تحليل بعد الانبعاج المرن للهياكل الفولاذية المستوية ذات المرابط والمستندة على أسس

أطروحة

مقدمة إلى كلية الهندسة في

جامعة بابل

كجزء من متطلبات نيل

الماجستير في شهادة

علوم

الـهندسة

من قبل

جواد طالب عبودي النصراوي

رمضان 1423 هـ **تشرين الثاني**
2002م

إشراف

أ.د.صبيح زكي الصراف أ.م.د.نمير عبد الامير علوش

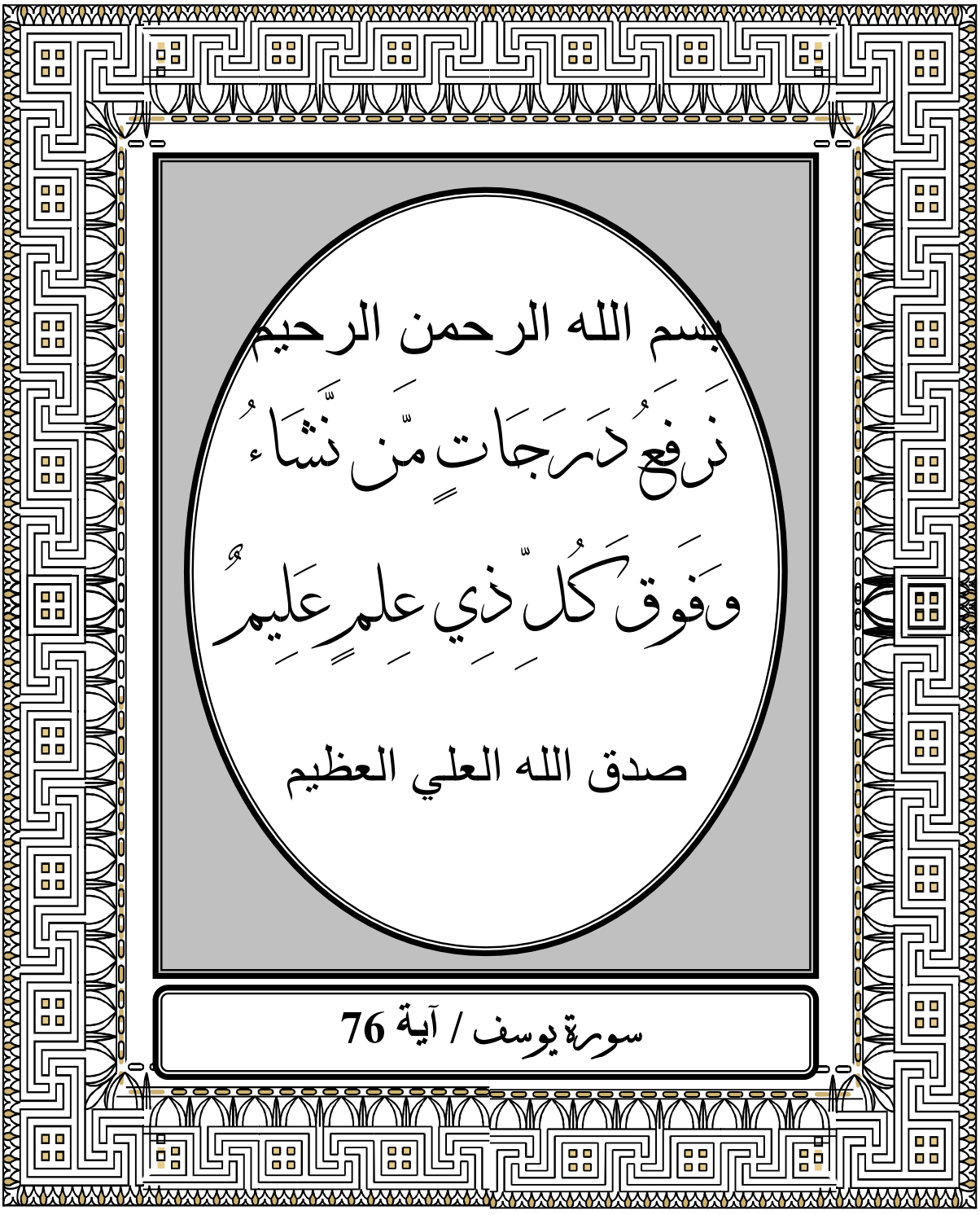
بسم الله الرحمن الرحيم
نَرفَعُ دَرَجَاتٍ مَّن نَّشَاءُ
وَفَوقَ كُلِّ ذِي عِلمٍ عَلِيمٌ
صدق الله العلي العظيم
سورة يوسف / آية 76


الى من سهرت الليالي من أجلي ....
والدتي العزيزة
الى من أشقى بعمره ورعاني ....
والدي العزيز
الى من أنار وا طريقي وأرشدوني ....
أساتذتي الأفاضل
الى من وقف الى جانبي ....
خالي العزيز
الى أصدقائي الأعزاء ....
أهدي جهدي المتواضع هذا

ACKNOWLEDGEMENT

I would like to express my gratitude to my supervisors Prof. Dr. Sabeeh Zaki Al-Sarraf and Dr. Nameer A. Alwash for their invaluable instructive guidance and encouragement during my study without which this work could not have been accomplished.

I also wish to offer my thanks to the Head and Staff members of the Department of Civil Engineering for all the facilities offered.

Acknowledgement is presented to the Head and Staff members of the advanced computer laboratory for their appreciable help.

Special words of thanks are devoted to my parents and my family for their patience and care during this work.

Finally, I would like to thank all my friends for their support and help in accomplishing this study, especially Hayder M. and Ali Kh.

Jawad Talib Aboudi

2005

ABSTRACT

In this investigation, a theoretical analysis is presented for predicting the pre- and post-buckling behavior of plane steel frames resting on elastic foundation with non-prismatic members, non-linear flexible steel connections and subjected to proportional and non-proportional increasing static loads including shear effect. The material of the frames is assumed to be isotropic and linearly elastic. Also, it is assumed that there is no-restrictions on the displacement values (large displacement analysis).

Beam-column approach is followed in the present study .A modified element presented is composed of two types of elements, namely, the beam-column (frame) element and the connection element. The moment-rotation behavior of steel connection is considered to be non-linear. The polynomial function is used to model the non-linear behavior of connection. The loading and unloading responses of the connection are also considered. The formulation of the beam-column element is based on Eulerian approach allowing for the influence of the axial force on bending stiffness. Changes in member chord length due to axial straining and flexural bowing are also taken into account.

In the post-buckling analysis, the incremental control with different load incrementation strategies and the modified Newton-Raphson method with different iterative strategies are used to obtain the complete load-displacement curve. Also, the determinant technique is used for detecting the intersection of load limit points.

In the present study, a multi-purpose computer program (NSHEEFF) has been coded in Quick-Basic 4.5 language for carrying out the proposed analysis and was implemented on personal computer types Pentium.

Several case studies are analyzed by using this program and the results show a good agreement with experimental and theoretical results by others.

As a result of this investigation, several important conclusions are obtained. Also, many recommendations are suggested for further work. One of the most important conclusions obtained from the results is the significant effect of connection flexibility that, gives differences in the investigation examples of about (15%-30%) taking in the account the effect of shear deformation.

LIST OF CONTENTS

SUBJECT ***PAGE***

CHAPTER FOUR: POST-BUCKLING ANALYSIS

CHAPTER FIVE: COMPUTER PROGRAM, TESTING AND DISCUSSION OF RESULTS

CHAPTER SIX: PARAMETRIC STUDIES

CHAPTER SEVEN: CONCLUSIONS AND RECOMMENDATIONS

NOTATION

SYMBOL	*DESCRIPTION*
A	: Cross-section area (mm^2).
A_o	:Equivalent area of cross section (mm^2).
$A_{(x)}$	:Variable area of cross section (mm^2).
[B]	:Matrix defined in equation (3.88)
$[\bar{B}]$	:Instantaneous static matrix.
b_1, b_2	:Bowing functions for prismatic member without shear.
$\bar{b}_1, \bar{b}_2$	:Bowing functions for prismatic member with shear.
C_b	:Length correction factor for bowing action.
C_1, C_2	:Stability functions for prismatic member without shear.
$\bar{C}_1, \bar{C}_2$	:Stability functions for prismatic member with shear.
D	:Depth ratio
E	:Modules of elasticity (N/mm^2).
{F}	:External forces.
$\{\bar{F}\}$	:Internal forces in local coordinates .
$\{F_r\}$	:Reference external forces.
{f}	:Internal forces of the nodal points in global coordinates.
G_1, G_2	:Quantities defined in equations (3.81) and (3.82).
$\{g^{(k)}\}$	:Geometric matrices defined in equations (3.105)and (3.106).
H	:Quantity defined in equation (3.83).
I	:Constant moment of inertia.
$I_{(x)}$	:Variable moment of inertia.
I_1	:Reference moment of inertia.
K	:Standardization constant for a connection.
R_{ki}	:Initial tangent stiffness of connection.
R_{kt}	:Tangent stiffness of connection.
λ_{cr}	:Elastic critical load factor.

ϕ :Rotational deformation (angle) within connection.

ϕ_1, ϕ_2 :End connection rotations.

J_{i-1} :Actual number of iterations required for convergence in the (i-1)th load step.

J_d :User-defined desired number of iterations for convergence.

L :Undeformed length of member (mm).

I_i :Arc-length.

M_1, M_2 :End moments (N.mm).

Q :Axial force (N).

Q_e :Euler load = π^2 EI/L^2.

q :Axial force parameter = Q/Q_E.

q_o :Modified axial force parameter for tapered member.

[R] :Transformation matrix.

m :Shape factor.

{S} :Member end forces in local coordinates.

[T] :Tangent stiffness matrix in global coordinates.

[t] :Tangent stiffness matrix in local coordinates.

$[T]_{mod.}$:New modified TSM in global coordinates.

U :Strain energy.

u :Relative axial displacement (mm).

{u} :Member end displacements in local coordinates (mm).

{v} :Member end displacements in global coordinates (mm).

$\{v_t\}$:Tangent displacements (mm).

W_e :Work done by the external forces (N.mm).

W_i :Work done by the internal forces (N.mm).

X :Horizontal coordinates axis.

Y :Vertical coordinates axis.

$y_{(x)}$:Lateral deflection function.

Δ :Increment.

$\{\Delta v_a\}_i$:Accumulated displacements within the ith load step (mm).

$\{\Delta v_r\}$:Residual displacements (mm).

$\{\Delta W\}$:Incremental work done (N.mm).

$\Delta\lambda_i^j$:The change in the load parameter.

$\Delta\lambda_i^1$:Initial increment of the load parameter.

Σ :Summation.

α, α'' :The angle between the local and global element coordinates in the deformed and undeformed configuration (rad.).

β_i :Modified bowing functions for non-prismatic member without shear.

$\overline{\beta}_i$:Modified bowing functions for non-prismatic member with shear.

γ_i :Modified stability functions for non-prismatic member without shear.

$\overline{\gamma}_i$:Modified stability functions for non-prismatic member with shear.

δ :Length increment changes.

ε_o :Effective axial strain.

θ_1, θ_2 :Relative end rotations (rad.).

λ :Load parameter.

μ :Shear parameter.

η :Axial strain.

π :3.1416…..

Note: Any other notation may be explained where it appears in the thesis.

الخلاصة

تتناول هذه الدراسة التحليل النظري للحصول على سلوك ما قبل وبعد الانبعاج للهياكل الحديدية المستوية والتي تحتوي على عناصر ذات مقاطع متغيرة ومستقرة على أسس مرنة من نوع (**Winkler**) ذات سلوكية خطية وكذلك على مفاصل حديدية ذات سلوكية لا خطية ومعرضة لزيادات مثاسبة وغير مثاسبة من الأحمال الساكنة والمسلطة على المفاصل فقط مع الأخذ بنظر الاعتبار تأثير تشوهات القص(**Shear Deformation Effect**). لقد فرض إن مادة هذه الهياكل تبقى مرنة وان علاقة الإجهاد–الانفعال لهذه المادة هي علاقة خطية. كذلك قد اخذ بنظر الاعتبار الازاحات الكبيرة **(Large Displacement Analysis)** وان لا محددات على قيم هذه الازاحات .

تبنت هذه الدراسة طريقة العمود–العتبة **(Beam-Column Approach)** وحيث قدمت الدراسة اشتقاق وتكوين نوعين من العناصر هي عنصر العمود–العتبة المتغير المقطع وعنصر المفصل. تم اعتبار العلاقة بين العزم والدوران في المفصل الحديدي علاقة لاخطية **(Non-Linear Moment-Rotation Behavior)**. إستُعمِلت دالة متعدد الحدود **(Polynomial)** لنمثيل السلوكية اللاخطية للمفاصل الحديدية وقد أُخِذَ بنظر الاعتبار احتمالية التحميل واللاتحميل في المفصل الحديدي. إن اشتقاق عنصر العمود–العتبة قد تم بالاعتماد على طريقة اويلر **(Eulerain Approach)** كما تم الأخذ بنظر الاعتبار تأثير القوة المحورية على صلابة العزم **(Bending Stiffness)** كما أخذ بنظر الاعتبار التغيرات في طول الوتر نتيجة الانفعال المحوري وتقوس الانحناء **(Flexural Bowing)** .

لغرض الحصول على سلوك الهياكل في مرحلة ما بعد الانبعاج فقد تم استخدام طريقة الحمل المتزايد مع إستراتيجيات مختلفة لزيادة الأحمال وكذلك تم استخدام طريقة

(***Newton Raphson***) المحورة مع إستراتيجيات مختلفة للحل المتكرر. أيضا تم استخدام تقنية المحدد لغرض التعرف على النقاط الحرجة (***critical points***).

ضمن متطلبات هذه الدراسة تم كتابة البرنامج (***NSHEEFF***) بلغة بيسك السريعة 4.5 ونفذ على حاسبة نوع (***Pentium***) . تم مقارنة النتائج المستحصلة مع نتائج أمثلة دراسات منشورة سابقا . كذلك تم تحميل مجموعة من المنشآت والتي تبين كل أنواع النقاط الحرجة والسلوك اللاخطي .

كنتيجة لهذه الدراسة فقد توصلت إلى عدة استنتاجات مهمة وكذلك تقديم عدة توصيات لغرض تطوير العمل المقدم. من أهم الاستنتاجات المستحصلة من خلال حل عدد من الأمثلة إن التصرف اللاخطي للمفصل هو تصرف ذو شأن ويجب الاهتمام به إثناء تحليل المنشآت , حيث يسبب فرق في نتائج الازاحات المستحصلة يتراوح تقريباً بين (15%-30%) مأخوذاً بنظر الاعتبار تأثير تشوهات القص .

Post-Buckling Analysis of Steel Plane Frames on Elastic Foundation With Flexible Connections

A thesis

Submitted to the College of Engineering

of the University of Babylon for Fulfillment

of the Partial of the Requirements

for the Degree of Master of Science in

Civil Engineering

By

Jawad Talib Aboudi
Al-Nasrawi

(B.Sc.)

November 2002 Ramathan 1423

Supervision

Prof. Dr. Sabeeh Z. Al-Sarraf

Dr. Nameer A. Alwash

1.1 Objective of The Thesis

The objective of this study is to make the theoretical basis for the large displacement and post-buckling analysis of non-prismatic plane steel frames with non-rigid connections, resting on elastic foundation and subjected to static loads including shear effect.

The present study is introduced in seven chapters. Chapter One presents the problem and the aim of the study. In Chapter Two, a brief review of early studies and the more advanced studies on the subject is given with an interpretation of results as possible.

Chapter Three establishes the derivation of the conventional tangent stiffness matrix for non-prismatic members in local and global coordinates and derivation of the modified tangent stuffiness matrix in global coordinates including shear effect which takes into account the two types of non-linearity at the same time. In addition, the iterative technique to be used for calculating the slip angle of the flexible connection is presented. Also, it introduces the special technique used for accounting the axial force when the flexural bowing in the member is included.

Chapter Four presents a description of the different numerical techniques used in solving the non-linear simultaneous equations. Also, the post-buckling behavior and types of instability points of plane steel frame are presented. Furthermore, this chapter introduces numerical algorithms for post-bucking analysis with different strategies for initial load incrementation and iterative process. Finally, a brief description of the types of the convergence criteria used in the iterative analyses has been presented.

In Chapter Five, the multi-purpose computer program (NSHEEFF) which has been coded in the present study in Quick Basic 4.5 language had been described. In addition, computer applications for testing the validity of the program (NSHEEFF), have been made and the results were compared with case studies reported by other researchers.

In Chapter Six, pre-and post-bucking analyses of prismatic and non-prismatic plane steel frames with rigid and flexible connections, resting on elastic foundation and subjected to static loads including shear effect are presented and discussed as six parametric studies.

Finally, Chapter Seven gives several conclusions and recommendations for future studies on this subject.

1.2 Post – Bucking Behavior of Structures

For most practical problems, it is quite unnecessary to trace such a convoluted load-displacement path as that shown in Figure (1). Indeed, where such a path is to be traced, most analyses would trace the static path ABCDEFGHIJ and thus infer the dynamic snaps. Although the analyses are therefore somewhat artificial, they may be very important.

For some problems, all that may appear to be required is the load level at the first limit point. However, without analysis techniques that allow the limit points to be passed, even this information may be unavailable or unreliable. Collapse loads are often associated with a failure to achieve convergence with the iterative solution procedure. However, it may be only the iterative solution that has collapsed (possibly as a consequence of round-off error). In such situation, the analyst is left with no information on the nature of the failure and may not even be sure that he has a structural rather than numerical collapse. In some situation, it may be important to obtain information on the nature of the load shedding, following the limit points, in order to assess the performance of the complete structure. Consequently, non-linear computer programs should be provided with solution procedures that will handle such non-linear behavior and snapping phenomena.

The present work (as will be explained in Chapter Four), involves the use of different techniques that handle such analysis without difficulty even when the structure exhibits stiffening or softening, limit or bifurcation point. Finally, it is worth while to know that the term "Post- Bucking Behavior" means the behavior of structures after the first load limit point even when the geometry of structure is changed.

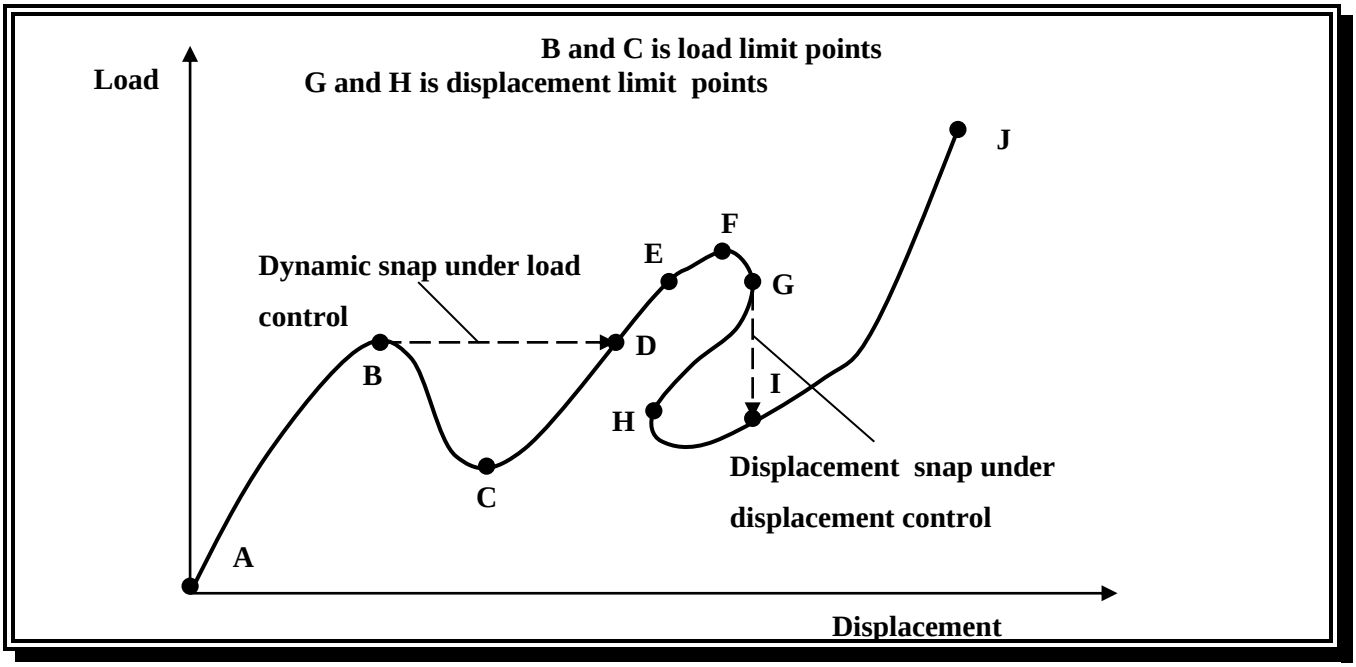

Fig.(1): Complex Load-Displacement Curve .

1.3 Non-Linear Behavior of Structures

Various behaviors are called "Non-Linear". Stress-strain relations may be non-linear in either a time-dependent or a time-independent way. Displacement may cause loads to alter their distribution or magnitude. Mating parts may stick or slip, gaps may open or close. Nonlinearity may be mild or severe .The problem may be static or dynamic. Many solutions have been proposed, and it is no surprise that no one is best for all problems.

1.3.1 Geometrical Non-linearity

The effects of geometrical non-linearity may be separated into three categories.

1.3.1.1 Stability Effect [Stability Non-Linearity]

The non-linearity in this type is mainly due to the coupling effect of axial force and flexural moment. The problem then may be solved by introducing stability functions which are dependent on the axial force parameter only ($q=Q/Q_{Euler}$). Then, the member end moments (M_1) and (M_2) for the prismatic member shown in Figure (2) are expressed in terms of member end rotations (θ_1) and (θ_2) as follows:

$$M_1 = \frac{EI}{L}(C_1\theta_1 + C_2\theta_2) \quad \text{..... (1)}$$

$$M_2 = \frac{EI}{L}(C_2\theta_1 + C_1\theta_2) \quad \text{..... (2)}$$

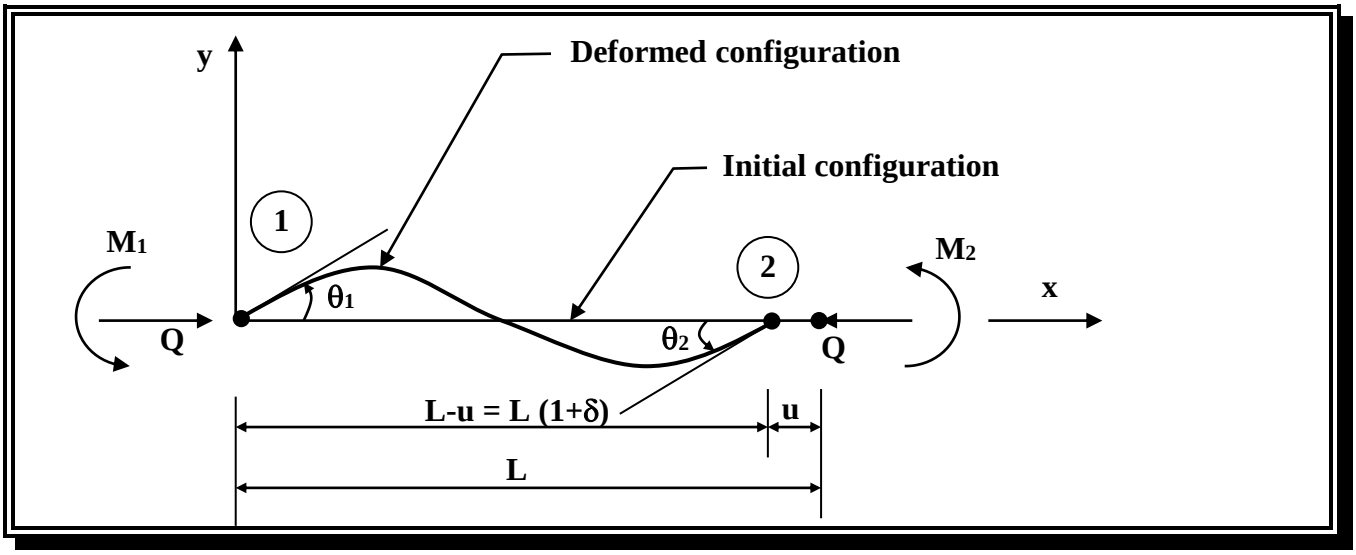

Fig.(2): Relative Member Deformations-End Forces .

1.3.1.2 Bowing Effect [Change in the Member Length Due to Bowing]:

This type of non-linearity is also caused by the interaction between bending and axial forces in the members. In a like manner, the presence of bending moments affects the axial stiffness of the member due to an apparent shortening of the member by the bending deformation. The problem then may be solved by introducing bowing functions, which are dependent on the axial force parameter (**q**). Then, the axial force **Q** is expressed in terms of relative axial displacement (**u)** as follows:

$$Q = \frac{EA}{L}(u - C_b.L) \quad \text{..... (3)}$$

and

$$C_b = b_1(\theta_1+\theta_2)^2 + b_2(\theta_1-\theta_2)^2 \quad \text{..... (4)}$$

However, all the previous equations are for prismatic member and to deal with non-prismatic member, some modification must be applied as discussed later in **Chapter Three**.

1.3.1.3 Large Displacement Effect

In which the non-linearity occurs when the deformation becomes large enough to cause significant changes in the geometry of the structure, so that the equilibrium equations must be formulated for the updated deformed configuration.

1.3.2 Connection Non-linearity

Connection non-linearity results due to the use of semi-rigid beam-to -column joints in unbraced steel frames. Since the relationship between the moment in the connection and rotation (slip angle) is non-linear, it follows that the stiffness matrix will contain the rotations and stiffnesses of connections that are not known in advance, and therefore requires an iteration technique to be used.

The assumption of rigid joint implies that the full displacement and slope continuities exist between adjoining members and that full (or a substantial percentage) of gravity moment is transferred from beam to column. On the other hand the assumption of ideally pinned connection implies that the beams will behave as if they were simply supported and that the columns will carry no gravity moments from the beams. Although the assumptions of fully rigid or ideally pinned connection behavior drastically simplify the analysis and design procedure, the validity of these assumptions may be questionable in some cases in which connection rigidities are intermediate between the fully rigid and pinned cases.

1.4 Shear Effect on Elastic Stability

The effect of shear force on the elastic stability of the beam-column element shown in Figure (3), will result in modifying the stability functions.

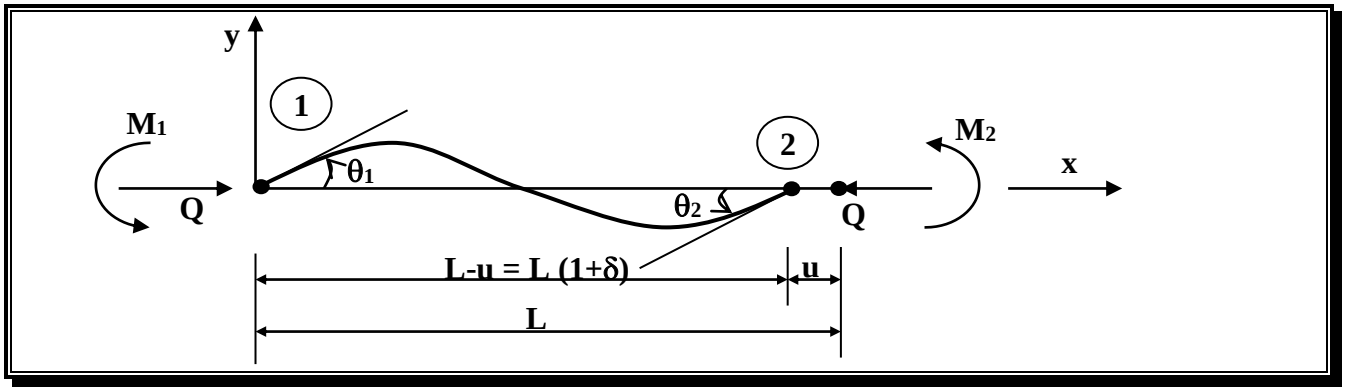

Fig.(3):Relative Member Displacements and Associated Forces in Local Coordinates for Non-Prismatic Member .

The modified stability functions can be derived by using the basic differential equation of the deflection curve. According to the first approach, which will be used in the present study, the basic differential equation is: -

$$\frac{d^2y}{dx^2} = -\frac{Mx}{EI} + \frac{n}{GA}\cdot\frac{dVx}{dx} \quad \text{.....(5)}$$

According to Figure (4), the bending moment, **Mx**, and the shear force, **Vx**, can be written as: -

$$Mx = \left(1 - \frac{x}{L}\right)M_1 - \frac{x}{L}M_2 + Qy \quad \text{.....(6)}$$

$$Vx = -\left(\frac{M_1 + M_2}{L}\right) + Q\frac{dy}{dx} \quad \text{.....(7)}$$

Substituting Equations (6) and (7) into Equation (5) yields: -

$$\left(1 - \frac{nQ}{GA}\right)\frac{d^2y}{dx^2} + \frac{Qy}{EI} = \frac{1}{EI}\left[M_1\left(\frac{x}{L} - 1\right) + \frac{M_2}{Q}\left(\frac{x}{L}\right)\right] \quad \text{.....(8)}$$

The general solution of Equation (8) in case of compression axial force **(q_o>0)** is: -

$$y = D_1.\sin(\omega x) + D_2.\cos(\omega x) + \frac{M_1}{Q}\left(\frac{x}{L} - 1\right) + \frac{M_2}{Q}\left(\frac{x}{L}\right) \quad \text{.....(9)}$$

Where;

$$\omega^2 = \frac{Q}{EI}\left(\frac{1}{1 - nQ/GA}\right) = \frac{\pi^2}{L^2}.\bar{q}_o \quad \text{.....(10)}$$

in which;

$$\bar{q}_o = \frac{q_o}{1 - \mu q_o} \quad \text{.....(11)}$$

With μ = The shear parameter and it is given in Table (1), and

Type	Shear Parameter (μ)
Solid Cross Section	$\frac{2n(1+\nu)\pi^2 Ie}{Ao\,L^2}$
Pratt Bracing 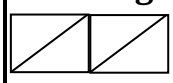	$\frac{EIe\pi^2}{L^2}\left[\frac{l_d.\cos(\alpha)}{(\cos(\varphi)+\sin(\varphi)\tan(\varphi))\cos(\varphi-\alpha)A_d El_c} + \frac{l_b}{A_b El_c}\right]$
X-Bracing 	$\frac{EIe\pi^2}{L^2}\left[\frac{l_d.\cos(\alpha)}{2(\cos(\varphi)+\sin(\varphi)\tan(\varphi))\cos(\varphi-\alpha)A_d El_c}\right]$

Warren Bracing 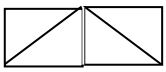	$\frac{EIe\pi^2}{L^2}\left[\frac{l_d.\cos(\alpha)}{(\cos(\varphi)+\sin(\varphi)\tan(\varphi))\cos(\varphi-\alpha)A_dEl_c}\right]$
Howe Bracing 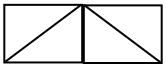	$\frac{EIe\pi^2}{L^2}\left[\frac{l_d.\cos(\alpha)}{(\cos(\varphi)+\sin(\varphi)\tan(\varphi))\cos(\varphi-\alpha)A_dEl_c}+\frac{l_b}{A_bEl_c}\right]$

Tab.(1):The Governing Equations of Shear Parameter(μ) For Any Type of Section

D_1, D_2 = Are integration constants, which can be found from boundary conditions, as follows: -

At x=0; y=0, then: -

$$D_2=M_1/Q \quad \text{.....(12)}$$

At x=L; y=0, then: -

$$D_1=-\frac{M_2}{Q}.\csc(\omega L)-\frac{M_1}{Q}.\cot(\omega L) \quad \text{.....(13)}$$

Now, substituting Equations (12) and (13) into Equation (9) yields: -

$$y=\left[-\frac{M_2}{Q}.\csc(\omega L)-\frac{M_1}{Q}.\cot(\omega L)\right].\sin(\omega x)+\frac{M_1}{Q}.\cos(\omega x)$$
$$+\frac{M_1}{Q}\left(\frac{x}{L}-1\right)+\frac{M_2}{Q}\left(\frac{x}{L}\right) \quad \text{.....(14)}$$

According to end conditions [***Al-Sarraf*** **[51]** (1986)] :-

$$\left(\frac{dy}{dx}\right)_{end1}=\frac{\theta_1-\frac{n(M_1+M_2)}{GAL}}{1-\mu q_o} \quad \text{.....(15)}$$

$$\left(\frac{dy}{dx}\right)_{end2}=\frac{\theta_2-\frac{n(M_1+M_2)}{GAL}}{1-\mu q_o} \quad \text{.....(16)}$$

Finally, applying Equations (15) and (16) into Equation (14), yields:-

$$M_1=\frac{EI_1}{L}\left(\overline{C}_1\theta_1+\overline{C}_2\theta_2\right) \quad \text{.....(17)}$$

$$M_2=\frac{EI_1}{L}\left(\overline{C}_2\theta_1+\overline{C}_1\theta_2\right) \quad \text{.....(18)}$$

Where;

$$\overline{C}_1=\frac{\overline{\alpha}[1-2(1-\mu q_o)\overline{\alpha}.\cot(2\overline{\alpha})]}{[\tan(\overline{\alpha})-\overline{\alpha}(1-\mu q_o)]} \quad \text{.....(19)}$$

$$\bar{C}_2 = \frac{\bar{C}_1[2(1-\mu q_o)\bar{\alpha} - \sin(2\bar{\alpha})]}{[\sin(2\bar{\alpha}) - 2\bar{\alpha}(1-\mu q_o)\cos(2\bar{\alpha})]} \quad \ldots\ldots(20)$$

And

$$\bar{\alpha} = \frac{\pi}{2}\sqrt{\bar{q}_o} = \frac{\pi}{2}\sqrt{\frac{q_o}{1-\mu q_o}} \quad \ldots\ldots(21)$$

In case of tension axial force, **(q_o<0)**, the modified stability functions can be derived in the same manner as before, which gives: -

$$\bar{C}_1 = \frac{\bar{\alpha}[1-2(1-\mu q_o)\bar{\alpha}.\coth(2\bar{\alpha})]}{[\tanh(\bar{\alpha}) - \bar{\alpha}(1-\mu q_o)]} \quad \ldots\ldots(22)$$

$$\bar{C}_2 = \frac{\bar{C}_1[2(1-\mu q_o)\bar{\alpha} - \sinh(2\bar{\alpha})]}{[\sinh(2\bar{\alpha}) - 2\bar{\alpha}(1-\mu q_o)\cosh(2\bar{\alpha})]} \quad \ldots\ldots(23)$$

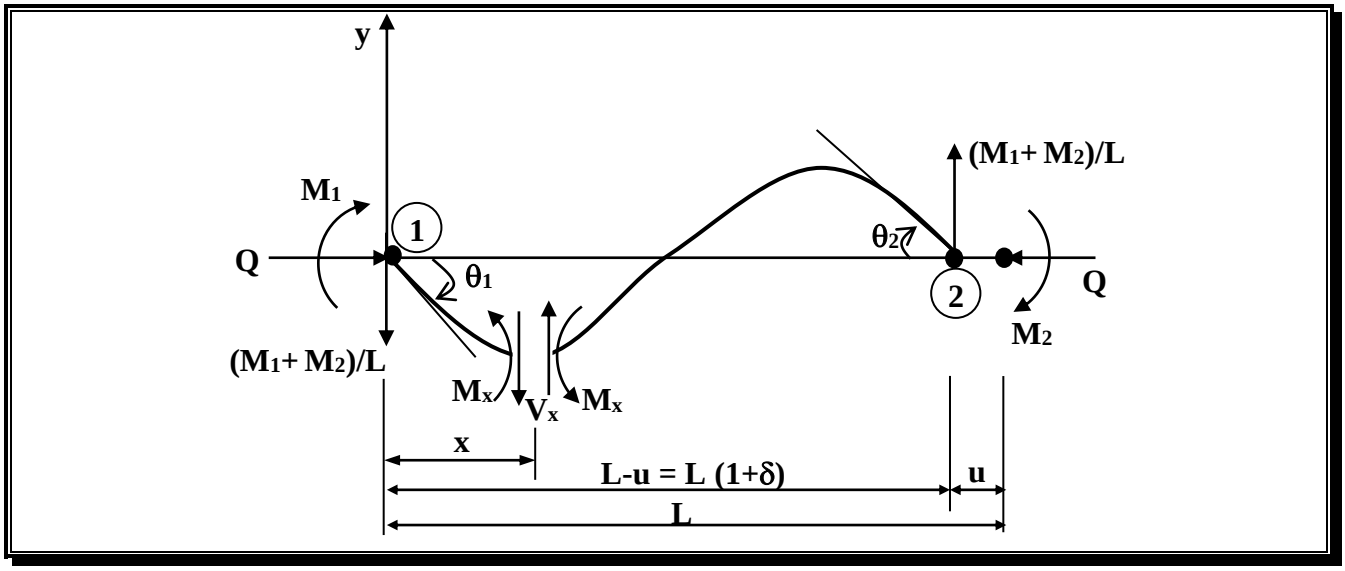

Fig.(4):Force System of Elastic Beam-Column

In the present study the approximate formula produced by ***Al-Sarraf*** **[30]**, for calculating stability functions for non-prismatic member, will be extended to include the effect of shear force, therefore, approximate formula of stability functions including shear effect for non-prismatic members are illustrated as follows **[80]**: -

$$\bar{\gamma}_1 = D^{\phi m/4}\,\bar{C}_1 \quad \ldots\ldots(24)$$

$$\bar{\gamma}_2 = D^{(\phi+1)m/4}\,\bar{C}_2 \quad \ldots\ldots(25)$$

$$\bar{\gamma}_3 = D^{(\phi+2)m/4}\,\bar{C}_1 \quad \ldots\ldots(26)$$

Where;

$\bar{\gamma}_i$: Are the stability functions of non - prismatic member including shear effect , and

$\bar{C}_1, \bar{C}_2$: Are the stability functions of prismatic member including shear effect.

1.5 Shear Effect on Flexural Bowing

When a prismatic member is subjected to bending, there is a shortening of the chord length, **Lc**. This change in length has been called bowing deformation or curvature shortening.

Bowing deformation, δ_b, was presented by ***Saffan*** **[7]** as: -

$$\delta_b = \frac{1}{2}\int_0^{Lc}\left(\frac{dy}{dx}\right)^2 dx \quad \text{.....(27)}$$

In addition to the effect of the combination of axial force and bending moments on the bowing phenomenon, the shearing force has a significant role in this operation. Thus, the modified bowing formula, $\bar{C}_b$, and the modified bowing functions, $\bar{b}_1$ and $\bar{b}_2$, including shear effect must be introduced. These functions were derived by ***Sideek*** **[74]**, as: -

$$\bar{C}_b = \bar{b}_1(\theta_1 + \theta_2)^2 + \bar{b}_2(\theta_1 - \theta_2)^2 \quad \text{.....(28)}$$

Where; For a compressive axial force ($q_o>0$): -

$$\bar{b}_1 = \frac{(\bar{C}1+\bar{C}2)^2}{4\pi^4 q_o^2}\left[\frac{2\bar{\alpha}(2\bar{\alpha}+\sin(2\bar{\alpha}).\cos(2\bar{\alpha}))}{\sin^2(2\bar{\alpha})} - 2 + \frac{(\bar{\alpha}\cos(2\bar{\alpha})-\bar{\alpha})(2\bar{\alpha}-\sin(2\bar{\alpha}))}{\sin^2(2\bar{\alpha})}\right]$$

.....(29)

$$\bar{b}_2 = \frac{(\bar{C}1+\bar{C}2)^2}{8\pi^4 q_o^2}\left[\frac{(2\bar{\alpha}-2\bar{\alpha}.\cos(2\bar{\alpha}))(2\bar{\alpha}-\sin(2\bar{\alpha}))}{\sin^2(2\bar{\alpha})}\right] \quad \text{.....(30)}$$

And, For a tensile force ($q_o<0$): -

$$\bar{b}_1 = \frac{(\bar{C}1+\bar{C}2)^2}{4\pi^4 q_o^2}\left[\frac{2\bar{\alpha}(2\bar{\alpha}+\sinh(2\bar{\alpha}).\cosh(2\bar{\alpha}))}{\sinh^2(2\bar{\alpha})} - 2 + \frac{(\bar{\alpha}\cosh(2\bar{\alpha})-\bar{\alpha})(2\bar{\alpha}-\sinh(2\bar{\alpha}))}{\sinh^2(2\bar{\alpha})}\right]$$

.....(31)

$$\bar{b}_2 = \frac{(\bar{C}1+\bar{C}2)^2}{8\pi^4 q_o^2}\left[\frac{(2\bar{\alpha}-2\bar{\alpha}.\cosh(2\bar{\alpha}))(2\bar{\alpha}-\sinh(2\bar{\alpha}))}{\sinh^2(2\bar{\alpha})}\right] \quad \text{.....(32)}$$

When the axial force is small (i.e. q_o approaches zero), computational difficulties arise in finding the modifying stability functions from their general expression. To avoid such difficulties, linear interpolation is suggested in the present study to be used in the range ($-0.1<q_o<0.1$), when the values of $\bar{C}_1$ and $\bar{C}_2$ at ($q_o=0$) can be found from Equations (22) and (23) using ***L'Hopital's*** rule as follows: -

$$\bar{C}_1 = \frac{4\pi^2+12\mu}{\pi^2+12\mu} \quad ; \quad \bar{C}_2 = \frac{2\pi^2-12\mu}{\pi^2+12\mu} \quad \text{.....(33a)}$$

And for **($-0.1<q_o<0.1$),** the values of $\bar{C}_1$ and $\bar{C}_2$ can be found as follows: -

$\bar{C}_i(\pm q_o)=\bar{C}_i(0)-[\bar{C}_i(0)-\bar{C}_i(\pm 0.1)]q_o/0.1$ **; i=1,2** .....(33b)

While for non-prismatic member an approximate formula for the effect of shear on the bowing functions is as follow **[75]**: -

$$\bar{C}_b = \bar{\beta}_1\theta^2_1 + 2\bar{\beta}_2\theta_1\theta_2 + \bar{\beta}_3\theta^2_2 \quad \text{.....(34)}$$

In which;

$\bar{C}_b$: Is the modified flexural bowing for non-prismatic member including shear effect, and

$\bar{\beta}_i$: Is the modified bowing functions for non-prismatic member including shear effect.

These functions are defined by: -

$$\bar{\beta}_1 = D^{-\phi m/4}\ (\bar{b}_1+\bar{b}_2) \quad \text{.....(35)}$$

$$\bar{\beta}_2 = D^{(1-\phi)m/4}\ (\bar{b}_1-\bar{b}_2) \quad \text{.....(36)}$$

$$\bar{\beta}_3 = D^{(2-\phi)m/4}\ (\bar{b}_1+\bar{b}_2) \quad \text{.....(37)}$$

Where;

$\bar{b}_1$ and $\bar{b}_2$: Are the bowing functions for prismatic member including shear effect .

1.6 Tangent Stiffness Matrix Including Shear Effect

The derivation of tangent stiffness matrix including shear effect follows the same procedure as that given in Equation (3.85), so we can substitute the modified stability and bowing functions including shear effect in matrix [t] given in Equation (3.85), instead of the ordinary stability and bowing functions. Accordingly: -

$$G_1 = -2\pi^2\left(\bar{\beta}_1\theta_1 + \bar{\beta}_2\theta_2\right) = \bar{\gamma}'_1\theta_1 + \bar{\gamma}'_2\theta_2 \quad \text{.....(38)}$$

$$G_2 = -2\pi^2\left(\bar{\beta}_2\theta_1 + \bar{\beta}_3\theta_2\right) = \bar{\gamma}'_2\theta_1 + \bar{\gamma}'_3\theta_2 \quad \text{.....(39)}$$

$$H = \frac{\pi^2}{\lambda_0^2} + \left(\bar{\beta}'_1\theta_1^2 + 2\bar{\beta}'_2\theta_1\theta_2 + \bar{\beta}'_3\theta_2^2\right) \quad \text{.....(40)}$$

1.7 The Equivalent Continuum Model For Beam-Column Like Lattice Structure

This method deals with the symmetrical lattice structure with respect to the longitudinal reference axis only. Non-symmetry in the lattice can result in coupling of the axial and transverse displacements. Therefore, only a symmetrical beam-like lattice structure will be considered here.

The equivalent model properties for prismatic beam-like lattice structure as shown in figure (5), can be identified as **[60]**: -

$$\overline{EI} = 2EA_cC^2 + 2EI_c \quad \text{.....(41)}$$

$\overline{EA}=2EA_c+\Sigma EA_{di}\cos^3$ ..... (42)

$\overline{GA}=GAs$…...……...……..(43)

Where;

$\overline{EI}$, $\overline{EA}$ and $\overline{GA}$: ..... Are the flexural, axial and shear rigidity of equivalent Continuum model,

ϕ : The angle between the diagonal and horizontal bars,

C : The distance between the longitudinal bar and the axis of Symmetry, and

GAs: The effective shear stiffness.

For the pin-jointed lattice, shown in Figure (5a), is given by: -

$GAs=2EA_d.\sin^2\phi.\cos\phi$ ……....(44)

And for the rigid-jointed lattice, shown in Figure (5b), is: -

$$GAs=\frac{\frac{24EI_c}{(1+\lambda_b)I_cL_b}}{\left[1+\frac{2(1+\lambda_b)I_cL_b}{(1+\lambda_c)I_bL_c}\right]} \quad \text{……...(45)}$$

$$\lambda_c=\frac{12EI_c}{Gn_cA_cL^2{}_c} \quad \text{……...(46)}$$

$$\lambda_b=\frac{12EI_b}{Gn_bA_bL^2{}_b} \quad \text{……..(47)}$$

n : The shear shape factor for the given cross-section geometry of the lattice members, and

c and **b** : Represent the chord and the battened member respectively.

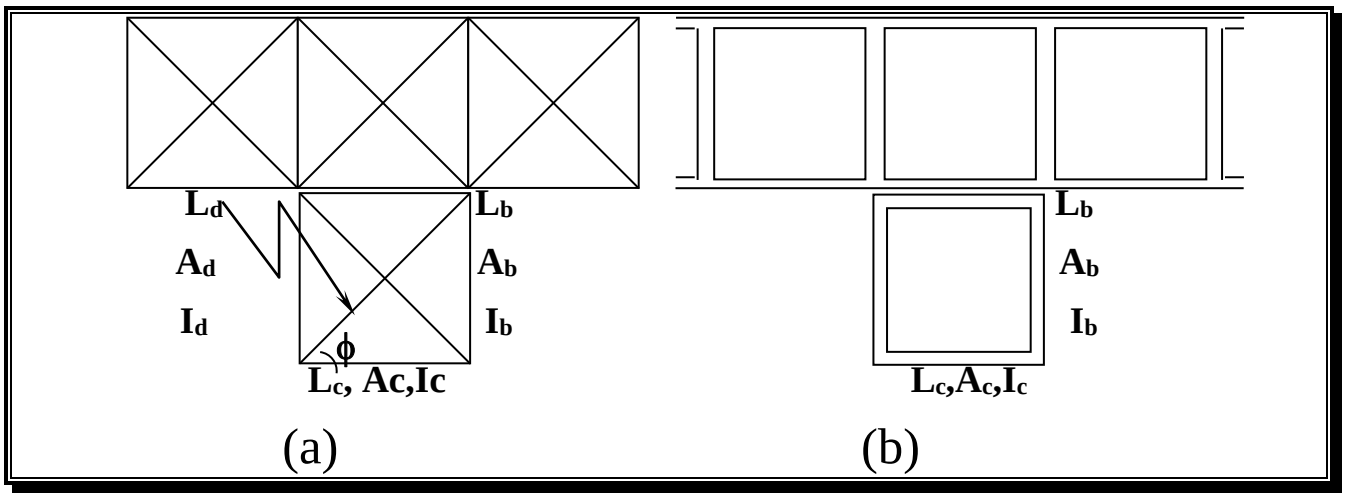

Fig.(5):Repeating Cells

In the present study we can use the same procedure as that obtained by ***Mc Callen and Romstad*** (1988) **[60]**, which is based on the equivalent continuum approach to obtained an equivalent continuum model for non-prismatic beam-like lattice structure, in which it's properties can be identified as: -

$$\overline{EI}=2EA_cC^2.\cos^3\alpha+2EI_c \quad \text{.....(48)}$$

$$\overline{EA}=2EA_c.\cos^3\alpha+\sum EA_{di}\cos^3\phi \quad \text{.....(49)}$$

$$\overline{GA}=GAs \quad \text{.....(50)}$$

In which;

α : Is the angle of the tapering.

1.8 Slip Angle of Non-linear Flexible Connection

It should be noted that because of the presence of the connections, the joint rotation and element end rotation are not the same, see Figures (6) and (7), where the element end rotation for a frame element with connections at the ends will be (θ_1-ϕ_1) and (θ_2-ϕ_2) respectively and that ϕ_1 and ϕ_2 are relative rotations of the beam-to-column connection.

Due to the presence of flexible connections at ends 1 and 2 of the element, the moment-rotation relationship of this element will be:

$$\begin{Bmatrix} M_1 \\ M_2 \end{Bmatrix} = \frac{EI_1}{L}\begin{bmatrix} \overline{\gamma}_1 & \overline{\gamma}_2 \\ \overline{\gamma}_2 & \overline{\gamma}_3 \end{bmatrix}\begin{Bmatrix} \theta_1-\phi_1 \\ \theta_2-\phi_2 \end{Bmatrix} \quad \text{.....(51)}$$

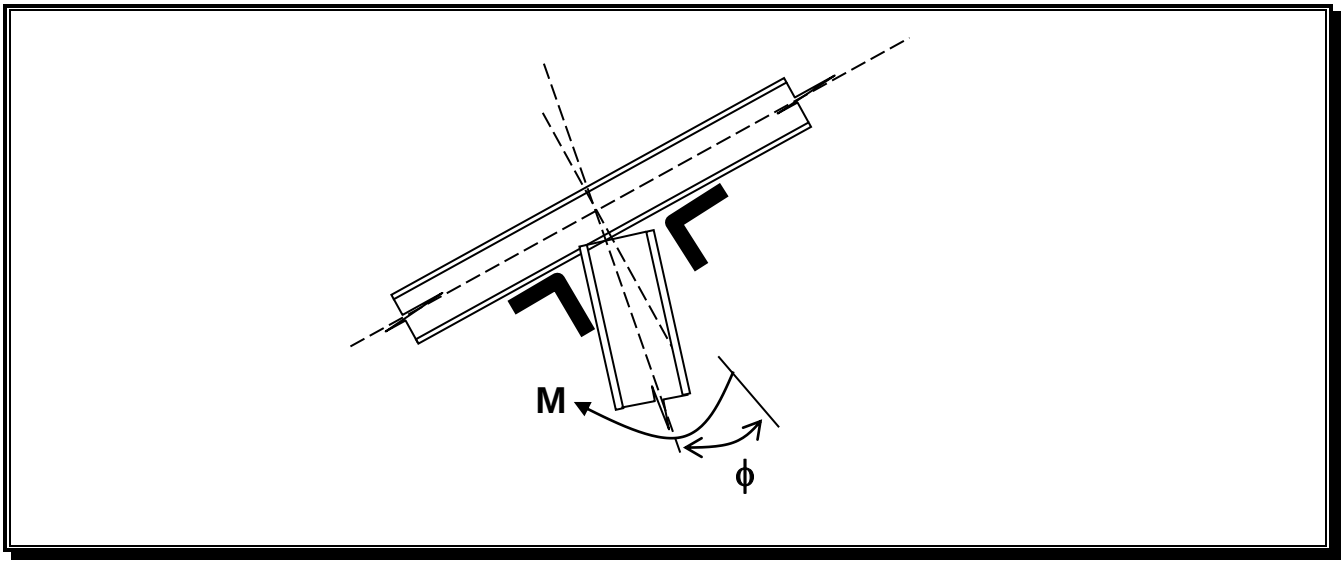

Fig.(6): Slip Angle of a Beam-Column Connection .

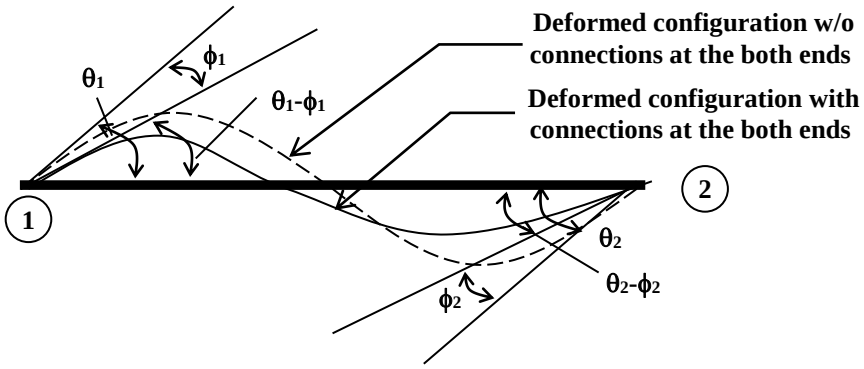

Fig.(7): End Rotation of a Beam-Column Element with Connections .

So, for a member with flexible connections at both ends;

$$\mathbf{M_1} = \frac{\mathbf{E I_1}}{\mathbf{L}}\left(\bar{\gamma}_1 \theta_1 + \bar{\gamma}_2 \theta_2 - \bar{\gamma}_1 \phi_1 - \bar{\gamma}_2 \phi_2\right) \quad \text{..... (52)}$$

$$\mathbf{M_2} = \frac{\mathbf{E I_1}}{\mathbf{L}}\left(\bar{\gamma}_2 \theta_1 + \bar{\gamma}_3 \theta_2 - \bar{\gamma}_2 \phi_1 - \bar{\gamma}_3 \phi_2\right) \quad \text{..... (53)}$$

Assuming two functions:

$$\mathbf{F_1(M_1, M_2)} = \mathbf{M_1} - \frac{\mathbf{EI_1}}{\mathbf{L}}\left(\bar{\gamma}_1 \theta_1 + \bar{\gamma}_2 \theta_2 - \bar{\gamma}_1 \mathbf{f_1(M_1)} - \bar{\gamma}_2 \mathbf{f_2(M_2)}\right) = \mathbf{0} \quad \text{..... (54)}$$

$$\mathbf{F_2(M_1, M_2)} = \mathbf{M_2} - \frac{\mathbf{EI_1}}{\mathbf{L}}\left(\bar{\gamma}_2 \theta_1 + \bar{\gamma}_3 \theta_2 - \bar{\gamma}_2 \mathbf{f_1(M_1)} - \bar{\gamma}_3 \mathbf{f_2(M_2)}\right) = \mathbf{0} \quad \text{..... (55)}$$

These two highly non-linear Equations (54) and (55) can be solved using conventional N-R iteration.

The new modified tangent stiffness matrix is used herein for the presence of connections. In the case of a rigid connection or a real hinge, linear **M-ϕ** relations may be used for these purposes as shown in Figure (8);

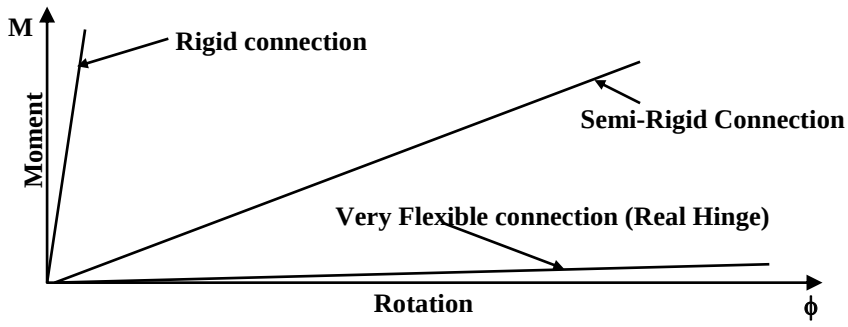

Fig.(8): Linear M-ϕ Relations .

1.9 Elastic Foundation

This part deals with the configuration and the strategy of analysis for the soil – structure interaction. There are two approaches in the analysis of structures consisting of members on elastic foundations. The first approach considered the foundation to be uniformly distributed ***Winkler*** type foundation. In the second approach, the foundation is represented by isolated (lumped) springs at the nodes of beam-column. The second approach will be adopted in the present study.

1.9.1 Elastic Foundation Properties

The constant of proportionality between the applied normal or shear stress at a point on the structure of soil and the corresponding surface displacement is the modulus of subgrade reaction for soil mass, or soil configuration at that point. The modulus of subgrade reaction gives the relationship between the soil pressure and the resulting deflection.

The subgrade reaction model of soil behavior was originally proposed by ***Winkler***, in (1867), characterize the soil as a series of unconnected linearly elastic springs. The deflection at any point (or any spring) occurs only where loading exists at that point. The obvious disadvantage of this soil model is the lack of continuity. Real soil is at least some extent continuous. A further disadvantage is that the spring modulus of the model (modulus of subgrade reaction) is dependent on the size of foundation. In spite of these drawbacks, the subgrade reaction approach has been widely employed in foundation practice because it provides a relatively simple means of analysis and enables factors, such as non-linearity, variation of soil stiffness with depth and layering of the soil profile to be taken into account. In order to characterize the behavior of a soil mass as being equivalent to a ***Winkler*** medium, the following conditions should be satisfied: -

1- The surface displacement at each point of the soil medium should be proportional to the applied normal stress. Plate bearing tests give approximate linearity especially when the loads are small.

2- The surface displacement of the soil medium outside the loaded region should be zero irrespective of the location or magnitude of the applied load. Real soil (another solid granular materials) does not fulfill this condition. The error is usually small in most computations.

Soil configuration can be presented by using two kinds of subgrade reaction modal along the foundation length, the normal and the tangential. The normal subgrade reaction modulus ($\mathbf{K_n}$) is defined as the load required to act normally on a unit area of the elastic foundation to produce a unit normal displacement. The tangential subgrade reaction modulus ($\mathbf{K_t}$) is defined as the load required to act tangentially on a unit area of elastic foundation to produce a unit horizontal displacement.

1.9.2 Modeling of Subgrade Reaction

The subgrade reaction can be represented in two ways, either consistent or lumped, which will be denoted as the soil stiffness matrix. The present study will be adept the lumped way.

1.9.2.1 Lumped (Isolated) Spring Approach

In this approach the foundation is represented by isolated springs at the nodes of the beam –column. Therefore, the theoretical derivation (stability functions, bowing function and transformation matrix) presented in this chapter can be used in this approach.

The lumped soil stiffness matrix, for the element shown in Figure (9) can be given as: -

$$\left[\overline{K}\right]_{(6\times6)} = \begin{bmatrix} K_t & & & & & 0 \\ & K_n & & & & \\ & & 0 & & & \\ & & & K_t & & \\ & & & & K_n & \\ 0 & & & & & 0 \end{bmatrix} \quad \text{.....(56)}$$

In which;

$\left[\overline{K}\right]$ is a (6×6) lumped soil stiffness matrix in local (intermediate) coordinates .

K_t : is the tangential (shear) nodal spring constant in x- direction .

K_n : is the normal spring constant in y - direction .

K_t and K_n can be obtained from the following equations: -

$$K_t = Kx.Sp.Dr \quad \text{.....(57)}$$

$$K_n = Ky.bw.Dr \quad \text{.....(58)}$$

In which;

Kx : is the tangential subgrade reaction modulus.

Ky : is the normal subgrade reaction modulus.

Sp : is the cross – section perimeter.

bw : is the width of the cross - section .

Dr : is the distribution ratio, defined by :-

Case (1) : when the member resting on elastic foundation is prismatic .

$Dr = \frac{L}{2}$ [at both ends]

in which : (**L**) is the length of the member .

Case (2): when the member resting on elastic foundation is tapered.

$\mathbf{Dr = \frac{L}{3}}$ (at the smallest end of the tapered element)

$\mathbf{Dr = \frac{2L}{3}}$ (at the largest end of the tapered element)

The matrix $[\bar{K}]$ is then to be added to the member tangent stiffness matrix in local coordinates $[\bar{T}]$, to get the total local tangent stiffness matrix.

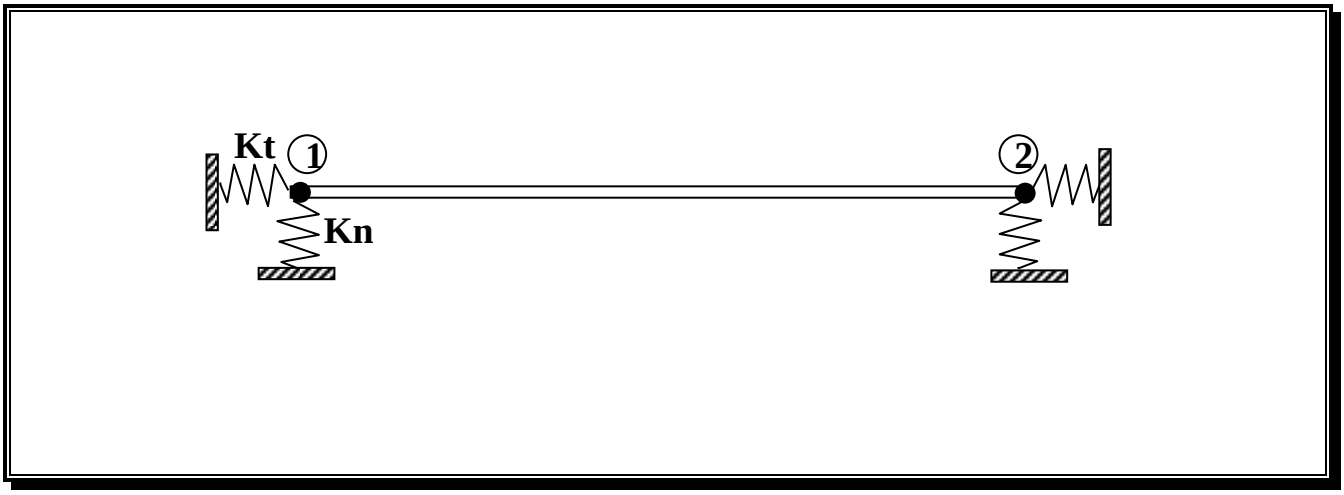

Fig.(9): Beam-Column Element on Elastic Foundation .

1.10 Applications for Testing the Program

Many examples are taken to verify the reliability of the program (NSHEEFF) and to examine the various solution schemes implemented in the program. Wherever possible, the results are compared with experimental, analytical and/or numerical results obtained by other investigators. These examples are

1. **3-Members extended frame.**
2. **Portal frame.**
3. **T-Shaped frame.**
4. **William's Toggle Frame.**
5. **Finite Beam on Elastic Foundation.**
6. **Fixed-Fixed Beam Resting on Elastic Foundation.**
7. **Fixed-Ended Vierendeel Frame.**
8. **Fixed-Ended X-Bracing truss Beam.**
9. **Cantilever Tapered Truss.**

One of these examples is showing below.

1.10.1 Example No. 1: (3-Member Extended Frame)

In 1996, ***Al-Raunduzy*** **[73]** solved this case using beam-column approach. Also, he used several methods for detecting the instability conditions and the extrapolation method was used to help in detecting such conditions. In his work, he detected a typical limit point at a load stage of 84.55 N. Also, he produced a complete load-displacement curve for vertical displacement of point B (see Figure (11)). Because he neglected the post-buckling analysis, the decreasing range in the post-buckling behavior did not appear.

Al-Mutairee in 2000, **[82]** solved this example, using the constant arc-length incrementation strategy with the arc-length iterative strategy.

AL-Khafaji A.Kh.**[84]** , solved the same example in 2002, but resting on elastic foundation with foundation length (**Lf=500 mm**) and soil stiffness (**Kn=50 kN/mm^2**), Figure (10) show this aim .

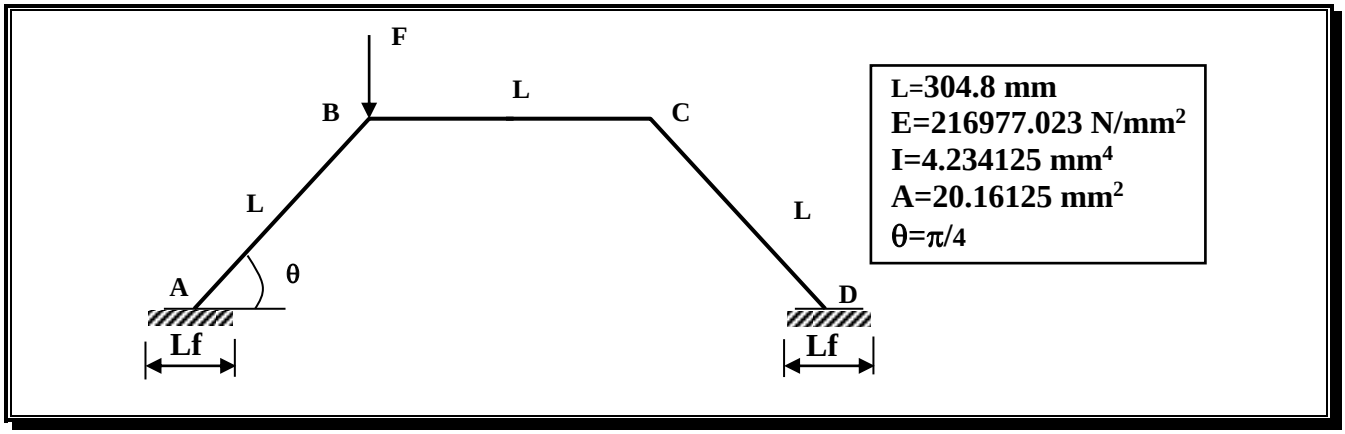

Fig.(10) : Geometry and Loading Conditions for Example No.1 .

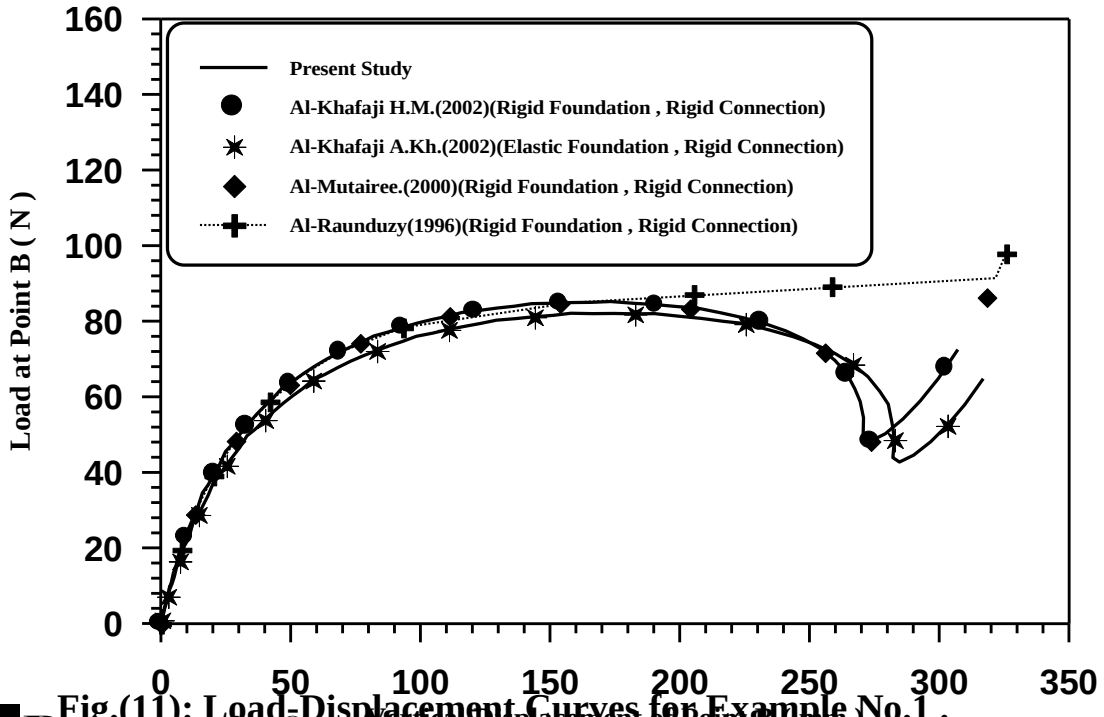

Fig.(11): Load-Displacement Curves for Example No.1 .

1.10 Parametric Studies

A parametric study is performed to assess the influence of several important paramertes on the behavior of elastic plane structures under static loading.

The selected parametric study to be discussed in this thesis can be summarized as follows:

1. Effect of the tapering ratio.

2 Effect of shear on the behavior of frames.

3 Effect of steel flexible connections on the behavior of frames.

4. Effect of subgrade reaction.

5. Effect of large displacement analysis.

Each one of these parameters was studied individually by analyzing a frame or more from the frames considered in this thesis as case studies.

1.11 Case Studies

A description for the six case studies selected to be analyzed in this thesis is presented here.

1.11.1 Case Study No. 1: (William's Toggle Frame)

1.11.2 Case Study No. 2: (Portal Frame with Tapered Members)

1.11.3 Case Study No. 3: (Gable Frame)

1.11.4 Case Study No. 4: (Fixed-Ended Vierendeel Frame)

1.11.5 Case Study No. 5: (Fixed-Ended X-Bracing Truss Beam)

1.11.6 Case Study No. 6: (3-Member Extended Frame)

One of these case studies was showing below.

The William's toggle frame was analyzed with seven values of tapering ratio (**D**) these are (**0.2,0.5,0.7,1,1.2,1.5 and 1.7**) respectively and for both rigid and flexible cases. The frame was analyzed for both rigid and flexible cases using the external-work load incrementation strategy with constant external-work iterative. The number of segments per each member is equal to (**3**). The reference load is (**Fr=1 lb**) and the desired number of iteration is (**Jd=3**).

For the case of William's toggle frame, it was observed that increasing the tapering ratio, [increase the depth of member at ends], leads to increase the stiffness of the frame. At the same time the associated displacement are reduced. The results of the analysis were presented as load-displacement curves in Figures (12), to, (14). Figure (15), show the relation between the critical load and tapering ratio. As shown in this figure, the best tapering ratio (**D**) for the three types of connection (rigid, linear and non-linear flexible connection) is in the range of (**1-1.2**). And the results were shown in Figures (16), (17), and (18), as load displacement curves. From the inspection of these results, the following observations may be drawn:

1. The critical load of a frame decreases with decreasing the stiffness of its connections (decreasing tangent stiffness of non-linear connection).
2. Connection flexibility affects the moment distribution of the frame
3. The approximate linear behavior of flexible connection gives results different from the non-linear (exact) behavior of connection and this effect increase if connection flexibility increases, so the non-linear behavior should be used in the representation of the flexible connection, and the approximate linear moment-rotation can be used at the initial stage of loading.

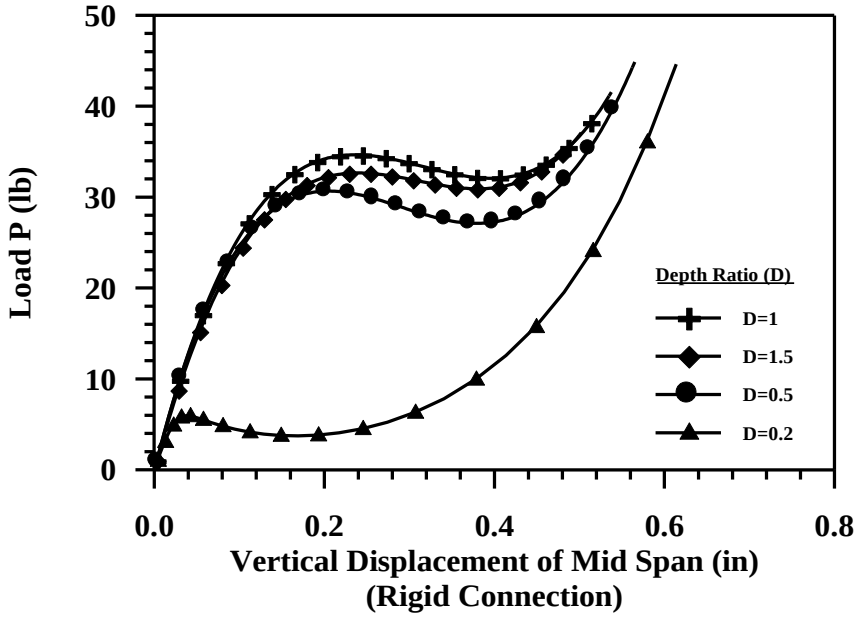

Fig.(12): Load-Displacement Curves for William's frame .

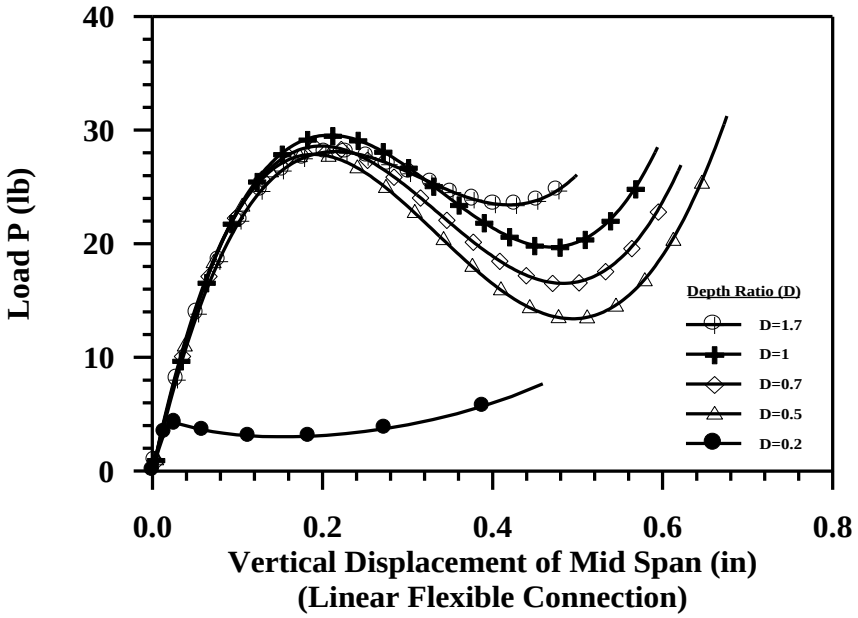

Fig.(13): Load-Displacement Curves for William's frame .

Fig.(14): Load-Displacement Curves for William's frame.

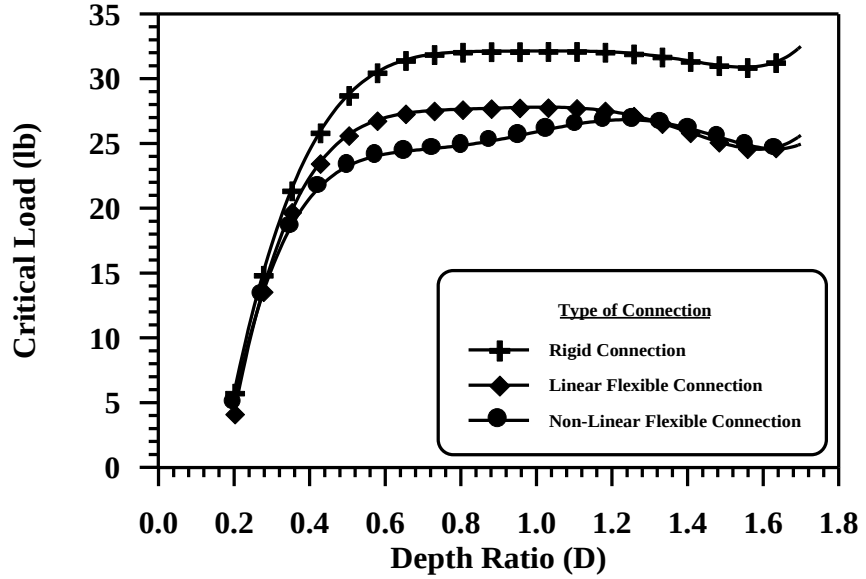

Fig.(15): Critical Load-Depth Ratios Curves for William's frame.

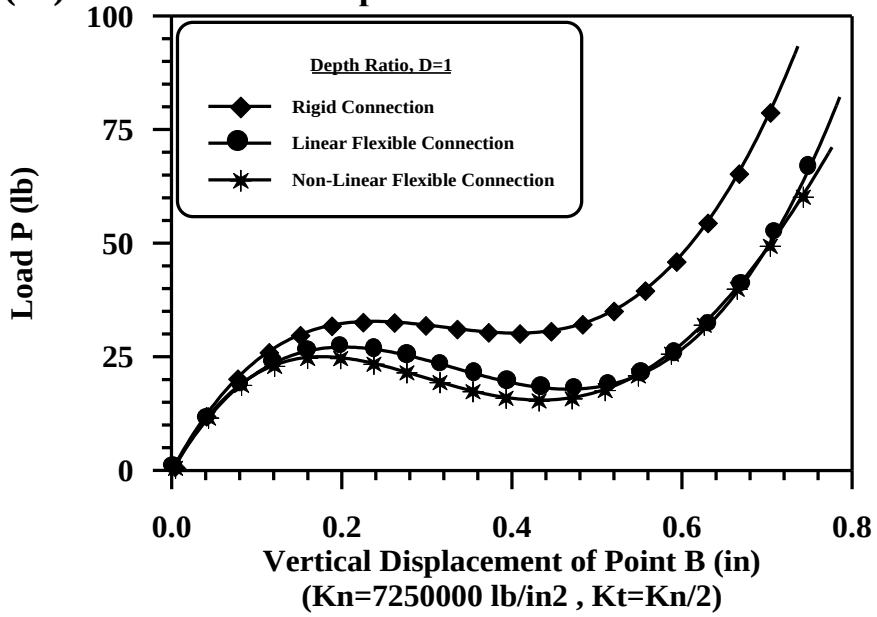

Fig.(16): Load-Displacement for William's frame .

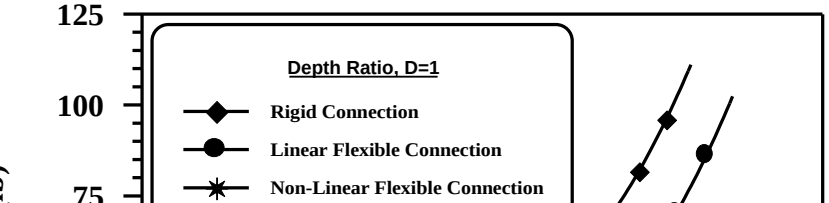

Fig.(17): Load-Displacement curve for William's frame.

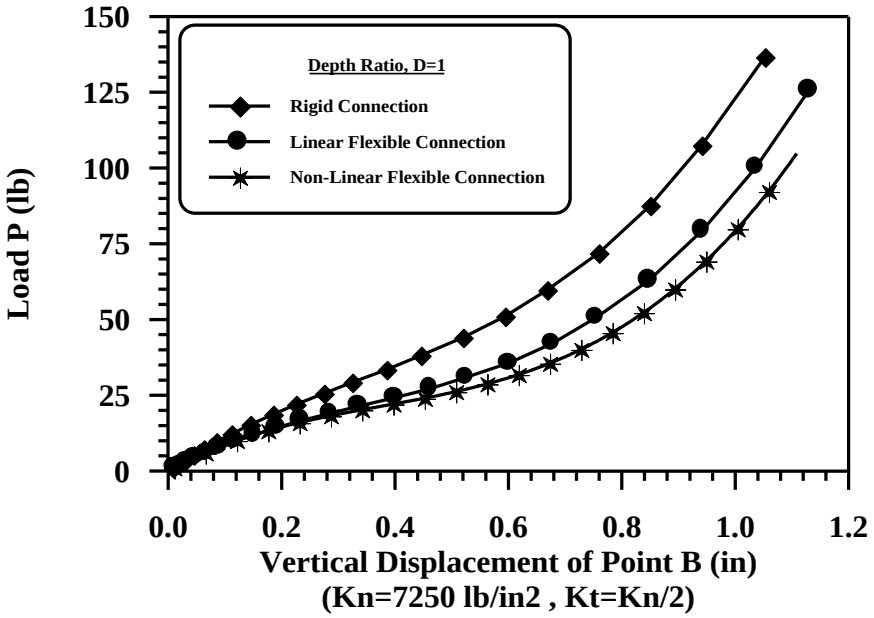

Fig.(18): Load-Displacement curve for William's frame.

7.1 Conclusions

Based on the results obtained in the present study, several conclusions may be drawn. These may be summarized as follows:

1. This investigation shows that the large displacement elastic behavior of plane steel frames with non-prismatic members resting on elastic foundation, subjected to static load including shear effect and having non-linear connections can be accurately predicted using the beam-column approach of analysis.
2. A comparison between the beam-column approach and finite element approach reveals similar results but the latter requires a larger number of elements than the former, a point which is in favor of the beam-column approach despite the fact that the derivations of the tangent stiffness matrix of the beam-column approach is more complicated than that of the finite element approach.
3. Shear effect plays a major role governing the behavior of the open-web structure and deep beams under static loads.
4. The method of equivalent system represents one of the most important and successful techniques, which enable us to replace the actual non-prismatic member with any arbitrary variation in its stiffness ($\mathbf{EI_x}$), with one of uniform stiffness ($\mathbf{EI_1}$). An exact as well as very accurate approximate solutions is obtained that drastically reduces the mathematical complexity of this problem.
5. When the depth ratio increases, the effect of shear deformation will be increased or in the other words the effect of shear deformation on non-prismatic member is greater than that of prismatic member.
6. When the slenderness ratio of structure decreases, the shear parameter increases and consequently the effect of shear on the behavior of that structure will be increased.
7. The effect of shear force will reduce the value of elastic critical load. This reduction in the value of critical load is larger in the cases of open-web structures and smaller or vanished in the cases of solid web structure.
8. The present modified tangent stiffness matrix which takes into account the two types of non-linearities at the same time (i.e. geometry and connection) and non-prismatic members efficient in giving accurate results of analysis of different types frames.
9. In all examples and case studies, the used load incrementation strategies are efficient for enabling the program to estimate the suitable size of load increments.
10. The determinant technique for sign detection used in the present study is found to be efficient for detecting the right sign of initial load increments.
11. The using of any iterative strategy excepts the constant load iterative strategy not only enable the program to pass limit points, but sometimes reduced the required computing time. And the used iterative strategies are efficient for enabling the program to change the load level and rapidly achieve the convergencey.

12. The arc-length incrementation strategies with the constant arc-length and minimum residual displacements iterative strategies represent the most efficient techniques in tracing entire load-displacement curves for different types of steel frames as well as a small CPU time is needed for the analysis.

13. The reference load (**Fr**) can be chosen from (1.3% to 2%) of the load at the first limit point, and desired number of iteration for convergence (**Jd**) can be chosen from (3 to 5), for any type of frames with both rigid and flexible connections.

14. The resistance of the frame to the static buckling load can improved through using tapered member with various tapering ratio for the same volume of steel, and the percentage of increment of this resistance depends on the geometry of frame and loading condition as well as the type of supports and joints.

15. Results of the analysis show that the displacements when the structure resting on linear elastic foundation are greater than those obtained when the structure is fixed - ended, by (20 - 60 %).

7.2 Recommendations

The following recommendations may be considered as an extension for the present study:

1. This subject requires to be supplemented by experimental results to be obtained from tests on a model or full scale plane steel frames under repeated loading having different types of steel connections, supports conditions using proportional and non-proportional cyclic loading.

2. The present work has been concerned mainly with effects of geometrical and connection non-linearities. A promising field for extending the present work is to include the material non-linearity.

3. The modified tangent stiffness matrix presented in this study may be modified to include more effects such as the end rigid gusset plates, the variation in the axial force in the member.

4. The post-buckling analysis may be extended to include more iterative strategies like the constant displacement and the minimum residual force iterative strategies.

5. Developing analysis by deriving the exact modified stability and bowing functions of non-prismatic member under compression and tension forces.

6. Extending the present study to consider dynamic analysis.

7. Developing the present study to consider the analysis of space frames.

Post-Buckling Analysis of Steel Plane Frames on Elastic Foundation With Flexible Connections

A thesis

Submitted to the College of Engineering of the University of Babylon for Fulfillment of the Partial of the Requirements for the Degree of Master of Science in Civil Engineering

By

Jawad Talib Aboudi Al-Nasrawi
(B.Sc.)

November 2002 Ramathan 1423

Supervision

Prof. Dr. Sabeeh Z. Al-Sarraf

Dr. Nameer A. Alwash

CHAPTER ONE

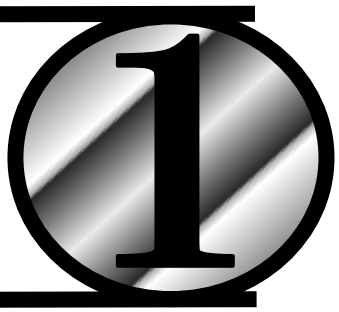

INTRODUCTION

1.1 General

Although the initial behavior of structural systems can very well be described by a linear computational model, all real structures exhibit a pronounced non-linear behavior when the loads and deformations become sufficiently large. However, the entire load-displacement curve of a structure may include both softening and stiffening behavior, the presence of load and displacement limit points and the possible bifurcation of the path. On the other hand, tapered members are used in many structural applications such as highway bridges, buildings, space and aircraft structures, as well as, in many mechanical components and machines. It is used in an effort to achieve a better distribution of strength and weight and sometimes to satisfy architectural and functional requirements. And while the connections constitute a small percentage of the weight of a structure, they have a relatively high labor content and hence represent a substantial percentage of the total framing cost. In addition, connection deformation is sometimes responsible for a substantial proportion of the overall deflection of a structure and often it has a significant bearing on the internal force distribution. Therefore, the non-linear behavior of framed structures having non-rigid connections and non-prismatic members becomes the subject of considerable researches. Towers or masts in such structures could have a solid cross-section or a lattice, batten and open-web ones, where the effect of shear deformation is rather dominant. Therefore, the study of the shear effect on stability and bowing functions takes a major role accordingly. So many considerable researches have considered the shear effect into the non-linear behavior and the large deformation analysis of the structures. As a brief explanation for the subject, some major definitions must be setted in order to understand the issue.

1.2 Non-Linear Behavior of Structures

Various behaviors are called "Non-Linear". Stress-strain relations may be non-linear in either a time-dependent or a time-independent way. Displacement may cause loads to alter their distribution or magnitude. Mating parts may stick or slip, gaps may open or close. Nonlinearity may be mild or severe .The problem may be static or dynamic. Many solutions have been proposed and it is no surprise that no one is the best for all problems.

In recent years, the non-linear behavior of framed structures has attracted a great deal of attention from designers and researchers. In a flexibly jointed structure there are three types of non-linearity; geometrical, connectional and material non-linearities of the steel framed structures. In the present study the last two types are taken with tapered members including shear effect and resting on elastic foundation.

1.2.1 Geometrical Non-linearity

The effects of geometrical non-linearity may be separated into three categories.

1.2.1.1 Stability Effect [Stability Non-Linearity]

The non-linearity in this type is mainly due to the coupling effect of axial force and flexural moment. The problem then may be solved by introducing stability functions which are dependent on the axial force parameter only ($\mathbf{q=Q/Q_{Euler}}$) **[3]**. So the well known slope-deflection equations for linear analysis are no longer valid since the axial load parameter is greater or smaller than zero which leads to the stiffness factor ($\mathbf{C_1}$) which is not to be equal to (**4**) and the stiffness carry over factor ($\mathbf{C_2}$) which is not to be equal to (**2**).Then, the member end moments ($\mathbf{M_1}$)and ($\mathbf{M_2}$)for the prismatic member shown in Figure (1.1) are expressed in terms of member end rotations (θ_1)and (θ_2)as follows:

$$\mathbf{M_1 = \frac{EI}{L}(C_1\,\theta_1 + C_2\,\theta_2)} \quad \text{..... (1.1)}$$

$$\mathbf{M_2 = \frac{EI}{L}(C_2\,\theta_1 + C_1\,\theta_2)} \quad \text{..... (1.2)}$$

in which;

$\mathbf{C_1}$ and $\mathbf{C_2}$: Conventional elastic stability functions, where,

C_1 : Flexural stiffness factor,

C_2 : Flexural moment carry-over factor,

E : Modulus of elasticity,

I : Moment of inertia, and

L : Member initial (undeformed) length.

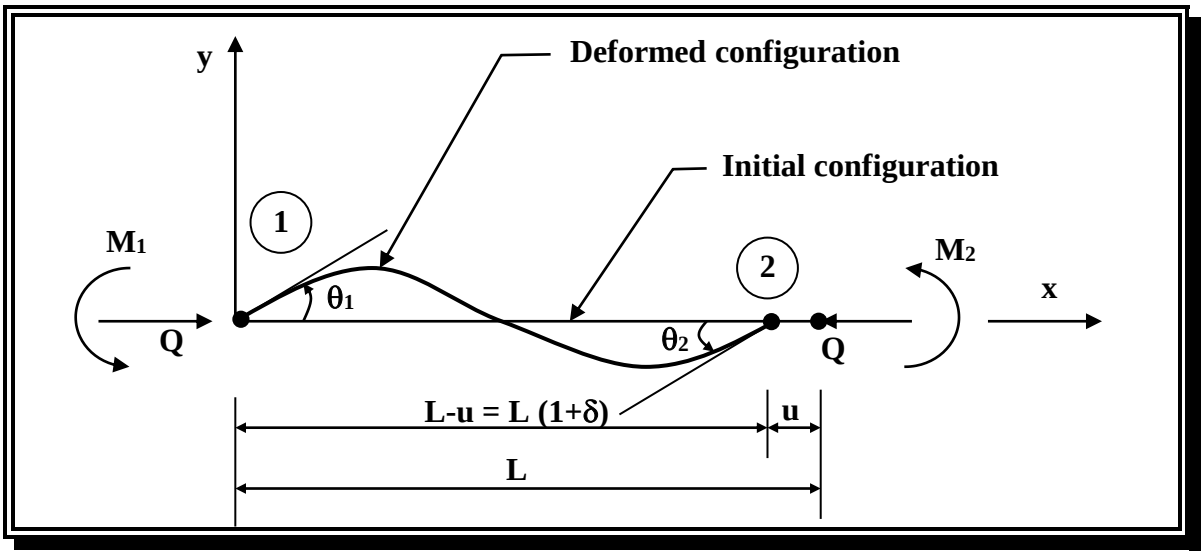

Fig.(1.1): Relative Member Deformations-End Forces .

1.2.1.2 Bowing Effect [Change in the Member Length Due to Bowing]:

This type of non-linearity is also caused by the interaction between bending and axial forces in the members. In a like manner, the presence of bending moments affects the axial stiffness of the member due to an apparent shortening of the member by the bending deformation. The problem then may be solved by introducing bowing functions, which are dependent on the axial force parameter (**q**). Then, the axial force **Q** is expressed in terms of relative axial displacement (**u)** as follows:

$$Q = \frac{E\,A}{L}(u - C_b.L) \quad \text{..... (1.3)}$$

and

$$C_b = b_1(\theta_1 + \theta_2)^2 + b_2(\theta_1 - \theta_2)^2 \quad \text{..... (1.4)}$$

in which;

A : Cross-sectional area,

$\mathbf{C_b}$: Length correction factor due to bowing action,

$\mathbf{b_1}$ and $\mathbf{b_2}$: Bowing functions.

However, all the previous equations are for prismatic member and to deal with non-prismatic member, some modification must be applied as discussed later in **Chapter Three**.

In linear elastic analysis of structures, the deformations are assumed to be small so that the interaction between bending and axial forces can be ignored and the equilibrium equations between the externally applied loads and the internal member end forces are formulated on the basis of the original (undeformed) configuration of structures. So, for linear analysis the axial force parameter **q** and bowing factors are ignored, so the stability functions become

$\mathbf{C_1=4}$ **and** $\mathbf{C_2=2}$ ..... (1.5)

1.2.1.3 Large Displacement Effect

In which the non-linearity occurs when the deformation becomes large enough to cause significant changes in the geometry of the structure, so that the equilibrium equations must be formulated for the updated deformed configuration.

There are several effects of non-linearity such as the initial axial, shear, flexural and any other effect that cause initial tensile, compressive, shear and flexure stresses in the members.

These effects can be treated as **Fixed Ended Action** (**F.E.A**) or as initial geometry. Geometrical non-linearity problems are sometimes referred to as large displacement problems, but actually whenever the first axial effect is taken into account the structure undergoes a so called non-linear small deflection analysis, the actual large displacements must include all the effects mentioned above or at least the first two ones where the effect of change in geometry pushed the solution hardly towards the **Elastica.** Such problems do not necessarily differ from the small displacement or linear ones, not because large displacement latterly occurs, but rather because axial forces exist which in the presence of lateral displacement exert a significant influnce on and play a dominant role in the stiffness of the member. Thus the difference between the large displacement analysis and small the deformation analysis comes from including higher order terms in the large displacement analysis. Figure (1.2) shows the deflected shape of a beam-column element. It may be seen that the curvature can be expressed as:

$$\phi = \frac{1}{R} = \frac{-\frac{d^2w}{dx^2}}{\left[1+\left(\frac{dw}{dx}\right)^2\right]^{1.5}} \quad \text{..... (1.6)}$$

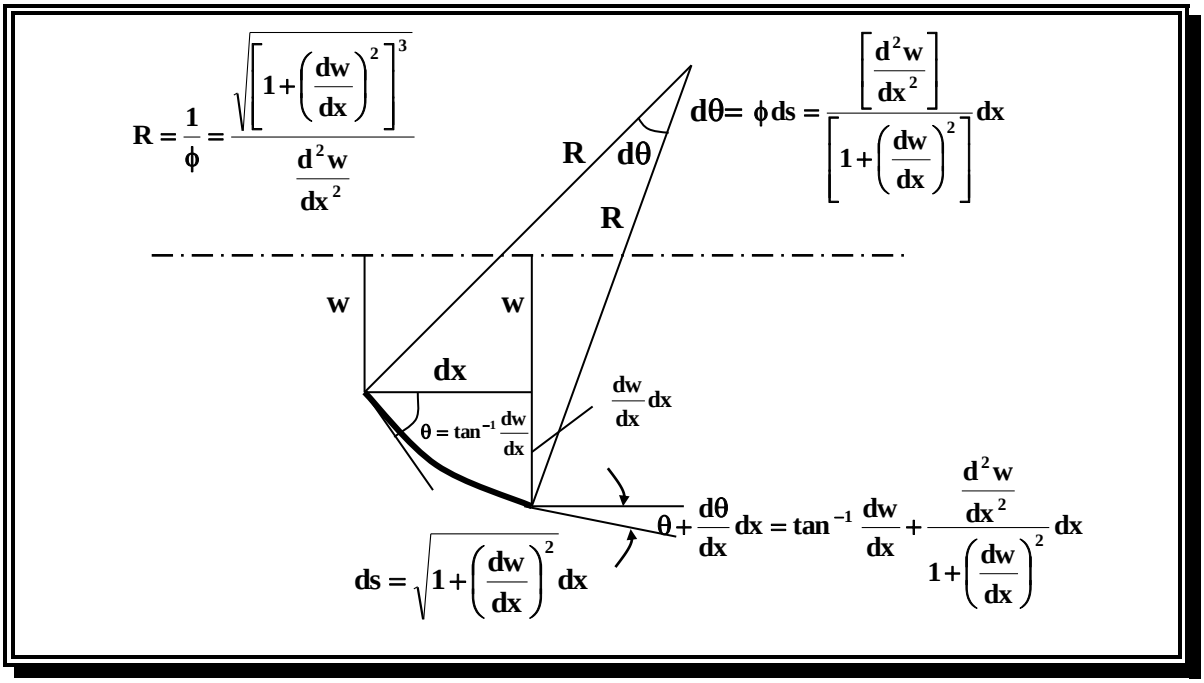

Fig.(1.2): Curvature and Deflection of Beam-Column Element .

In the small deformation theory, the term (**dw/dx**) will have small values, therefore, the square of the term will be very small compared with one and then the term (**dw/dx**) is neglected. In large deformations, the term (**dw/dx**) will have a considered effect on the curvature value and it cannot be neglected. If the term (**dw/dx**) in Equation (1.6) is considered in the analysis, the analysis becomes so complicated that it can be solved only by using the elliptical integrals. Hence, this method is inapplicable in structures.

The complicated large displacement problem is then solved by considering small relative deformations in the member with a large joint displacement. So, the small deformation theory is still applicable to the relative large member deformations and the problem produced by assuming large joint displacements may then be solved by satisfying the equilibrium condition in the last (updated) configuration of structure.

The direct stiffness method, which is usually used in the structural analysis, is then used in the analysis. The use of matrix methods in the analysis, especially the direct stiffness method, makes it easy for the

problem to be programmed and the use of the computer programs for the analysis of framed structures becomes possible.

In comparison with linear problems, for which the terms constituting the stiffness matrix of the structure are linear and constants, the stiffness for geometrically non-linear problems contains terms that are non-linear functions of the deformations of the structure and member axial forces.

The change in the stiffness of the framed structure happens in two ways, hardening and softening. In the hardening, the stiffness of the structure will increase by load increasing. Most of the structures have softening properties, which are a reduction in the stiffness of the structure with increasing load.

Softening may cause a zero stiffness condition i.e., a condition at which a small load increment may cause a large displacement. The load condition at which this zero stiffness occurs is called the elastic critical load. There are many methods for determining the critical load, some of these methods will be discussed in this study.

1.2.2 Connection Non-linearity

Connection non-linearity results due to the use of semi-rigid beam-to -column joints in unbraced steel frames. Since the relationship between the moment in the connection and rotation (slip angle) is non-linear, it shows that the stiffness matrix will contain the rotations and stiffnesses of connections that are not known in advance, and therefore requires an iteration technique to be used.

The assumption of rigid joint implies that the full displacement and slope continuities exist between adjoining members and that full (or a substantial percentage) of bending moment is transferred from beam to column. On the other hand the assumption of ideally pinned connection implies that the beams will behave as if they were simply supported and that the columns will carry no bending moments from the beams. Although the assumptions of fully rigid or ideally pinned connection behavior drastically simplify the analysis and design procedure, the validity of these assumptions may be questionable in some cases in which connection rigidities are intermediate between the fully rigid and pinned cases.

Depending on the degree of restraint offered by steel connections, the AISC specification **[62]** recommend three different types of steel framing:

1. Type (1) construction-rigid framing-assumes rigid beam-to column connections.

2. Type (2) Construction-simple framing- assumes that beam-to-column connections are free to rotate under gravity loads.
3. Type (3) Construction-semi-rigid framing-calls for elastic frame analysis accounting for behavior of semi-rigid beam-to-column connections.

However, the load and resistance factor design specification (LRFD) classifies only two types of steel frames **[52]**:

1. Type FR-full restrained construction-assumes that beam-to-column connections have sufficient rigidity to hold the original angles between intersecting elements virtually unchanged.
2. Type PR-partially restrained construction-assumes that beam-to-column connections possess an insufficient rigidity to keep the original angle between intersecting members unchanged.

Thus, it can be noticed that types FR and PR of LRFD specification are analogous to types 1 and 3 of the AISC specification respectively. The LRFD specification permits to consider type 2 as a special case of type PR.

The analysis and the design of types FR and PR frames are different for a simple reason that the effect of connection flexibility in type PR frames must be taken into account. Since connection is a highly indeterminate element, rigorous analysis study of its behavior is quite formidable task. However, because of the absence of reliable analytical methods for predicting accurately the connection behavior and since there is still a lack of semi-rigid frame analysis approach suitable for office practice, type3 construction is rarely considered in analysis.

1.3 Post – Buckling Behavior of Structures

For most practical problems, it is quite unnecessary to trace such a convoluted load-displacement path as that shown in Figure (1.3). Indeed, where such a path is to be traced, most analyses would trace the static path ABCDEFGHIJ and thus infer the dynamic snaps. Although the analyses are therefore somewhat artificial, they may be very important.

For some problems, all that may appear to be required is the load level at the first limit point. However, without analysis techniques that allow the limit points to be passed, even this information may be unavailable or unreliable. Collapse loads are often associated with a failure to achieve convergence with the iterative solution procedure. However, it may be only the iterative solution that has collapsed (possibly as a consequence of round-off error). In such situation, the analyst is left with no information on the nature of the failure and may not even be sure that he has a structural rather than numerical collapse. In some situation, it may be important to obtain information on the nature of the load shedding,

following the limit points, in order to assess the performance of the complete structure. Consequently, computer programs should be provided with solution procedures that will handle such non-linear behavior and snapping phenomena.

The present work (as will be explained in Chapter Four), involves the use of different techniques that handle such analysis without difficulty even when the structure exhibits stiffening or softening, limit or bifurcation point. Finally, it is worth to know that the term "Post- Bucking Behavior" means the behavior of structures after the first load limit point even when the geometry of structure is changed.

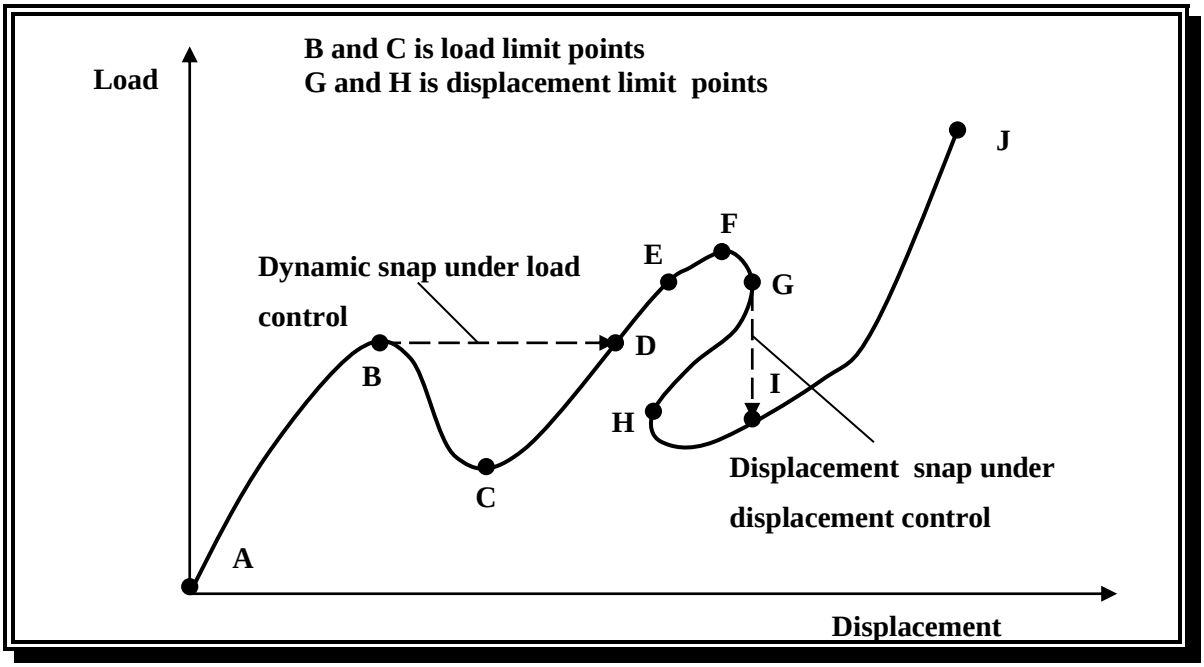

Fig.(1.3): Complex Load-Displacement Curve [85].

1.4 Objective of The Present Study

The objective of this study is to make the theoretical basis for the large displacement and post-buckling analysis of non-prismatic plane steel frames with semi-rigid connections, resting on elastic foundation and subjected to static loads including shear effect.

The present study is introduced in seven chapters. Chapter One presents the problem and the aim of the study. In Chapter Two, a brief review of early studies and the more advanced studies on the subject is given with an interpretation of results as possible.

Chapter Three establishes the derivation of the conventional tangent stiffness matrix for non-prismatic members in local and global coordinates and derivation of the modified tangent stuffiness matrix in global coordinates including shear effect which takes into account the two types of non-linearity at the same time. In addition, the iterative technique to be

used for calculating the slip angle of the flexible connection is presented. Also, it introduces the special technique used for accounting the axial force when the flexural bowing in the member is included.

Chapter Four presents a description of the different numerical techniques used in solving the non-linear simultaneous equations. Also, the post-buckling behavior and types of instability points of plane steel frame are presented. Furthermore, this chapter introduces numerical algorithms for post-bucking analysis with different strategies for initial load incrementation and iterative process. Finally, a brief description of the types of the convergence criteria used in the iterative analyses has been presented.

In Chapter Five, the multi-purpose computer program (NSHEEFF) which has been coded in the present study in Quick Basic 4.5 language had been described. In addition, computer applications for testing the validity of the program (NSHEEFF), have been made and the results were compared with case studies reported by other researchers.

In Chapter Six, pre-and post-bucking analyses of prismatic and non-prismatic plane steel frames with rigid and flexible connections, resting on elastic foundation and subjected to static loads including shear effect are presented and discussed as six parametric studies.

Finally, Chapter Seven gives several conclusions and recommendations for further studies on this subject.

CHAPTER TWO

REVIEW OF LITERATURE

2.1 General

This review covers five aspects. The first one is the developments in the elastic stability and large displacement analysis of plane steel structures. The second is the developments in the analysis of frames and beam-like lattice structures including shear effects. The third is the developments in the analysis of frames with flexible connections. The fourth is the developments in the analysis of frames resting on elastic foundation .The fifth is the developments in the post- buckling analysis.

2.2 Basic Theory Literature

Considerable amount of literature on the elastic analysis of steel framed structures has been undertaken and many researches, papers and books have been published to determine the real behavior of the structures by establishing the load-deflection response.

In 1956, ***Livesely*** and ***Chandler*** **[3]** developed a computer program for analyzing plane frames comprised of prismatic linear elastic members and subjected to in-plane loads applied only at the joints. They neglected the effect of flexural bowing and chord rotation and assumed no change occurs in geometry.

In 1963, ***Saafan*** **[7]** presented a non-linear formulation for in-plane frames. He took into account the effects of instability caused by axial force, bowing of deformed members and finite deflections. He developed a computer program for analyzing elastic plane frames subjected to in-plane forces. The effect of rigid gusset plates was included in the program. His solution procedure involves iterations on the displacement. The

conventional Newton-Raphson method with one load step has been used in his iteration procedure.

In 1973, ***Oran*** **[13]** derived a tangent stiffness matrix for linear elastic in-plane prismatic member according to the conventional beam-column theory. In his derivation, he included besides the effect of the axial force on the stiffness of the member, the effect of flexural bowing of deformed member and made no restrictions on the displacements of frame. Although large joint displacements were assumed, relative member deformations were assumed to be small enough to justify the using of the beam-column theory. He assumed also that the loads are applied at joints only.

In 1974, ***Oran*** **[15]** used the same principles presented above for the derivation of the tangent stiffness matrix for in-plane and in-space non-prismatic members.

In 1974, ***James, et. al*** **[16]** derived a general curvature expression for arbitrary rotations for a beam element. Then, they derived a beam element stiffness matrix and by using the finite element method, they solved a number of problems and compared it with others. They used an incremental-iterative procedure in their solution using the conventional Newton-Raphson method as an iterative technique. They concluded that the derived general curvature expression gives displacement responses, which are approximately the same as those obtained by other researchers.

In 1976, ***Oran*** and ***Kassimali*** **[21]** suggested a method for the analysis of large deformations and stability of elastic framed structures using the general beam-column type method, which was developed by ***Oran*** **[13]**. They used two techniques in solving the non-linear problem. The first one consists of applying the loads in small increments, then determining the corresponding changes in the configuration of the structure from a sequence of linearized analyses. According to the authors, this technique does not involve iteration, but requires that the tangent stiffness matrix be updated at each load level. The second technique is an iterative one in which for any desired load level, an approximate solution is first assumed or calculated. It is then improved step-by-step using a Newton-Raphson type of iteration until the joint equilibrium equations are satisfied within a prescribed tolerance. They used two coordinate systems, Lagrangian and Eulerion (updated Lagrangian). The first one deals with the initial undeformed configuration while the other coordinate system deals with the last configuration of the system. They found the possibility of reducing the required computational work for plane frames could be achieved by introducing some approximations such as:

1. Using Lagrangian coordinates.

2. Neglecting the bowing effect then the tangent stiffness matrix would be a function of axial force parameters only.
3. Using undeformed member length in writing member equilibrium equations.

They applied their work to many case studies and found that their results – compared with others-were the closest to the exact solutions.

In 1977, ***Wood and Zienkiewicz*** **[25]** Presented a continuum approach for the geometrically non-linear analysis of beams, frames and arches in a total Largrangian coordinate system by using the finite element method. They solved their non-linear equilibrium equations by Newton-Raphson method for which a number of examples were solved.

In 1979, ***Al-Sarraf*** **[30]** produced modified stability functions for uniformly tapered beam-columns having wide flange, box section and other cross-sectional shapes. This modification made possible the rapid prediction of the elastic critical load of structures with non-prismatic members by using a hand computing method. Also, he produced an approximate formula for the modified stability functions. Two examples were solved by using the exact and approximate modified stability functions.

In 1983, ***Wen*** and ***Rahimzadeh*** **[41]** studied the non-linear elastic plane and space frame analysis by using finite element method. Large deformations and changes in geometry were considered in their study. Numerical examples were checked and the comparison with other methods indicates that their method is competitive.

In 1983, ***Kassimali*** **[42]** presented a numerical procedure for large deformation analysis of elastic-plastic frames. The procedure was based on the Eulerion formulation, which was developed initially for elastic systems and then extended to include the elastic-plastic effects.

Local member force-deformation relationships were based on the beam-column approach and changes in chord lengths due to axial strains and flexural bowing were taken into account. His extended study gave excellent results with previous methods for treating both the geometrical and material non-linearity at the same time.

In 1987, ***Chajes*** and ***Churchill*** **[53]** presented the basic concepts involved in the construction of the solving the non-linear problem. These are the linear incremental method, the non-linear incremental method and the direct method. They derived the governing equation for each method and the procedure used to plot the load-deflection curve. In both the linear and non-linear incremental methods, the load is applied as a series of small steps. They concluded that the linear incremental method requires the use

of smaller load increments than those necessitated by the non-linear incremental method, because the latter is an iterative method. In the direct method, which is an iterative method, they applied the entire load as a single step.

In 1996, ***Al-Raunduzy*** **[73]** presented a theoretical analysis for estimating the plane large displacement elastic stability behavior of steel frames subjected to either proportional or non-proportional increasing static or dynamic loads applied at joints only by using beam-column approach. The formulation of the beam-column element was based on Eulerian approach allowing for the interaction between the bending moment and the axial force stiffness. The Changes into member chord length due to axial strain and flexural bowing were taken into account. The load-deflection responses of frames were obtained by using an incremental load control Newton-Raphson iterative technique. Several methods for detecting the instability condition of the frames were presented and extrapolation method was used to hold in detaching such a condition.

2.3 Shear Deformation of Lattice, Batten and Laced Elements

In general, the researches and studies have raised a significant interest in this field since the great efforts of ***Timoshenko*** and ***Gere*** **[4].**

In 1973, ***J.D Renton*** **[14]** studied the buckling in long, regular pin-jointed trusses due to the axial force using finite deference method. Small deflection theory was used. Exact solution was found, and approximate formula was derived which may compare with the critical loads for analogous columns buckling due to bending and shear. He concluded that results taken from his formula are identical to those from ***Timoshenko*** and ***Gere***.

In 1974, ***A.K. Noor*** **[18]** presented a mixed between force and displacement methods to analyzed the geometric and material non-linear pin-jointed three dimension trusses. The proposed method was examined by using a computer. For convenience, the constitutive relations were assumed to in the form of ***Ramberg-Osgood*** polynomials and the individual members of the truss were assumed to remain straight and stable under loading, i.e. no change in length (axial and bowing effects) was taken into account. So, he adopts the beam theory rather than the beam-column theory. He examined two-bar truss, two bay plane truss, and transmission tower case studies to check his method.

In 1982, ***Svensson*** and ***Kragerup*** **[40]** investigated the imperfection sensitivity of laced columns, this imperfection consisting of both a laced and an overall geometric imperfection. They presented a simple numerical

method for solving both elastic and elastic-plastic problem and the collapse load was finally predicted.

In 1983, ***Gelu Onu*** **[43]** studied the shear effect in beam stiffness matrix. He adopted the beam theory using the energy method and so he formalized the stiffness, the geometric stiffness, and the consistent mass matrix for the four degrees of freedom beam element including shear effect by coupling the transverse displacement field and the shear angular displacement field.

In 1986, ***S.Z. Al-Sarraf*** **[51]** studied the shear effect on the elastic stability of frames; Modified small deflection stability functions for prismatic beam-column having any solid cross-sectional shapes, laced or battened built-up sections were developed in terms of shear flexibility and axial load parameter which make possible the rapid prediction of the elastic critical load of structures taking into consideration the effect of the shear force in the members by using a hand computing method. The modified stability functions were related to existing tabulated stability functions of ***Livesley*** and ***Chandler***. The approximate formula predicts the accurate elastic critical load to within 1%.

In 1991,***R.R.A.Issa*** and ***M.L.Chow*** **[68]**, used the techniques of discrete field analysis to investigate the critical buckling loads for various two dimensions X-braced truss configurations and geometry. An explicit formula was developed for determining loads having a form of independent of the number of panels. The study indicates that the modified ***Eular*** critical load may vary up to **(**85 %**)** of loads obtained by discrete field analysis.

In 1992, ***V.Paramasiran, et. al*** **[70]**, published a technique note on the ***Timoshenko*** beam finite element with four D.O.F. and convergence of $\mathbf{O(h^4)}$. They stated that when transverse shear deformations and rotary inertia in beams are important, elements based on the ***Timoshenko*** beam theory are useful, and they are completely free of locking and perform equally and efficiently in thick as well as in thin beam range.

In 1995, ***N.A.H.Alwash*** **[72]**, studied the non-linear behavior of reinforced concrete vierendeel trusses subjected to concentrated loads as well as distributed loads. In his work he included the effect of shear deformation using the bending slope approach and derived the stability functions for this approach in such structures. He neglected the bowing effect, and the change in geometry of the chord, but took the effect of axial force in the geometrical non-linear stiffness matrix. So, his work is closer to the approximate theory (small deflection theory) rather than the exact large deflection one.

In 1997, ***Kh.Sideek*** **[74]**, presented a theoretical analysis for predicting a large displacement elastic stability behavior including shear effect for both ordinary space frames and cable-frame interactions subjected to concentrate or distributed static loads. He used the beam-

column theory in his analysis. The shear effect on stability analysis was adopted for both bending and total slope approaches. He proposed new bowing functions due to twisting action and derived these functions.

In 1998, ***Al-Bidairy*** **[76]** presented a theoretical analysis of the plane large displacement elastic stability of steel beam-like lattice frames including shear and damping effects. He made a comparison between the different non-linear incremental methods to decide which of each method is the best and the more efficient. He concluded that the conventional Newton-Raphson method with incremental load represent the most efficient and most rapid technique. Also, he found that the modified Newton-Raphson method needs more load increment and more numbers of elements to reach the correct solution.

2.4 Analysis of Frames with Flexible Connection

Although many research works have been conducted on the force-deformation behavior of steel framing connections, only a few attempts have been made to incorporate the connection deformations into structural analysis of the frame.

According to ***Monforton*** and ***Wu*** **[6]** in 1963, ***Rathbun*** **[1]** in 1936, developed modification to slope-deflection equations to account for the deformation of linearly elastic connections (analogous to rotational springs) at the ends of the beam. They also presented modifications to the stiffness and carry over factors and the fixed-end moments to permit frames with elastic connections to be analyzed by the moment distribution method.

In 1970, ***Romstad*** and ***Subramanian*** **[10]** presented a modified conventional technique for the elastic stability analysis of frames to incorporate the effect of flexible connection, and they adopted the basic assumption that the member end-connections behave as either pinned or completely rigid, and analytical methods developed to incorporate this behavior were cumbersome for even moderately large frames.

In 1974, ***Lightfoot*** and ***Messurier*** **[17]** incorporated linearly elastic connection into the direct stiffness method.

In 1975, ***Frye*** and ***Morris*** **[20]** presented an iterative analysis procedure for planar linear, rectangular steel frames incorporating the non-linear elastic behavior of seven beam-to-column connection types. The analysis procedure involved repeated cycles of linear analysis, to determine a set of connection secant stiffness, Ks, which could be used to predict the displacement and internal forces in real structure. As illustrated in Figure (2.1), the final secant stiffness at a given connection would produce a

moment, $\mathbf{M_f}$, and a rotation, ϕ_f, corresponding to a point on the non-linear moment-rotation curve.

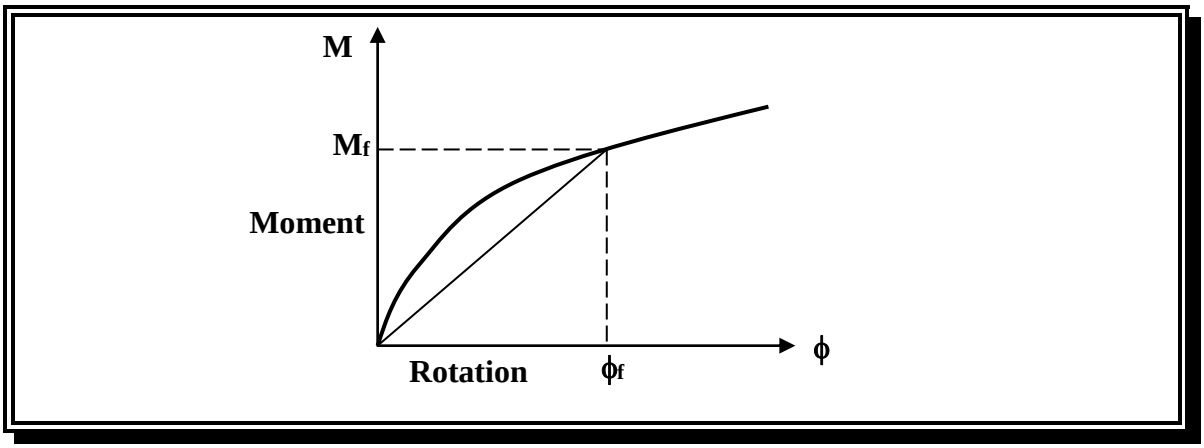

Fig.(2.1): Connection Moment-Rotation Curve and Secant Stiffness .

In 1981, ***Moncarz*** and ***Gerstle*** **[33]** presented an iterative non-linear elastic analysis procedure by modifying the conventional linear elastic stiffness matrix to take into account the presence of non-linear elastic connection by using two rotational springs at the ends of beam-column element and then determining the modified stiffness matrix after applying the static condensation technique to eliminate the additional two rotational D.O.F. and determining the modified fixed end force vector.

They trilinearized the M-ϕ curve for the connection and then corporated the M-ϕ curve in a cyclic loading analysis to determine the effect of repeated loading on lateral displacements (drifts) of the frames under service loading conditions. They found that the effect of proportional loading on the non-linear structures, results in an overestimate of the way (drift) over that due to a more realistic loading history (non proportional loading), and also they found that the assumption of linear elastic response of flexible connection seems reasonable and appears to give a good prediction for the actual frame response under working load.

In 1984, ***Ang*** and ***Morris*** **[44]** generalized the Frye and Morris procedure to permit the analysis of three-dimensional rectangular frames with non-linear flexible connections. They considered only one non-linear connection force-displacement relationship, the M-ϕ one, which they modeled using Ramberg-Osgood function. They analyzed an 11- story unbraced frame, first modeling the non-linear behavior of the top and set angle beam-to-column connection and then assuming the connection to be rigid.

In 1986, ***Yu*** and ***Shanmugam*** **[47]** derived a modified stiffness matrix which takes into account the effect of partial rigidity of the joints (in

terms of fixity factor), effect of flexural on axial stiffness and geometric changes effect.

They used the modified stiffness matrix in an elastic stability analysis of braced and unbraced steel frames with semi-rigid joints. They found that buckling capacity of frames could significantly be increased even for a marginal increase in the degree of fixity of joints, and they found that bracing semi-rigid frames improves their resistance to buckling.

The monotonic load-deflection response of frames with flexible connection was traced by using an incremental load control Newton-Raphson iterative technique.

They derived three local tangent stiffness matrices for simulating presence of plastic hinges, these tangent stiffness matrices were taken into account incremental changes in plastic moment capacity. They analyzed a four-story frame up to collapse using an end-plate steel connection and then using rigid connection assumption. They found that the frame with flexible connection drifted more than the frame with rigid connection.

In 1987, ***George E. Blandford*** **[57]**, studied the elastic response of plane frames including non-linear semi-rigid connection behavior, post-bucking strength of thin-walled steel members and first-order geometric non-linearity. Semi-rigid connection behavior was modeled by using an exponential approximation of the connection flexibility-moment relationship.

In 1989, ***Shi*** and ***Atluri*** **[63]** presented the procedure for non-linear analysis of space frames with non-linear flexible joints and subjected to static and dynamic loads. A complementary energy approach based on a weak form of the compatibility condition as a whole of a frame member, and of the joint equilibrium conditions for the frame, was found to be the best suited for the analysis of flexibly jointed frames. In the presented case an explicitly expression for the tangent stiffness matrix is given when:

1. Each frame member, along with the flexible connections at its ends, was represented by a single finite element,
2. Each member can undergo arbitrarily large rigid rotations and only moderate relative rotations, and
3. The non-linear bending-stretching coupling is accounted for each member. Semi-rigid connection behavior is modeled using Ramberg-Osgood function. Several examples, with both quasi-static and dynamic loading are included to illustrate the accuracy and efficiency of the developed methodology.

In 1994, ***Al-Sadder*** **[71]** presented a theoretical analysis for estimating the in-plane large displacement elastic-plastic stability behavior of steel frames having non-linear steel connections. Yielding is considered to be concentrated at a member ends, and changes in member chord length due to axial stain and flexural bowing are taking into account. The moment-

rotation behavior of steel connection is considered to be non-linear. The standardized Ramberg-Osgood function is used to model the non-linear behavior of connection.

In 2002, ***Al-Khafaji H.M.*****[85]** , presented a theoretical analysis for predicting the pre- and post-buckling behavior of plane steel frame with non-prismatic members,non-linear flexible steel connections and subjected to proportional and non-proportional increasing static loads applied at joints only. He assumed that there was no-restrictions on the displacement values (large displacement analysis).

2.4.1 Mathematical Modeling of Non-Linear Moment–Rotation Behavior of Beam – to – Column Steel Connection

Two different approaches were used in the past to model the moment-rotation behavior of beam-to-column connection.

The first type of these was carried out in conjunction with an experimental investigation of a particular connection type. Both elastic and plastic analyses of a typical connection were conducted. According to the incorporating phenomena observed in experiment, one or more expressions (which involve factors specific to the connection tested) were derived as approximate representations of the moment-rotation behavior.

Several of these mathematical models have been shown in Table (2.1) **[54]**. It can be seen from this table that the majority of them are bilinear, or nearly so, and thus are incapable to follow the experimental moment-rotation curves closely. Several of them would be somewhat cumbersome to use.

The second approach to M-ϕ modeling is a more general one that can be applied to any connection for which appropriate experimental M-ϕ data are available. According to this approach, the geometric parameters that most strongly affect on the moment-rotation behavior of a particular connection type is to be first identified, then comparative experimental M-ϕ data are to be used to isolate the effect of each parameter in turn. Thereafter, a conventional form of non-linear mathematical function is to be selected to model the M-ϕ behavior and a regression analysis can then be performed to fit the function to the available experimental data.

According to ***Morris*** and ***Packer*** in 1987 **[54]**, ***Somner*** in 1969 **[9]** was the first who apply such a procedure based on his own tests on a series of header plate connections. He assumed a standardized moment-rotation equation of the form:

$$\phi = C_1 (KM) + C_2 (KM)^3 + C_3 (KM)^5 \quad \text{..... (2.1)}$$

where;

C_i : Dimensionless constant evaluated from a regression analysis (according to ***Somner*** $C_1=5.1 \times 10^{-5}$, $C_2=6.2 \times 10^{-10}$, $C_3=2.4 \times 10^{-3}$),

K : Standardization factor which scales the ordinates on the M-ϕ curve and is a function of the significant geometric parameters such as plate thickness, depth, bolt diameter, etc.

In 1975, ***Frye*** and ***Morris*** **[20]** proposed a polynomial model (following ***Somner's*** method) in which a polynomial (see Figure (2.2)) was used to represent the connection M-ϕ behavior of seven different connection types. The standardization procedure involves the representation of the moment-rotation curves for all the seven connection types by a single function of the form

$$\phi = \sum_{i=1}^{\infty} C_i (K M)^i \quad \text{..... (2.2)}$$

where

C_i **and K** are as defined by Equation (2.1).

However, there is a major drawback in this model since the nature of a polynomial is to peak and trough within a certain range, the stiffness of

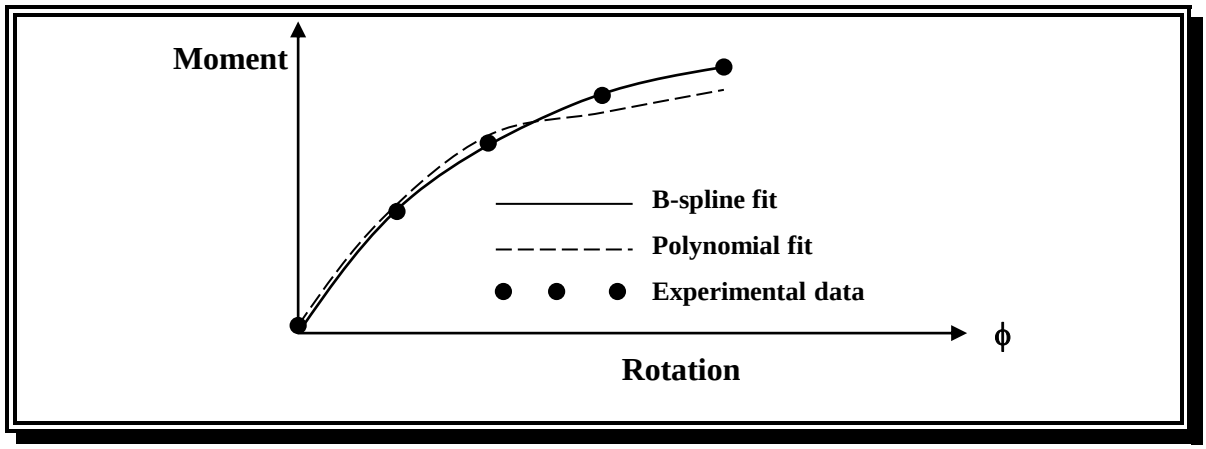

Fig.(2.2): B-Spline and Polynomial Curve Fit Models .

the connection may be negative, which is physically unjustifiable. To overcome this, ***Jones et al.,*** in 1982 **[37]** used a cubic B-spline curve (See Figure (2.2)) fitting technique to improve the polynomial model. Although the cubic B-spline model gives a good representation of connection behavior and circumvents the problem of negative stiffness, a large number of data are necessary for curve fitting process.

In 1984, ***Ang and Morris*** **[44]** replaced the polynomial function by a form of the function given by ***Ramberg*** and ***Osgood*** (1943) in the

developing of standardized moment-rotation expression for five common connection types. The function has the form:

$$\frac{\phi}{\phi_o} = \frac{KM}{(KM)_o}\left[1+\left(\frac{KM}{(KM)_o}\right)^{n-1}\right] \quad \text{..... (2.3)}$$

where ϕ_o, $(K\ M)_o$ **and n** are coefficients evaluated in the curve fitting process.

2.5 Analysis of Frames Beam-column Supported or Driven into Elastic Foundation

The analysis of frames, beams or any other structural element resting or embedded into elastic foundation is very common in engineering. A considerable research has been made on this field because of the major importance of such condition in the structure response under static loads, but a little has dealt with the beam – column element.

In frameworks with some of their members supported or driven into elastic soil, the structural behavior of frame works will be influenced significantly by the restraint caused by the elastic foundation and the amount of influence will be depended on the flexural rigidity of the embedded members and the soil modulus.

In 1946, ***Hetenyi*** **[2],** developed the analysis of beams on an elastic foundation on the assumption that the reaction forces of the foundation are proportional at every point to the deflection of the beam at the point. According to the author, this assumption was introduced first by ***E. Winkler*** in 1867 and formed the basic of ***H.Zimmermann*** classical work on the analysis of the railroad track, published in 1888.

In 1961, ***Wang, et al*** **[5],** presented the analysis of continuous beam–column on elastic ***Winkler*** foundation by using modified slope-deflection equation and moment distribution methods, and demonstrated the computation of constant axial force and constant soil modulus.

In 1974, ***Gupta*** **[19],** studied the problem of bending in axially constrained beams on ***Winkler–type*** elastic foundation. The considered beam is either fixed end beam or hinged end beam. The non-linear problem is approached by a deferential equation method as well as by finite element method. Linear solution for deflection (which neglects axial constraint effects) is also tried. Numerical results are presented which show that for a low modulus of subgrade reaction, the linear solution for deflection yields deflection values which may be several times higher than the exact solution.

In 1976, ***Avnet et al***, **[23],** presented a Fourier series analysis technique for performing the elastic stability beam-column supported by continuous ***Winkler*** supports. This method involves the solution of the

governing differential equation by Fourier series technique and enabling completely arbitrary boundary conditions to be considered for the beam-column. Axial force and soil stiffness are both considered to be constant along the beam – column.

In 1976, ***Wang J.*** **[24]** , investigated the buckling of cantilever bars on elastic foundation using some suitable function to be found to represent the buckling modes . Two cases were considered, pin jointed – free and fixed –free beam – column. He presented an example problem considering a uniform elastic bar supported by an elastic foundation of constant stiffness and carrying an axial force varying along the length of the bar.

In 1978, ***AL-Sarraf*** **[29],** presented modified slope – deflection equations by using the modified stability functions, for a uniform beam – column supported by a continuous ***Winkler's*** foundation, which was developed and tabulated for different values of axial force parameters and relative stiffness – depth parameters. They enabled the rapid prediction of the elastic critical loads of structure with some members supported on or driven in to elastic soil, having constant modulus of subgrade reaction by using a hand computing method.

The axial force is taken to be constant along the strut. Approximate formulae of the modified stability functions were derived.

In 1980, ***Beaufait*** **[32],** organized the mid point difference method for solving the basic differential equation for the elastic deformation of a beam supported on elastic non–linear foundation with rigid or elastic discrete supports. An iterative approach was used in solving the non-linear problem .The method of analysis, as programmed for a computer solution considered the continuous elastic, non-linear foundation to be active only when the beam is pressing against the foundation, the foundation was assumed to be inactive in the regions where the beam has been displaced away from the foundation. Two examples were presented to illustrate the application of the method of analysis.

In 1986, ***Yankelevsky and Eisenberger,*** **[48],** introduced an exact stiffness matrix for a beam – column on elastic foundation based on a direct analytical solution. In their formulation, nodes are required only at places of discontinuity in stiffness, loading or support conditions and therefore only a few elements are required for a common problem to yield an exact solution. The efficiency and accuracy were demonstrated through two examples, which gave an excellent agreement with the results of other researchers.

In 1986, ***Razaqpur*** **[50],** used the exact shape function from the solution of governing differential equation, to determine the stiffness and equivalent joint load matrices for a beam – column finite element resting on a ***winkler – type*** elastic foundation. The degrees of freedom at the nodes are assumed to be lateral displacement and flexural rotation. The resulting

matrices are similar to the corresponding matrices of ordinary beam elements. To verify the proposed formulation, a continuous beam – column on elastic foundation was analyzed. The result match existing solutions obtained by other analytical procedures.

In 1988, ***Anthoni*** and ***Tso*** **[59],** developed a numerically integrated finite element for the analysis of three – dimensional non-linear ***winkler*** foundation. Together with the stiffness matrix of a linear beam – column element, they used to solve the problem of beams, columns and beam – columns on linear and non-linear foundation in two and three dimensions.

The coupling between the axial and lateral directions was taken into account, including the actual distribution of the axial force. The Newton – Raphson method was used in the solution. Excellent results were illustrated by comparisons with available solutions.

In 1997, ***AL- Hachami*** **[75],** presented a theoretical analysis for predicting the large displacement elastic stability analysis of plane and space structures subjected to static loading. He studied the behavior of beam – column resting on elastic foundation, piles driven into soil, and large displacement of submarine pipelines. Two approaches were used in the analysis of structures consisting of members resting on linear elastic foundation. In the first approach, the elastic foundation was represented by isolated springs at the nodes of members. In the second approach, the foundation was considered to be uniformly distributed springs along the member. Modified formulae for stability and bowing functions were derived.

In 1998, ***Chen*** **[78],** proposed a new numerical approach for solving the problem of a beam resting on linear elastic foundation .The differential quadrature (**DQ**) was used in this approach to descretize the governing differential equations defined on all elements, the transition conditions defined on the interelement of two adjacent elements and the boundary condition of the beam. Numerical results of the solutions of beams resting on linear elastic foundations obtained by the (**DQ**) were presented.

In 1999, ***T. Hong, J.G. Teng*** and ***Y.F. Luo*** **[81]**, described a finite element method for the large deflection analysis of axisymmetric shells and plates on a non-linear tensionless elastic foundation. They modeled any form of non-linear elastic foundation by using the discrete data points. The analysis was then validated by comparison with existing results for circular plates and beams as the only existing results for shells on tensionless foundations were found to be in error. Following this verification, the analysis was applied to investigate the behavior of shallow spherical shells subjected to a central concentrated load on tensionless linear elastic foundations. A number of insightful conclusions regarding the behavior of such structure-foundation systems were drawn. The numerical results for

shells were believed to be the first correct results, which may be useful in benchmarking results from other sources in the future.

In 2001, ***AL-Rubai*** **[83],** studied the non -linear behavior of prismatic members in plane structures with some members resting on non -linear ***Winkler*** foundation. He used the equation $\left(\mathbf{P}=\frac{\delta}{\mathbf{a}+\mathbf{b}\delta}\right)$ and developed it to be very efficient in estimating the non-linear behavior of soil. The elastic foundation was represented by isolated springs at the nodes of members only. Excellent results were achieved compared with available solutions.

In 2002, ***Al-Khafaji A.Kh.*** **[84]**, presented a theoretical analysis for non-prismatic members in plane structure resting on non-linear elastic ***Winkler*** foundation. He used the polynomial function to be the relation between the deflection and the load. Both lumped and consistent methods were used in his study to calculate the stiffness of soil.

2.6 Post-Buckling Analysis

The problem of buckling of structures has grown in importance because of several interrelated developments. The need to cover large spans without intermediate supports and at the same time the very small ratio of the weight of structural material to the unit area covered due to economical considerations, made the buckling capacity of these structures a determining factor for their design and also for the selection of their form.

General theoretical formulations and computational techniques for the analysis of structures have been extensively studied in recent years. The majority of the work has been concentrated in non-linearities produced from changes of geometry, because these types of structure are more likely to fail by instability before significant non-linear material response is observed.

In 1980, ***Bergan*** **[31]** discussed characteristic types of non-linearities in structural systems and various ways of illustrating such non-linearities were suggested. The use of the current stiffness parameter for characterizing non-linear systems was discussed and some new formulations and applications of this parameter were suggested. Also, a new class of solution technique utilizing simultaneous iteration of he loading parameter as well as the displacements was proposed.

In 1981, ***Crisfield*** **[34]** made a modification to the ***Riks's*** approach discussed previously so that it is suitable for use with the finite element method. The procedure was then applied in conjunction with modified Newton-Raphson method in both its original and accelerated forms. The resulting techniques were not only allow limit points to be passed, but also, improve the convergence characteristics of the iterative procedures. The author also, solved some problems including the large deflection analysis of elastic shallow shells.

In 1987, ***Hsiao and Hou*** **[55]** presented finite element formulation and numerical procedure for the geometrically non-linear and post-buckling analysis of in-plane frames. A conventional formulation combined with small deflection beam theory with the inclusion of the effect of axial force was adopted. A body-attached coordinate system was used to distinguish between rigid body and deformational rotations. The deformational nodal rotational angles were assumed to be small, and the membrane strain along the deformed beam to be constant. Superimposing the bending and the geometric stiffness matrices of the elementary beam element and the stiffness matrix of the linear bar element obtained the element stiffness matrix. An incremental iterative method based on the Newton-Raphson method combined with a constant arc-length control method was employed for the solution of the non-linear equilibrium equations. In order to improve convergence properties of the equilibrium equation, a two-cycle iteration scheme was introduced. Nine examples were presented to demonstrate the accuracy and efficiency of the proposed method.

In 1988,***Chan*** **[58]** presented a geometric and material non-linear analysis method for framed structures, by using a solution technique of minimizing the residual displacements. The new technique "Minimum Residual Displacements", was used together with the concept of the effective tangent stiffness matrix for braced members. In an inelastic analysis, the elastic perfectly plastic material model was employed. Four examples were solved to verify the efficiency and accuracy of the proposed method. He concluded that the proposed method was capable of handling geometric and/or material non-linear problems in beam-columns and frames exhibiting snapping softening and stiffening behavior.

In 1989, ***Meek and Loganathan*** **[64]** presented a solution strategy for the geometrically non-linear analysis of elastic space frame structures subjected to static loads by using finite element method. To trace the load-deflection paths of space frames undergoing large deformations, the updated Lagrangian approach was adopted. For large joint rotations, ***Oran's*** approach was used. The solution strategy is based on the constant arc-length method proposed by ***Crisfield*** **[34]**, and the conventional Newton-Raphon method. Some modifications were applied to the ***Crisfield*** method in order to pass the bifurcation and limit point regions when the solution strategy exhibits imaginary roots. A complete non-linear static analysis was presented for at two-hinged deep arch and a shallow geodesic dome to illustrate the validity of this method.

In 1990, ***Wong and Tin-Loi*** **[66]** developed a method for the elastic non-linear analysis of framed structures depending on the finite element method. They described the main forms of Lagrangian coordinate systems and their relative merits were also discussed. They used partially updated Lagrangian coordinate system that takes advantages of the merits inherent in both the updated and the total Lagrangian descriptions. They used a solution strategy that rests on a judicious combination of the well-known Newton-Raphson iterative scheme and a modification to the modified arc-

length method **[34]**, proposed by them. The proposed variation of the modified arc-length technique enables a solution at the limit point to be calculated. They solved three examples and got very accurate results compared with the experimental results obtained by others.

In 1992, ***Fujh, et.al.*** **[69]** presented a modified version of displacement control titles "Variable Displacement Control" to overcome the turning points of the displacement on snapping-back and looping equilibrium path. As a remedial measure to overcome the drawback of the conventional displacement control, the tangent vector of the path is examined and the component with the maximum absolute value is located. The corresponding displacement or loading parameter detected by the above examination will serve at the best control parameter in the sense that its turning point is most unlikely to occur in local path geometry. Two examples were solved to demonstrate the validity of the proposed method and good agreement was obtained.

In 1998, ***Al-Uraiby*** **[77]** presented a theoretical analysis for predicting the pre-and post-bucking behavior of plane steel frames with non-prismatic members subjected to static loads. The analysis was for the large displacement behavior and adopts the beam-column approach. The formulation of the beam-column element is based on Eulerian approach allowing for the influence of the axial force on bending stiffness. The formulation of a tangent stiffness matrix for non-prismatic member in local and global coordinates in such study takes into account the geometrical non-linearity. In the post-buckling analysis, the incremental load control with different load incrementation strategies and modified Newton-Raphson method with different iterative strategies were used.

In 2000, ***Al-Mutairee*** **[82]** developed the work of ***Al-Uraiby*** **[77]** to deal with dynamic loading. Also, he made a comparison between the different iterative strategies and the different incremental strategies to decide which of each group is the best, more efficient and general. He concluded that the arc-length load incrementation strategy with the constant arc-length and minimum residual displacements iterative strategies represent the most efficient and the most rapid techniques.

From the preceding review of literature, No literature was found that considers the non-linear analysis of plane steel frames with non-prismatic members and flexible connections subjected to static loads including the post-buckling behavior and shear effect. Such study cases is presented well in the present work.

CHAPTER SIX

6

PARAMETRIC STUDIES

6.1 Introduction

A parametric study is performed to assess the influence of several important paramertes on the behavior of elastic plane structures under static loading.

The selected parametric study to be discussed in this chapter can be summarized as follows:

1. Effect of the tapering ratio.

2 Effect of shear on the behavior of frames.

3 Effect of steel flexible connections on the behavior of frames.

4. Effect of subgrade reaction.

5. Effect of large displacement analysis.

Each one of these parameters was studied individually by analyzing a frame or more from the frames considered in this chapter as case studies.

6.2 Case Studies

A description for the six case studies selected to be analyzed in this chapter is presented here.

6.2.1 Case Study No. 1: (William's Toggle Frame)

This structure which was considered in **Chapter Five** as example No. 4 (Figure (5.13)), is treated here to study the effect of flexible connection on behavior of the frame. Figure (6.1) shows the moment-rotation behavior of this frame.

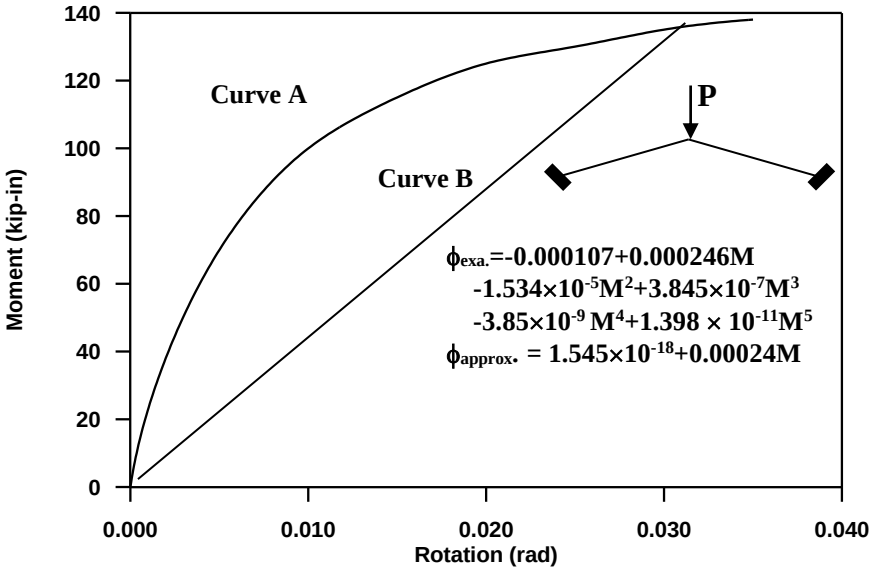

Fig.(6.1): Moment-Rotation Behavior [65].

6.2.2 Case Study No. 2: (Portal Frame with Tapered Members)

Figure (6.2), shows the geometry and loading conditions for this case study. This frame had been analyzed by ***Al-Uraiby B.*** **[77]** and ***Al-Khafaji H.M.*****[85]**.

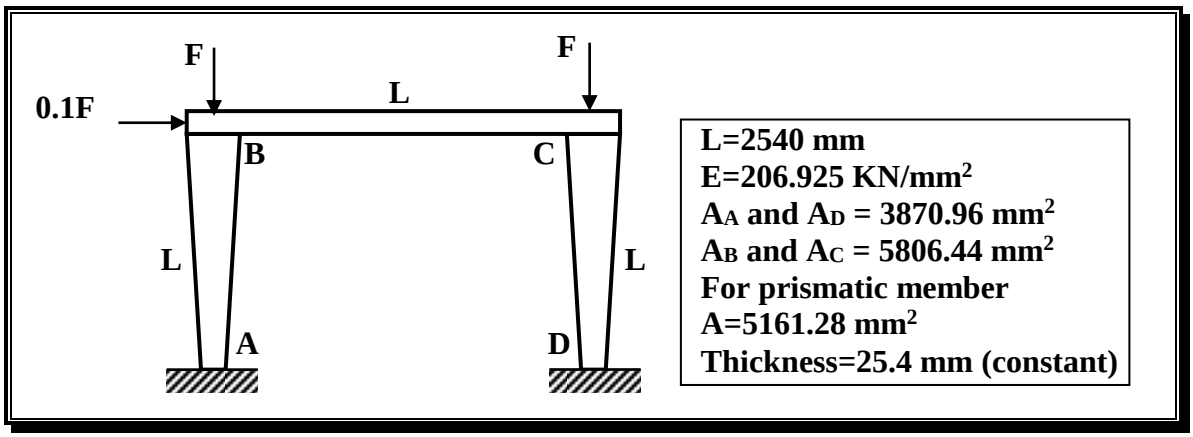

Fig.(6.2): Geometry and Loading Conditions for Case Study No.2 .

6.2.3 Case Study No. 3: (Gable Frame)

The geometry, properties and loading conditions for this case study are shown in Figure (6.3).

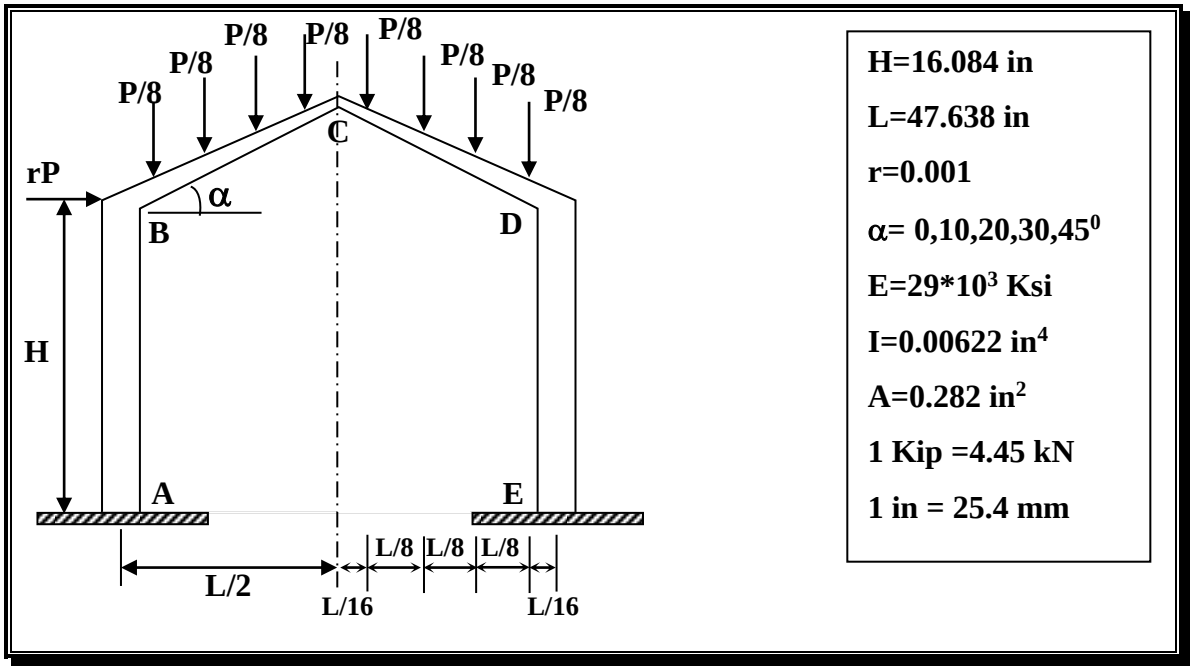

Fig.(6.3): Geometry and Loading Conditions for Case Study No.3 .

6.2.4 Case Study No. 4: (Fixed-Ended Vierendeel Frame)

The geometry, properties and loading conditions for this case study are shown in Figure (6.4). This Structure was analyzed in **Chapter Five** as Example No.7.

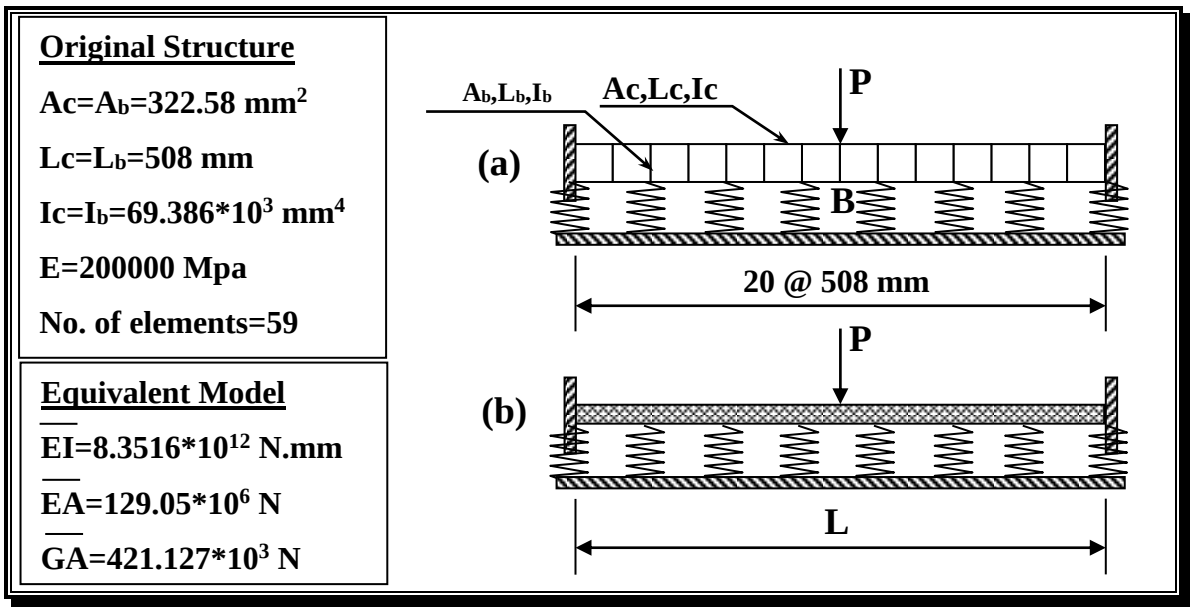

Fig.(6.4) : Geometry and Loading Condition of Case Study No.4 .

6.2.5 Case Study No. 5: (Fixed-Ended X-Bracing Truss Beam)

The geometry, properties and loading conditions for this case study are shown in Figure (6.5). This Structure was analyzed in **Chapter Five** as Example No.8.

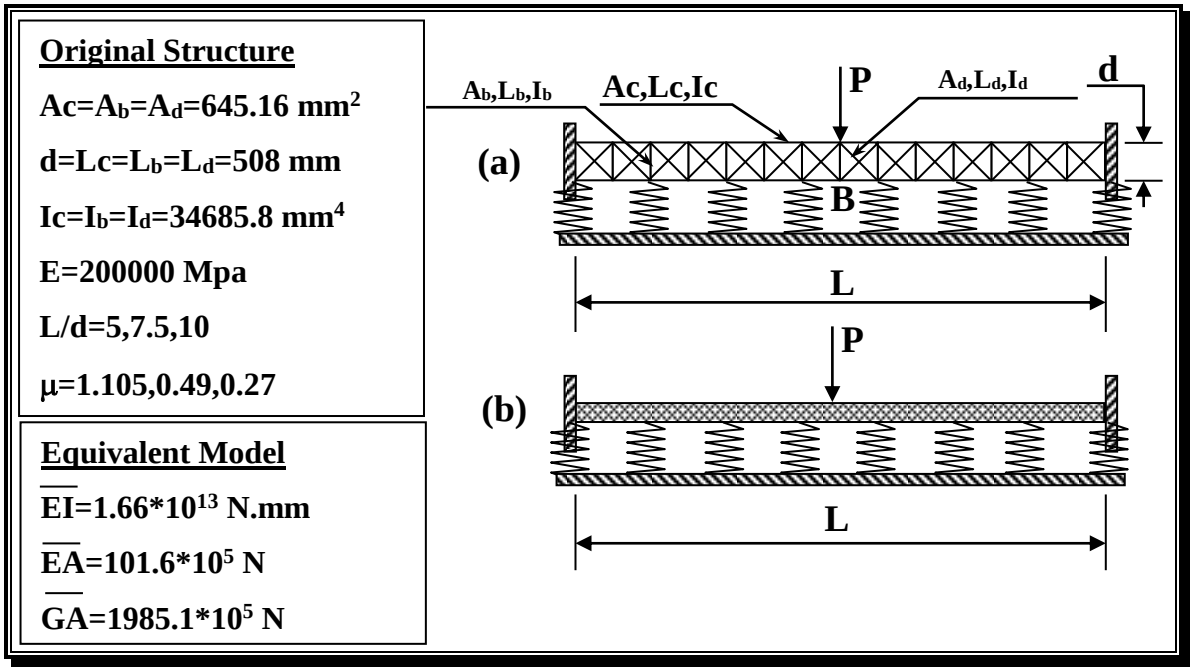

Fig.(6.5) : Geometry and Loading Condition of Case Study No.8 .

6.2.6 Case Study No. 6: (3-Member Extended Frame)

The geometry, properties and loading conditions for the 3-Member extended frame, chosen to be the sixth case study in this chapter, are shown in Figure (6.6).

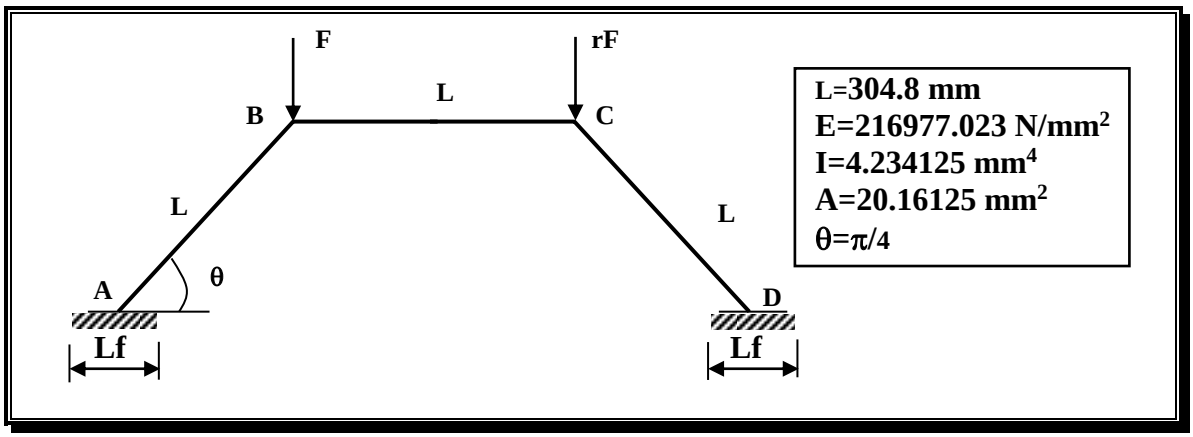

Fig.(6.6) : Geometry and Loading Conditions for Case Study No.6 .

6.3 Parametric Studies

Parametric studies were performed to assess the influence of several important parameters on the static behavior of the plane elastic steel frames under static load with non-prismatic members resting on elastic foundation, non-linear flexible connections and including shear effect. Also, a discussion for the results obtained from such parametric studies is presented. It is important to mention that all the following parametric studies are carried out for the same volume of steel when changing the tapering ratios.

6.3.1 Effect of Tapering Ratio

To asses the effect of tapering ratio (**D**) on the post-buckling behavior of frames with flexible connections, non-prismatic members, resting on elastic foundation and subjected to static loads including shear effects, the William's toggle frame as shown in Figure (5.12), the portal frame as shown in Figure (6.2) and the gable frame as shown in Figure (6.3) were analyzed.

Frame containing members whose bending moments vary along its length can be prepared more economically by tapering the members. With this technique a large cross-sections can be used in reign where bending moments are high. On the other hand, smaller cross-sections can be used where the external bending moments are low. As mentioned, the tapering was made so that the same volume or weight of the material is achieved.

The William's toggle frame was analyzed with seven values of tapering ratio (**D**) these are (**0.2,0.5,0.7,1,1.2,1.5 and 1.7**) respectively and for both rigid and flexible cases. The frame was analyzed for both rigid and flexible cases by using the external-work load incrementation strategy with constant external-work iterative. The number of segments per each member is equal to (**3**). The reference load is (**Fr=1 lb**) and the desired number of iteration is (**Jd=3**). The portal frame was analyzed with four values of tapering ratio (**D**) these are (**0.5,1,1.5,2 and 2.5**) respectively and for both rigid and flexible cases. The frame was analyzed for both rigid case and flexible case [linear beam-to-column joint with constant stiffness equal to **10EI/L**] by using the arc-length load incrementation strategy and the minimum residual displacement iterative. The number of segments per each non-prismatic member is equal to (**3**). The reference load is (**Fr=500 kN**) and the desired number of iteration is (**Jd=3**).

The gable frame was analyzed with four values of tapering ratio (**D**) these are (**1,1.2,1.5 and 1.7**) respectively, and with five values of angle (α) of gable frame .The frame was analyzed by using the arc-length load incrementation strategy with the arc-length iterative. The number of

segments per each non-prismatic member is equal to (**8**). The reference load is (**Fr=0.0075 Kips**) and the desired number of iteration is (**Jd=3**).

For the case of William's toggle frame, it was observed that increasing the tapering ratio, [increase the depth of member at ends], leads to increase the stiffness of the frame. At the same time the associated displacements are reduced. The results of the analysis were presented as load-displacement curves in Figures (6.7), to, (6.9). Figure (6.10), shows the relation between the critical load and tapering ratio. As shown in this figure, the best tapering ratio (**D**) for the three types of connection (rigid, linear and non-linear flexible connection) is in the range of (**1-1.2**).

Figures (6.11), to, (6.14), show the results of portal frame as load-displacement curves. Figures (6.15) and (6.16), show the relation between the critical load and tapering ratio (**D**). The critical load increases with decreasing the tapering ratio up to a certain values of (**D**) after which the structure change its behavior and critical load decreases. The best tapering ratio (**D**), in this case is (**D=2**).

The results of gable frame are shown in Figures (6.17), to, (6.19), as load-displacement curves. As shown in these figures, when the angle of the gable increases the vertical deflection decreases because the share of axial force from external load is more than the share of vertical component, these lead to increase the stiffness of the frame.

The results discussed as follows: the resistance of a structure can be improved when the volume of steel is distributed according to the distribution of the bending stresses. For example for William's frame, the decrease of the depth at the mid section and the increase at the ends increases the resistance of the frame because the moment at the ends is larger than the moments at mid section. However, the best tapering ratio at which the greater stiffness of the structure is obtained depends on the geometry of the frame and the loading conditions.

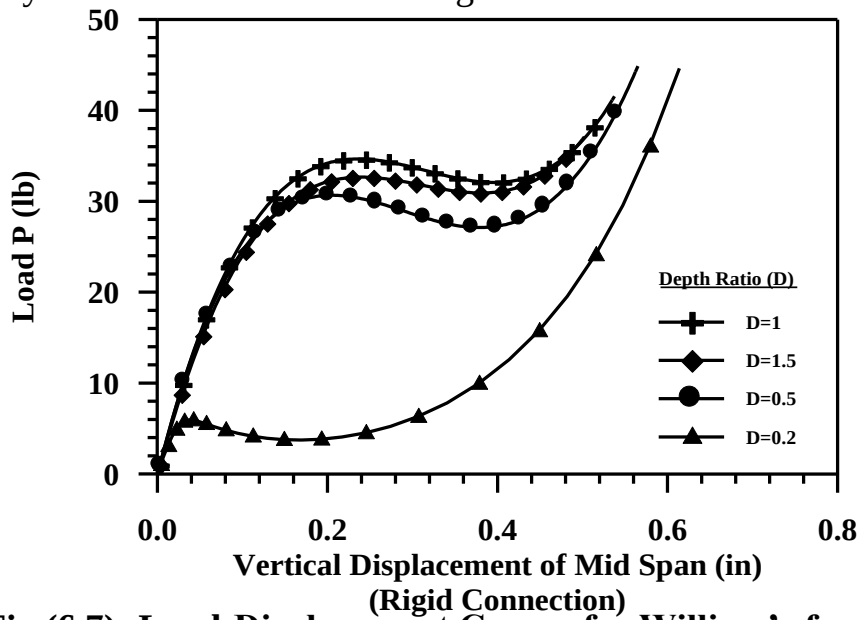

Fig.(6.7): Load-Displacement Curves for William's frame .

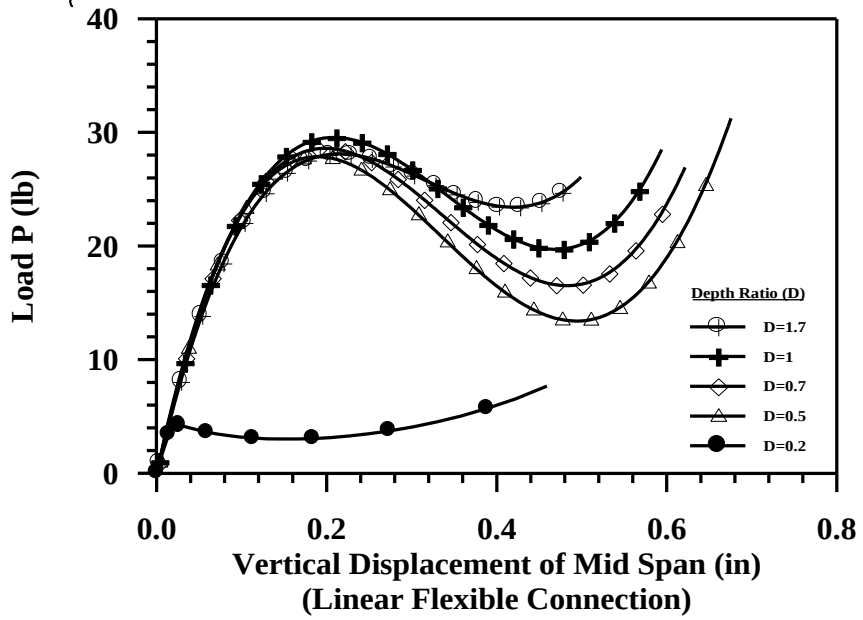

Fig.(6.8): Load-Displacement Curves for William's frame .

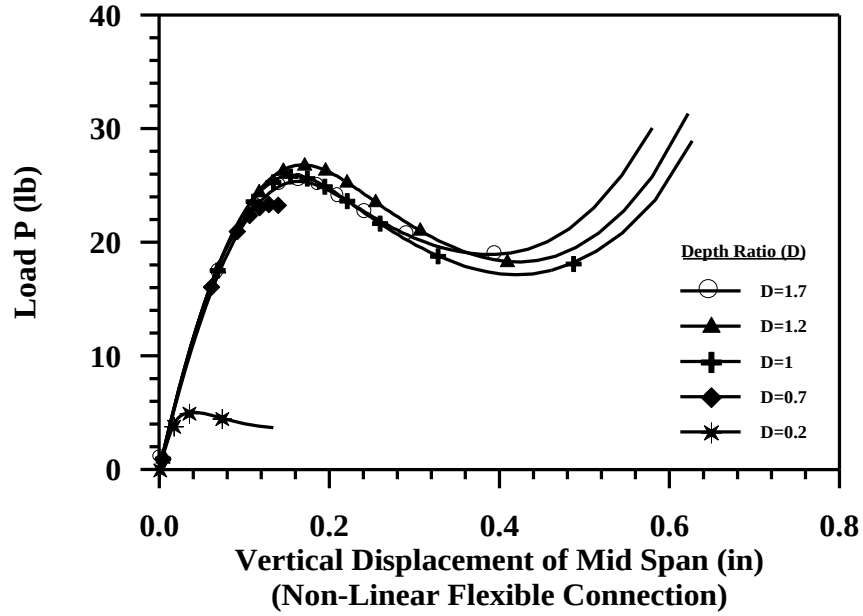

Fig.(6.9): Load-Displacement Curves for William's frame.

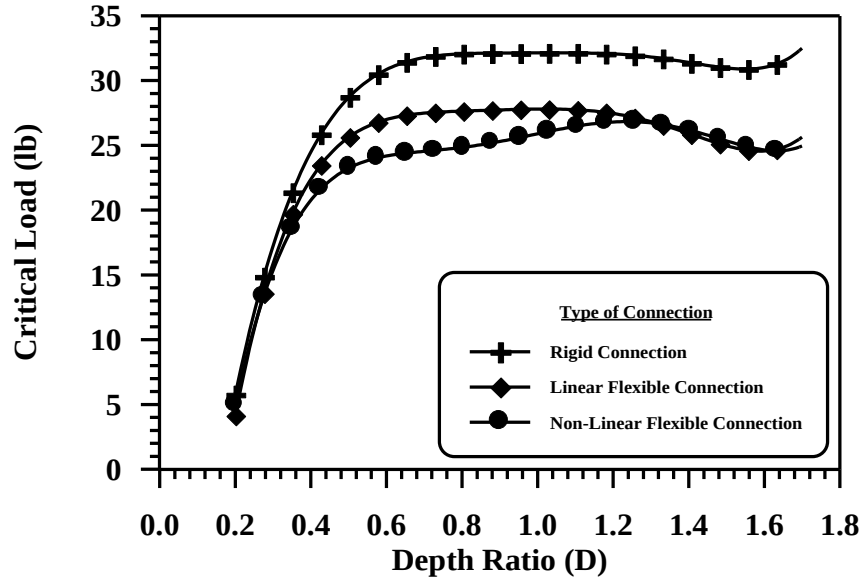

Fig.(6.10): Critical Load-Depth Ratios Curves for William's frame.

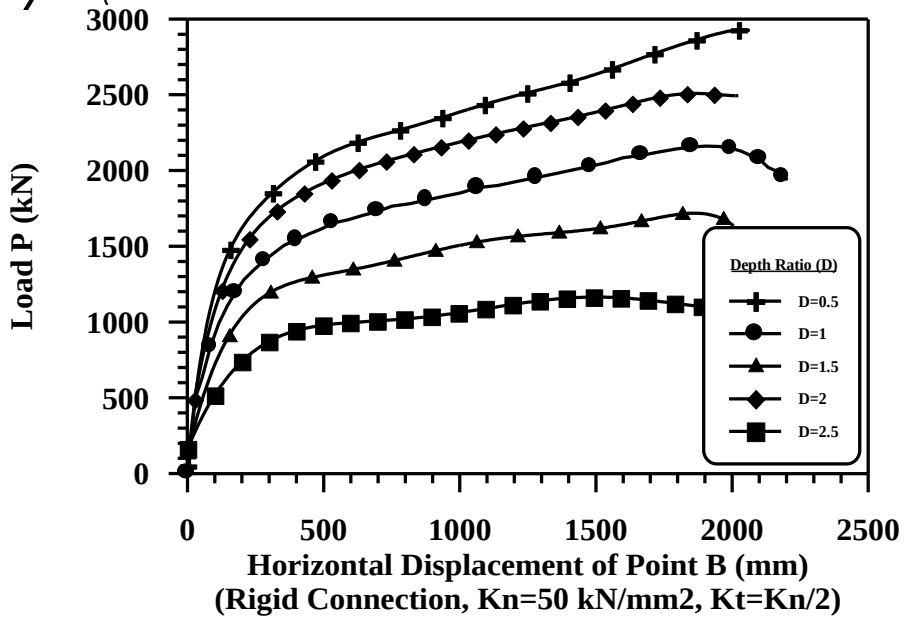

(Rigid Connection, Kn=50 kN/mm2, Kt=Kn/2)

Fig.(6.11): Load-Displacement Curves for Portal frame .

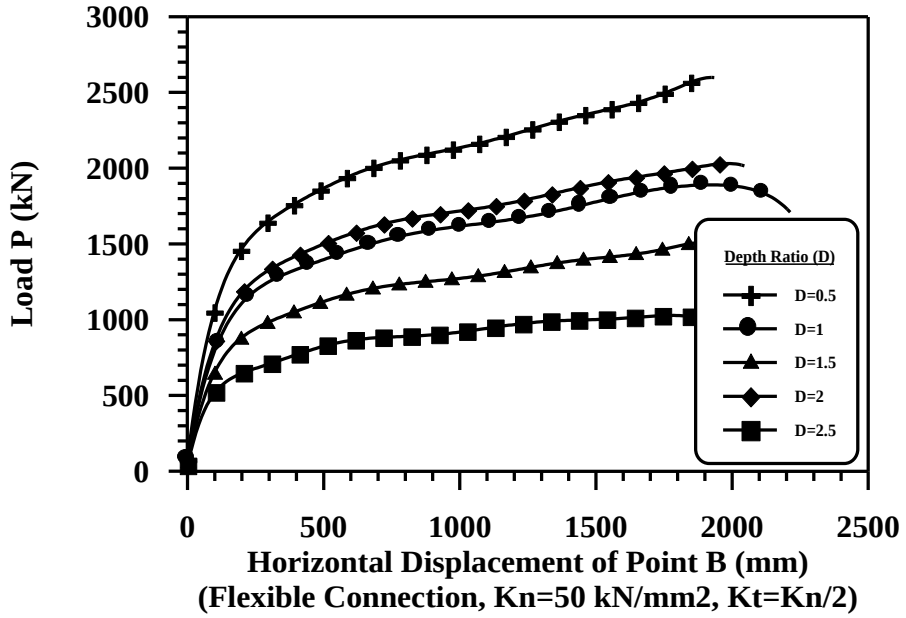

(Flexible Connection, Kn=50 kN/mm2, Kt=Kn/2)

Fig.(6.12): Load-Displacement Curves for Portal frame .

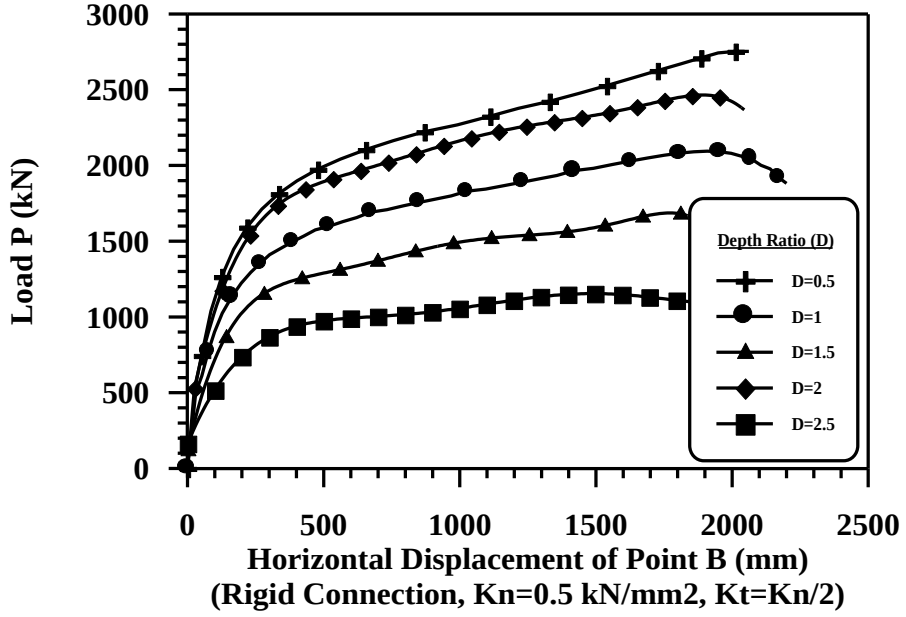

(Rigid Connection, Kn=0.5 kN/mm2, Kt=Kn/2)

Fig.(6.13): Load-Displacement Curves for Portal frame .

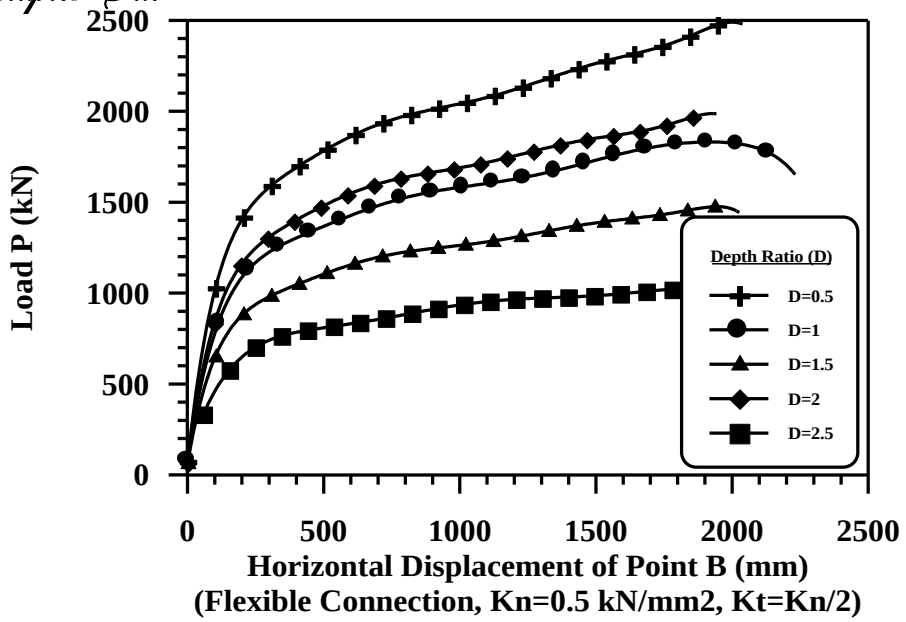

Fig.(6.14): Load-Displacement Curves for Portal frame

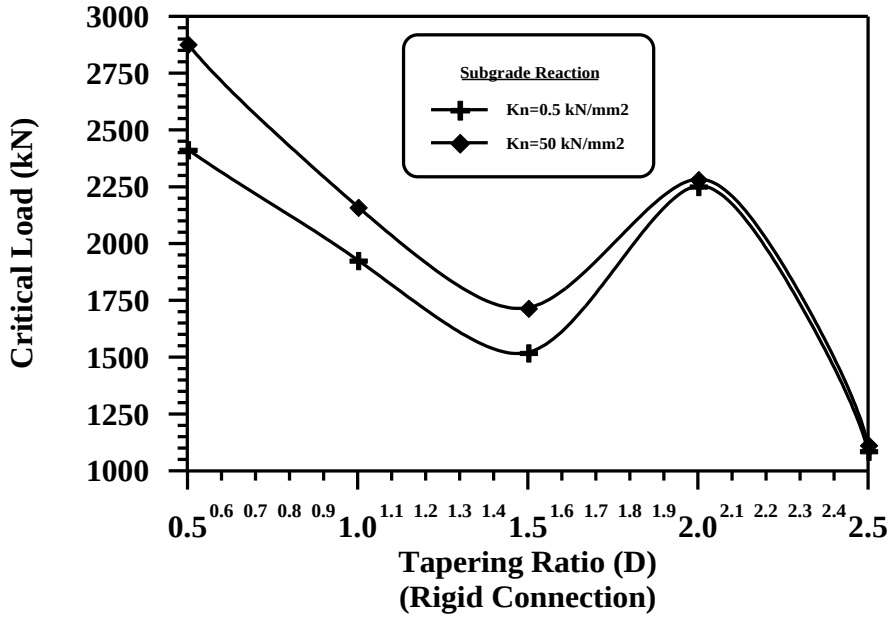

Fig.(6.15):Critical Load-Displacement Curves for Portal frame

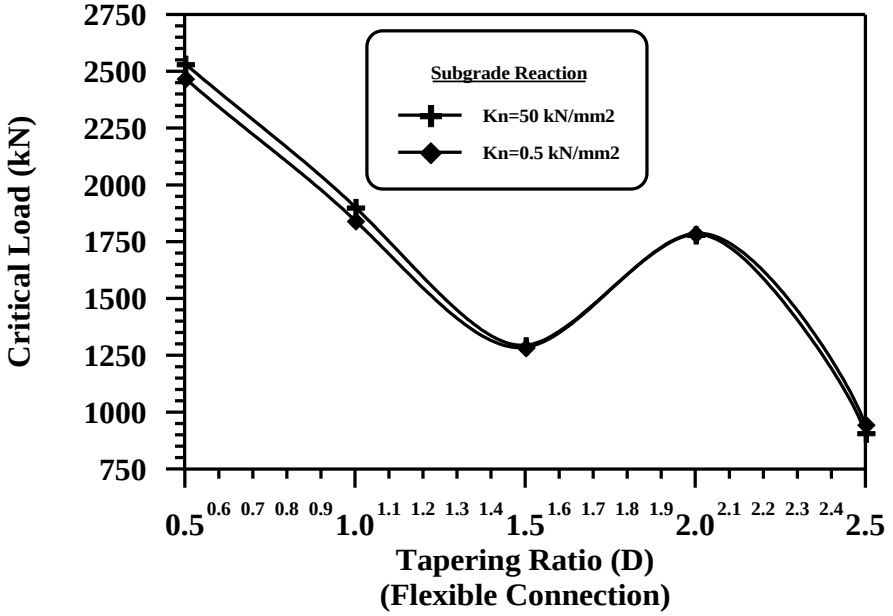

Fig.(6.16):Critical Load-Displacement Curves for Portal frame

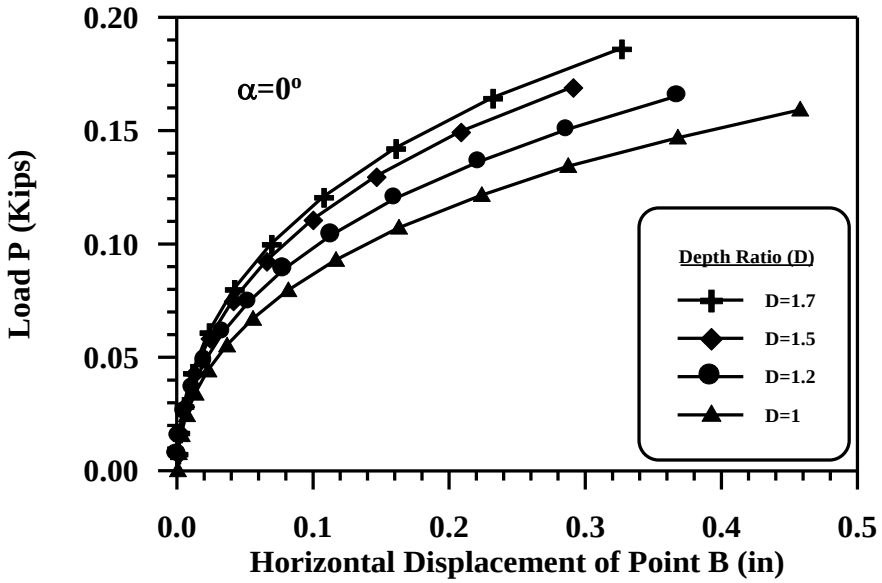

Fig.(6.17): Load- Displacement Curves for Gable frame .

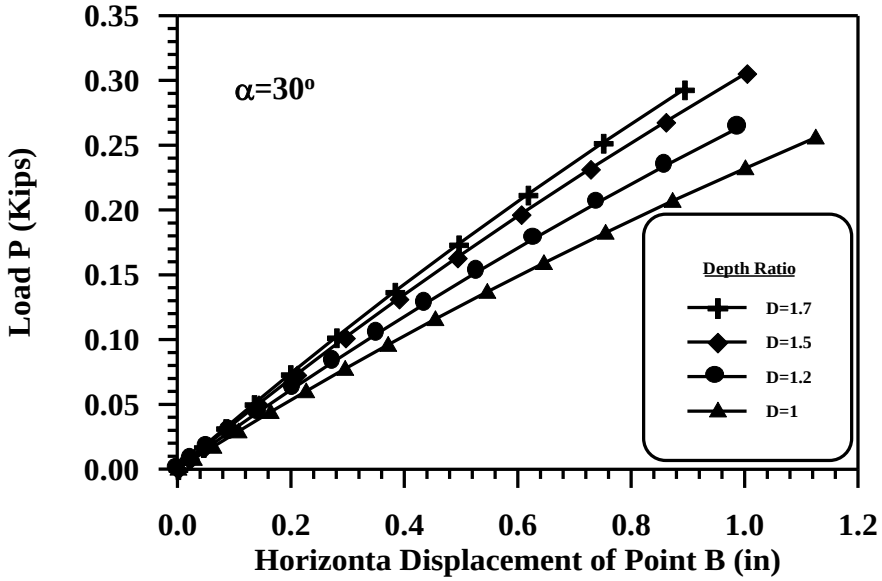

Fig.(6.18): Load- Displacement Curves for Gable frame.

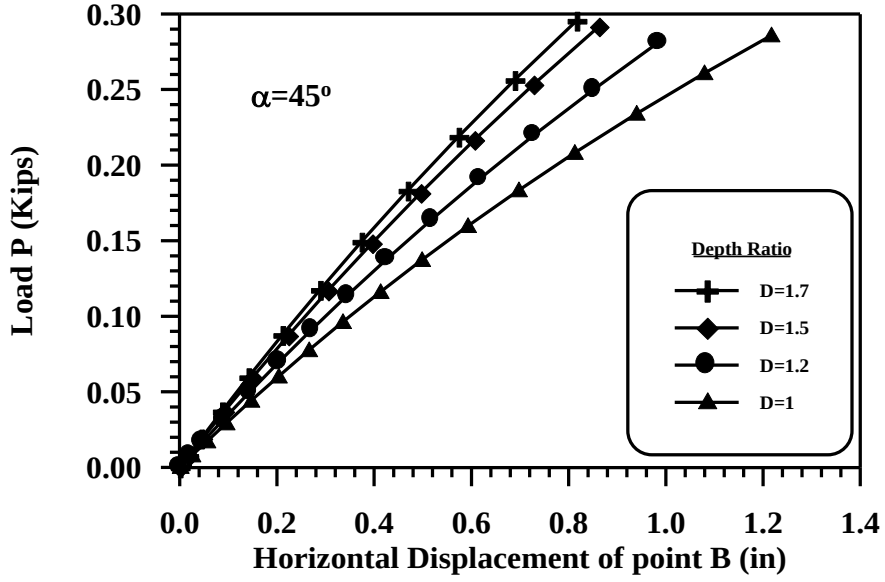

Fig.(6.19): Load- Displacement Curves for Gable frame

6.3.2 Effect of Shear on the behavior of Frame

To verify the effect of shear on the behavior of frame and beam-like lattice structure under static loading, the Vierendeel frame shown in Figure (6.4), has been chosen as a case study.

To show the effect of slenderness ratio on the value of shear parameter (μ) and accordingly on the shear deformation of structures, the fixed-ended x-bracing beam, Figure (6.5), has been chosen as a case study.

The Vierendeel frame was analyzed twice, first without shear and other with shear, for three values of subgrade reaction (**Kn=0.05,0.005 Kn/mm^2, and zero**),by using the equivalent continuum model presented in **Chapter Three**, and divided into (**10**) elements each one has a value of shear parameter (μ) equals to (**227.536**). The frame was analyzed by using the arc-length load incrementation strategy with the arc-length iterative strategy. The reference load is (**Fr=100 kN**) and the desired number of iteration is (**Jd=3**). The results were shown in Figure (6.20), as load-displacement curves.

The X-bracing beam was analyzed twice, first without shear and other with shear, for four values of slenderness ratio (**L/d=2.5,5,7.5, and 10**), and for three value of subgrade reaction (**Kn=0.05,0.005 kN/mm^2, and zero**), using the equivalent continuum model presented in **Chapter Three**, and divided into (**10**) elements each one has value of shear parameter (μ) according to Table (6.1). The frame was analyzed using the arc-length load incrementation strategy with the arc-length iterative. The reference load is (**Fr=100 kN**) and the desired number of iteration is (**Jd=3**). The results were shown in Figures (6.21), (6.22), and (6.23), as load-displacement curves.

As mentioned previously, in Chapter Three, the effect of the shear force will reduce the value of critical load and increase the deflection as shown in Table (6.1). It can be seen from Figure (6.20), that the deflection of Vierendeel frame increases when the shear effect is included. That means the structure became softer and close to the original structure when the shear effect is included **[76]**.

It can be seen from Figures (6.21), (6.22), and (6.23), and Table (6.1), when (**L/d=2.5**), and as it is expected the effect of shear deformation on the response of the structure becomes as shown in Table (6.1), and this effect decreases for a large value of slenderness ratio (**L/d**). This behavior is due to fact that, when the slenderness ratio decreases, the shear parameter (μ) increase and consequently, the shear effect on the response of structures will increase.

Table (6.1a): A comparison between the solution of X-bracing beam with and without shear for subgrade reaction (Kn=0.05 kN/mm^2)

No.	Slenderness ratio(L/d)	Shear Parameter (μ)	The load (kN)	Max. deflection (mm)		% Effect of shear deformation
				Without shear	With shear	
1	2.5	61.404	8000	21.29	69.52	69.38
2	5	15.351	8000	87.48	118.47	26.16
3	7.5	6.823	8000	105.85	128.32	17.51
4	10	3.838	-	-	-	-

Table (6.1b): A comparison between the solution of X-bracing beam with and without shear for subgrade reaction (Kn=0.005 kN/mm^2)

No.	Slenderness ratio(L/d)	Shear Parameter (μ)	The load (kN)	Max. deflection (mm)		% Effect of shear deformation
				Without shear	With shear	
1	2.5	61.404	8000	22.84	81.15	71.85
2	5	15.351	8000	149.86	214.68	30.19
3	7.5	6.823	8000	303.28	347.32	12.68
4	10	3.838	8000	410.12	440.38	6.87

Table (6.1c): A comparison between the solution of X-bracing beam with and without shear for subgrade reaction (Kn=0)

No.	Slenderness ratio(L/d)	Shear Parameter (μ)	The load (kN)	Max. deflection (mm)		% Effect of shear deformation
				Without shear	With shear	
1	2.5	61.404	8000	22.93	82.86	72.33
2	5	15.351	8000	160.98	234.16	31.25
3	7.5	6.823	8000	367.97	414.23	11.17
4	10	3.838	8000	560.88	605.32	7.34

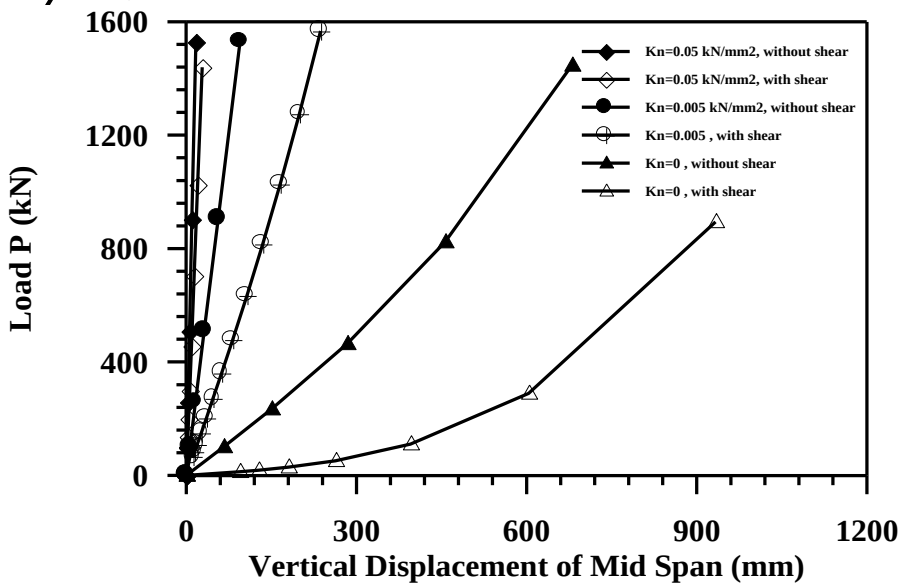

Fig.(6.20): Load-Displacement Curves for Vierendeel frame.

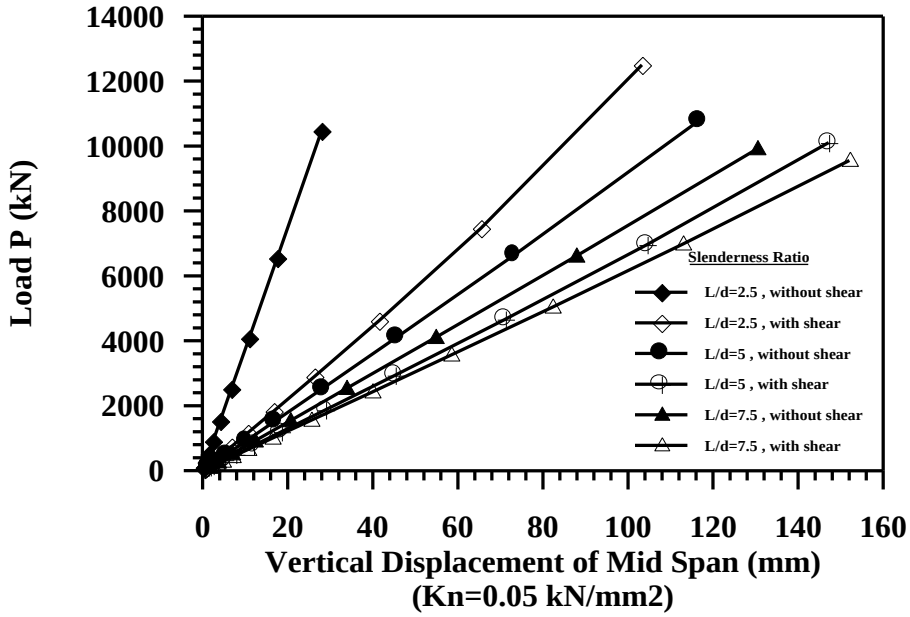

Fig.(6.21): Load-Displacement Curves for X-Bracing Truss Beam .

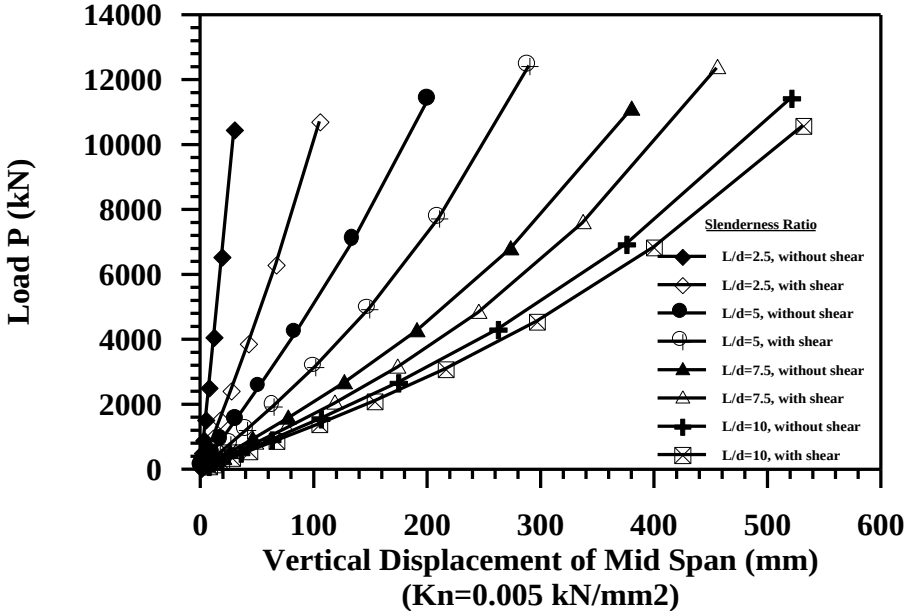

Fig.(6.22): Load-Displacement Curves for X-Bracing Truss Beam.

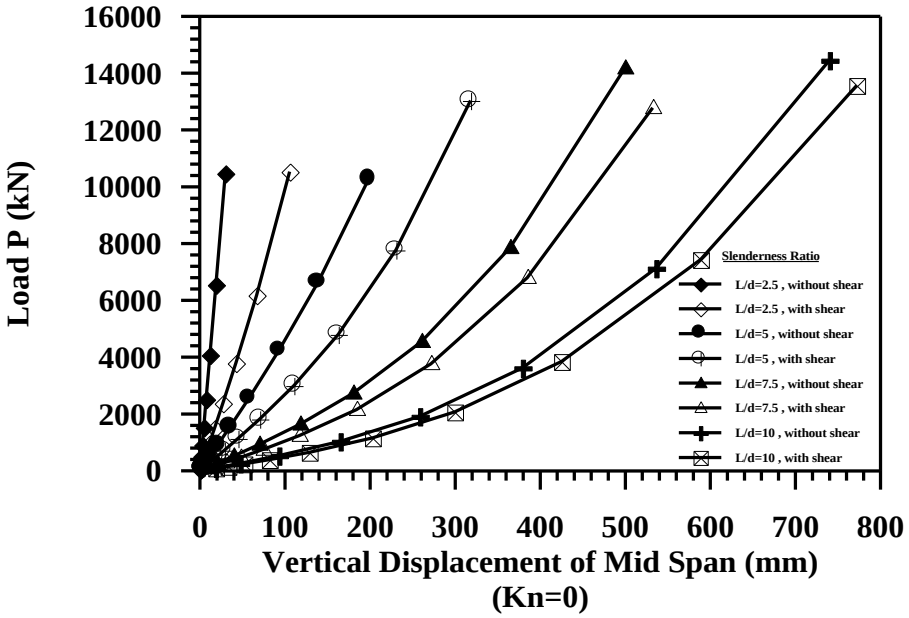

Fig.(6.23): Load-Displacement Curves for X-Bracing Truss Beam.

6.3.3 Effect of steel flexible connections on behavior of frames

As discussed earlier, most of the connections in a real steel structure are flexible and their effect on structure behavior must be considered in any realistic analytical procedure. The behavior of a connection is best described by its moment-relative rotation relationship. **Frye and Morris [20]** and others proposed several relationships to describe this behavior. It can be seen from these relationships that they are non-linear almost from the start of loading. A polynomial function can be used to represent the non-linear moment-rotation curve of a connection, and its adopted in the present study.

To assess the effect of varying stiffness of the connection on the behavior of frames under static loads, in this part the William's toggle frame (the same William's toggle frame considered in **Chapter Five**), was analyzed.

The William's toggle frame was analyzed by using the external-work load incrementation strategy with the constant external-work iterative strategy. The reference load is (**Fr = 1 lb**) and the desired number of iteration is (**Jd = 3**).

Figure (6.1) shows the moment-rotation behavior for the flexible connections used in case study No. 1. And the results were shown in Figures (6.24), (6.25), and (6.26), as load displacement curves.

From the inspection of these results, the following observations may be drawn:

1. The critical load of a frame decreases with decreasing the stiffness of its connections (decreasing tangent stiffness of non-linear connection).
2. Connection flexibility affects the moment distribution of the frame.
3. The approximate linear behavior of flexible connection gives results different from the non-linear (exact) behavior of connection and this effect increases if connection flexibility increases, so the non-linear behavior should be used in the representation of the flexible connection, and the approximate linear moment-rotation can be used at the initial stage of loading.

The study of flexible connected frames presented in this part, has demonstrated the importance of connection behavior in affecting the overall stability and behavior of steel frames. It should be noted that, in really, fully rigid and ideally pinned connections do not exist. All connections exhibit behavior somewhere in between these two extreme cases. The fully rigid and ideally pinned joint idealizations are just design simplifications.

Since flexibly connected frame behavior is, to a large extent, affected by connection behavior, additional and systematic research into connection behavior is deemed necessary.

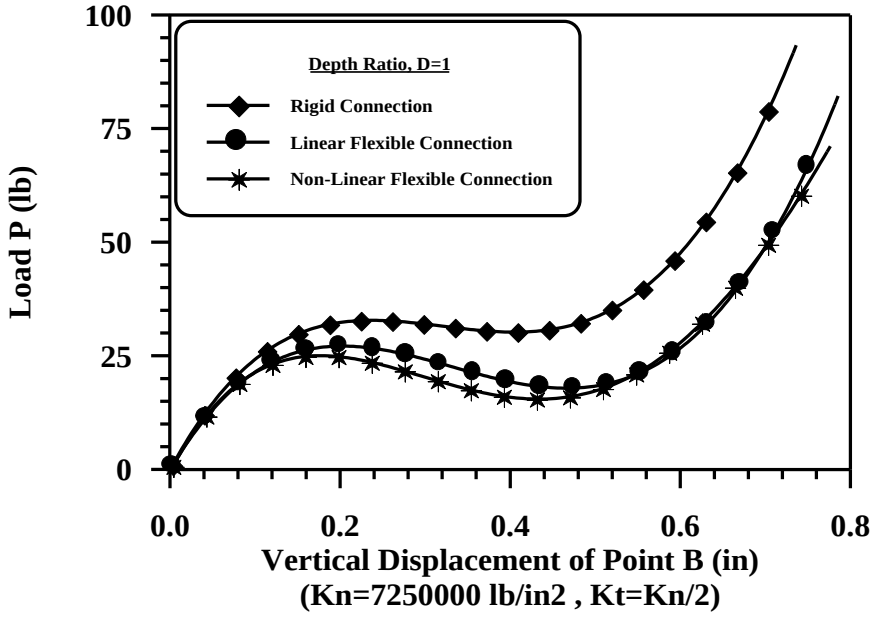

Fig.(6.24): Load-Displacement for William's frame .

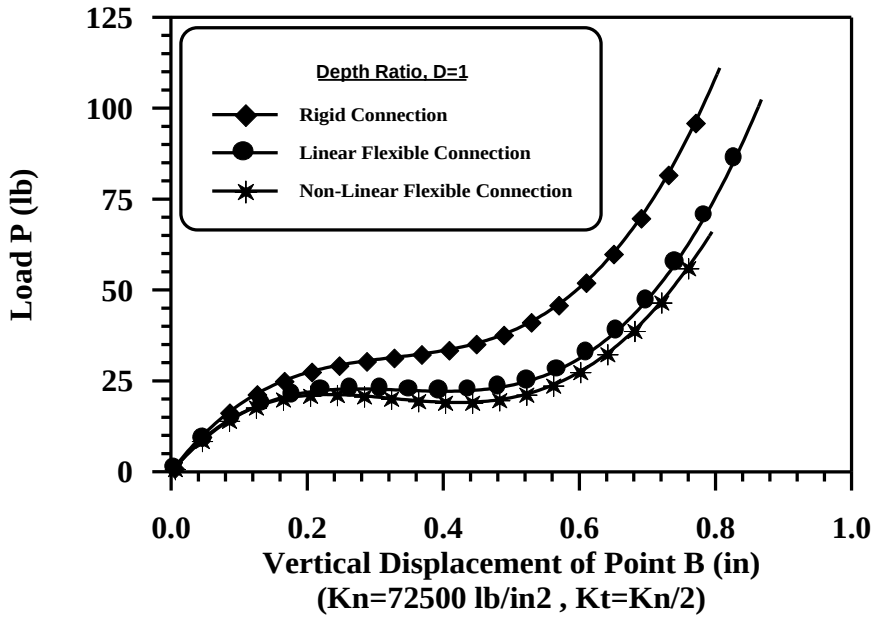

Fig.(6.25): Load-Displacement curve for William's frame.

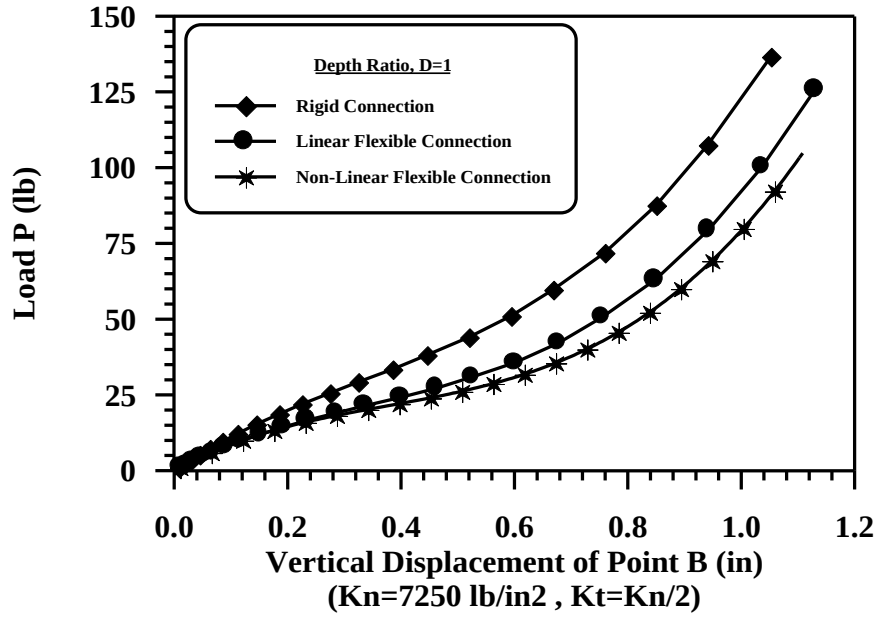

Fig.(6.26): Load-Displacement curve for William's frame.

6.3.4 Effect of Subgrade Reaction on the behavior of Frame

The subgrade reaction is divided into two types, the first one is the normal subgrade reaction (**Kn**) which is the relation between the normal soil pressure at a point and the resulting deflection at that point, Figures (6.20), to (6.23), and Figures (6.27), to (6.31), show the effect of normal subgrade reaction, as shown in these figures, when the normal subgrade reaction decreases, the deflection of the frame increases and the pressure of the soil decreases, while the second type is the tangential subgrade reaction (**Kt**), which is the relation between the shearing stress and the resulting deflection along the pile perimeter or the foundation surface, Figures (6.11), to (6.14), Figures (6.24), to (6.26), show the effect of tangential

subgrade reaction, as shown in these figures, when the tangential subgrade reaction decreases the deflection of the frame increases, and the limit point decreases .

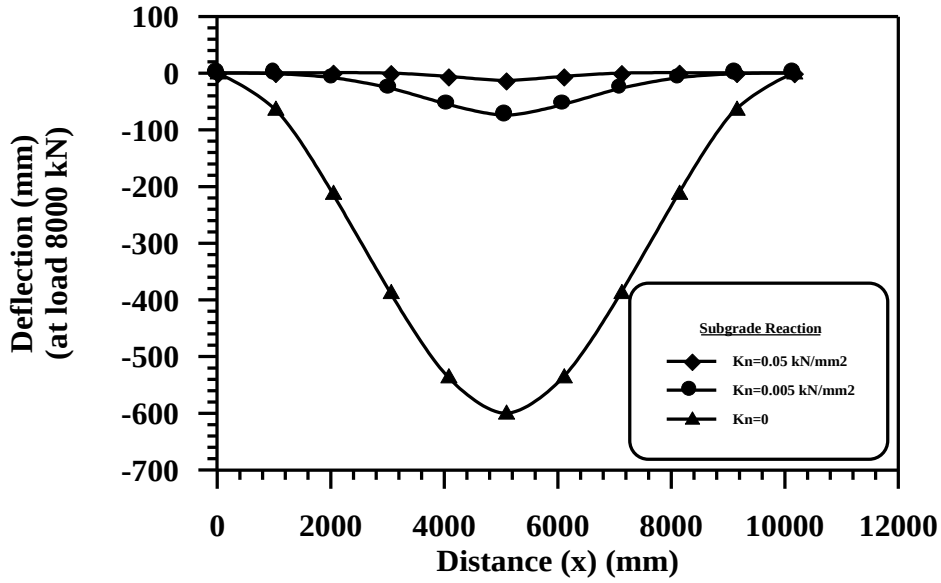

Fig.(6.27): Deflection curve for Vierendeel frame .

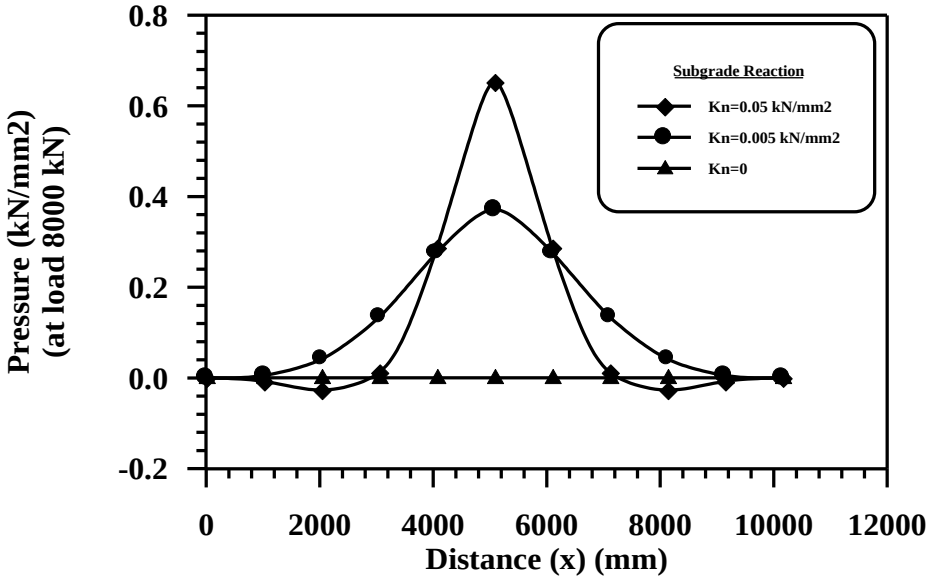

Fig.(6.28): Pressure curve for Vierendeel frame .

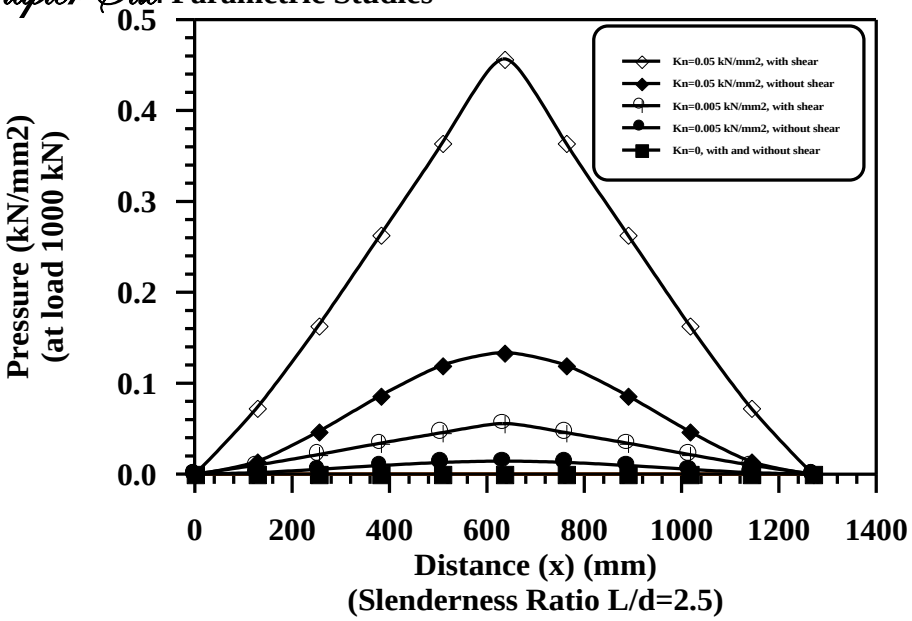

Fig.(6.29): Pressure curve for X-Bracing Truss Beam.

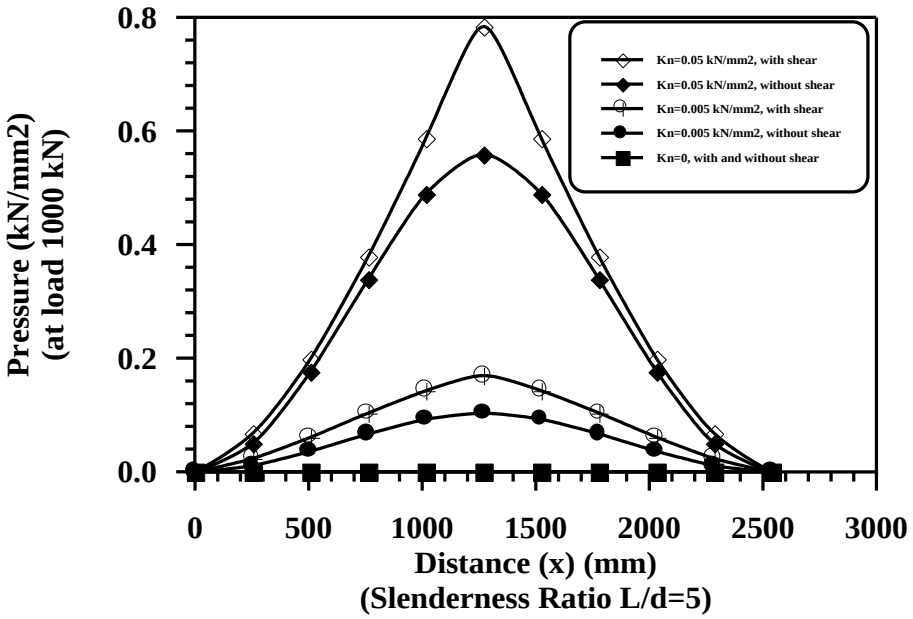

Fig.(6.30): Pressure curve for X-Bracing Truss Beam .

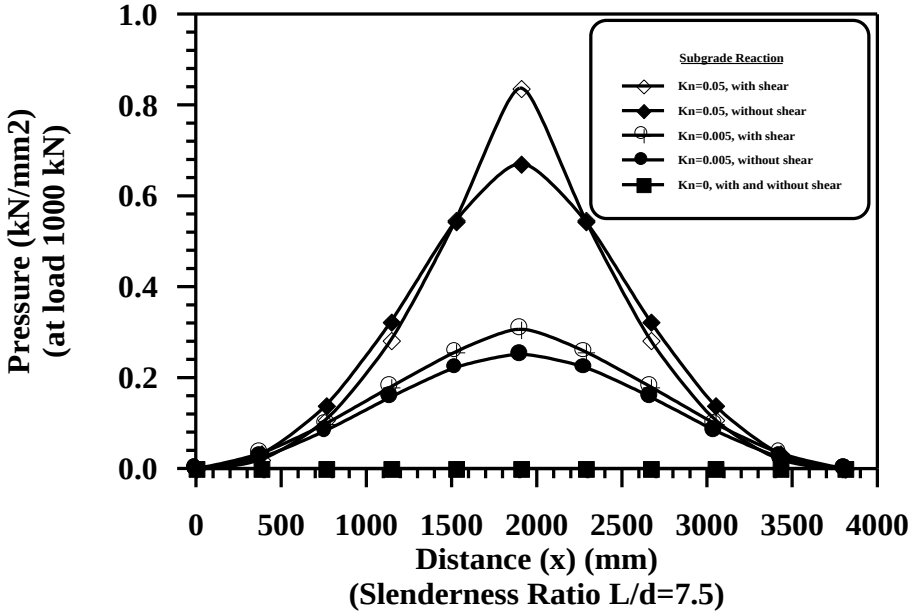

Fig.(6.31): Pressure curve for X-Bracing Truss Beam.

6.3.6 Effect of Large Displacement Analysis on Behavior of Structure

To show the effect of large displacement analysis on the behavior of structure, 3-members extended frame Figure (6.6) [case study No.6] has been chosen for this aim, this frame was analyzed with four values of the vertical load ratio these are (**r=1, 0.999, 0.996, 0.99, and 0.95**), and two values of subgrade reaction (**Kn=50000, and 5000 N/mm2, Kt=Kn/2**). The frame was analyzed for both rigid case and flexible case [linear beam-to-column joint with constant stiffness equal to **10EI/L**] using the arc-length load incrementation strategy with the arc-length iterative. The reference load is (**Fr=1 N**) and the desired number of iteration is (**Jd=3**).

Figures (6.32), to (6.35), show the results of this case study, as shown in these figures, when the vertical load ratio decreases (**r** less than **1**), (i.e. unsymmetrical frame), leads to increase the axial force and the deflection increases too.

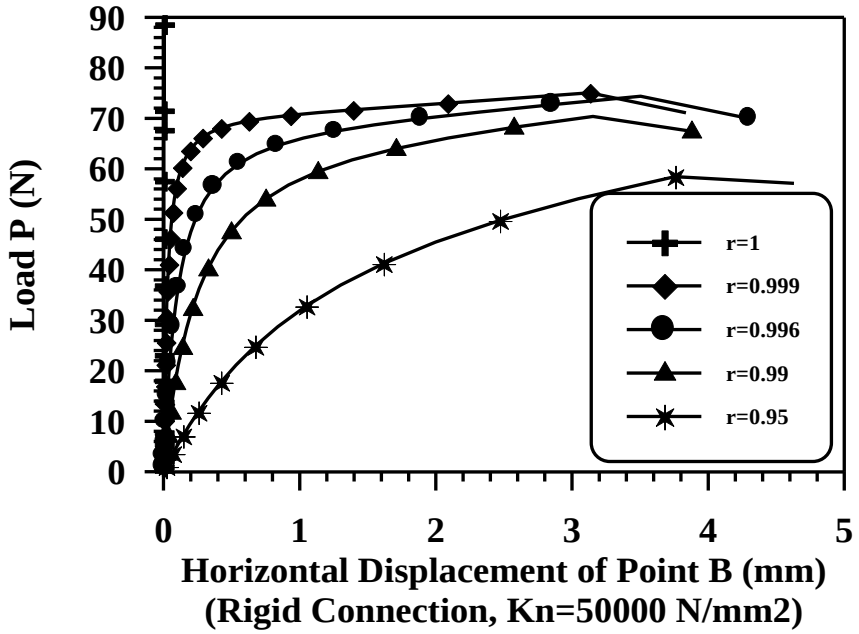

Fig.(6.32): Load-Displacement curve for 3-Member Extended frame.

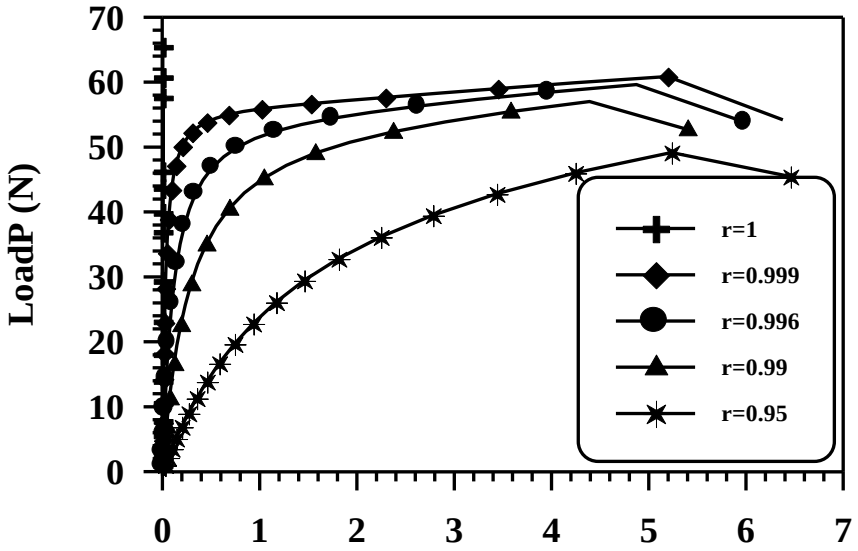

Fig.(6.33): Load-Displacement curve for 3-Member Extended frame.

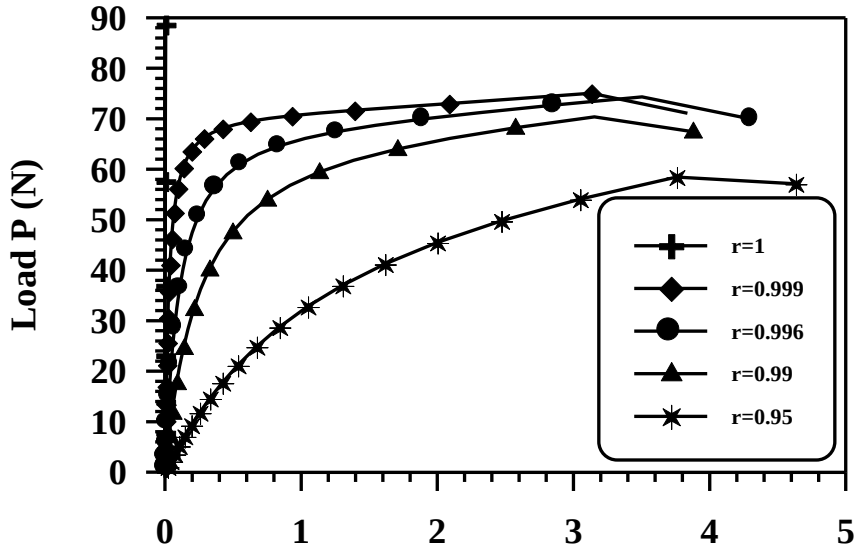

Fig.(6.34): Load-Displacement curve for 3-Member Extended frame.

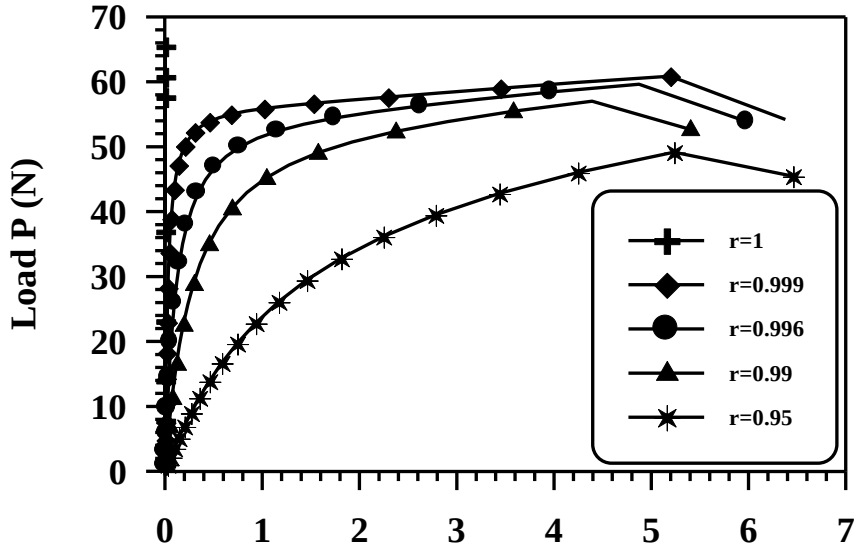

Fig.(6.35): Load-Displacement curve for 3-Member Extended frame.

CHAPTER SEVEN

7

CONCLUSIONS AND RECOMMENDATIONS

7.1 Conclusions

Based on the results obtained in the present study, several conclusions may be drawn. These may be summarized as follows:

1. This investigation shows that the large displacement elastic behavior of plane steel frames with non-prismatic members resting on elastic foundation, subjected to static load including shear effect and having non-linear connections can be accurately predicted by using the beam-column approach of analysis.
2. A comparison between the beam-column approach and the finite element approach reveals similar results but the latter requires a larger number of elements than the former, a point which is in favor of the beam-column approach despite the fact that the derivations of the tangent stiffness matrix of the beam-column approach is more complicated than that of the finite element approach.
3. Shear effect plays a major role governing the behavior of the open-web structure and the deep beams under static loads see Tab.(6.1).
4. The method of equivalent system represents one of the most important and successful techniques, which enable us to replace the actual non-prismatic member with any arbitrary variation in its stiffness ($\mathbf{EI_x}$), with one of uniform stiffness ($\mathbf{EI_1}$). An exact as well as a very accurate approximate solution is obtained that drastically reduces the mathematical complexity of this problem.
5. When the depth ratio increases, the effect of shear deformation will be increased or in other words the effect of shear deformation on non-prismatic member is greater than that of prismatic member.

6. When the slenderness ratio of a structure decreases, the shear parameter increases and consequently the effect of shear on the behavior of that structure will be increased.

7. The effect of shear force will reduce the value of elastic critical load. This reduction in the value of the critical load is larger in the cases of open-web structures and smaller or vanished in the cases of solid web structure.

8. The present modified tangent stiffness matrix which takes into account the two types of non-linearities at the same time (i.e. geometry and connection) and non-prismatic members are efficient in giving accurate results of analysis of different types frames.

9. In the all examples and case studies, the use of load incrementation strategies is efficient for enabling the program to estimate the suitable size of load increments.

10. The determinant technique for a sign detection used in the present study is found to be efficient for detecting the right sign of the initial load increments.

11. The using of any iterative strategy excepts the constant load iterative strategy and not only enables the program to pass limit points, but sometimes reduces the required computing time. And the use of iterative strategies is efficient for enabling the program to change the load level and rapidly achieves the convergencey.

12. The arc-length incrementation strategies with the constant arc-length and minimum residual displacements iterative strategies represent the most efficient techniques in tracing entire load-displacement curves for different types of the steel frames as well as a small CPU time is needed for the analysis.

13. The reference load (**Fr**) can be chosen from (1.3% to 2%) of the load at the first limit point, and a desired number of iteration for the convergence (**Jd**) can be chosen from (3 to 5), for any type of frames with both rigid and flexible connections.

14. The resistance of the frame to the static buckling load can be improved through using tapered member with various tapering ratios for the same volume of steel, and the percentage of increment of this resistance depends on the geometry of the frame and loading condition as well as the type of supports and joints.

15. The results of the analysis show that the displacements when the structure resting on linear elastic foundation are greater than those obtained when the structure is fixed -ended, by (20 - 60 %).

7.2 Recommendations

The following recommendations may be considered as an extension for the present study:

1. This subject requires to be supplemented by experimental results to be obtained from tests on a model or full scale plane steel frames under repeated loading having different types of steel connections, supports conditions by using proportional and non-proportional cyclic loading.
2. The present work has been concerned mainly with effects of geometrical and connection non-linearities. A promising field for extending the present work is to include the material non-linearity.
3. The modified tangent stiffness matrix presented in this study may be modified to include more effects such as the end rigid gusset plates, the variation in the axial force in the member.
4. The post-buckling analysis may be extended to include more iterative strategies like the constant displacement and the minimum residual force iterative strategies.
5. Developing analysis by deriving the exact modified stability and bowing functions of non-prismatic member under compression and tension forces.
6. Extending the present study to consider dynamic analysis.
7. Developing the present study to consider the analysis of space frames.

CHAPTER THREE

THEORY AND DERIVATION

3.1 General

The objective of this chapter is to provide the theoretical basis for the analysis of plane steel structures having non-prismatic members, non-rigid connections, resting on elastic foundation and subjected to static loads including shear effects.

The complete derivation of the conventional tangent stiffness matrix for non-prismatic member in local and global coordinates is presented. The approximate formula **[30]**, for the modified stability and bowing functions including shear effect have been presented too. In addition, a modeling technique for beam-like lattice structures, in which the shear has a significant effect, has been presented.

In addition, a new modified tangent stiffness matrix is derived which takes into account the presence of elastic flexible linear and/or non-linear connection for non-prismatic beam-column resting on elastic foundation under static load including shear effect. Also, a significant difficulty has been encountered in calculating end bending moments and connection rotation due to presence of two highly non-linear equations for each beam-column member. This difficulty has been overcome by solving the two non-linear equations using conventional Newton-Raphson iteration or by using Iterative Analysis Method. Finally, the special procedure used in the calculations of member axial force has been explained in details.

3.2 Modeling of a Beam-Column Element

The modeling of the geometrically non-linear behavior of an elastic beam-column element has been the subject of researches of a number of workers. In general, two approaches can be used:

1. Finite Element Approach **[25,53,55]**.
2. Beam-Column Approach **[13,15,42]**.

In the first approach, the basic idea is relatively simple in theory, but a large number of elements is often needed for satisfactory accuracy. In the

second approach, member force-deformation relations are determined from a more complex, but also more refined, analysis so that fewer elements are generally needed than in the case of a finite element approach.

3.2.1 Finite Element Approach

In this approach, the incremental stiffness matrix in Lagrangian coordinates system has been derived by using the principle of stationary potential energy which leads finally to the expression: -

$$[K_1]\{\Delta x\}=\{\Delta P\} \qquad (3.1)$$

In which $[K_1]$ is the incremental stiffness matrix that relates the incremental displacement $\{\Delta x\}$ to the corresponding incremental element forces $\{\Delta P\}$.

The incremental stiffness matrix in Equation (3.1) consists of the sum of four distinct matrices, that is: -

$$[K]=[K_0]+[K_P]+\frac{EA}{2}[K_1]+\frac{EA}{3}[K_2] \qquad (3.2)$$

Where;

$[K_0]$	:	Conventional linear stiffness matrix.
$[K_P]$	:	Initial stress matrix, which is a linear function of the axial force "**Q**" presented at the beginning of the incremental step.
$[K_1]$,$[K_2]$	:	Non-linear stiffness matrices, consisting respectively of terms that are linear and quadratic functions of the incremental elemental displacements.

In some instances, the non-linear effects due to the change in element forces and displacements occurring during the incremental step are very small compared to the non-linear effects of the forces and deformations that exist at the beginning of the step. When is this, the case $[K_1]$ and $[K_2]$ can be neglected and the stiffness takes the form

$$[K_T]=[K_0]+[K_P] \qquad (3.3)$$

the stiffness matrix will depend only on the internal forces and deformations existing at the beginning of the load step, commonly referred to as tangent stiffness matrix, and used in linear incremental method. If the total load is applied in one step, the $[K_P]$ matrix in Equation (3.2) is set equal to zero, and a stiffness matrix is then called secant stiffness matrix, and used in direct stiffness method. On the other hand, the incremental stiffness matrix, Equation (3.2) is used with all its components in the non-linear incremental method.

To transform the stiffness matrix from local, **[K]**, to global, **[T]**, coordinates, the transformation matrix, **[R]**, is used as

$$[T] = [R]\,[K]\,[R]^T \qquad (3.4)$$

in which the superscript **T** denotes transpose and

$$[R]=\begin{bmatrix}[r] & 0\\ 0 & [r]\end{bmatrix};\quad [r]=\begin{bmatrix}m & -n & 0\\ n & m & 0\\ 0 & 0 & 1\end{bmatrix} \quad \text{..... (3.5)}$$

with $m = \cos\alpha$, $n = \sin\alpha$ ..... (3.6)

where α is the angle between the global and local element coordinate axes.

3.2.2 Beam-Column Approach

In the beam-column approach, Eulerian or updated Lagrangian coordinates are used in developing element stiffness matrix. The effect of geometrical non-linearity is accounted for by coordinate transformation. In formulating the element force-displacement relationships, the basic stiffness matrix obtained is transformed into the element global stiffness matrix by coordinates transformation. The non-linear behavior of the element is represented by the incremental tangent stiffness matrix.

The element developed in the present study is based on the beam-column approach. The term "beam-column" generally refers to an initially straight member subjected to a prescribed combination of axial and lateral loads. In the "conventional beam-column theory" **[22]**, which is as indicated constitutes the basic of the present analysis, the axial force is considered to be much larger than the effects associated with the flexural deformation of the member.

3.2.2.1 System Equilibrium Equation

The equilibrium equations of the structure as a whole can be written symbolically **[22]**

$$f_i(x_1, x_2, \ldots, x_n) - F_i = 0 \quad \text{for } i=1, 2, \ldots, n \quad \text{..... (3.7)}$$

in which x_i = generalized coordinates (essentially, translations and rotations of the joints); F_i = load terms (prescribed external forces and moments acting at the joints); and f_i= non-linear functions representing resultant internal forces corresponding to x_i (obtained by combining member end forces acting at the respectively joints). When the problem is analyzed by the beam-column approach, **{f}** can not be expressed explicitly in terms of **{x}**, because, as previously indicated, member axial force do remain in the picture as auxiliary parameters.

Equation (3.7) can be rewritten in terms of differentials as:

$$\{\Delta F\}=[T]\{\Delta x\} \quad \text{..... (3.8)}$$

where **{Δx}** and **{ΔF}** represent displacements and load increments respectively, and

$$[\mathbf{T}] = \left[\frac{\partial \mathbf{f_i}}{\partial \mathbf{x_i}}\right] \quad \text{..... (3.9)}$$

is the "system tangent stiffness matrix". As will become apparent shortly, Equation (3.8) plays a central role in practically all computational methods that have been suggested for the solution of Equation (3.7).

3.2.2.2 Member Force – Deformation Relation

A typical non-prismatic member of a planner-framed structure, in which a deformed configuration produced by external loads applied at the joints, let **{F}** and **{v}** denote member end forces and end displacements, in global coordinates as shown in Figure (3.1.a).

It should be noted that the elements $\mathbf{v_1}$, $\mathbf{v_2}$, $\mathbf{v_4}$ and $\mathbf{v_5}$ of the 6×1 vector **{v}** represent member end translations, non-dimensionalized via division by **L**, and the corresponding element **{F}**, i.e. $\mathbf{F_1}$, $\mathbf{F_2}$, $\mathbf{F_4}$ and $\mathbf{F_5}$ represent member end forces multiplied by **L**.

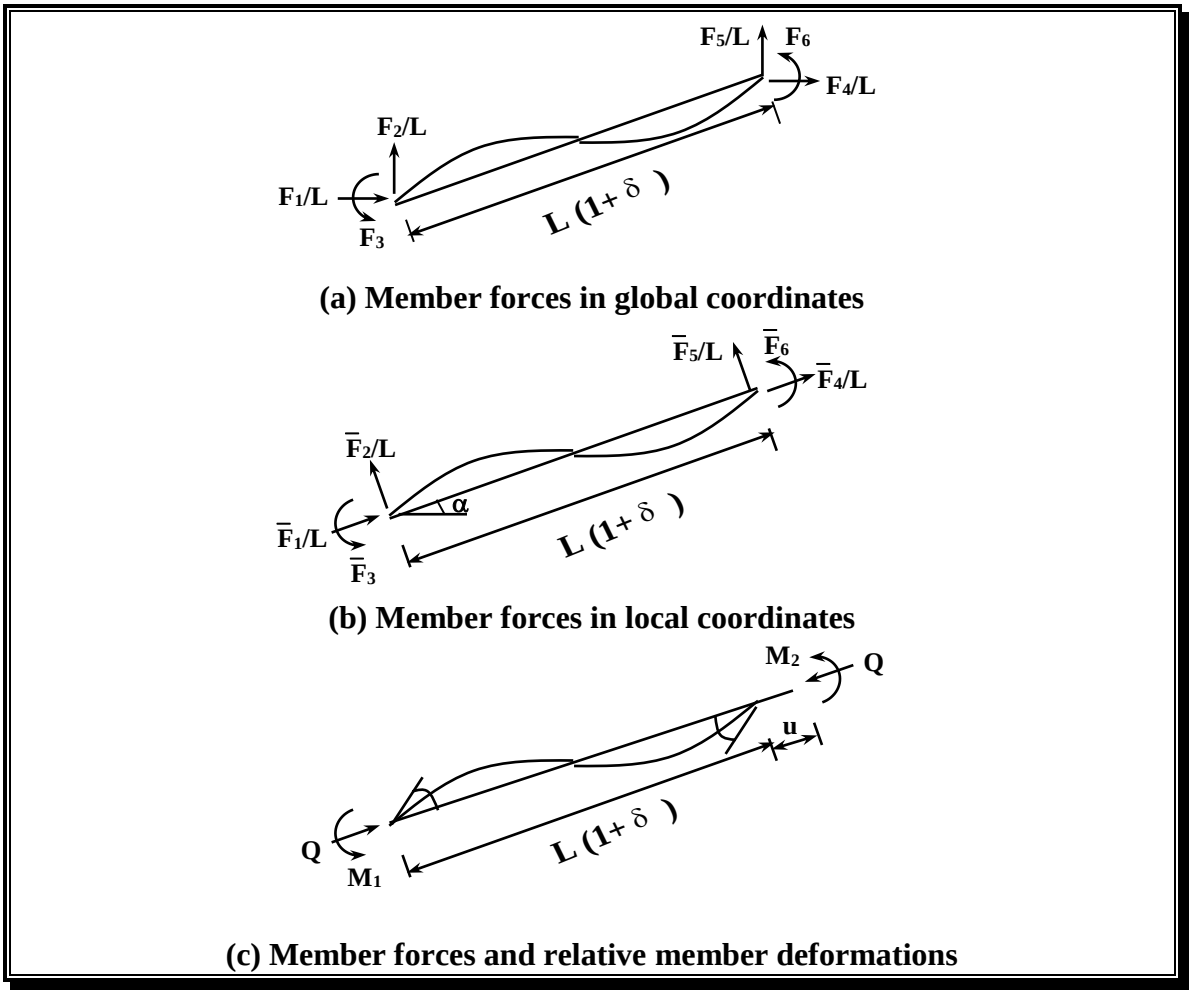

Fig.(3.1): Member End Effects .

Within the limitations of the beam-column theory **[13]**, the governing differential equation **[4]**, of a typical non-prismatic member (Figure 3.2) of an elastic plane frame is

$$\left(\mathbf{E\,I_{(x)}\,y''}\right)'' + \mathbf{Q\,y''} = \mathbf{0} \quad \text{..... (3.10)}$$

subjected to boundary conditions

$$\mathbf{y(0) = 0;\ \ y'(0) = \theta_1;\ y(L) = 0;\ y'(L) = \theta_2} \quad \text{..... (3.11)}$$

Where;

$y(x)$: Lateral deflection function,

Q : Axial force,

E : Modulus of elasticity,

$I_{(x)}$: Variable moment of inertia,

L : Initial length,

θ_1, θ_2 : Prescribed end rotations,

and the prime superscript on **y(x)** denotes one differentiation with respect to **x**.

The solution of Equation (3.10) is of the form

$$\mathbf{y(x) = \theta_1 y_1(x) + \theta_2 y_2(x)} \quad \text{..... (3.12)}$$

In which $\mathbf{y_1(x)}$ and $\mathbf{y_2(x)}$ are particular solutions subject to boundary conditions.

$$\mathbf{y_1(0) = 0;\ y'_1(0) = 1;\ y_1(L) = 0;\ y'_1(L) = 0} \quad \text{..... (3.13)}$$

$$\mathbf{y_2(0) = 0;\ y'_2(0) = 0;\ y_2(L) = 0;\ y'_2(L) = 1} \quad \text{..... (3.14)}$$

In order to separate relative member deformations from rigid body displacements, an Eulerian local reference system is sometimes introduced. Thus the immediate fundamental problem is introduced to that of expressing relative member end forces $\mathbf{M_1}$, $\mathbf{M_2}$ and **Q** in terms of relative member deformations θ_1, θ_2 and **u** as shown in Figure (3.2). The basic member force-deformation relations can be expressed as **[15]**

$$\mathbf{M_1} = \frac{\mathbf{E\,I_0}}{\mathbf{L}}\left(\gamma_1\,\theta_1 + \gamma_2\,\theta_2\right) \quad \text{..... (3.15)}$$

$$\mathbf{M_2} = \frac{\mathbf{E\,I_0}}{\mathbf{L}}\left(\gamma_2\,\theta_1 + \gamma_3\,\theta_2\right) \quad \text{..... (3.16)}$$

$$\mathbf{Q = E\,A_0\,(\eta - C_b)} \quad \text{..... (3.17)}$$

in which;

η : Axial strain (η=u/L)

$\mathbf{I_o}$: Reference moment of inertia,

γ_i : generalized stability functions,

A_0 : Equivalent area of cross section defined by

$$A_0 = \frac{L}{\int_0^L \frac{dx}{A_{(x)}}} \quad \text{..... (3.18)}$$

When $A_{(x)}$ is the variable area of cross section, and it is in the form :-

$$A_{(x)} = A_1\left(1 + C\frac{x}{L}\right)^n \quad \text{..... (3.19)}$$

The equivalent area of the cross-section is important to determine the axial force (**Q**) as in Equation (3.17).

For the tapared member as shown in Figure (3.3), the relationship between the axial force and the axial deformation may be in general expressed by using equivalent area (A_o) as follows: -

$$Q = (E\ A_o / L)\ u \quad \text{..... (3.20)}$$

The axial deformation under constant axial force may be obtained as follows:

$$u = \frac{Q}{E}\int_0^L \frac{dx}{A_{(x)}} \quad \text{..... (3.21)}$$

Substituting Equation (3.20) into Equation (3.21) yields Equation (3.18). Substituting Equation (3.19) into Equation (3.18) yields

$$A_0 = \frac{L}{\int_0^L \frac{dx}{A_1\left(1 + c\frac{x}{L}\right)^n}} \quad \text{..... (3.22)}$$

Here, the integration result depends on the shape factor **n**. Where (**n**) may be defined as: -

$$n = \frac{\log\left(\frac{A_2}{A_1}\right)}{\log D} \quad \text{..... (3.23)}$$

Where;

A_1: Area of small side, and

A_2: Area of large side

D: Depth ratio ($D=d_2/d_1$)

For **n** = 1

$$\mathbf{A_0} = \frac{\mathbf{D-1}}{\mathbf{\ln D}}\mathbf{A_1} \quad \text{..... (3.24)}$$

For **n** ≠ 1

$$\mathbf{A_0} = \frac{(\mathbf{D-1})(\mathbf{1-n})}{\mathbf{D^{1-n}-1}}\mathbf{A_1} \quad \text{..... (3.25)}$$

If the member is prismatic (i.e., **D** =1), then $\mathbf{A_0 = A_1}$.

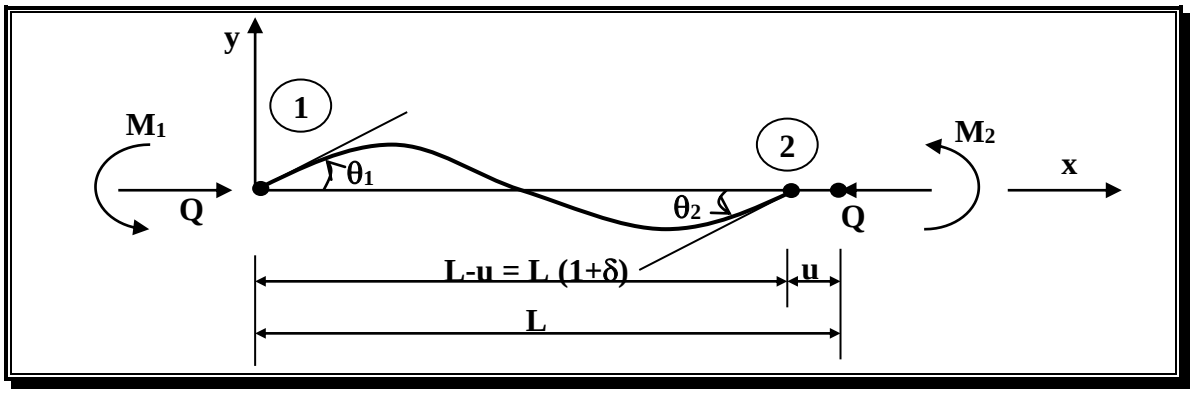

Fig.(3.2):Relative Member Displacements and Associated Forces in Local Coordinates for Non-Prismatic Member .

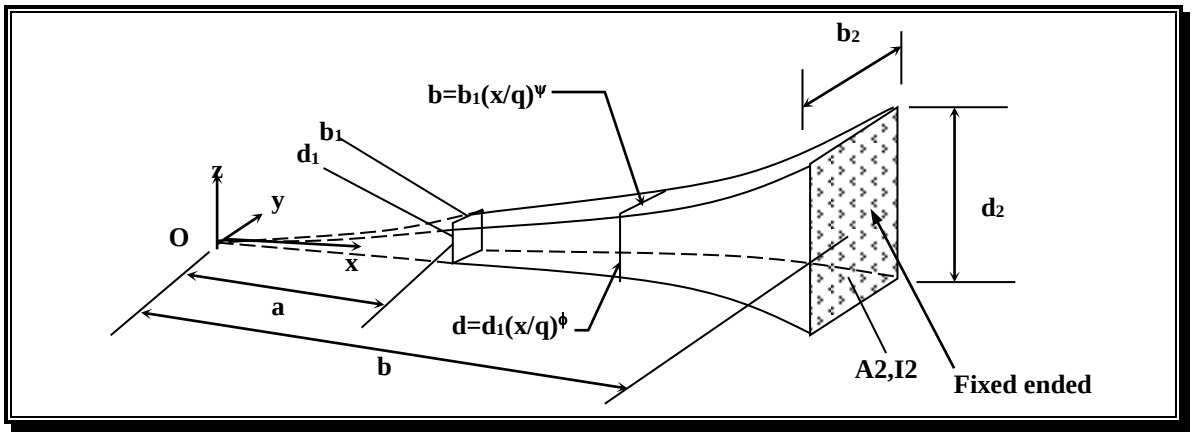

Fig.(3.3): Tapered Cantilever Beam with Rectangular Cross-Section .

The length correction factor for bowing action, $\mathbf{C_b}$, is of the form

$$\mathbf{C_b} = \beta_1\theta_1^2 + 2\beta_2\theta_1\theta_2 + \beta_3\theta_2^2 \quad \text{..... (3.26)}$$

in which (β_1) is the generalized bowing functions.

From the general moment – curvature relation, and in view of Equations (3.12), (3.13), (3.14), (3.15) and (3.16)

$$\gamma_1 = -\frac{I_1}{I_0} L y_1''(0) \quad \text{..... (3.27)}$$

$$\gamma_2 = -\frac{I_1}{I_0} L y_2''(0) = \frac{I_2}{I_1} L y_1''(L) \quad \text{..... (3.28)}$$

$$\gamma_3 = \frac{I_2}{I_0} L y_2''(L) \quad \text{..... (3.29)}$$

in which I_1 and I_2 are moments of inertia at node **1** and **2**, respectively. Similarly, the bowing functions are given by:

$$\beta_1 = \frac{1}{2L} \int_0^L (y_1')^2 \, dx \quad \text{..... (3.30)}$$

$$\beta_2 = \frac{1}{2L} \int_0^L y_1' y_2' \, dx \quad \text{..... (3.31)}$$

$$\beta_3 = \frac{1}{2L} \int_0^L (y_2') dx \quad \text{..... (3.32)}$$

Note that γ_i and β_i may be viewed as functions of a dimensionless axial force parameter, q_0, defined by

$$q_0 = \frac{Q L^2}{\pi^2 E I_o} \quad \text{..... (3.33)}$$

For the special case of a prismatic member (**EI** = constant), one have

$$\gamma_1 = \gamma_3 = C_1 \; ; \; \gamma_2 = C_2 \quad \text{..... (3.34)}$$

and $$C_b = b_1(\theta_1 + \theta_2)^2 + b_2(\theta_1 - \theta_2)^2 \quad \text{..... (3.35)}$$

from which

$$\beta_1 = \beta_3 = b_1 + b_2 \; ; \; \beta_2 = b_1 - b_2 \quad \text{..... (3.36)}$$

in which C_1, C_2 = conventional stability functions of prismatic member (see Appendix (A)), and, b_1, b_2 = bowing functions of prismatic member (see Appendix (A)).

3.2.2.3 Modified Stability Function-Approximate Formula

The full derivations of modified stability functions for non-prismatic members produced by ***Al-Sarraf*** **[30]**, are presented here in detail.

Figure (3.3) shows the non-prismatic beam-column element subjected to constant axial force (**Q**). The basic differential equation of elastic curve is: -

$$E I_{(x)} \frac{d^2y}{dx^2} + Qy = M_1 \frac{x-b}{L} + M_2 \frac{x-a}{L} \quad \text{..... (3.37)}$$

Where;

y : is the lateral deflection at distance (**x**) along the member ,

a : is the distance of end (**1**) from the origin (**0**) (point of zero depth)

b : is the total distance (**b=a+L**)

A member may be uniformly tapered in either one or two direction. Therefore, the depth **d(x)** may be expressed by :-

$$d_{(x)} = d_1 \left(\frac{x}{a} \right) \text{.....(3.38)}$$

The moment of inertia of the cross-sectional area of the member about the axis of buckling may be expressed in the form: -

$$I_{(x)} = I_1 \left(\frac{x}{a} \right)^m \quad \text{..... (3.39)}$$

Where;

I(x) : is the moment of inertia at distance (**x**) from the origin (**0**) ,

m : is the shape factor that depends on the cross-sectional shape and dimensions of the member .

The shape factor (m) may be evaluated by observing that Equation (3.39) must give (**$I_{(x)}=I_2$**) when (**x=b**).This condition yields the relation:-

$$m = \frac{\log\left(\frac{I_2}{I_1} \right)}{\log D} \quad \text{..... (3.40)}$$

Therefore, the shape factor can be determined once the dimensions of the end cross-sections which are known. For members of rectangular cross-sections, the shape factor is equal to either (**1**) or (**3**) depending on the axis about which buckling occurs. A member having an open web, or an open box section consisting of equal area at the corner, has a value of (**2**) and a tapared member with solid circular or square cross-section has a value of (**4**). For member of wide flange shape or closed box section, the shape factor will be between the limits (**2.1-2.6**).

The solution of the basic differential equation of elastic curve for non-prismatic members, Equation (3.37), depends on the value of the shape factor (**m**), for (**m=4**), the exact evaluating of these functions are very easy, and for (**m=3,2.4,2** and **1**), the presence of Bassel functions makes the problem very complicated and involves the use of higher mathematics, (i.e.

the use of Bassel functions of the first and second kind and other associated functions which are beyond the scope of this study), therefore , the present study is based on a good approximation to the modified stability functions for non-prismatic member produced by ***Al-Sarraf*** **[30]**.

$$\gamma_1 = D^{\phi m/4} C_1 \quad \text{..... (3.41)}$$

$$\gamma_2 = D^{(\phi+1)m/4} C_2 \quad \text{..... (3.42)}$$

$$\gamma_3 = D^{(\phi+2)m/4} C_1 \quad \text{..... (3.43)}$$

Where;

$\gamma_1, \gamma_2, \gamma_3$: Are the stability functions of non-prismatic member.

C_1, C_2: Are the stability functions of prismatic member with constant moment of inertia ($D^{\phi m/2} I_1$) , and have axial load parameter ($q=q_o/D^{\phi m/2}$)

and ϕ is a correction factor. The value of ϕ depends on the shape factor **m**. for $m = 4$, $\phi = 1$ and for $m \leq 3$, ϕ is obtained from

$$\phi = 10.4 + 0.08\,(3-m) \quad \text{..... (3.44)}$$

These approximate formula for the modified stability functions can be used for compression, zero, tensile axial force by using the suitable prismatic stability functions (C_1) and (C_2) in each case and it has a good accuracy to the exact value.

3.2.2.4 Modified Bowing Function

In connection with prismatic members, ***Saafan*** **[7]** derived the relations:

$$b_1 = \frac{(C_1 + C_2)(C_2 - 2)}{8\pi^2 q} \quad \text{..... (3.45)}$$

$$b_2 = \frac{C_2}{8(C_1 + C_2)} \quad \text{..... (3.46)}$$

Which are useful mainly in calculating the numerical values of b_1 and b_2 for a given value of **q**. ***Oran*** **[13]** established the following alternate relations, which play a major role in the derivation of consistent and symmetric tangent stiffness matrices:

$$b_1 = -\frac{C_1' + C_2'}{4\pi^2} \quad \text{..... (3.47)}$$

$$b_2 = -\frac{C_1' - C_2'}{4\pi^2} \quad \text{..... (3.48)}$$

in which a prime superscript denotes one differentiation with respect to **q**.

While Equations (3.45) and (3.46) appear to represent special relations that may not be directly extended to tapered members, Equations (3.47) and (3.48) do reflect an inherent property of the general beam-column problem, as seen from the following analysis.

Assuming that the axial force **[15], Q**, is applied first and is followed by $\mathbf{M_1}$ and $\mathbf{M_2}$, the work of external forces (which, incidentally, is stored as strain energy) is given by

$$\mathbf{U = \frac{1}{2}\left(M_1\,\theta_1 + M_2\,\theta_2\right) + QLC_b + \frac{QL\varepsilon_o}{2}} \quad \text{..... (4.49)}$$

in which ε_0 is effective axial strain given by

$$\mathbf{\varepsilon_0 = \frac{Q}{EA_0}} \quad \text{..... (3.50)}$$

By substituting Equations (3.15), (3.16), (3.26), (3.33) and (3.50) into Equation (3.49)

$$\mathbf{U = \frac{EI_0}{2L}\left[\left(\gamma_1\theta_1^2 + 2\gamma_2\theta_1\theta_2 + \gamma_3\theta_2^2\right) + 2\pi^2 q_0\left(\beta_1\theta_1^2 + 2\beta_2\theta_1\theta_2 + \beta_3\theta_2^2\right) + \frac{\pi^4 q_0^2}{\lambda_0^2}\right]} \text{... (3.51)}$$

Then, differentiating with respect to $\mathbf{q_0}$ (while θ_1 and θ_2 remain constant):

$$\mathbf{\frac{dU}{dq_0} = \frac{EI_0}{2L}\left[\left(\gamma_1'\theta_1^2 + 2\gamma_2'\theta_1\theta_2 + \gamma_3'\theta_2^2\right) + 2\pi^2\left(\beta_1\theta_1^2 + 2\beta_2\theta_1\theta_2 + \beta_3\theta_2^2\right)\right.}$$

$$\mathbf{\left. + 2\pi^2 q_0\left(\beta_1'\theta_1^2 + 2\beta_2'\theta_1\theta_2 + \beta_3'\theta_2^2\right) + \frac{2\pi^4 q_0^2}{\lambda_0^2}\right]} \quad \text{..... (4.52)}$$

in which

$$\mathbf{\lambda_0^2 = \frac{A_0 L^2}{I_0}} \quad \text{..... (3.53)}$$

and a prime superscript on γ_i or β_i indicates one differentiation with respect to $\mathbf{q_o}$.

Assume now that the loading sequence is reversed, i.e., suitable end moments are first applied to produce the end rotations θ_1 and θ_2, while **Q** remains equal to zero. Next the axial force, **Q**, is applied gradually while θ_1 and θ_2 are kept constant. During the second stage of the indicated loading sequence

$$\mathbf{dU = QL\,d\eta = QL\,(d\varepsilon_o + dC_b)} \quad \text{..... (3.54)}$$

Substituting Equations (3.26), (3.33), (3.50) and (3.53) into Equation (3.54),

$$\frac{dU}{dq_0} = \frac{EI_0}{2L}\left[\frac{2\pi^4 q_0}{\lambda_0^2} + 2\pi^2 q_0\left(\beta'_1\theta_1^2 + 2\beta'_2\theta_1\theta_2 + \beta'_3\theta_2^2\right)\right] \quad (3.55)$$

Finally, equating the right-hand sides of Equations (3.52) and (3.55) yields

$$\beta_i = -\frac{\gamma'_i}{2\pi^2} \quad ; \quad \text{for} \quad i = 1,2,3 \quad (3.56)$$

3.2.2.5 Modified Bowing Functions- Approximate Formula

In connection with approximate stability functions presented in Equations (3.41), (3.42) and (3.43), the values of (γ_i) can be obtained as: -

$$\gamma_1 = D^{\phi m/4} C_1 \quad (3.57)$$

$$\gamma_2 = D^{(\phi+1)m/4} C_2 \quad (3.58)$$

$$\gamma_3 = D^{(\phi+2)m/4} C_1 \quad (3.59)$$

$$q_o = D^{\phi m/2} q \quad (3.60)$$

The derivative of the modified stability functions with respect to the axial force parameter, q_o , is obtained by using the chain rule theory .

$$\gamma'_1 = [D^{\phi m/4} / D^{\phi m/2}] C'_1 = D^{-\phi m/4} C'_1 \quad (3.61)$$

$$\gamma'_2 = D^{(1-\phi)m/4} C'_2 \quad (3.62)$$

$$\gamma'_3 = D^{(2-\phi)m/4} C'_1 \quad (3.63)$$

and by using the same theory , the second derivatives with respect to, q_o are:-

$$\gamma''_1 = D^{-3\phi m/4} (C''_1) \quad (3.64)$$

$$\gamma''_2 = D^{(1-3\phi)m/4} (C''_2) \quad (3.65)$$

$$\gamma''_3 = D^{(1-3\phi)m/4} (C''_1) \quad (3.66)$$

Where;

$$C'_1 = -2\pi^2 (b_1+b_2) \quad (3.67)$$

$$C'_2 = -2\pi^2 (b_1-b_2) \quad (3.68)$$

$$C''_2 = -2\pi^2 (b'_1+b'_2) \quad (3.69)$$

$$C''_1 = -2\pi^2 (b'_1-b'_2) \quad (3.70)$$

Now, substituting Equations (3.61),(3.62) and (3.63) into Equation (3.59) , utilizing Equations (3.67) and (3.68) yield the relationships between the bowing functions of non-prismatic members and that of prismatic one as follows:-

$\beta_1 = D^{-\phi m/4}\ (b_1+b_2)$ ..... (3.71)

$\beta_2 = D^{(1-\phi)m/4}\ (b_1-b_2)$ ..... (3.72)

$\beta_3 = D^{(2-\phi)m/4}\ (b_1+b_2)$ ..... (3.73)

and it is derivatives with respect to ,q_o , are :-

$\beta'_1 = D^{-3\phi m/4}\ (b'_1+b'_2)$ ..... (3.74)

$\beta'_2 = D^{(1-3\phi)m/4}\ (b'_1-b'_2)$ ..... (3.75)

$\beta'_3 = D^{(2-3\phi)m/4}\ (b'_1+b'_2)$ ..... (3.76)

It may be noted that the modified bowing functions are exact for a member having the shape factor (m=4), and are approximate with good accuracy for other shape factors. These functions can be used for compression, zero and tensile axial force by using the suitable stability and bowing functions and their derivatives in each case.

To check the correctness of this approximate method and the reliability of program (NSHEEFF), a comparison is made with the results obtained by ***Al-Damerchi*** **[79]** who used the exact method and by ***Oran*** **[15]** who used the numerical method. ***Oran's*** example is a tapered member with rectangular cross-section and depth varying linearly form **(h)** at end 1 (**x**=0) to **(h/2)** at end 2 (**x=L**); (i.e., the shape factor **m**=3 and the depth ratio **(D=2)**. His numerical results correspond to a fixed value of step size $\Delta x = 0.01\ L$. The comparison is given in Table (3.1).

3.2.2.6 Tangent Stiffness Matrix for Relative Deformations

The relation between incremental values of **Si** and **ui** can be expressed as **[15]**

$\{\Delta S\} = \{t\}\{\Delta u\}$ ..... (3.77)

where **[t]** is the tangent stiffness matrix for relative deformations with

$$t_{ij} = \frac{\partial S_i}{\partial u_j} + \frac{\partial S_i}{\partial q_0}\frac{\partial q_o}{\partial u_j} \quad ; \quad \text{for} \quad i,j = 1,2,3 \quad \text{..... (3.78)}$$

The derivatives $\partial q_0/\partial u_j$, are to be obtained from Equation (3.17) which by virtue of equations (3.26), (3.33) and (3.53), can be rewritten in the form

$$\frac{\pi^2 q_o}{\lambda_o^2} = \eta - \left(\beta_1\theta_1^2 + 2\beta_2\theta_1\theta_2 + \beta_3\theta_2^2\right) \quad \text{..... (3.79)}$$

Using a notation consistent with that of Ref.**[13]**

Table (3.1): Comparison between the approximate stability and bowing functions form [85] with those obtained by exact method from Al-Damerchi [79] and a numerical method from Oran [15]

q_o	Functions	Al-Khafaji H.	Al-Damerchi	Oran
		Approximate	Exact	Numerical
0.6	γ_1	0.7022	0.68144	0.681
	γ_2	1.0871	1.08991	1.090
	γ_3	0.2483	0.23939	0.239
	γ'_1	-4.0028	-4.08915	-4.088
	γ'_2	1.1119	1.15115	1.151
	γ'_3	-1.4152	-1.44507	-1.445
	γ''_1	-6.0501	-6.36374	-6.360
	γ''_2	2.9177	3.08605	3.085
	γ''_3	-2.1390	-2.24837	-2.248
	β_1	0.2028	0.20716	0.2071
	β_2	-0.0563	-0.05832	-0.0583
	β_3	0.0171	0.07321	0.0732
0.7	γ_1	0.2681	0.23682	0.237
	γ_2	1.2148	1.22262	1.223
	γ_3	0.0948	0.08227	0.082
	γ'_1	-4.7199	-4.84696	-4.846
	γ'_2	1.4662	1.52761	1.528
	γ'_3	-1.6687	-1.71281	-1.712
	γ''_1	-8.4835	-9.00686	-9.002
	γ''_2	4.2792	4.56816	4.5665
	γ''_3	-2.9994	-3.18214	-3.181
	β_1	0.2391	0.24555	0.2455
	β_2	-0.0743	0.07739	-0.0773
	β_3	0.0845	0.08677	0.0868
0.8	γ_1	-0.2522	-0.29934	-0.299
	γ_2	1.3862	1.40188	1.402
	γ_3	-0.0892	-0.10720	-0.107
	γ'_1	-5.7527	-5.95041	-5.949
	γ'_2	1.9989	2.09982	2.100
	γ'_3	-2.0339	-2.10265	-2.102
	γ''_1	-12.5410	-13.47864	-13.471
	γ''_2	6.5906	7.12039	7.1175
	γ''_3	-4.4339	-4.6194	-4.761
	β_1	0.2914	0.30145	0.3014
	β_2	-0.1013	-0.10638	-0.1063
	β_3	0.103	0.10652	0.1065

$$\frac{\partial q_0}{\partial \theta_1} = \frac{G_1}{\pi^2 H}\ ;\ \frac{\partial q_0}{\partial \theta_2} = \frac{G_2}{\pi^2 H};\ \frac{\partial q_0}{\partial \eta} = \frac{1}{H} \quad \text{..... (3.80)}$$

where;

$$G_1 = -2\pi^2\left(\beta_1\theta_1 + \beta_2\theta_2\right) = \gamma_1'\theta_1 + \gamma_2'\theta_2 \quad \text{..... (3.81)}$$

$$G_2 = -2\pi^2\left(\beta_2\theta_1 + \beta_3\theta_2\right) = \gamma_2'\theta_1 + \gamma_3'\theta_2 \quad \text{..... (3.82)}$$

$$H = \frac{\pi^2}{\lambda_0^2} + \left(\beta_1'\theta_1^2 + 2\beta_2'\theta_1\theta_2 + \beta_3'\theta_2^2\right) \quad \text{..... (3.83)}$$

Substituting Equations (3.15), (3.16) and (3.80) into Equation (3.78) yields

$$[t] = \frac{E I_0}{L}\begin{bmatrix} \gamma_1 + \frac{G_1^2}{\pi^2 H} & \gamma_2 + \frac{G_1 G_2}{\pi^2 H} & \frac{G_1}{H} \\ \gamma_2 + \frac{G_1 G_2}{\pi^2 H} & \gamma_3 + \frac{G_2^2}{\pi^2 H} & \frac{G_2}{H} \\ \frac{G_1}{H} & \frac{G_2}{H} & \frac{\pi^2}{H} \end{bmatrix} \quad \text{..... (3.84)}$$

Note that [**t**] is symmetric and as previously indicated, a prime superscript on γ_i or β_i indicates one differentiation with respect to q_0.

3.2.2.7 Tangent Stiffness Matrix in Global Coordinates

Let **[T]** denote the 6×6 member tangent stiffness matrix in the global coordinates shown in Figure (3.4).

{ΔF} = [T] {Δv} ..... (3.85)

and **[B]** the 6 × 3 instantaneous static matrix so that

{F} = [B] {S} ..... (3.86)

{Δu} = [B]^T {Δv} , ... (3.87)

in which the superscript **T** denotes transpose and , **{Δu}**and **{Δv}**are incremental displacements in local and global coordinates respectively .

For geometric considerations, **[B]** can be defined as: -

$$[B] = \begin{bmatrix} -\frac{n}{1+\delta} & -\frac{n}{1+\delta} & m \\ \frac{m}{1+\delta} & \frac{m}{1+\delta} & n \\ 1 & 0 & 0 \\ \frac{n}{1+\delta} & \frac{n}{1+\delta} & -m \\ -\frac{m}{1+\delta} & -\frac{m}{1+\delta} & -n \\ 0 & 1 & 0 \end{bmatrix} \quad \text{..... (3.88)}$$

with **n=sin(α)** ; **m=cos(α)**..... (3.89)

Note that the angle (α) , refers to the deformed configuration of member .

The relative local member deformations can be expressed directly in terms of global displacements, **{v}**, by noting that

$$\theta_1 = \theta'_1 + \Delta v_3 - \rho \quad \text{..... (3.90)}$$

$$\theta_2 = \theta'_2 + \Delta v_6 - \rho \quad \text{..... (3.91)}$$

$$v = -\delta L = L - L_c \quad \text{..... (3.92)}$$

$$\text{With} \quad \rho = \alpha - \alpha'' \quad \text{..... (3.93)}$$

In these Equations θ'_i = 1,2 are the nodal rotations of the equilibrium configuration of the i-th increment, Δv_i, i=3,6 are the incremental nodal rotations in the global coordinates, α'' refers to the orientation of the chord in the undeformed configuration, as shown in Figure (3.4), and ρ is the angle of rotation of the chord, L_c is the member chord length of deformed configuration.

For arbitrary large chord rotations **[52]**

$$\tan\alpha'' = \frac{y_2 - y_1}{x_2 - x_1} \quad \text{..... (3.94)}$$

$$\tan\alpha = \frac{y_2 - Lv_5 - y_1 - Lv_2}{X_2 + Lv_4 - X_1 - Lv_1} \quad \text{..... (3.95)}$$

$$L = \left[(x_2 - x_1)^2 + (y_2 - y_1)^2\right]^{0.5} \quad \text{..... (3.96)}$$

and

$$L_c = L(1+\delta) = L - u = [(x_2 + Lv_4 - x_1 - Lv_1)^2 + (y_2 + Lv_5 - y_1 - Lv_2)^2]^{0.5} \quad \text{..... (3.97)}$$

in which **y** and **x** is the global coordinates of member joints in the initial undeformed configuration. Now, to compute the tangent stiffness matrix in global coordinates, Equation (3.86) should be rewritten in incremental form

$$\{\Delta F\} = [B]\{\Delta S\} + \{\Delta B\}\{S + \Delta S\} \quad \text{..... (3.98)}$$

Substitute Equations (3.77) and (3.87) into Equation (3.97) yields

$$\{\Delta F\} = [B][t][B]^T\{\Delta v\} + [\Delta B]\{S\} \quad \text{..... (3.99)}$$

in which {**S**} refers to the internal forces at the end of load step, and

$$[\Delta B]=\begin{bmatrix} \frac{-\Delta n(1+\delta)+n\Delta\delta}{(1+\delta)^2} & \frac{-\Delta n(1+\delta)+n\Delta\delta}{(1+\delta)^2} & \Delta m \\ \frac{\Delta m(1+\delta)-m\Delta\delta}{(1+\delta)^2} & \frac{\Delta m(1+\delta)-m\Delta\delta}{(1+\delta)^2} & \Delta n \\ 0 & 0 & 0 \\ \frac{\Delta n(1+\delta)-n\Delta\delta}{(1+\delta)^2} & \frac{\Delta n(1+\delta)-n\Delta\delta}{(1+\delta)^2} & -\Delta m \\ \frac{-\Delta m(1+\delta)+m\Delta\delta}{(1+\delta)^2} & \frac{-\Delta m(1+\delta)+m\Delta\delta}{(1+\delta)^2} & -\Delta n \\ 0 & 0 & 0 \end{bmatrix} \quad \text{..... (3.100)}$$

in which

$$\Delta_m=\frac{\left[mn(\Delta v_2-\Delta v_5)+n^2(-\Delta v_1+\Delta v_4)\right]}{(1+\delta)} \quad \text{..... (3.101)}$$

$$\Delta_n=\frac{\left[m^2(-\Delta v_2+\Delta v_5)+nm(\Delta v_{`1}+\Delta v_4)\right]}{(1+\delta)} \quad \text{..... (3.102)}$$

$$\Delta\delta=\left[n(-\Delta v_2+\Delta v_5)+m(-\Delta v_1+\Delta v_4)\right] \quad \text{..... (3.103)}$$

Equations (3.101), (3.102) and (3.103) can be obtained from the geometry of Figure (3.5).

To obtain [**T**], let an arbitrary element of [**ΔB**] be written as **[13]**

$$\Delta B_{ik}=\sum_{j=1}^{6} g_{ij}^{(k)}\,\Delta v_j \quad \text{..... (3.104)}$$

Thus, defining three 6×6 matrices, [$\mathbf{g^{(1)}}$], [$\mathbf{g^{(2)}}$] and [$\mathbf{g^{(3)}}$], which incidentally, are symmetric **[42]**:

$$[g^{(1)}]=[g^{(2)}]=\frac{1}{(1+\delta)^2}\begin{bmatrix} -2mn & m^2-n^2 & 0 & 2mn & -(m^2-n^2) & 0 \\ m^2-n^2 & 2mn & 0 & -(m^2-n^2) & -2mn & 0 \\ 0 & 0 & 0 & 0 & 0 & 0 \\ 2mn & -(m^2-n^2) & 0 & -2mn & m^2-n^2 & 0 \\ -(m^2-n^2) & -2mn & 0 & m^2-n^2 & 2mn & 0 \\ 0 & 0 & 0 & 0 & 0 & 0 \end{bmatrix} \quad \text{... (3.105)}$$

and

$$\left[g^{(3)}\right]=\frac{1}{(1+\delta)}\begin{bmatrix} -n^2 & mn & 0 & n^2 & -mn & 0 \\ mn & -m^2 & 0 & -mn & m^2 & 0 \\ 0 & 0 & 0 & 0 & 0 & 0 \\ n^2 & -mn & 0 & -n^2 & mn & 0 \\ -mn & m^2 & 0 & mn & -m^2 & 0 \\ 0 & 0 & 0 & 0 & 0 & 0 \end{bmatrix} \quad \text{..... (3.106)}$$

From Equation (3.104)

$$[\Delta B]\{S\}=\left[\sum_{k=1}^{3} S_k\left[g^{(k)}\right]\right]\{\Delta v\} \quad \text{..... (3.107)}$$

Finally, comparing Equation (3.99) and (3.85) gives

$$[T]=[B][t][B]^T+\sum_{k=1}^{3}\delta_k\left[g^{(k)}\right] \quad \text{..... (3.108)}$$

note that **[T]** is symmetric.

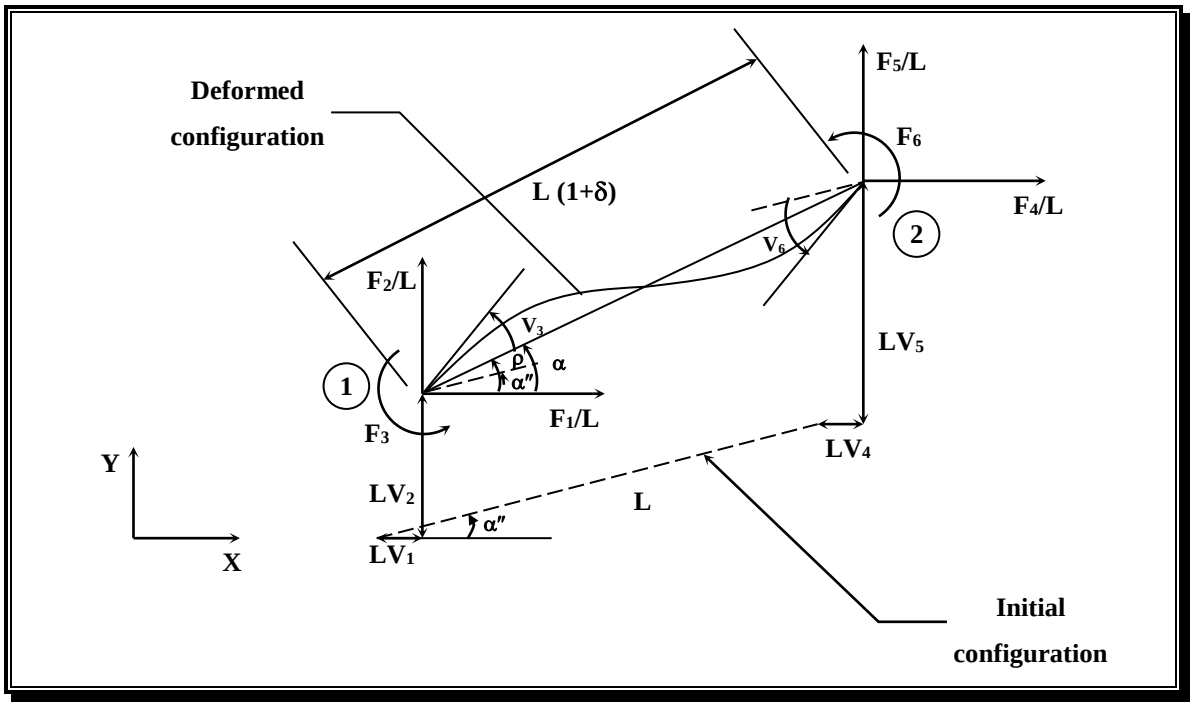

Fig.(3.4): Member Force and Deformations in Global Coordinates .

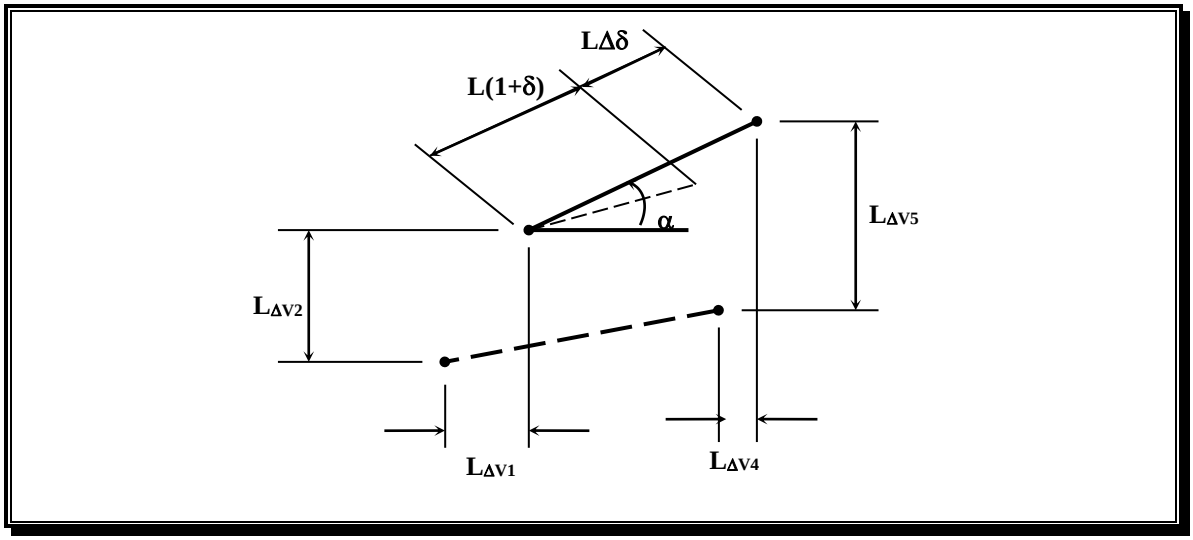

Fig.(3.5): Relative Member Incremental Displacement in Local and Global Coordinates .

3.3 Shear Effect

There are a little researches have covered shear effect on the stability and bowing functions of non-prismatic members. Most of researches used approximate methods for including such effect by converting a non-prismatic member to a prismatic one with the depth equal to the average of the upper and lower depths for non-prismatic member. The approximate method is preferred to exact one because of it's simplicity, while in the exact method the presence of Bessel functions in the solution of the differential equation makes the problem very complicated as it was mentioned earlier.

In the present study, an approximate method proposed by ***Al-Sarraf*** **[30]**, for calculating stability functions and by ***Oran*** **[15],** for calculating bowing functions of non-prismatic members is used and it is extended to including the effect of shear on stability and bowing functions on such members as it will be explained below.

3.3.1 Shear Flexibility Parameter

The shear effect on elastic stability analysis depends on the type of structure, whether it is open or closed web structure. The open web structure exhibits relatively higher shear deformation than the solid one. Therefore, we must introduce a parameter that gives us a sense about how much the effect of shear deformation will be on that structure, or we can say that, when this parameter has a large value, this means that the effect of shear deformation is high and vice versa.

The derivations of shear flexibility parameter produced by ***Lin*** and ***Glouser*** **[11]**, and by ***Timoshenko*** and ***Gere*** **[4]**, are presented in this study as follows.

3.3.2 Shear Flexibility Parameter of Solid Members

Consider an element of length, **a**, of a structural member as shown in Figure (3.6), acted upon by axial force, **Q**, shearing force, **V**, and bending moment, **M**.

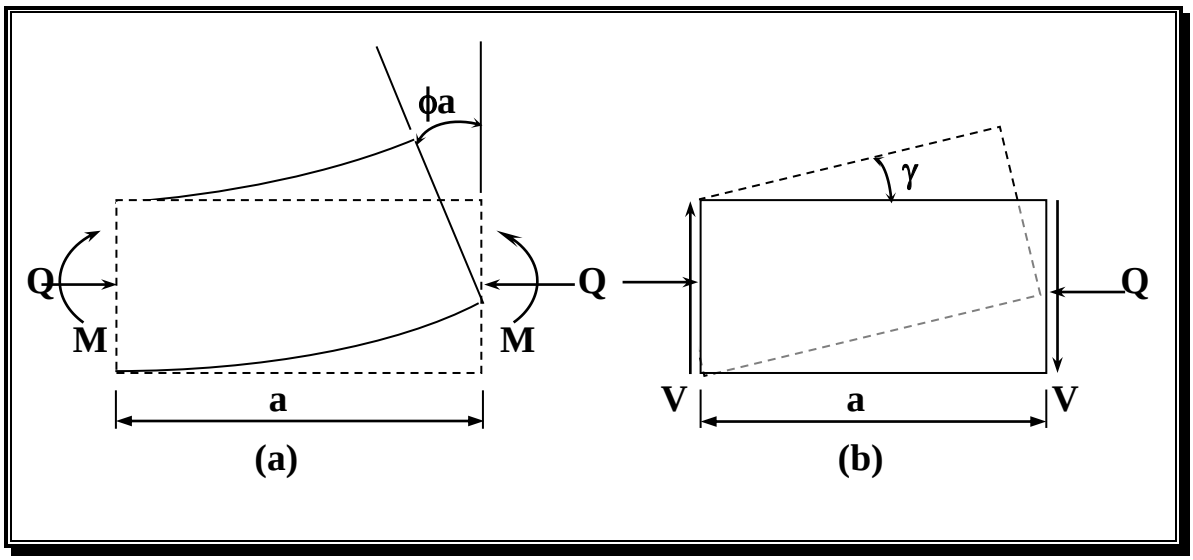

Fig.(3.6): Element of Length (a) of Structural Member Under :
(a) Bending Forces, (b) Shear Forces

The deformation is separated in two parts; (1) Bending and (2) Shear. Bending produces a change in slope in length (**a**) of: -

$$\varphi a = \frac{Ma}{EI} \quad \text{.....(3.109)}$$

and shear produce a change in slope of :-

$$\gamma = \frac{nV}{GA} \quad \text{.....(3.110)}$$

Where;

EI : The flexural rigidity of the structural member ,

GA : The shear rigidity of the structural member , and

n : The shear shape factor see Tab.(3.2) .

Thus within the length (**a**) , the ratio of change in slope caused by shear to that caused by moment is defined as " Shear Flexibility Parameter" and it is equal to :-

$$\mu = \frac{nQe}{GA} \quad \text{.....(3.111)}$$

Tab.(3.3) illustrates the shear flexibility parameter of solid and lacing members .

NO.	Type of section	n
1	Rectangular cross-section	1.2
2	Circular cross-section	1.4
3	I-section bent about Miner axes	1.2A/Af= (1.4-2.8)
4	I-section bent about Major axes	A/Aw= (2-6)

Tab.(3.2):The Shape Factor Typical Values [76]

Where;

A : cross-sectional area ,

Af : area of the flange,

Aw : area of the web .

Type	Shear Parameter (μ)	Eqs. NO.
Solid Cross Section	$\frac{2n(1+\nu)\pi^2 Ie}{Ao\,L^2}$	3.112
Pratt Bracing 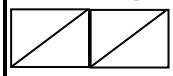	$\frac{EIe\pi^2}{L^2}\left[\frac{l_d.\cos(\alpha)}{(\cos(\varphi)+\sin(\varphi)\tan(\varphi))\cos(\varphi-\alpha)A_d El_c}+\frac{l_b}{A_b El_c}\right]$	3.113
X-Bracing 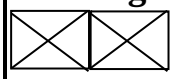	$\frac{EIe\pi^2}{L^2}\left[\frac{l_d.\cos(\alpha)}{2(\cos(\varphi)+\sin(\varphi)\tan(\varphi))\cos(\varphi-\alpha)A_d El_c}\right]$	3.114
Warren Bracing 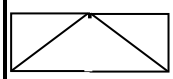	$\frac{EIe\pi^2}{L^2}\left[\frac{l_d.\cos(\alpha)}{(\cos(\varphi)+\sin(\varphi)\tan(\varphi))\cos(\varphi-\alpha)A_d El_c}\right]$	3.115
Howe Bracing 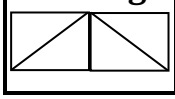	$\frac{EIe\pi^2}{L^2}\left[\frac{l_d.\cos(\alpha)}{(\cos(\varphi)+\sin(\varphi)\tan(\varphi))\cos(\varphi-\alpha)A_d El_c}+\frac{l_b}{A_b El_c}\right]$	3.116

Tab.(3.3):The Governing Equations of Shear Parameter(μ) For Any Type of Section [76]

α : Is the angle of tapared (α=0 for prismatic member)

ϕ : Is the angle between the horizontal and diagonal bars.

Ao : Equivalent cross-section area (**Ao**=$\mathbf{A_1}$ for prismatic)

Ie : Is the equivalent moment of inertia ($\mathbf{Ie=D^{m/2}.\ I_1}$), (**D=1** for prismatic)

3.3.3 The Effect of Shearing Force on The Critical Load

When deriving the critical load for the column is shown in Figure (3.7) without considering the shear effect, the bending moment, **Mx**, at any cross-section (n-n), is: -

$$\mathbf{M(x) = - Q\ (\delta - y)} \qquad \text{.....(3.117)}$$

Or

$$\mathbf{EI}\frac{\mathbf{d^2y}}{\mathbf{dx^2}} = \mathbf{Q}(\boldsymbol{\delta} - \mathbf{y}) \qquad \text{.....(3.118)}$$

Solving this equation yields [***Timoshenko*** and ***Gere*** **[4]** 1961].

$$\mathbf{Qcr} = \frac{\boldsymbol{\pi}^2\mathbf{EI}}{\mathbf{4L^2}} \qquad \text{.....(3.119)}$$

which is the smallest critical load for the bar shown in Figure (3.7).

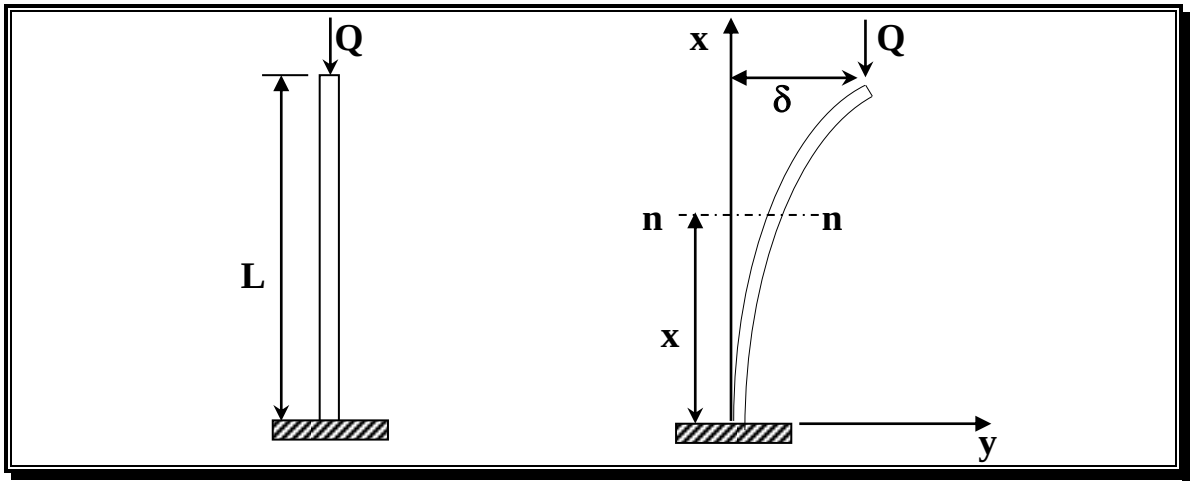

Fig.(3.7):Buckling Load For a Column With One End Fixed and The Other Free

When buckling occurs, however, there is a shearing force acting on the cross-sections of the bar. The effect of these forces on the critical load will now be discussed for the column which is shown in Figure (3.8). The

shearing force, **V**, acting on an element of a length (**dx**) between cross-sections,(n-n) and (m-m) has the magnitude of :-

$$\mathbf{V} = \mathbf{Q}\frac{\mathbf{dy}}{\mathbf{dx}} \qquad \text{.....(3.120)}$$

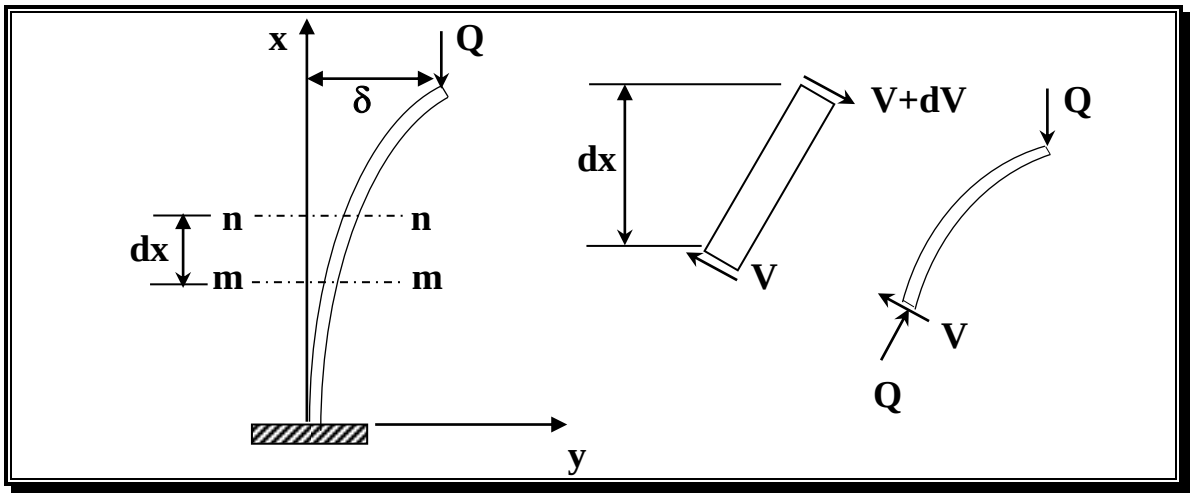

Fig.(3.8): Shear Force in Beam-column Element

The change in slope of the curve produced by the shearing force is $(\frac{\mathbf{nV}}{\mathbf{GA}})$, where $(\frac{\mathbf{V}}{\mathbf{A}})$ is the average shear stress obtained by dividing the shear force, **V**, by the cross-sectional area, **A**, (**G**) is the shear modulus of elasticity, and (**n**) is a numerical factor, which is called the shape factor, by which the average shear stress must be multiplied to obtain the shear stress at the centroid of the cross-section. Expressions for shape factor for different shapes of element cross-section are given in Tab. (3.2).

The rate of change of slope produced by the shearing force, **V**, represents the additional curvature due to the shear and is equal to: -

$$\frac{\mathbf{n}}{\mathbf{GA}}\cdot\frac{\mathbf{dV}}{\mathbf{dx}} = \frac{\mathbf{nQ}}{\mathbf{GA}}\cdot\frac{\mathbf{d^2y}}{\mathbf{dx^2}} \qquad \text{.....(3.121)}$$

The total curvature of the deflection curve is then obtained by adding the curvature produced by the shearing force to the curvature produced by the bending moment. So, the differential equation of the deflection curve becomes: -

$$\frac{\mathbf{d^2y}}{\mathbf{dx^2}} = \frac{\mathbf{Q(\delta - y)}}{\mathbf{EI}} + \frac{\mathbf{nQ}}{\mathbf{GA}}\cdot\frac{\mathbf{d^2y}}{\mathbf{dx^2}} \qquad \text{.....(3.122)}$$

Or

$$\frac{\mathbf{d^2y}}{\mathbf{dx^2}} = \frac{\mathbf{Q}}{\mathbf{EI}\left(\mathbf{1} - \frac{\mathbf{nQ}}{\mathbf{GA}}\right)}(\mathbf{\delta - y}) \qquad \text{.....(3.123)}$$

The general solution for this differential equation results in the following expression [***Timoshenko*** and ***Gere*** (1961)].

$$\frac{Q}{EI\left(1-\frac{nQ}{GA}\right)}=\frac{\pi^2}{4L^2} \quad \text{.....(3.124)}$$

from which;

$$Qcr=\frac{Qe}{1+\frac{nQe}{GA}} \quad \text{.....(3.125)}$$

Where;

$Qe=\frac{\pi^2EI}{4L^2}$ represent the ***Eular*** critical load for the case (a column with one end fixed and the other free).

Thus, owing to the action of shearing force, the critical load diminished in the ratio $\left(\frac{1}{1+\frac{nQ}{GA}}\right)$. For a column with hinged ends, Equation (3.125) can also be used provided that **(Qe)** is taken as the Eular critical load for this case equal to $\left(\frac{\pi^2EI}{L^2}\right)$.

Another approach can be used in deriving the critical load by considering the deformation of the element **(nm)** is shown in Figure (3.9) cut from the column shown in Figure (3.8).

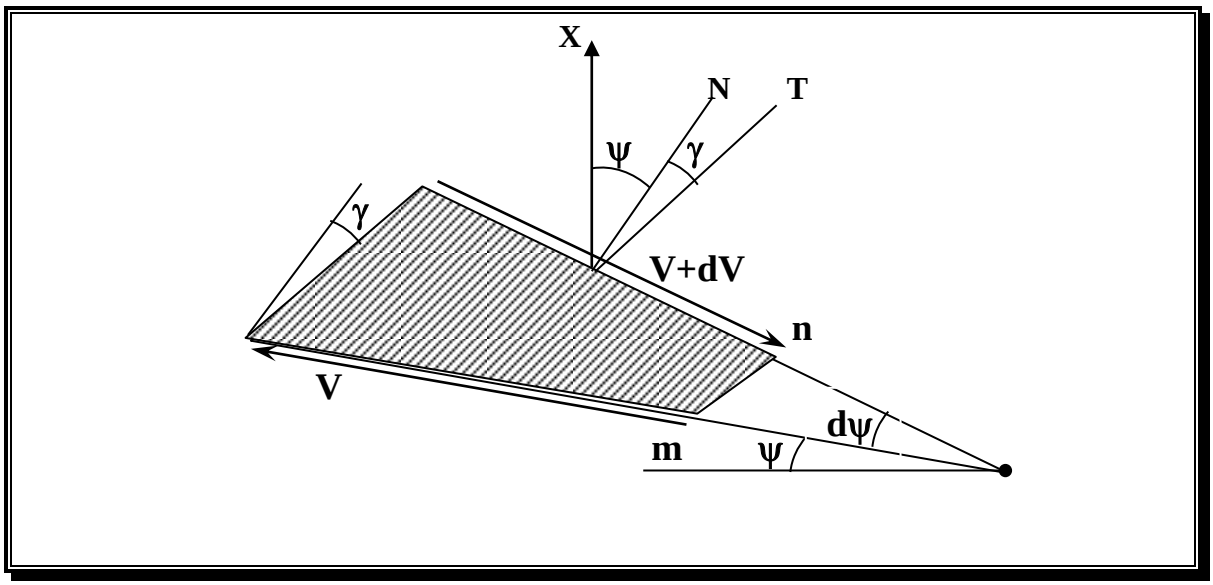

Fig.(3.9): The Deformation of the Beam-Column Element Due to Shearing Force

The angle **(ψ)** represents the change in slope due to the bending moment **(Mx)**, measured from the vertical axis, **X**, to the normal, **N**, to the cross section. Due to shearing strains,**γ**, there is an additional slope measured from the normal, **N**, to the tangent, T, to the axis of the deflected column. Thus, the total slope of the deflected curve will be: -

$$\frac{dy}{dx} = \psi + \gamma = \psi + \frac{nV}{GA} \quad \text{.....(3.126)}$$

The axial force, Q, has a component in the direction, N, is equal to **(Q.cos(ψ) ≅Q)**, and a component,V, is equal to **(Q.sin(ψ) ≅Qψ)**,substituting in Equation(3.126) yields:-

$$\frac{dy}{dx} = \psi + \frac{nQ\psi}{GA} = \psi\left(1 + \frac{nQ}{GA}\right) \quad \text{.....(3.127)}$$

Note that **(** $\frac{d\psi}{dx} = \frac{Mx}{EI} = \frac{Q(\delta - y)}{EI}$ **)**, the following expression for the curvature can be obtained as: -

$$\frac{d^2y}{dx^2} = \frac{Q(\delta - y)}{EI}\left(1 + \frac{nQ}{GA}\right) \quad \text{.....(3.128)}$$

Solving this differential equation gives the critical load as: -

$$Qcr = \frac{\sqrt{1 + {4nQe}/{GA}} - 1}{{2n}/{GA}} \quad \text{.....(3.129)}$$

Where **(Qe)** represents the ***Eular*** critical load, which is equal to **(** $\pi^2 EI / 4L^2$ **)** for a fixed-free column and **(** $\pi^2 EI / L^2$ **)** for a hinged-hinged column.

The difference between Equation (3.125) and Equation (3.129) is due to the fact that, in the derivation of Equation (3.125), the shear force is calculated from the total slope of the deflection curve, **(dy/dx)**, whereas in the derivation of Equation (3.129), only the angle of rotation of the cross-section is used.

In the present study, only the first approach for determining the shear effect [Equation (3.125) will be used because it is more safe than the second approach.

3.3.4 Shear Effect on Elastic Stability

The effect of shear force on the elastic stability of the beam-column element which is shown in Figure (3.2), will result in modifying the stability functions.

The modified stability functions can be derived by using the basic differential equation of the deflection curve. According to the first approach, which will be used in the present study, the basic differential equation is:-

$$\frac{d^2y}{dx^2} = -\frac{Mx}{EI} + \frac{n}{GA}.\frac{dVx}{dx} \quad \text{.....(3.130)}$$

According to Figure (3.10), the bending moment, **Mx**, and the shear force, **Vx**, can be written as:-

$$Mx = \left(1 - \frac{x}{L}\right)M_1 - \frac{x}{L}M_2 + Qy \quad \text{.....(3.131)}$$

$$Vx = -\left(\frac{M_1 + M_2}{L}\right) + Q\frac{dy}{dx} \quad \text{.....(3.132)}$$

Substituting Equations (3.131) and (3.132) into Equation (3.130) yields: -

$$\left(1 - \frac{nQ}{GA}\right)\frac{d^2y}{dx^2} + \frac{Qy}{EI} = \frac{1}{EI}\left[M_1\left(\frac{x}{L} - 1\right) + \frac{M_2}{Q}\left(\frac{x}{L}\right)\right] \quad \text{.....(3.133)}$$

The general solution of Equation (3.133) in case of compression axial force **(q_o>0)** is: -

$$y = D_1.\sin(\omega x) + D_2.\cos(\omega x) + \frac{M_1}{Q}\left(\frac{x}{L} - 1\right) + \frac{M_2}{Q}\left(\frac{x}{L}\right) \quad \text{.....(3.134)}$$

where;

$$\omega^2 = \frac{Q}{EI}\left(\frac{1}{1 - nQ/GA}\right) = \frac{\pi^2}{L^2}.\bar{q}_o \quad \text{.....(3.135)}$$

in which;

$$\bar{q}_o = \frac{q_o}{1 - \mu q_o} \quad \text{.....(3.136)}$$

with μ = The shear parameter and it is given in Table (3.3), and

D_1 , D_2 = Are integration constants, which can be found from boundary conditions, as follows:-

At x=0 ; y=0 , then:-

$$D_2 = M_1/Q \quad \text{.....(3.137)}$$

At x=L ; y=0 , then:-

$$D_1 = -\frac{M_2}{Q}.\csc(\omega L) - \frac{M_1}{Q}.\cot(\omega L) \quad \text{.....(3.138)}$$

Now, substituting Equations (3.137) and (3.138) into Equation (3.134) yields: -

$$y=\left[-\frac{M_2}{Q}.\csc(\omega L)-\frac{M_1}{Q}.\cot(\omega L)\right].\sin(\omega x)+\frac{M_1}{Q}.\cos(\omega x)$$
$$+\frac{M_1}{Q}\left(\frac{x}{L}-1\right)+\frac{M_2}{Q}\left(\frac{x}{L}\right) \quad \text{.....(3.139)}$$

According to end conditions [***Al-Sarraf*** **[51]** (1986)] :-

$$\left.\frac{dy}{dx}\right)_{end1}=\frac{\theta_1-\frac{n(M_1+M_2)}{GAL}}{1-\mu q_o} \quad \text{.....(3.140)}$$

$$\left.\frac{dy}{dx}\right)_{end2}=\frac{\theta_2-\frac{n(M_1+M_2)}{GAL}}{1-\mu q_o} \quad \text{.....(3.141)}$$

Finally, applying Equations (3.140) and (3.141) into Equation (3.139), yields:-

$$M_1=\frac{EI_1}{L}\left(\bar{C}_1\theta_1+\bar{C}_2\theta_2\right) \quad \text{.....(3.142)}$$

$$M_2=\frac{EI_1}{L}\left(\bar{C}_2\theta_1+\bar{C}_1\theta_2\right) \quad \text{.....(3.143)}$$

where;

$$\bar{C}_1=\frac{\bar{\alpha}\left[1-2(1-\mu q_o)\bar{\alpha}.\cot(2\bar{\alpha})\right]}{\left[\tan(\bar{\alpha})-\bar{\alpha}(1-\mu q_o)\right]} \quad \text{.....(3.144)}$$

$$\bar{C}_2=\frac{\bar{C}_1\left[2(1-\mu q_o)\bar{\alpha}-\sin(2\bar{\alpha})\right]}{\left[\sin(2\bar{\alpha})-2\bar{\alpha}(1-\mu q_o)\cos(2\bar{\alpha})\right]} \quad \text{.....(3.145)}$$

and

$$\bar{\alpha}=\frac{\pi}{2}\sqrt{\bar{q}_o}=\frac{\pi}{2}\sqrt{\frac{q_o}{1-\mu q_o}} \quad \text{.....(3.146)}$$

In case of tension axial force, **($q_o<0$)**, the modified stability functions can be derived in the same manner as before, which gives:-

$$\bar{C}_1=\frac{\bar{\alpha}\left[1-2(1-\mu q_o)\bar{\alpha}.\coth(2\bar{\alpha})\right]}{\left[\tanh(\bar{\alpha})-\bar{\alpha}(1-\mu q_o)\right]} \quad \text{.....(3.147)}$$

$$\bar{C}_2=\frac{\bar{C}_1\left[2(1-\mu q_o)\bar{\alpha}-\sinh(2\bar{\alpha})\right]}{\left[\sinh(2\bar{\alpha})-2\bar{\alpha}(1-\mu q_o)\cosh(2\bar{\alpha})\right]} \quad \text{.....(3.148)}$$

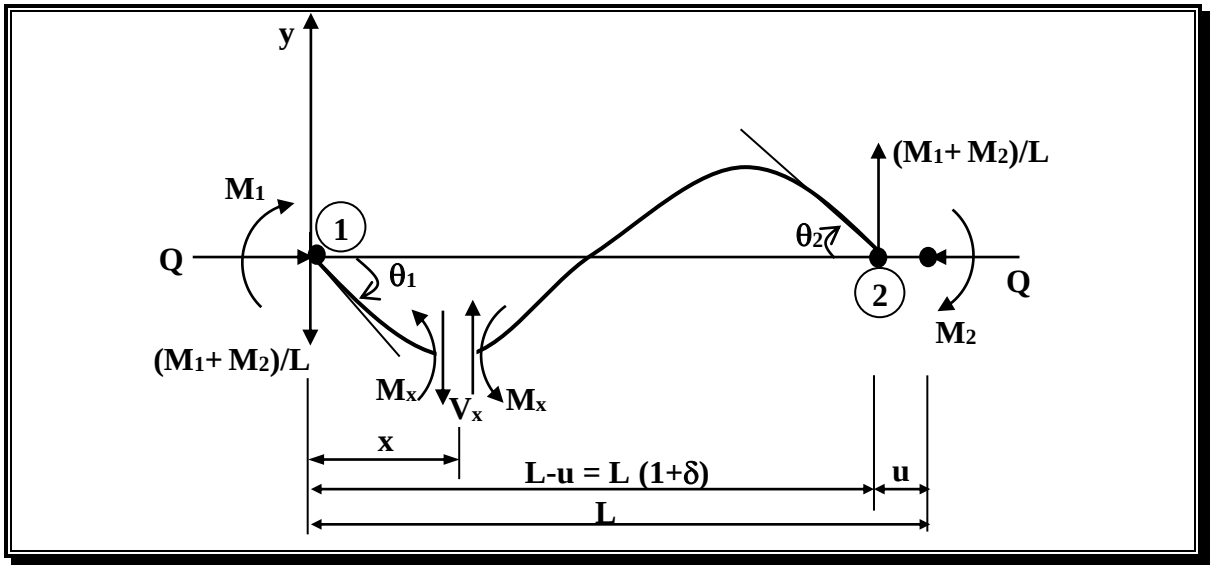

Fig.(3.10):Force System of Elastic Beam-Column

In the present study the approximate formula produced by ***Al-Sarraf*** **[30]**, for calculating stability functions for non-prismatic member, will be extended to include the effect of shear force, therefore, approximate formula of stability functions including shear effect for non-prismatic members are illustrated as follows **[80]**: -

$$\bar{\gamma}_1 = D^{\phi m/4}\,\bar{C}_1 \quad \text{..... (3.149)}$$

$$\bar{\gamma}_2 = D^{(\phi+1)m/4}\,\bar{C}_2 \quad \text{..... (3.150)}$$

$$\bar{\gamma}_3 = D^{(\phi+2)m/4}\,\bar{C}_1 \quad \text{..... (3.151)}$$

where;

$\bar{\gamma}_i$: Are the stability functions of non - prismatic member including shear effect , and

$\bar{C}_1, \bar{C}_2$: Are the stability functions of prismatic member including shear effect.

3.3.5 Shear Effect on Flexural Bowing

When a prismatic member is subjected to bending, there is a shortening of the chord length, **Lc**. This change in length has been called bowing deformation or curvature shortening.

Bowing deformation, δ_b, was presented by ***Saffan*** **[7]** as: -

$$\delta_b = \frac{1}{2}\int_0^{Lc}\left(\frac{dy}{dx}\right)^2 dx \quad \text{.....(3.152)}$$

In addition to the effect of the combination of axial force and bending moments on the bowing phenomenon, the shearing force has a significant

role in this operation. Thus, the modified bowing formula, $\bar{C}_b$, and the modified bowing functions, $\bar{b}_1$ and $\bar{b}_2$, including shear effect must be introduced. These functions were derived by ***Sideek*** **[74]**, as: -

$$\bar{C}_b = \bar{b}_1(\theta_1 + \theta_2)^2 + \bar{b}_2(\theta_1 - \theta_2)^2 \quad \text{.....(3.153)}$$

Where; For a compressive axial force ($q_o>0$): -

$$\bar{b}_1 = \frac{(\bar{C}1+\bar{C}2)^2}{4\pi^4 q_o^2}\left[\frac{2\bar{\alpha}(2\bar{\alpha}+\sin(2\bar{\alpha}).\cos(2\bar{\alpha}))}{\sin^2(2\bar{\alpha})} - 2 + \frac{(\bar{\alpha}\cos(2\bar{\alpha})-\bar{\alpha})(2\bar{\alpha}-\sin(2\bar{\alpha}))}{\sin^2(2\bar{\alpha})}\right]$$

.....(3.154)

$$\bar{b}_2 = \frac{(\bar{C}1+\bar{C}2)^2}{8\pi^4 q_o^2}\left[\frac{(2\bar{\alpha}-2\bar{\alpha}.\cos(2\bar{\alpha}))(2\bar{\alpha}-\sin(2\bar{\alpha}))}{\sin^2(2\bar{\alpha})}\right] \quad \text{.....(3.155)}$$

and, For a tensile force ($q_o<0$):-

$$\bar{b}_1 = \frac{(\bar{C}1+\bar{C}2)^2}{4\pi^4 q_o^2}\left[\frac{2\bar{\alpha}(2\bar{\alpha}+\sinh(2\bar{\alpha}).\cosh(2\bar{\alpha}))}{\sinh^2(2\bar{\alpha})} - 2 + \frac{(\bar{\alpha}\cosh(2\bar{\alpha})-\bar{\alpha})(2\bar{\alpha}-\sinh(2\bar{\alpha}))}{\sinh^2(2\bar{\alpha})}\right]$$

.....(3.156)

$$\bar{b}_2 = \frac{(\bar{C}1+\bar{C}2)^2}{8\pi^4 q_o^2}\left[\frac{(2\bar{\alpha}-2\bar{\alpha}.\cosh(2\bar{\alpha}))(2\bar{\alpha}-\sinh(2\bar{\alpha}))}{\sinh^2(2\bar{\alpha})}\right] \quad \text{.....(3.157)}$$

When the axial force is small (i.e. q_o approaches zero), computational difficulties arise in finding the modifying stability functions from their general expression. To avoid such difficulties, linear interpolation is suggested in the present study to be used in the range ($-0.1<q_o<0.1$), when the values of $\bar{C}_1$ and $\bar{C}_2$ at ($q_o=0$) can be found from Equations (3.147) and (3.148) using ***L'Hopital's*** rule as follows: -

$$\bar{C}_1 = \frac{4\pi^2+12\mu}{\pi^2+12\mu} \quad ; \quad \bar{C}_2 = \frac{2\pi^2-12\mu}{\pi^2+12\mu} \quad \text{.....(3.158a)}$$

and for **($-0.1<q_o<0.1$),** the values of $\bar{C}_1$ and $\bar{C}_2$ can be found as follows:-

$\bar{C}_i(\pm q_o)=\bar{C}_i(0)-[\bar{C}_i(0)-\bar{C}_i(\pm 0.1)]q_o/0.1$; $i=1,2$ .....(3.158b)

While for non-prismatic member an approximate formula for the effect of shear on the bowing functions is as follow **[75]**: -

$$\bar{C}_b = \bar{\beta}_1\theta^2_1 + 2\bar{\beta}_2\theta_1\theta_2 + \bar{\beta}_3\theta^2_2 \quad \text{.....(3.159)}$$

in which;

$\bar{C}_b$: Is the modified flexural bowing for non-prismatic member including shear effect, and

$\bar{\beta}i$: Is the modified bowing functions for non-prismatic member including shear effect.

These functions are defined by:-

$$\bar{\beta}_1 = D^{-\phi m/4}\ (\bar{b}_1+\bar{b}_2) \quad \text{..... (3.160)}$$

$$\bar{\beta}_2 = D^{(1-\phi)m/4}\ (\bar{b}_1-\bar{b}_2) \quad \text{..... (3.161)}$$

$$\bar{\beta}_3 = D^{(2-\phi)m/4}\ (\bar{b}_1+\bar{b}_2) \quad \text{..... (3.162)}$$

where;

$\bar{b}_1$ and $\bar{b}_2$: Are the bowing functions for prismatic member including shear effect .

3.3.6 Tangent Stiffness Matrix Including Shear Effect

The derivation of tangent stiffness matrix including shear effect follows the same procedure as that given in Equation (3.85), so we can substitute the modified stability and bowing functions including shear effect in matrix [t] given in Equation (3.85), instead of the ordinary stability and bowing functions. Accordingly: -

$$G_1 = -2\pi^2\left(\bar{\beta}_1\theta_1+\bar{\beta}_2\theta_2\right)=\bar{\gamma}_1'\theta_1+\bar{\gamma}_2'\theta_2 \quad \text{..... (3.163)}$$

$$G_2 = -2\pi^2\left(\bar{\beta}_2\theta_1+\bar{\beta}_3\theta_2\right)=\bar{\gamma}_2'\theta_1+\bar{\gamma}_3'\theta_2 \quad \text{..... (3.164)}$$

$$H = \frac{\pi^2}{\lambda_0^2}+\left(\bar{\beta}_1'\theta_1^2+2\bar{\beta}_2'\theta_1\theta_2+\bar{\beta}_3'\theta_2^2\right) \quad \text{..... (3.165)}$$

3.3.7 The Equivalent Continuum Model For Beam-Column Like Lattice Structure

Many researchers made their attempts to model large lattice structures with significant non-linear behavior because of excessive processing time or storage requirements for the actual structure, a mong those, ***Noor*** **[18]** and others. The present work, however will adopted the equivalent continuum model proposed by ***Mc Callen*** and ***Romstad*** (1988)**[60]**, in which a simple equivalent model has been developed for geometrically non-linear analysis of prismatic beam-like lattice structure. Two important features of the model are the simplicity of the calculation of the continuum properties and the ability of the continuum to accurately predict the behavior of rigid-joint as well as pin-joint lattices. The equivalence of the continuum and lattice is

established by requiring the strain energy of the continuum to equal the strain energy of the lattice for a finite set have assumed deformation modes.

This method deals with the symmetrical lattice structure with respect to the longitudinal reference axis only. Non-symmetry in the lattice can result in coupling of the axial and transverse displacements. Therefore, only a symmetrical beam-like lattice structure will be considered here.

The equivalent model properties for prismatic beam-like lattice structure as shown in figure (3.11), can be identified as **[60]**: -

$$\overline{EI}=2EA_cC^2+2EI_c \quad \text{(3.166)}$$

$$\overline{EA}=2EA_c+\sum EA_{di}\cos^3\phi. \quad \text{(3.167)}$$

$$\overline{GA}=GAs \quad \text{(3.168)}$$

Where;

$\overline{EI}$, $\overline{EA}$ and $\overline{GA}$: Are the flexural , axial and shear rigidity of equivalent Continuum model,

ϕ : The angle between the diagonal and horizontal bars,

C : The distance between the longitudinal bar and the axis of symmetry, and

GAs : The effective shear stiffness.

For the pin-jointed lattice, shown in Figure (3.11a), is given by: -

$$GAs=2EA_d.\sin^2\phi.\cos\phi \quad \text{(3.169)}$$

and for the rigid-jointed lattice, shown in Figure (3.11b), is: -

$$GAs=\frac{\frac{24EI_c}{(1+\lambda_b)I_cL_b}}{\left[1+\frac{2(1+\lambda_b)I_cL_b}{(1+\lambda_c)I_bL_c}\right]} \quad \text{(3.170)}$$

where;

$$\lambda_c=\frac{12EI_c}{Gn_cA_cL^2_c} \quad \text{(3.171)}$$

$$\lambda_b=\frac{12EI_b}{Gn_bA_bL^2_b} \quad \text{(3.172)}$$

with ;

n : The shear shape factor for the given cross-section geometry of the lattice members, and

c and **b** : represent the chord and the battened member respectively.

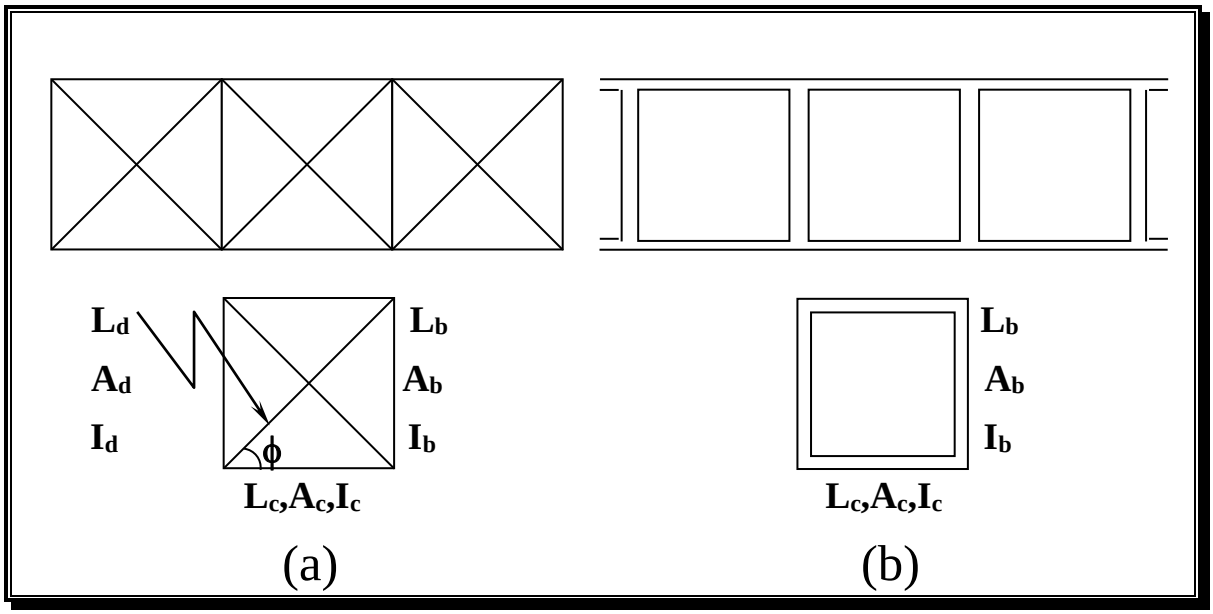

Fig.(3.11):Repeating Cells

In the present study we can use the same procedure as that obtained by ***Mc Callen and Romstad*** (1988) **[60]**, which is based on the equivalent continuum approach to obtained an equivalent continuum model for non-prismatic beam-like lattice structure, in which its properties can be identified as: -

$$\overline{EI}=2EA_cC^2.\cos^3\alpha+2EI_c \quad \text{.....(3.173)}$$

$$\overline{EA}=2EA_c.\cos^3\alpha+\sum EA_{di}\cos^3\phi \quad \text{.....(3.174)}$$

$$\overline{GA}=GAs \quad \text{.....(3.175)}$$

in which;

α : Is the angle of the tapering.

3.4 The Standardized Moment – Rotation Functions

The primary distortion of a steel beam-to-column connection is the rotational deformation **(ϕ)** caused by the bending moment **(M)**. Because of the complexity of connection behavior, the moment-rotation function is virtually always determined experimentally.

There are two ways that connection moment-rotation relationships can be incorporated into a structural analysis program.

(a) The moment-rotation information for every connection of every type can be used in the procedure, which is described by ***Somner*** **[9]** (i.e., following ***Somner's*** method). Since for any given type of connection,

there are a number of “size parameter’s” such as depth , angle thickness,

etc., this requires the storing of an extremely large amount of information.

(b) It is impractical to incorporate into a computer program the individual moment-rotation functions for the many possible sizes and geometries of the common connection types. Fortunately, those for all connections of a given type are similar. Hence, it is convenient to develop a standardized moment-rotation function for each connection type, expressed in terms of the connection size parameters. Then, when the parameters for a given connection are known, they can be substituted into the standardized function in order to generate the specific moment-rotation function for the connection.

The previous studies used Equations (2.2) and (2.3) as the standardized functions to represent the moment-rotation curves for the seven and five common connection types respectively **[20, 44]**.

Dimensionless factor **k** in the Equations (2.2) and (2.3) scales the ordinates on the curve of moment-rotation relationship, by accounting for their dependence upon the connection size parameters. It has the form

$$\mathbf{k} = \prod_{j=1}^{m} \mathbf{q}_j^{\mathbf{a}_j} \quad \text{..... (3.176)}$$

where $\mathbf{q_j}$ = numerical value of the jth size parameter, $\mathbf{a_j}$ = dimensionless exponent which indicates the effect of the jth size parameter on the moment-rotation relationship, and **m** = number of size parameters.

The evaluation of the exponents $\mathbf{a_j}$ in Equation (3.176) follows the procedure described by ***Somner*** (1969) **[9]**. A pair of experimentally obtained moment-rotation curves for two connections that are identical except for parameter $\mathbf{q_j}$ is considered.

The relationship between moments $\mathbf{M_1}$ and $\mathbf{M_2}$, for connections 1 and 2, at a particular rotation $\boldsymbol{\phi}$ is assumed to have the form

$$\frac{\mathbf{M_1}}{\mathbf{M_2}} = \left[\frac{\mathbf{q_j^2}}{\mathbf{q_j^1}}\right]^{\mathbf{a_j}} \quad \text{..... (3.177)}$$

where $\mathbf{q_j^1}$ and $\mathbf{q_j^2}$ are the numerical values of parameter $\mathbf{q_j}$ for connections 1 and 2 respectively.

Rewriting Equation (3.177)

$$\mathbf{a_j} = \frac{\log\left(\mathbf{M_1}/\mathbf{M_2}\right)}{\log\left(\mathbf{q_j^2}/\mathbf{q_j^1}\right)} \quad \text{..... (3.178)}$$

parameters $\mathbf{a_j}$ are calculated from Equation (3.178), for several rotation ϕ, for every available combination of experimental curves, such as 1 and 2, 1 and 3, and 2 and 3, and the mean value is used.

When values have been calculated for all **m** of the exponents $\mathbf{q_i}$, Equation (3.176) is used to evaluated factor **k**. Then, for a given ϕ, values of $\mathbf{K}\times\mathbf{M}$ for the various combinations of parameters are calculated and an average $\mathbf{K} \times \mathbf{M}$ value is computed. The procedure is repeated for several ϕ values. Then pairs of coordinate ($\mathbf{K} \times \mathbf{M}$ and ϕ) are input to curve fitting program, which evaluates constants $\mathbf{C_i}$, $\mathbf{\phi_0}$, $\mathbf{[KM]_0}$ and **n** in Equation (2.2) and (2.3). More details are given by References **[20, 44]**.

3.5 Modeling of Non-linear Flexible Connection

The behavior of flexible connection is usually described by the moment-rotation curves of the connection in which the slope of the curve corresponds to the rotational rigidity of the connections. Many models have been proposed to represent the behavior of the connections. For simplicity, the linear semi-rigid model has been widely used, with concepts such as effective length **[37]**, rigidity factors **[17]** and linear rotational springs **[44, 38]**. However, the approximation of a linear semi-rigid connection is good only when the force at the connection is quite small. When the moment acting at the connection is not small, the rigidity of the connection may change dramatically compared with the initial rigidity, and the structure becomes more flexible.

The non-linear behavior of the flexible connections can be approximated by bilinear or trilinear functions, or expressed by some types of functions, for example, polynomial ***Rambera-Osgood*** **[44]** functions. The bilinear and trilinear models are simple and present no problems in determining the rigidity of the connections but they are not accurate enough.

In general, by curve fitting the experimental data, many types of functions were generated to approximate the non-linear behavior of the flexible connections.

Because the behavior of non-linear flexible connections is actually represented, in a computational model, by the instantaneous rotational stiffness of the connection, i.e., the slope of the moment-rotation curve, the property of the function used for the moment-rotation curve is very important for the numerical analysis of flexibly jointed frame structures.

By considering the properties of a moment-rotation curve, it is evident that a non-linear mathematical expression for the curve must satisfy the following requirements:

1. **$\mathbf{M=0}$ at $\mathbf{\phi=0}$** (the curve passes through the origin).

2. **$dM/d\theta = ki$ at $\phi = 0$** (the slope of the curve at the origin is equal to the initial elastic stiffness of the connection).
3. For any value of ϕ the slope of the expression corresponds to the tangent stiffness of the connection.
4. The parameters in the expression are physically meaningful.
5. The parameters are easily and accurately determinable.
6. The expression is of relatively simple form.

A polynomial expression **[85]**

$$\phi = a + b M + c M^2 + d M^3 + \dots \quad \text{..... (3.179)}$$

can be used and has a considerable accuracy for the moment-rotation relation.

In the present study, the non-linear connection moment-rotation behavior is represented by a polynomial function **[85]**. Here, **a, b, c** and **d** are obtained from a polynomial regression of experimental data. By taking a sufficient number of terms, almost any M-ϕ curve can be closely fitted, but the parameters have very little physical meaning. Also, negative values of the slope (stiffness) of the function may occur within the working range of the connection**]**. So, it should be noted that the fitting polynomial expression must satisfy the above requirements.

The standardized moment-rotation functions can be used here when the parameters for a given connection are known.

The connection will have different stiffnesses during its loading or unloading conditions (Figure (3.12)). If the connection is under loading condition, the instantaneous or tangent stiffness is to be used, i.e.:

$$R_k = R_{kt} = \left.\frac{dM}{d\phi}\right]_{\phi=\phi} = \left.\frac{1}{f'_{(m)}}\right]_{\phi=\phi} \quad \text{..... (3,180)}$$

For unloading condition, the initial stiffness is to be used (***Moncarz*** and ***Gerstle*** **[33]**), i.e.:

$$R_k = R_{ki} = \left.\frac{dM}{d\phi}\right]_{\phi=0} = \left.\frac{1}{f'_{(m)}}\right]_{\phi=0} \quad \text{..... (3,181)}$$

To determine whether a connection is in a loading or unloading condition, the moment at each connection of the frame is monitored at every load step. An increase in moment indicates loading and a decrease signifies unloading.

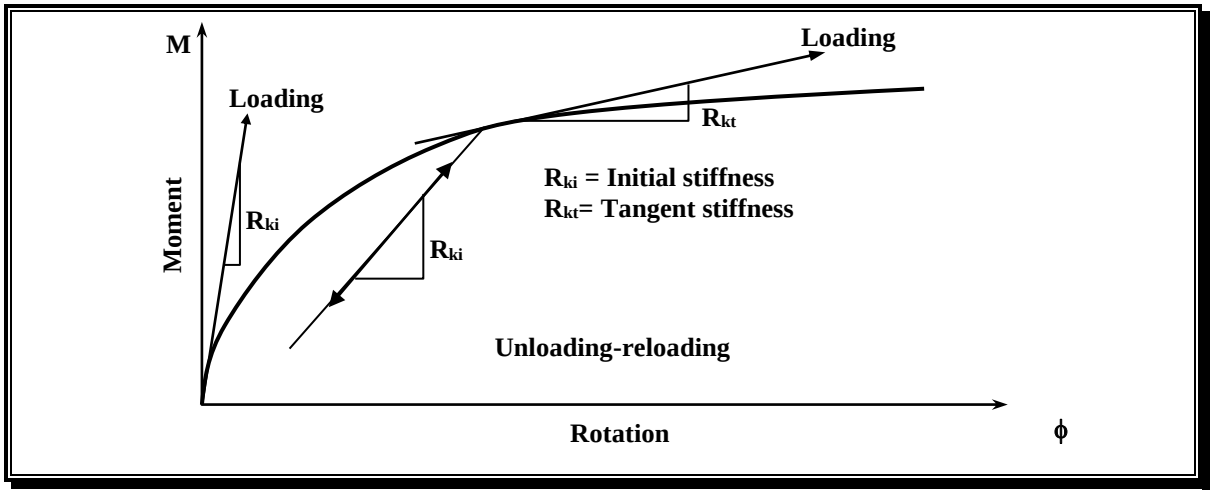

Fig.(3.12): Loading-Unloading Behavior or Steel Connections [56].

3.6 Modification of incremental beam-column stiffness matrix to account for presence of a connection

Assuming that the axial and shearing deformation of the connection are negligible, the incremental force-displacement relationship of a connection can be written as:

$$\begin{Bmatrix} \Delta M_{1cn} \\ \Delta M_{2cn} \end{Bmatrix} = \begin{bmatrix} R_k & -R_k \\ -R_k & R_k \end{bmatrix} \begin{Bmatrix} \Delta_{v1cn} \\ \Delta_{v2cn} \end{Bmatrix} \quad \text{..... (3.182)}$$

where $\Delta v_1 cn$ and $\Delta v_2 cn$ are the incremental rotational D.O.F. of the connection, Figure (3.13).

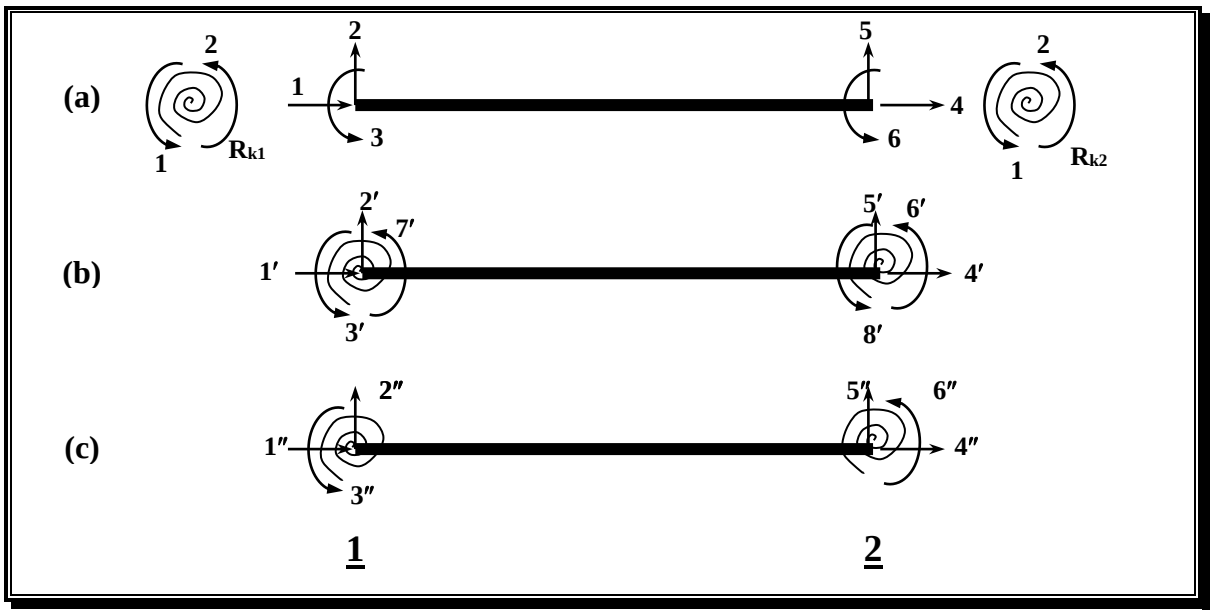

Fig.(3.13): Modification of Beam-Column Element to Account for Presence of Connection [56].

For a frame beam-column element, the incremental force-displacement relationship is:

$$\begin{Bmatrix} \Delta F_1 \\ \Delta F_2 \\ \Delta F_3 \\ \Delta F_4 \\ \Delta F_5 \\ \Delta F_6 \end{Bmatrix} = \begin{bmatrix} k_{11} & k_{12} & k_{13} & k_{14} & k_{15} & k_{16} \\ & k_{22} & k_{23} & k_{24} & k_{25} & k_{26} \\ & & k_{33} & k_{34} & k_{35} & k_{36} \\ & & & k_{44} & k_{45} & k_{46} \\ & & & & k_{55} & k_{56} \\ & & & & & k_{66} \end{bmatrix} \begin{Bmatrix} \Delta v_1 \\ \Delta v_2 \\ \Delta v_3 \\ \Delta v_4 \\ \Delta v_5 \\ \Delta v_5 \end{Bmatrix} \quad \text{..... (3.183)}$$

where $\mathbf{k_{ij}}$ are the entries of the 6 × 6 frame element tangent stiffness matrix in global coordinate system, Equation (3.108).

The three elements shown in Figure (3.13.a) can be jointed together as in Figure (3.13.b) by enforcing equilibrium and compatibility at their junctions. In particular, the kinematics matrix relating the D.O.F of the elements in Figures (3.13.a, 3.13.b) can be written as:

$$[T'_{ff}] = \begin{bmatrix} 0 & 0 & 1 & 0 & 0 & 0 & 0 & 0 \\ 0 & 0 & 0 & 0 & 0 & 0 & 1 & 0 \\ 1 & 0 & 0 & 0 & 0 & 0 & 0 & 0 \\ 0 & 1 & 0 & 0 & 0 & 0 & 0 & 0 \\ 0 & 0 & 0 & 0 & 0 & 0 & 0 & 0 \\ 0 & 0 & 0 & 1 & 0 & 0 & 0 & 0 \\ 0 & 0 & 0 & 0 & 1 & 0 & 0 & 0 \\ 0 & 0 & 0 & 0 & 0 & 0 & 0 & 1 \\ 0 & 0 & 0 & 0 & 0 & 0 & 0 & 1 \\ 0 & 0 & 0 & 0 & 0 & 1 & 0 & 0 \end{bmatrix} \quad \text{..... (3.184)}$$

The equilibrium relationship between the two systems using the contra gradient law, is then $[T_{ff}']^T$ and the stiffness matrix of the element in Figure (3.13.b) is therefore:

$$\mathbf{[k'_{CN}] = [T_{ff}']^T [k'f] [T_{ff}']} \quad \text{..... (3.185)}$$

where

$$[k'f]=\begin{bmatrix} R_{k1} & -R_{k1} & & & & & & \\ -R_{k1} & R_{k1} & & & & & & \\ & & k_{11} & \cdots & k_{16} & & & \\ & & \vdots & & \vdots & & & \\ & & k_{61} & & k_{66} & & & \\ & & & & & R_{k2} & -R_{k2} & \\ & & & & & -R_{k2} & R_{k2} & \end{bmatrix} \quad \text{..... (3.186)}$$

Since the D.O.F 7′ and 8′ in Figure (3.13.b) are internal D.O.F., they can be condensed out the stiffness matrix $[k'_{CN}]$ by static condensation. The modified frame element tangent stiffness matrix accounting for the presence of connections at the ends, (Figure (3.13.c)),

Can be written as **[56]**:

$$[kgfc] = [T_{f'f''}]^T [k'_{CN}] [T_{f'f''}] \quad \text{..... (3.187)}$$

where;

$$[T_{f'f''}]=\begin{bmatrix} & & [I] & \\ & \dfrac{1}{R_k^*}\begin{bmatrix} k_{16}k_{36}-k_{13}(R_{k_2}+k_{66}) & k_{13}k_{36}-k_{16}(R_{k1}+k_{33}) \\ k_{26}k_{36}-k_{23}(R_{k_2}+k_{66}) & k_{23}k_{36}-k_{26}(R_{k_1}+k_{33}) \\ Rk_1(R_{k_2}+k_{66}) & -R_{k_1}k_{36} \\ k_{36}k_{46}-k_{34}(R_{k_2}+k_{66}) & k_{34}k_{36}-k_{46}(R_{k_1}+k_{33}) \\ k_{36}k_{56}-k_{35}(R_{k_2}+k_{66}) & k_{35}k_{36}-k_{56}(R_{k_1}+k_{33}) \\ -R_{k_2}k_{36} & Rk_2(R_{k_1}+k_{33}) \end{bmatrix}^T & \end{bmatrix} \quad (3.188)$$

in which [I] is a 6 × 6 identity matrix and

$$Rk^* = (R_{k1} + k_{33})(R_{k2} + k_{66}) - k^2_{36} \quad \text{..... (3.189)}$$

Substitute Equation (3.185) into Equation (3.187) enables the modified frame elemental tangent stiffness matrix to be written as:

$$[k_t]_{mod} = [T_{f'f''}]^T [T_{ff'}]^T [k'_f] [T_{ff''}] [T_{f'f''}] \quad \text{..... (3190)}$$

where $[k_t]_{mod}$ is the modified element tangent stiffness matrix in global coordinates **[56]**.

3.7 Slip Angle of Non-linear Flexible Connection

It should be noted that because of the presence of the connections, the joint rotation and element end rotation are not the same, see Figures (3.14) and (3.15), where the element end rotation for a frame element with connections at the ends will be (θ_1-ϕ_1) and (θ_2-ϕ_2) respectively and that ϕ_1 and ϕ_2 are relative rotations of the beam-to-column connection.

Due to the presence of flexible connections at ends 1 and 2 of the element, the moment-rotation relationship of this element will be:

$$\begin{Bmatrix} M_1 \\ M_2 \end{Bmatrix} = \frac{EI_1}{L} \begin{bmatrix} \bar{\gamma}_1 & \bar{\gamma}_2 \\ \bar{\gamma}_2 & \bar{\gamma}_3 \end{bmatrix} \begin{Bmatrix} \theta_1 - \phi_1 \\ \theta_2 - \phi_2 \end{Bmatrix} \quad \text{..... (3.191)}$$

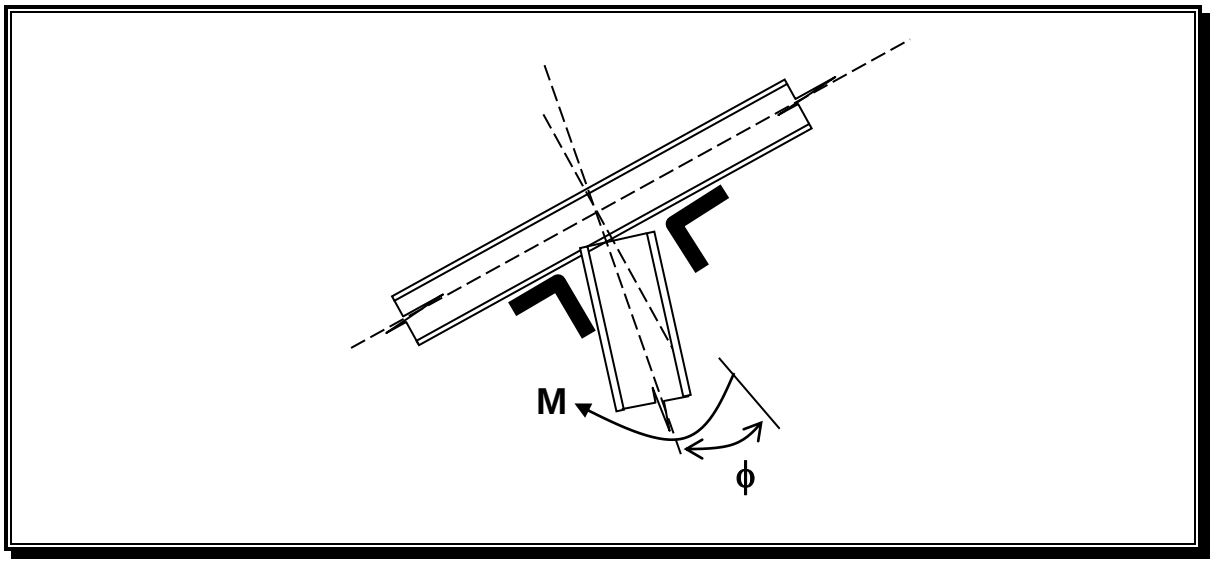

Fig.(3.14): Slip Angle of a Beam-Column Connection .

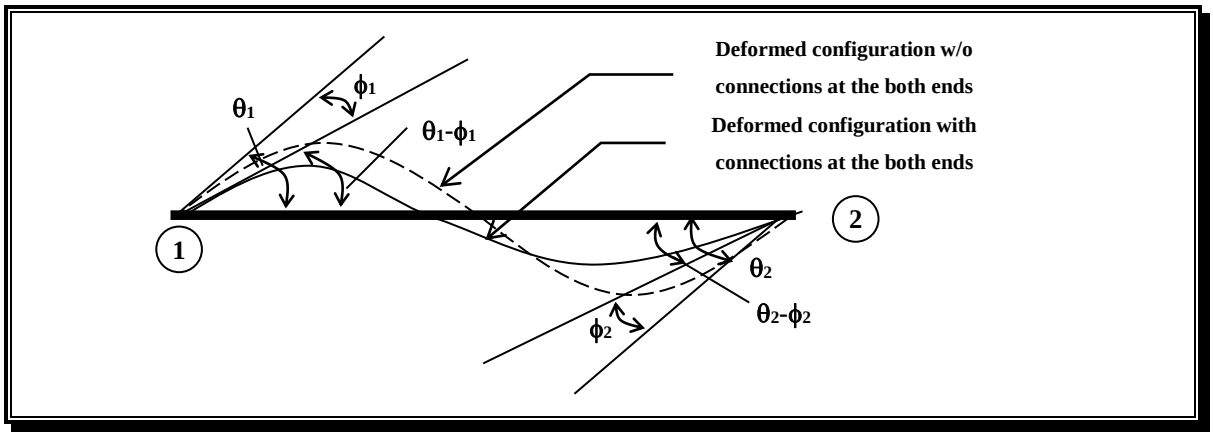

Fig.(3.15): End Rotation of a Beam-Column Element with Connections .

Note that there are four unknowns in Equation (3.191) (i.e., M_1, M_2, ϕ_1 and ϕ_2), therefore; in order to solve the element end moments, two more equations are required. The connection model equation, Equation (3.179), for ends 1 and 2 of the element is:

$$\phi_1 = f_1(M_1) \quad \text{..... (3.192)}$$

$$\phi_2 = f_2(M_2) \quad \text{..... (3.193)}$$

where the functions f_1 and f_2, referring to the expressions on the right-hand side of Equation (3.179), will furnish the additional two equations required.

Strictly, θ_1 and θ_2 will be calculated from Equations (3.90) and (3.91) and are independent whether the connection being linear or non-linear.

So, for a member with flexible connections at both ends;

$$\mathbf{M_1} = \frac{\mathbf{EI_1}}{\mathbf{L}}\left(\bar{\gamma}_1\,\theta_1 + \bar{\gamma}_2\,\theta_2 - \bar{\gamma}_1\,\phi_1 - \bar{\gamma}_2\,\phi_2\right) \quad \text{..... (3.194)}$$

$$\mathbf{M_2} = \frac{\mathbf{EI_1}}{\mathbf{L}}\left(\bar{\gamma}_2\,\theta_1 + \bar{\gamma}_3\,\theta_2 - \bar{\gamma}_2\,\phi_1 - \bar{\gamma}_3\,\phi_2\right) \quad \text{..... (3.195)}$$

A substitution of Equations (3.192) and (3.193) into Equations (3.194) and (3.195) gives

$$\mathbf{M_1} = \frac{\mathbf{EI_1}}{\mathbf{L}}\left(\bar{\gamma}_1\,\theta_1 + \bar{\gamma}_2\,\theta_2 - \bar{\gamma}_1\,\mathbf{f_1}(\mathbf{M_1}) - \bar{\gamma}_2\,\mathbf{f_2}(\mathbf{M_2})\right) \quad \text{..... (3.196)}$$

$$\mathbf{M_2} = \frac{\mathbf{EI_1}}{\mathbf{L}}\left(\bar{\gamma}_2\,\theta_1 + \bar{\gamma}_3\,\theta_2 - \bar{\gamma}_2\,\mathbf{f_1}(\mathbf{M_1}) - \bar{\gamma}_3\,\mathbf{f_2}(\mathbf{M_2})\right) \quad \text{..... (3.197)}$$

assuming two functions:

$$\mathbf{F_1}(\mathbf{M_1},\mathbf{M_2}) = \mathbf{M_1} - \frac{\mathbf{EI_1}}{\mathbf{L}}\left(\bar{\gamma}_1\,\theta_1 + \bar{\gamma}_2\theta_2 - \bar{\gamma}_1\,\mathbf{f_1}(\mathbf{M_1}) - \bar{\gamma}_2\,\mathbf{f_2}(\mathbf{M_2})\right) = \mathbf{0} \quad \text{.. (3.198)}$$

$$\mathbf{F_2}(\mathbf{M_1},\mathbf{M_2}) = \mathbf{M_2} - \frac{\mathbf{EI_1}}{\mathbf{L}}\left(\bar{\gamma}_2\,\theta_1 + \bar{\gamma}_3\theta_2 - \bar{\gamma}_2\,\mathbf{f_1}(\mathbf{M_1}) - \bar{\gamma}_3\,\mathbf{f_2}(\mathbf{M_2})\right) = \mathbf{0} \quad \text{.. (3.199)}$$

These two highly non-linear Equations (3.198) and (3.199) can be solved by using conventional N-R iteration, so that:

$$\begin{Bmatrix}\mathbf{M_1^{k+1}}\\ \mathbf{M_2^{k+1}}\end{Bmatrix} = \begin{Bmatrix}\mathbf{M_1^{k}}\\ \mathbf{M_2^{k}}\end{Bmatrix} - \begin{bmatrix}\dfrac{\partial \mathbf{f_1^k}}{\partial \mathbf{M_1}} & \dfrac{\partial \mathbf{f_1^k}}{\partial \mathbf{M_2}}\\ \dfrac{\partial \mathbf{f_2^k}}{\partial \mathbf{M_1}} & \dfrac{\partial \mathbf{f_2^k}}{\partial \mathbf{M_2}}\end{bmatrix}^{-1} \begin{Bmatrix}\mathbf{F_1^K}\left(\mathbf{M_1^k},\,\mathbf{M_2^k}\right)\\ \mathbf{F_2^k}\left(\mathbf{M_1^k},\mathbf{M_2^k}\right)\end{Bmatrix} \quad \text{..... (3.200)}$$

$$\mathbf{EM_1} = \left|\frac{\mathbf{M_1^{K+1}} - \mathbf{M_1^k}}{\mathbf{M_1^k}}\right| \quad , \quad \mathbf{EM_2} = \left|\frac{\mathbf{M_2^{k+1}} - \mathbf{M_2^k}}{\mathbf{M_2^k}}\right| \quad \text{.....(3-201)}$$

The iteration process continues until both $\mathbf{EM_1}$ and $\mathbf{EM_2}$ satisfy the convergence criterion simultaneously.

The value of $\mathbf{EM_1}$ and $\mathbf{EM_2}$ is usually in the range (1×10^{-3} - 1×10^{-10}) **[85]**.

Having $\mathbf{M_1}$ and $\mathbf{M_2}$ been obtained, ϕ_1 and ϕ_2 can be calculated from Equations (3.192) and (3.193).

The new modified tangent stiffness matrix is used herein for the presence of connections. In the case of a rigid connection or a real hinge, linear **M-**ϕ relations may be used for these purposes as shown in Figure (3.16);

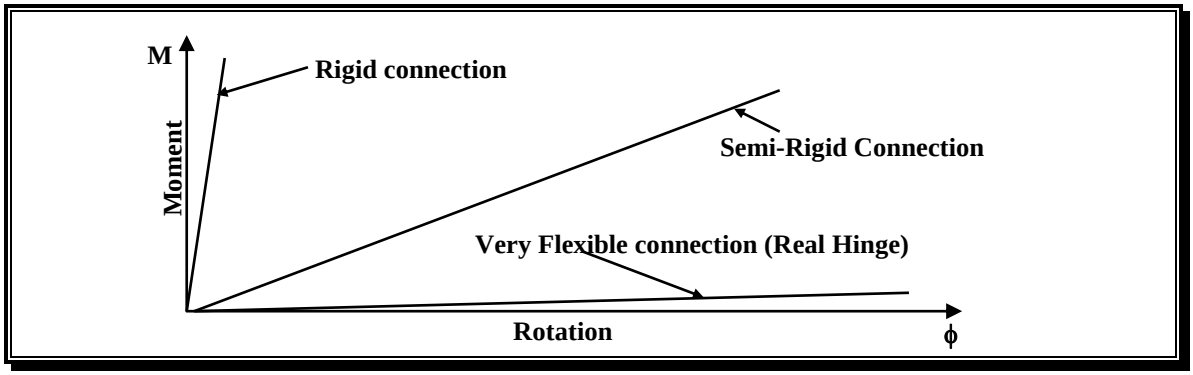

Fig.(3.16): Linear M-ϕ Relations .

In which $\phi = \frac{1}{R_k} M$ ..... (3.202)

$$R_k = R_{ki} = \left.\frac{dM}{d\phi}\right]_{\phi=\phi} \quad \text{..... (3.203)}$$

where $R_k = \begin{cases} \approx 0 & \text{for pinned connection} \\ \approx \infty & \text{for rigid connection} \end{cases}$ ..... (3.204)

Another method can be used as an iterative successive approximation method to determine the slip angle of non-linear flexible connection. This method is called "**Iterative Analysis Method**", and the procedure for this method is as follows **[20, 44]**:

Because of the non-linearity of the connection behavior, an iterative analysis procedure is used. It is based on that the structural deflection and internal forces can be obtained from a single analysis, provided the correct stiffness is assumed for each connection.

Thus, repeated cycles of an iterative procedure are performed to determine appropriate stiffness characteristics for the various connections. When they have been determined with sufficient accuracy, they are employed in analysis to calculate the correct structural displacements and forces.

Consider the structure whose member end connections have non-linear moment-rotation functions, as in Figure (3.17), of the form

$\phi = g(M)$ ..... (3.205)

where **g(M)** is a non-linear function of the moment acting on the connection.

This function is replaced by a linear one of the form

$\phi = \frac{1}{S_1} M$ ..... (3.206)

where S_1 is the slope of the initial tangent to the M-ϕ curve.

The moment-rotation functions for all other connections in the structure are similarly linearized, the corresponding member force-displacement relationships are determined. If the moment at the connection originally considered is M_1, the corresponding rotational deformations is

$$\phi_1 = \frac{1}{S_1} M_1 \quad \text{..... (3.207)}$$

However, the rotation calculated from the correct non-linear relationship, Equation (3.205), is

$$\phi'_1 = g(M_1) \quad \text{..... (3.208)}$$

A better approximation to the connection moment-rotation function is, thus,

$$\phi = \frac{1}{S_2} M \quad \text{..... (3.209)}$$

where $$S_2 = \frac{M_1}{\phi'_1} \quad \text{..... (3.210)}$$

Equation (3.210) and similar relationships for the other connections are then used to calculate the new member force-displacement relationships and a second linear analysis is performed.

The procedure is repeated until the rotation of each connection, calculated from the linear relationship for the current cycle, is sufficiently close to the non-linear relationship of the form of Equation (3.205). The convergence of the above procedure can be hastened by using only some fraction of the difference between ϕ' and ϕ, rather than the total difference.

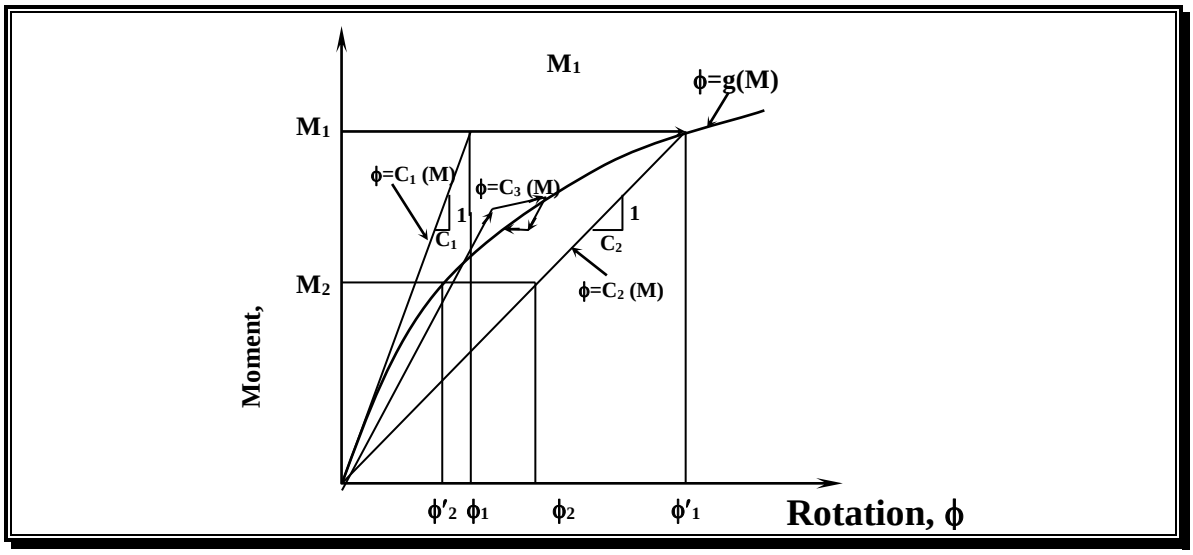

Fig.(3.17): Iterative Analysis Procedure .

3.8 Calculation of Member Axial Force

An important computational difficulty arises in determining {**S**} from {**u**}. This is due to the fact that the expression for member axial force, **Q**, as given by Equation (3.17) involves bowing function, $\bar{\beta}_1$, $\bar{\beta}_2$ and $\bar{\beta}_3$, which, in turn, are functions of the axial force parameter, q_o. The problem can be solved, however, by two alternative iterative procedures.

(i) The first procedure is very slow and needs a large number of iterations to get the actual value of the member axial force **[7]**. The procedure is summarized in the following steps.

1- Calculate member axial force Q_i at the **i** iteration, using Equation (3.17), and then the axial force parameter q_{oi}.

2- Calculate all stability and bowing functions.

3- Calculate the new value of $\bar{C}_b$.

4- Calculate the new value of Q_{i+1} and q_{oi+1}.

5- Determine $\Delta q_o = q_{oi+1} - q_{oi}$.

6- The iteration continues until, $|\Delta q_o| \le e$ in which, **e** is a prescribed tolerance.

(ii) The second procedure which is faster than the first one and needs a very small number of iterations **[42]**, can be summarized as follows:

Noting that q_o is the only unknown in Equation (3.17), let

$$k(q_o) = \frac{\pi^2}{\lambda_0^2} q_0 + \bar{C}_b - \frac{u}{L} = 0 \quad \text{..... (3.211)}$$

Let q_{oi} be an approximate solution of this equation. By using a first-order Taylor series expansion, Equation (3.211) can be rewritten as

$$k(q_{oi} + \Delta q_{oi}) = k(q_{oi}) + k'(q_{oi})\Delta q_{oi} = 0 \quad \text{..... (3.212)}$$

in which a prime superscript denotes a differentiation with respect to q_o, and

$$k'(q_{oi}) = \frac{\pi^2}{\lambda_o^2} + \bar{C}'_b \quad \text{..... (3.213)}$$

A new value is thus obtained for q_o:

$$q_{oi+1} = q_{oi} + \Delta q_{oi} = q_{oi} - \frac{k(q_{oi})}{k'(q_{oi})} \quad \text{..... (3.214)}$$

and the iteration continues until

$$|\Delta q_o| \le e \quad \text{..... (3.215)}$$

In Equations (3.17) and (3.213), $\bar{C}_b$ and $\bar{C}'_b$ are given by

$$\bar{C}_b = \bar{\beta}_1(\theta_1-\phi_1)^2 + 2\bar{\beta}_2(\theta_1-\phi_1)(\theta_2-\phi_2)+\bar{\beta}_3(\theta_2-\phi_2)^2 \quad \text{..... (3.216)}$$

$$\begin{aligned}\bar{C}'_b = {} & \bar{\beta}'_1(\theta_1-\phi_1)^2 + 2\bar{\beta}_1(\theta_1-\phi_1)(\theta'_1-\phi'_1)+2\bar{\beta}'_2(\theta_1-\phi_1)(\theta_2-\phi_2)\\ & +2\bar{\beta}_2(\theta'_1-\phi'_1)(\theta_2-\phi_2)+2\bar{\beta}_2(\theta_1-\phi_1)(\theta'_2-\phi'_2)+\bar{\beta}'_3(\theta_2-\phi_2)^2\\ & +2\bar{\beta}_3(\theta_2-\phi_2)(\theta'_2-\phi'_2) \quad \text{..... (3.217)}\end{aligned}$$

in which θ'_1, θ'_2 equal to zero for member with connection at both ends and are independent whether the connection being linear or non-linear, and

$$\phi'_1 = \left(\frac{d}{dM_1}f_1(M_1)\right).\frac{dM_1}{dq_o} \quad \text{..... (3.218)}$$

$$\phi'_2 = \left(\frac{d}{dM_2}f_2(M_2)\right).\frac{dM_2}{dq_o} \quad \text{..... (3.219)}$$

where $f_1(M_1)$, $f_2(M_2)$ are equations of M-ϕ curve, for ends 1 and 2 respectively.

$$M_1 = \frac{EI_1}{L}\left[\bar{\gamma}_1\theta_1+\bar{\gamma}_2\theta_2-\bar{\gamma}_1 f_1(M_1)-\bar{\gamma}_2 f_2(M_2)\right] \quad \text{..... (3.220)}$$

$$M_2 = \frac{EI_1}{L}\left[\bar{\gamma}_2\theta_1+\gamma_3\theta_2-\bar{\gamma}_2 f_1(M_1)-\bar{\gamma}_3 f_2(M_2)\right] \quad \text{..... (3.221)}$$

to obtain (ϕ'_1, ϕ'_2), (dM_1/dq_o and dM_2/dq_o) must be obtained, thus

$$\frac{dM_1}{dq_o} = \frac{EI_1}{L}\left[\bar{\gamma}'_1\theta_1+\bar{\gamma}'_2\theta_2-\bar{\gamma}_1 f'_1(M_1)\frac{dM_1}{dq_o}-\bar{\gamma}'_1 f_1(M_1)-\bar{\gamma}_2 f'_2(M_2)\frac{dM_2}{dq_o}-\bar{\gamma}'_2 f_2(M_2)\right]$$

..... (3.222)

$$\frac{dM_2}{dq_o} = \frac{EI_1}{L}\left[\bar{\gamma}'_2\theta_1+\bar{\gamma}'_3\theta_2-\bar{\gamma}_2 f'_1(M_1)\frac{dM_1}{dq_o}-\bar{\gamma}'_2 f_1(M_1)-\bar{\gamma}_3 f'_2(M_2)\frac{dM_2}{dq_o}-\bar{\gamma}'_3 f_2(M_2)\right]$$

..... (3.223)

Solving the two equations simultaneously, $\frac{dM_1}{dq_o}$ and $\frac{dM_2}{dq_o}$ are obtained.

Noting that $\bar{\gamma_1}$, $\bar{\gamma_2}$, $\bar{\gamma_3}$, $\bar{\gamma'_1}$, $\bar{\gamma'_2}$ and $\bar{\gamma'_3}$ are based on values of previous iteration cycle.

3.9 Simplified Formulation

It can be seen from the foregoing presentation that consideration of the flexural bowing and stability effects complicates the non-linear analysis of plane frames considerably. The analysis can be simplified and the necessity of iterations in determining member axial forces can be avoided

by neglecting the bowing and stability effects. The influence of these simplifying approximations on the non-linear response of plane frames is investigated in subsequent chapters.

3.10 Elastic Foundation

This part deals with the configuration and the strategy of analysis for the soil – structure interaction. There are two approaches in the analysis of structures consisting of members on elastic foundations. The first approach considered the foundation to be uniformly distributed ***Winkler*** type foundation. In the second approach, the foundation is represented by isolated (lumped) springs at the nodes of beam-column. The second approach will be adopted in the present study.

3.10.1 Elastic Foundation Properties

The constant of proportionality between the applied normal or shear stress at a point on the structure of soil and the corresponding surface displacement is the modulus of subgrade reaction for soil mass, or soil configuration at that point. The modulus of subgrade reaction gives the relationship between the soil pressure and the resulting deflection.

The subgrade reaction model of soil behavior was originally proposed by ***Winkler***, in (1867), characterized the soil as a series of unconnected linearly elastic springs. The deflection at any point (or any spring) occurs only where loading exists at that point. The obvious disadvantage of this soil model is the lack of continuity. Real soil is at least some extent continuous. A further disadvantage is that the spring modulus of the model (modulus of subgrade reaction) is dependent on the size of foundation. In spite of these drawbacks, the subgrade reaction approach has been widely employed in foundation practice because it provides a relatively simple means of analysis and enables factors, such as non-linearity, variation of soil stiffness with depth and layering of the soil profile to be taken into account. In order to characterize the behavior of a soil mass as being equivalent to a ***Winkler*** medium, the following conditions should be satisfied: -

1- The surface displacement at each point of the soil medium should be proportional to the applied normal stress. Plate bearing tests give approximate linearity especially when the loads are small.

2- The surface displacement of the soil medium outside the loaded region should be zero irrespective of the location or magnitude of the applied load. Real soil (another solid granular materials) does not fulfil this condition. The error is usually small in most computations.

Soil configuration can be presented by using two kinds of subgrade reaction modal along the foundation length, the normal and the tangential. The normal subgrade reaction modulus ($\mathbf{K_n}$) is defined as the load required to act normally on a unit area of the elastic foundation to produce a unit normal displacement. The tangential subgrade reaction modulus ($\mathbf{K_t}$) is defined as the load required to act tangentially on a unit area of elastic foundation to produce a unit horizontal displacement.

3.10.2 Modeling of Subgrade Reaction

The subgrade reaction can be represented in two ways, either consistent or lumped, which will be denoted as the soil-stracture interaction stiffness matrix. The present study will be adept the lumped way.

3.10.2.1 Lumped (Isolated) Spring Approach

In this approach the foundation is represented by isolated springs at the nodes of the beam –column. Therefore, the theoretical derivation (stability functions, bowing function and transformation matrix) presented in this chapter can be used in this approach.

The lumped soil-stracture interaction stiffness matrix, for the element shown in Figure (3.18) can be given as: -

$$\left[\overline{K}\right]_{(6\times6)} = \begin{bmatrix} K_t & & & & & 0 \\ & K_n & & & & \\ & & 0 & & & \\ & & & K_t & & \\ & & & & K_n & \\ 0 & & & & & 0 \end{bmatrix} \quad \text{.....(3.224)}$$

In which;

$\left[\overline{K}\right]$ is a (6×6) lumped soil-stracture interaction stiffness matrix in local (intermediate) coordinates .

$\mathbf{K_t}$: is the tangential (shear) nodal spring constant in x- direction .

$\mathbf{K_n}$: is the normal spring constant in y - direction .

$\mathbf{K_t}$ and $\mathbf{K_n}$ can be obtained from the following equations **[84]**: -

$$\mathbf{K_t = Kx.Sp.Dr} \quad \text{.....(3.225)}$$

$$\mathbf{K_n = Ky.bw.Dr} \quad \text{.....(3.226)}$$

In which;

Kx : is the tangential subgrade reaction modulus.

Ky : is the normal subgrade reaction modulus.

Sp : is the cross – section perimeter.

bw : is the width of the cross - section .

Dr : is the distribution length, defined by **[84]** :-

Case (1) : when the member resting on elastic foundation is prismatic .

$\mathbf{Dr} = \frac{\mathbf{L}}{\mathbf{2}}$ [at both ends]

in which : (**L**) is the length of the member .

Case (2): when the member resting on elastic foundation is tapered.

$\mathbf{Dr} = \frac{\mathbf{L}}{\mathbf{3}}$ (at the smallest end of the tapered element)

$\mathbf{Dr} = \frac{\mathbf{2L}}{\mathbf{3}}$ (at the largest end of the tapered element)

The matrix $[\overline{\mathbf{K}}]$ is then to be added to the member tangent stiffness matrix in local coordinates $[\overline{\mathbf{T}}]$, Equation (3.108), to get the total local tangent stiffness matrix.

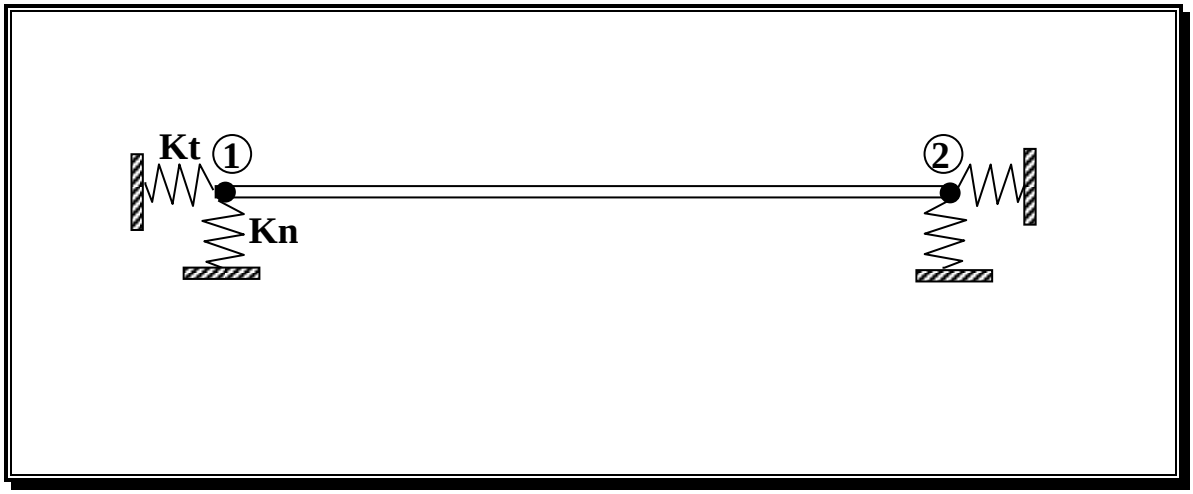

Fig.(3.18): Beam-Column Element on Elastic Foundation .

CHAPTER FOUR

4

POST-BUCKLING ANALYSIS

4.1 General

This chapter presents a description of the different numerical techniques used in solving non-linear simultaneous equations.

The chapter introduces the instability condition of elastic plane steel frames and presents different methods for the detection of instability and the calculation of the elastic critical loads.

In addition, this chapter introduces the post-buckling behavior of elastic plane steel frames. Furthermore, presents different strategies for initial load incrementation and iterative process.

A brief description of the types of convergence criteria usually used in the computer programs is also presented in this chapter.

4.2 Solution Techniques for Non-Linear Problems

The elastic analysis of frame structures by means of the finite element method or beam-column method in the post-buckling range inevitably involves the solution of large systems of non-linear equations. The techniques used in solving the non-linear problems are:

1. Linear Incremental Method.
2. Iterative Methods.
3. Incremental-Iterative Methods (Non-Linear Incremental Methods).

4.2.1 Linear Incremental Method

In this method, the load is applied to the structure as a series of equal or unequal increments and for each of these load increments, the change in deformation is determined by using a linear analysis (see Figure (4.1)).

Thus, the non-linear problem is analyzed as a series of linear problems. A so-called tangent stiffness matrix, based on the last configuration of the structure (beginning of load step) is constructed. The total displacements and internal forces existing at the end of any load increment are obtained by summing the incremental changes in displacements and internal forces up to that point for more details, see references **[53]**.

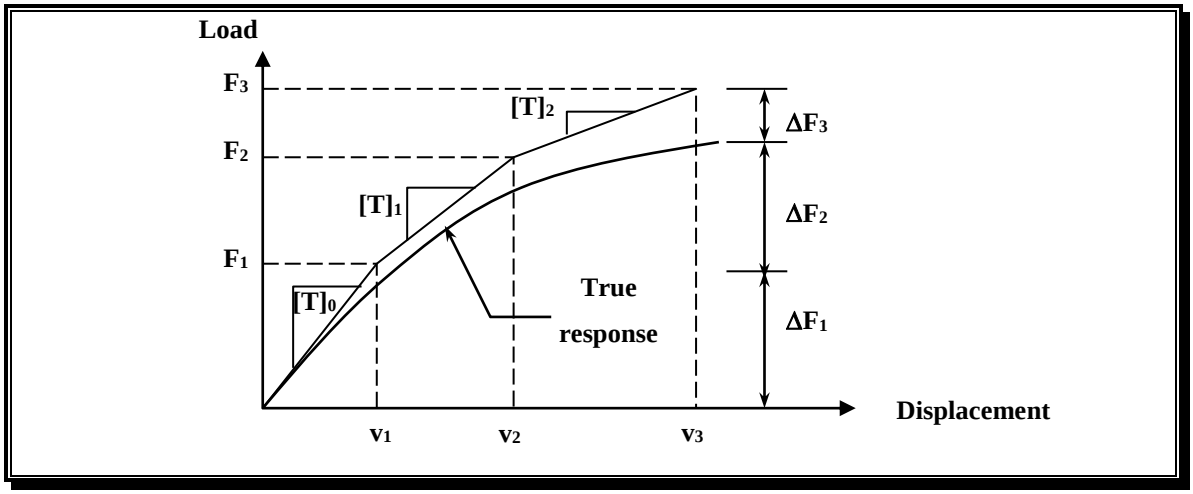

Fig.(4.1): Linear Incremental Method .

4.2.2 Iterative Methods

In these methods an attempt is made to correct solution by using successive iterations. There are many types of iterative methods such as:

1. Conventional Newton-Raphson (N-R) Method.
2. Modified N-R Method.
3. Combined Conventional and Modified N-R Method.
4. Direct Method.

4.2.2.1 Conventional N-R Method

The conventional N-R method is one of the oldest and best known methods used in solving the non-linear problem **[21]**.

For simplicity, consider first a single degree of freedom (D.O.F) system with a load level, $\{F\}_i$ and assume that the corresponding deformed configuration of the system which may be denoted symbolically by $\{v\}_i$ is known, as shown in Figure (4.2).

Now to determine the configuration $\{v\}_{i+1}$ corresponding to a load level $\{F\}_{i+1}$ where

$$\{F\}_{i+1} = \{F\}_i + \{\Delta F\} \quad \text{..... (4.1)}$$

in which;

{ΔF} is the additional applied load.

Using a linearized analysis, the change in configuration **{Δv}** is first computed from:

$$\{\Delta F\} = [T]_o \{\Delta v\}_1 \quad \text{..... (4.2)}$$

in which tangent stiffness matrix, $[T]_o$ is evaluated at the beginning of the load interval; i.e., at load level $\{F\}_i$, $\{u\}_i + \{\Delta\}_i$ represents an approximate configuration in sense that joint equilibrium equations are not necessary satisfied at the load level $\{F\}_{i+1}$. This approximate solution is then corrected by a N-R iteration until equilibrium equations are satisfied within prescribed tolerance.

From the approximate configuration $\{v\}_i + \{\Delta v\}_i$, a new tangent stiffness matrix is updated, then the internal forces corresponding to that configuration $\{f\}_j$ can be determined as:

$$\{f\}_j = [T]_j \{v\}_j \quad \text{..... (4.3)}$$

in which

$$\{v\}_j = \{v\}_i + \sum_{j=1}^{n} \{\Delta v\}_j \quad \text{..... (4.4)}$$

where $\{v\}_j$ is the vector of total displacements after the **j** iterations. Then, the out-of - balance forces $\{\Delta w\}_j$ can be obtained from

$$\{\Delta w\}_j = \{F\}_{i+1} - \{f\}_j \quad \text{..... (4.5)}$$

The unbalanced joint forces are then treated as a load increment and the correction vector, $\{\Delta v\}_{j+1}$, is obtained from the incremental relationship

$$[T]_j \{\Delta v\}_{j+1} = \{\Delta w\}_j \quad \text{..... (4.6)}$$

A new approximate configuration is then obtained by using of Equation (4.3). The process continues until the latest correction vector is sufficiently small.

The N-R method requires that the tangent stiffness be formed and then triangulated in each step. This is expensive if the problem has many D.O.F. Accordingly, various modifications have been proposed.

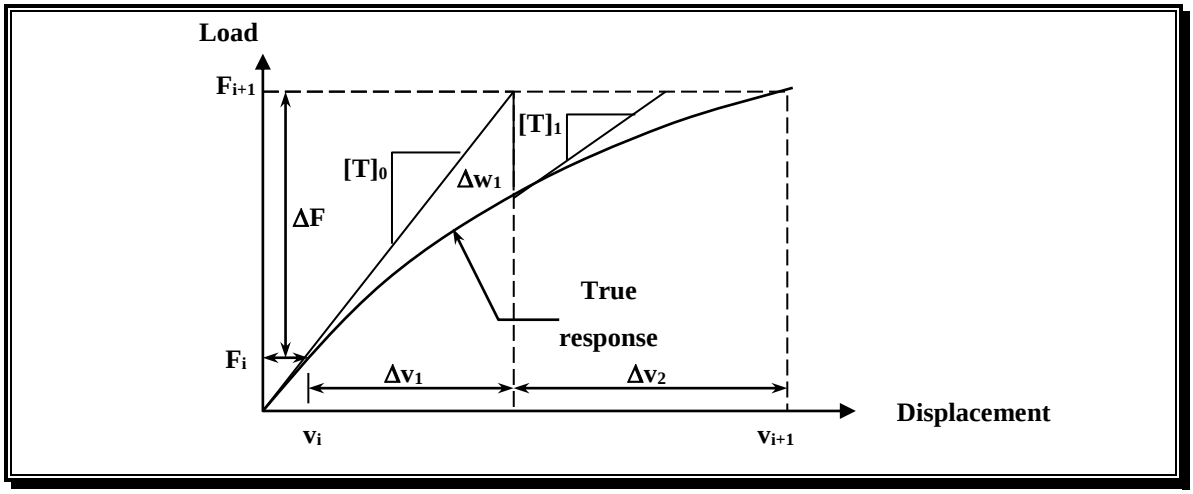

Fig.(4.2): Conventional Newton-Raphson Method

4.2.2.2 Modified N-R Method

This method differs from the conventional N-R method only in that the tangent stiffness matrix is not updated (constant stiffness iteration). The process is depicted one-dimensionally in Figure (4.3).

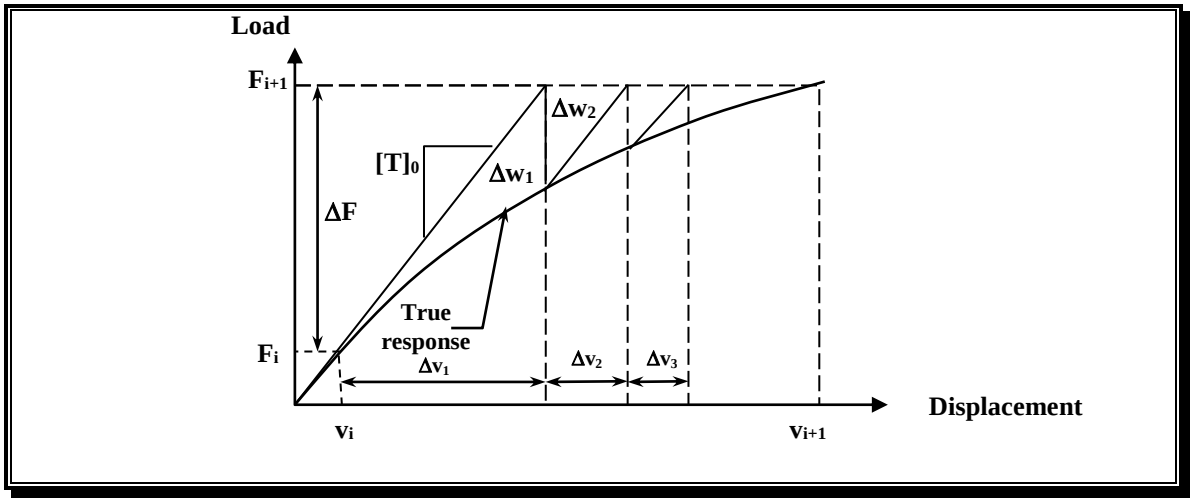

Fig.(4.3): Modified Newton-Raphson Method .

As compared with conventional N-R method, Modified N-R method requires more steps for convergence, but each step is done more quickly by avoiding the expensive repetitions of forming reducing stiffness matrix **[T]**.

4.2.2.3 Combined Conventional and Modified N-R Method

In this method (Figure 4.4), the stiffness is held constant for several iterations and is updated when the rate of convergence begins to deteriorate (number of iterations exceeds maximum limit).

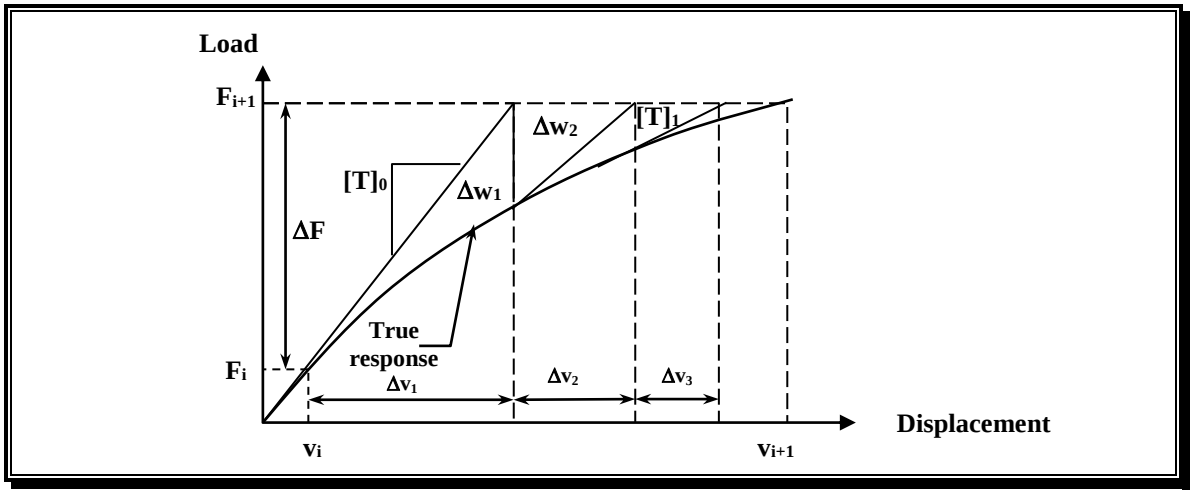

Fig.(4.4): Combined Conventional and Modified Newton-Raphson Method .

4.2.2.4 Direct Method

In this method **[53]**, the deformation corresponding to any load along the load-deformation curve is obtained by applying the load in a single step. The method thus deals with total deformations and total loads. The direct method can be used to obtain the deformations corresponding to a single load-deflection curve as shown in Figure (4.5)

In this method, the desired deformation is related to the applied load by so-called secant stiffness matrix i.e.:

$$[ks]\{v\}_A = \{F\}_A \quad \text{..... (4.7)}$$

For more details, see reference **[53]**.

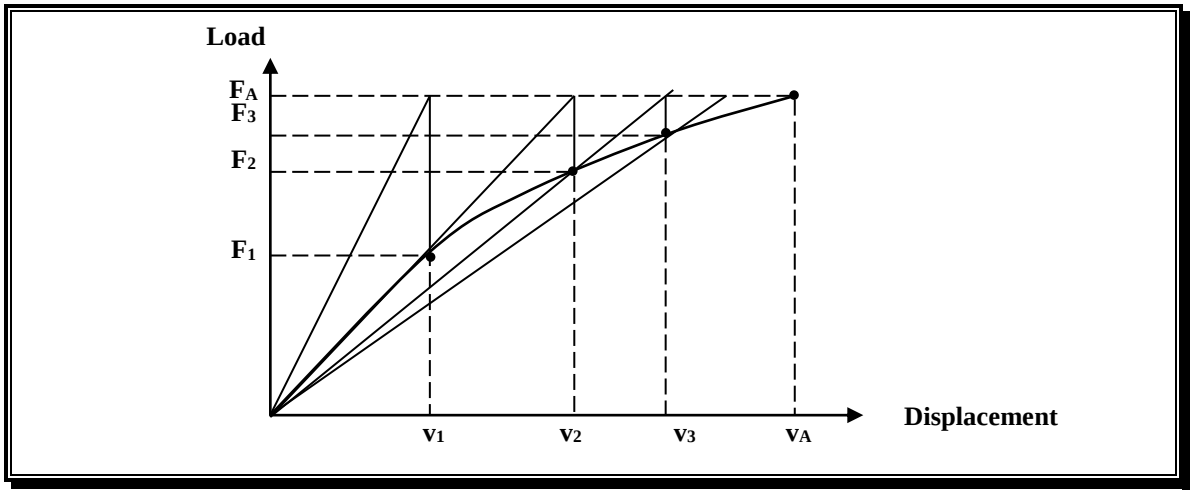

Fig.(4.5): Iterative Procedure for Direct Method .

4.2.3 Incremental-Iterative Methods

In framework with a considerable geometrical non-linearity, if the total load is applied in a single step, the iterative method may lose convergency and fail. Also, if the linear incremental method is used, the solution may drift further and further from the true solution at each load increment. For these two reasons the incremental-iterative methods are widely used in the non-linear analysis.

In these methods the load is applied as a series of increments and at each increment, iterative solution is carried out to find the true response of the structure (see Figure (4.6)).

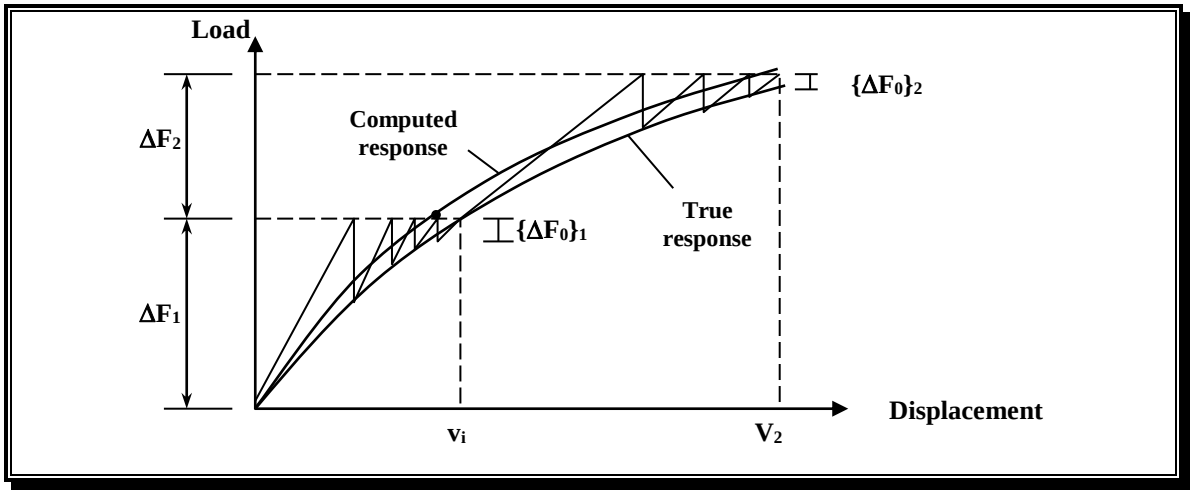

Fig.(4.6): Incremental-Iterative Method .

The three N-R methods discussed in the previous section may be used in the iteration process at each load step. In addition, another N-R methods can be used, for more details about these methods see references **[26]**.

4.3 Detection of Instability

In ordinary parlance, a system is said to be stable if a small disturbance causes only a small response to the disturbance. Similarly a system is said to be unstable if a small disturbance causes a very large response. In terms of structural stability if a structure is stable then any small disturbance will cause only a small additional deformation.

As an example considers the beam is shown in Figure (4.7). The beam is subjected to an axial compressive force P. From the stiffness and carry over factor relations derived by ***Livesley*** and ***Chandler*** **[3]**, the moment – rotation relationship is given by

$$M = (EI / L)\, C_1\, \theta \quad \text{..... (4.8)}$$

For a given value of **M**, a plot of **EIθ/ML** vs. **q** is shown in Figure (4.8). If **M** is treated as a disturbing force then evidently θ will be the response to the disturbance. It can be seen form Figure (4.8), as **q** approaches 2.045, then however small **M** is, θ tends to approach infinity. In other words at a value of **q** = 2.045, the structure reaches the limit of its stability. Since we have assumed that the structure remains elastic however large the deformations, one can say that at **q**=2.045, the structure reaches the limit of its elastic stability.

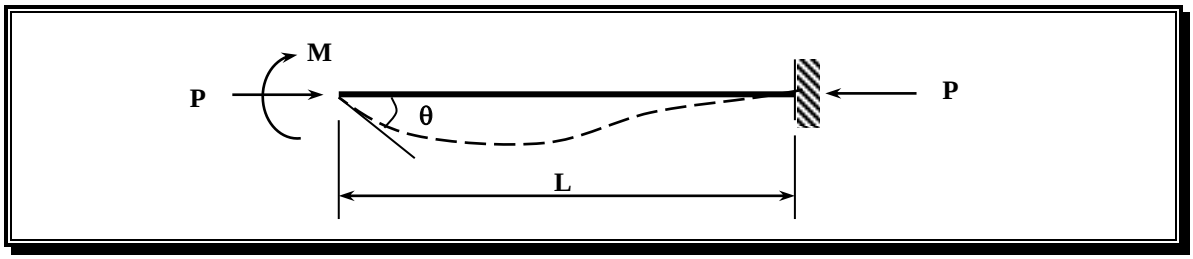

Fig.(4.7): Prismatic Beam Under Effects of Axial Force and Disturbing Moment .

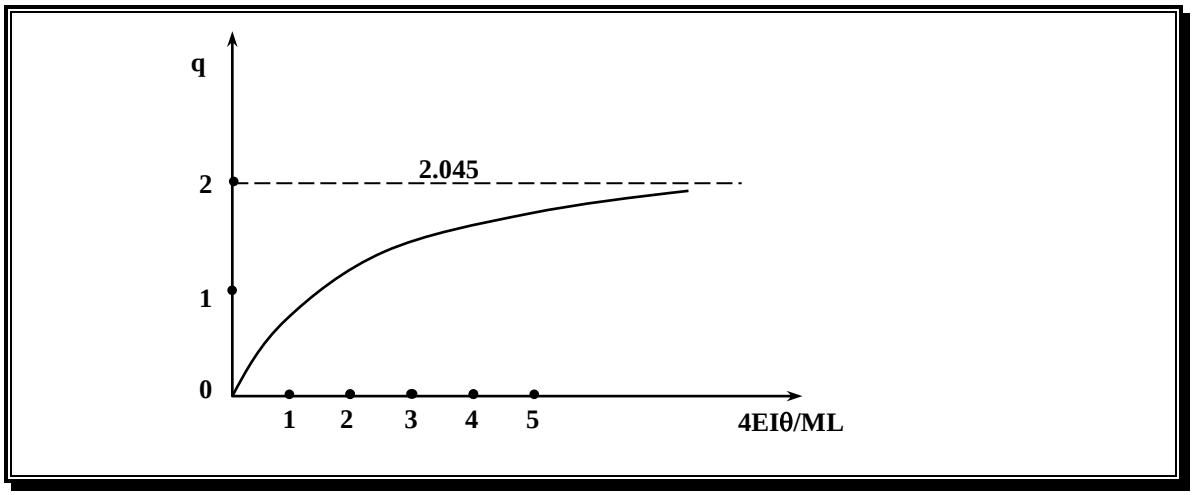

Fig.(4.8): Axial Force Parameter vs. 4 EIθ / ML Relationship .

As long as the structure remains in stable equilibrium, there is only one available path for the load-deflection curve that satisfies the equilibrium condition. In other words, for any load level there is only one available set of deflection and the determinant of the stiffness matrix is positive.

During the analysis most structures lose their stiffness (softening) until the determinant of the stiffness matrix becomes zero. The zero stiffness point has two categories, the first, which is the bifurcation point, at which behind that point there are two possible paths satisfy equilibrium conditions. This means that there are two configurations, reference and buckled configuration are both possible equilibrium configurations. The first path refers to the reference configuration and it is called the primary

path, while the other one is called the secondary path, which is followed by most structures.

The buckling theory presumes the existence of a bifurcation point. So the buckling represents a bifurcation point. Actually, a bifurcation point exists if the column is perfectly straight, perfectly uniform, perfectly free of end moments and lateral loads and forces are perfectly centered and perfectly axial. In reality there are always imperfections. If there is any imperfection, the column displays no bifurcation point and structures in general display the second category of zero stiffness point i.e. limit points.

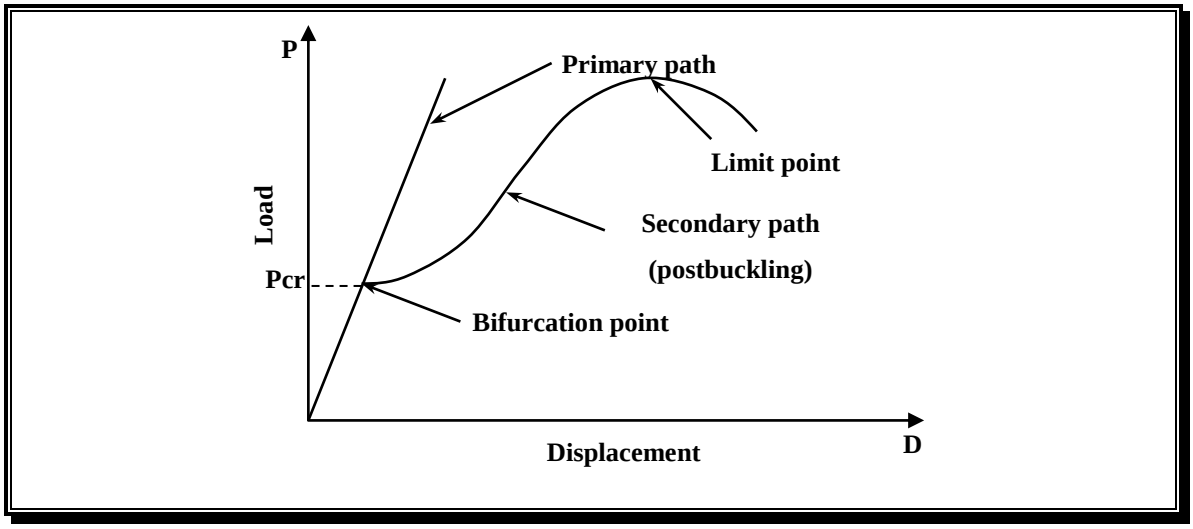

Fig.(4.9): Imperfect Structure .

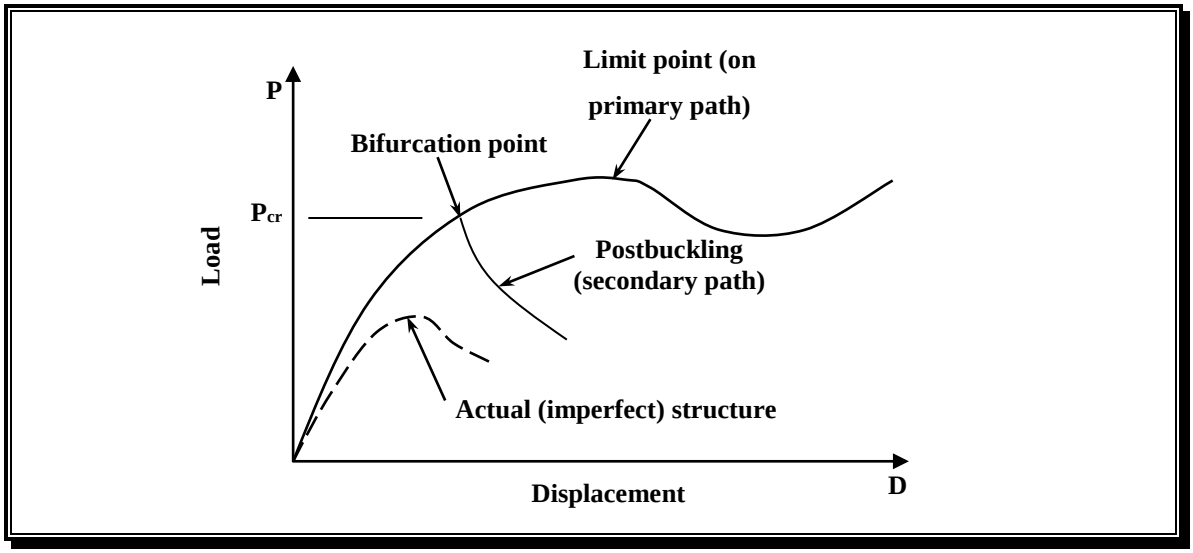

Fig.(4.10): Imperfection Sensitive Structure .

A real structure may collapse at a load quite different from that predicated by linear bifurcation buckling analysis. Figure (4.9) and (4.10)

illustrate some of the ways a structure may behave. In figure (4.9), the primary or pre-buckling path happens to be linear. At bifurcation, either of two adjacent and infinitesimally close equilibrium positions is possible. Therefore, for **P > Pcr** a real (imperfect) structure follows the secondary path. The secondary (post-buckling) path rises, which means that the structure has post-buckling strength. This structure finally collapses at a limit point. Another type of behavior is depicted in Figure (4.10). Here the perfect (idealized) structure has a non-linear primary path. The post-buckling path falls, so there is no post-buckling strength. If the primary path is close to a falling secondary path, the structure is called imperfection sensitive, which means that the collapse load of the actual structure is strongly affected by small changes in direction of loads, manner of support, or changes in geometry. A real structure, which has imperfections, displays a limit point rather than bifurcation as shown by the dashed line.

In some of these studies, the post-critical behavior of the structure is not considered because the analysis at such a stage considers a negative stiffness matrix and a special procedure must be used to determine the behavior of the structure at that stage. So, the analysis always stops at the first limit point (some structures have even more than one limit point) and that stage of load will be considered as the critical load.

4.3.1 Interpolation Method [85]

Many researchers view that a lack of convergence in the iteration processes indication of collapse and elastic instability **[21]**. This reasoning, while it is clearly justified from the theoretical point of view, appears to be unreliable as a practical criterion.

The aim here is to obtain the value of the load for which the determinant of the tangent stiffness matrix vanishes by using the interpolation process. The extrapolation process can be highly useful since through this process, one can change the load increment and make it smaller and smaller near the limit point. At specified load applying stage, the interpolation process can be highly precise detecting instability condition especially when a large number of load increments have been used i.e. a small load step. This process is often used when the mentioned determinant of tangent stiffness matrix changes its sign form positive to negative or from negative to positive, in the following two load increments applied as shown in Figure (4.11). Herein, an approximated value of λ_{cr} can be estimated as:

$$\lambda_{cr} = \frac{D_i \lambda_{i+1} - \lambda_i D_{i+1}}{D_i - D_{i+1}} \quad \text{..... (4. 9)}$$

in which

λ_{cr} : The approximate value for the elastic critical load factor,

λ_i, D_i : The load factor and the determinate of the tangent stiffness matrix at ith load step.

Note: the interpolation method used in the present study to calculate the elastic critical loads.

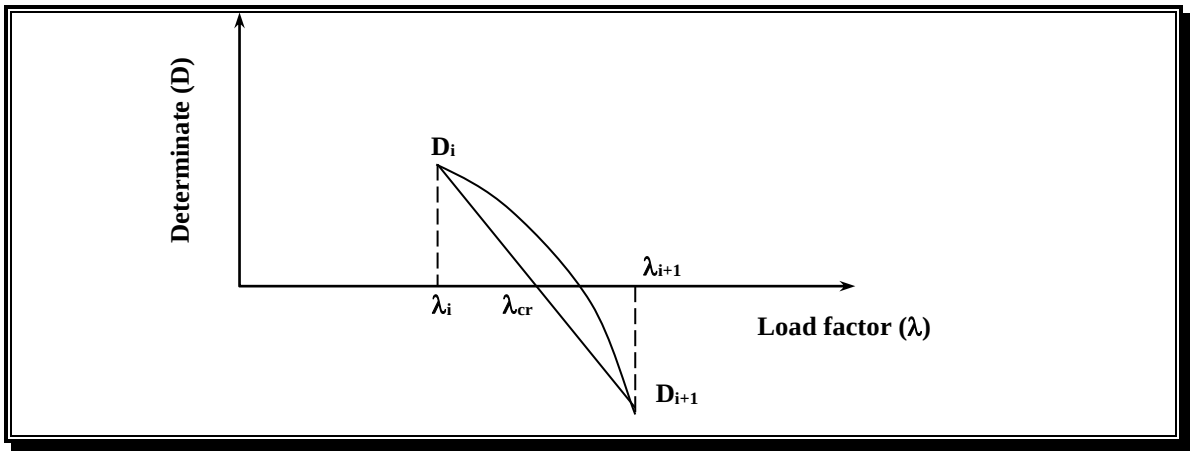

Fig.(4.11): Determinate Versus Load Factor Curve.

4.4 Post-Bucking Behavior of Structures

In the usual non-linear behavior in terms of stiffening or softening systems, two phenomena are of a particular interest; occurrence of limit points and bifurcation of the path into several branches (Figure (4.12)).

In the case of limit point the solution process can only continue beyond the limit point by decreasing the applied loads. Bifurcation is more dramatic phenomenon in which a new equilibrium path suddenly occurs by branching. It is important not only to establish that a bifurcation point exist, but also to be able to proceed with the solution along the secondary branch.

Considerable effort has been devoted to the development of numerical techniques for the solution of non-linear structural problems. Ideally, a solution method should be able to trace the entire pre-and post-critical load path of a structure which may include both softening and stiffening behavior, the presence of load and displacement limit points (see Figure (4.13)), and the possible bifurcation of the path.

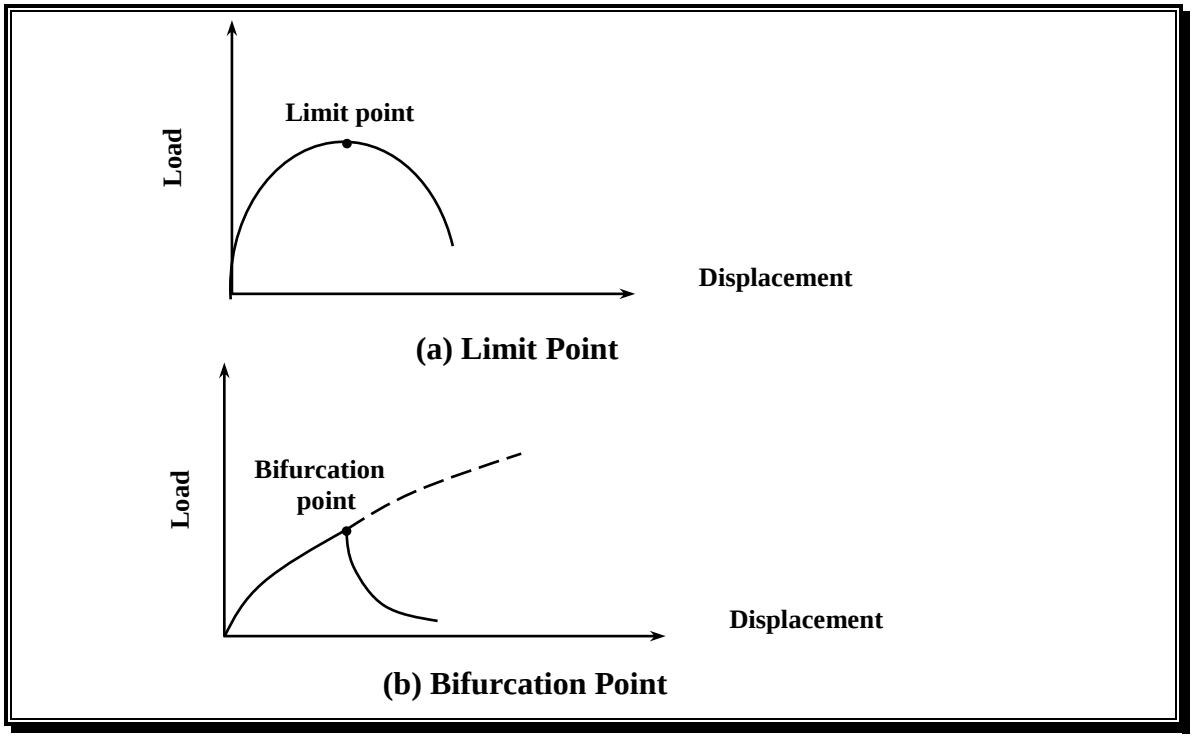

Fig.(4.12): Important Phenomena in Non-Linear Problems.

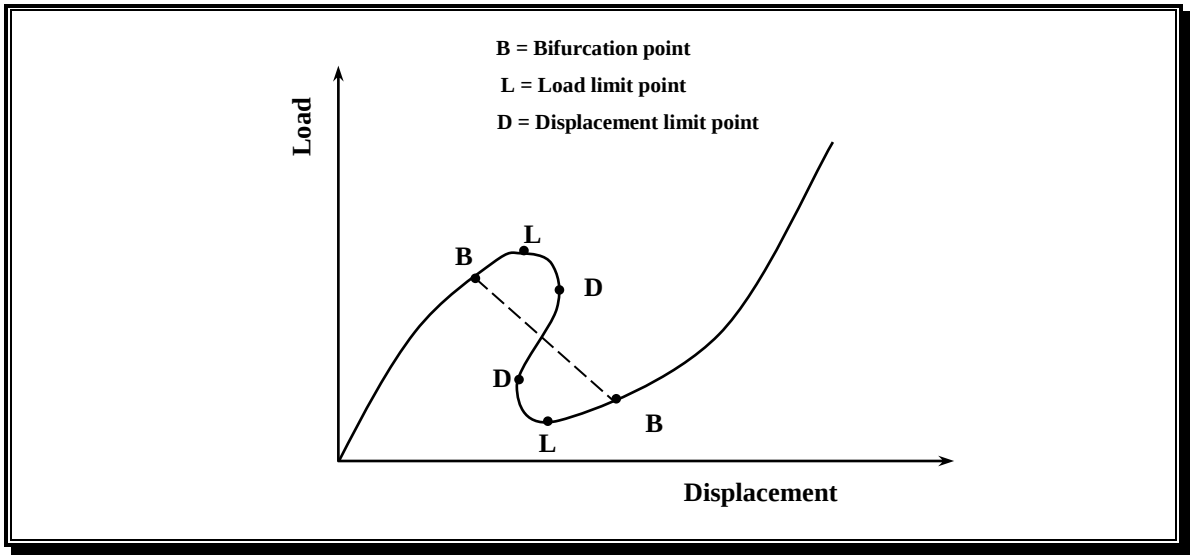

Fig.(4.13): Static Load Path of a Structure .

4.5 Numerical Algorithm for Post-Buckling Analysis

It is a consequence of any discrete formulation (e.g. the finite element method), that the deformation of a given structure is described by a set of (N) deformation parameters, also called generalized coordinates. In this context the load-deformation history of a structure presents itself as a curve in a (N+1) dimensional space spanned by the deformation parameters and the magnitude of the applied loads. Such a curve is usually referred to

as equilibrium path or deformation path. The problem of elastic stability is intimately connected with singularities that occur some where along the path under consideration. These singular points are better known as critical points. Well known is their classification into limit points and bifurcation points. In principle, the elastic stability formulations should be relevant to the problem at hand and should have the capability to:

1. Compute the critical points, i.e. limit or bifurcation points.
2. Trace parts of the path or paths' (branches) connected with these points. In another way of saying that the method should have the capability to compute post-buckling or post-critical equilibrium states.

The incremental-iterative solution method for non-linear elastic problems is ideally suited to obtain the complete static load-deflection response of a structure. In the incremental-iterative method each load increment consists of the application of an increment of external load and subsequent iterations to restore equilibrium.

In this section, the notation adopted is to use the subscript **i** to denote load increment number **i**, and the superscript **j** to denote iterative cycle **j** (within load step i). Iterative cycles commence at j=1, which is defined here to correspond to an increment of external load. The equilibrium iterations commence at j=2. It is clear now that there are two distinct strategies required for the successful completion of a single load increment in an incremental-iterative method:

1. Selection of a suitable external load increment for the first iterative cycle. The chosen increment is termed an initial load increment and a particular strategy used to determine it is termed a load incrementation strategy.
2. Selection of an appropriate iterative strategy for application in subsequent iterative cycles [J≥2] with the aim of restoring equilibrium as rapidly as possible. If iterations are performed on the load parameter as well as the nodal displacement, then an additional constraint equation involving the change in the load parameter is required. It is the from of this constraint equation which distinguishes the various iterative strategies.

A description of the incremental-iterative method for a single load increment **i** is as in Figure (4.14). It is assumed that perfect convergence has been achieved at a conclusion of the (i-1) th load increment, so that the solution (λ_{i-1}, $\{v\}_{i-1}$) is known to satisfy the total equilibrium.

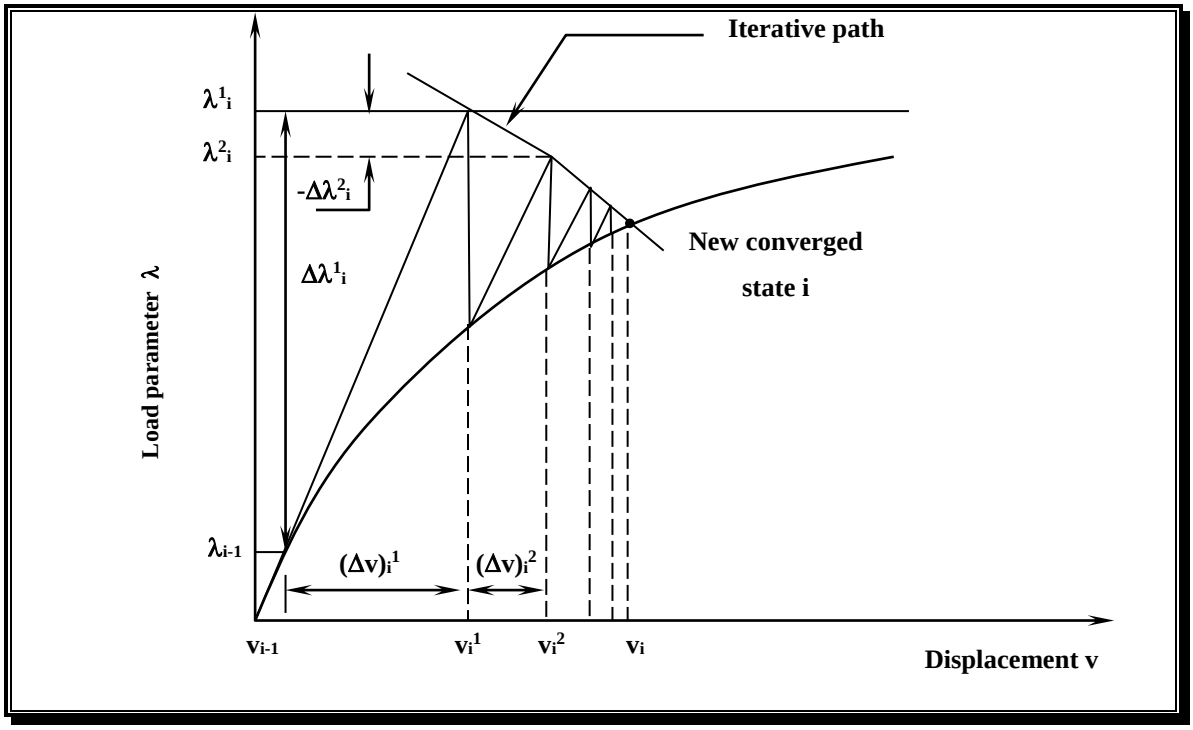

Fig.(4.14): The New Incremental-Iterative Scheme with Modified Newton-Raphson Method and Variable Load Parameter Applied to a Single Degree of Freedom System [59].

At the first iterative cycle (**j**=1), the new load increment commence with the computation of the tangent stiffness matrix $\mathbf{[T]_i}$ based on the known displacements and forces at the conclusion of the previous load increment. The "tangent displacement", $\mathbf{\{v_t\}_i}$ for this increment are then computed as the solution of **[59]**,

$$\mathbf{[T]_i \{v_t\}_i = \{F_r\}_i} \quad \text{..... (4.10)}$$

in which $\mathbf{\{F_r\}_i}$ is the reference external load vector, typically as specified in the input data for the problem. Next, the value of the initial load increment $\Delta\lambda_i^1$ is determined according to a particular incrementation strategy.

The incremental displacements are then evaluated by scaling the tangent displacements

$$\mathbf{\{\Delta v\}_i^1 = \Delta\lambda_i^1 \{v_t\}_i} \quad \text{..... (4.11)}$$

The total displacements and load level updated from those at the conclusion of the previous load step by:

$$\mathbf{\{v\}_i^1 = \{v\}_{i-1} + \{\Delta v\}_i^1} \quad \text{..... (4.12)}$$

$$\lambda_i^1 = \lambda_{i-1} + \Delta\lambda_i^1 \quad \text{..... (4.13)}$$

At this stage the solution invariably does not satisfy the total equilibrium and so additional iterative cycles are required to restore equilibrium.

The well-known Newton-Raphson or modified Newton-Raphson iterative strategies are incapable of passing limit points because the load level is held constant whilst iteration to convergence. The load parameter λ_i^j must be allowed to vary if limit points are to be overcome. With a varying load parameter, a general solution technique evolves if it is assumed that, for any iteration ($j \geq 2$), within load step **i**, the incremental change in the displacements can be written as the solution of

$$[T]_i \{\Delta v\}_i^j = \Delta\lambda_i^j \{F_r\}_i + \{\psi\}_i^{j-1} \quad \text{..... (4.14)}$$

in which

$$\{\psi\}_i^{j-1} = \{F\}_i^{j-1} - \{f\}_i^{j-1} \quad \text{..... (4.15)}$$

where

$\{f\}_i^{j-1}$ is the internal force vector typically computed by summing the elemental contributions in the usual way **[21]**.

$\{F\}_i^{j-1}$ is the external force vector at conclusion of the previous iteration which is for proportional loading may be expressed as

$$\{F\}_i^{j-1} = \lambda_i^{j-1} \{F_r\}_i \quad \text{..... (4.16)}$$

$\{\psi\}_i^{j-1}$ is the net internal out-of-balance force acting on the structure at the conclusion of the previous iteration.

The right side of Equation (4.14) is linear in $\Delta\lambda_i^{j-1}$ and so that the final solution can be written as the linear combination of two vectors

$$\{\Delta v\}_i^j = \Delta\lambda_i^j \{v_t\}_i + \{\Delta v_r\}_i^j \quad \text{..... (4.17)}$$

in which; $\{v_t\}_i$ is the tangent displacements, already computed for (j=1),

$\{\Delta v_r\}_i^j$ is the residual displacements obtained as the solution of

$$[T]_i \{\Delta U_r\}_i^j = \{\psi\}_i^{j-1} \quad \text{..... (4.18)}$$

The variation of the load parameter $\Delta\lambda_i^j$ is obtained by solving an appropriate constraint equation as described in iterative strategies. Equation (4.17) then gives the incremental change to the nodal displacements for this iteration, and the total displacement and load level are updated from the previous iteration by

$$\{v\}_i^j = \{v\}_i^{j-1} + \{\Delta v\}_i^j \quad \text{..... (4.19)}$$

$$\lambda_i^j = \lambda_i^{j-1} + \Delta\lambda_i^j \quad \text{..... (4.20)}$$

It is useful herein to illustrate the solution technique sued in this study after post-buckling.

As shown in Figure (4.15), after post-buckling the change in the load parameter ($\Delta\lambda$) (compute from the iterative strategies) begins negative,

then it transforms to positive and so on (negative, positive, negative, …, etc) until convergence is achieved. While the change in load parameter before post-buckling (computed from the iterative strategies), is always negative as shown in Figure (4.14).

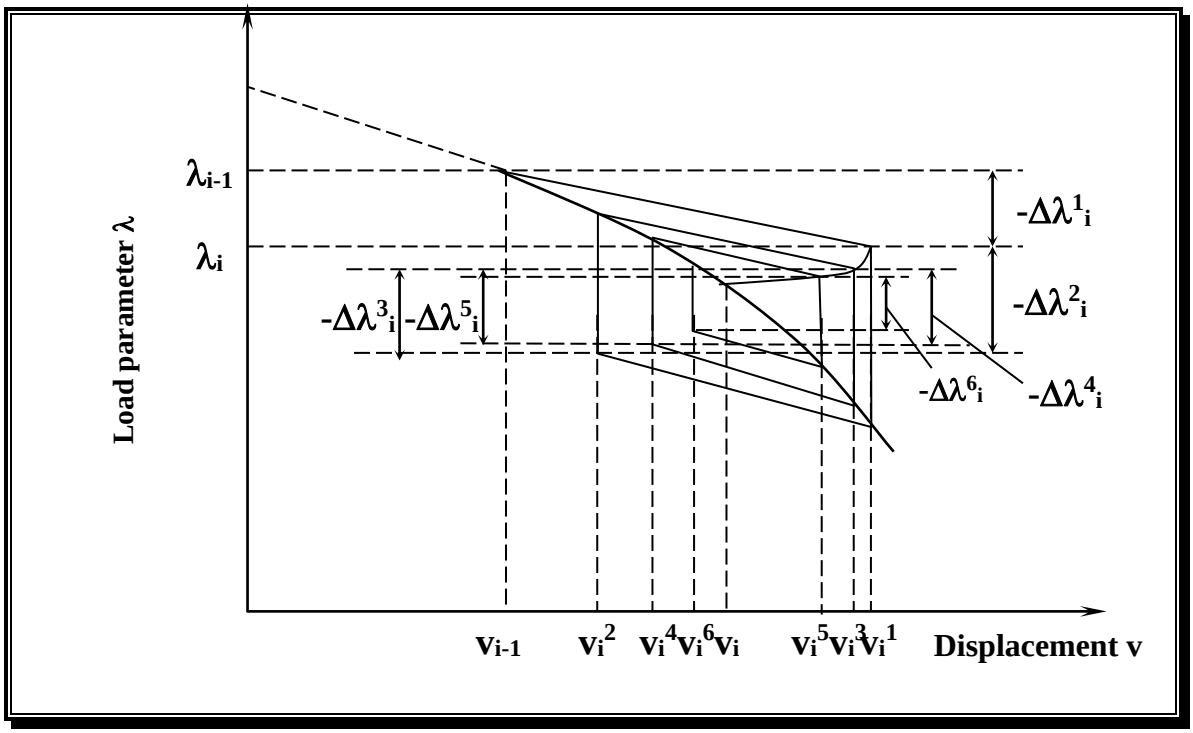

Fig.(4.15): The Incremental-Iterative Scheme with Modified Newton-Raphson Method and Variable Load Parameter After the Limit Point Applied to a Single Degree of Freedom System.

4.5.1 Load Incrementation Strategies

When commencing a load step from converged state (**i-1**) to a new converged state **i**, an initial load increment $\Delta\lambda_i^1$ must be chosen. The choice of increment size is important and should reflect the current degree of non-linearity. If the initial load increment is too large the convergence will be slow or may not occur at all. If the initial load increment is too small then the efficiency of the solution suffers as more converged states are computed than are strictly necessary for an adequate definition of the load-deflection response. The automatically chosen load increment must also be of the correct sign, necessitating measures capable of detecting when maximum and minimum points on the load-deflection curve have been passed.

An effective load incrementation strategy should result in a sequence of solutions (λ_i,$\{v\}_i$) which adequately define the load-deflection characteristic of the structure throughout the entire range of loading. The

progression of the solution should be driven by the specification of the following input parameters:

1. $\Delta\lambda_i^1$, the commencing load level.
2. **Jd,** is the desired number of iterations for convergence.
3. The exponent γ which will be explained later).
4. The tolerance **(tol.)** for convergence.

A number of the methods for controlling the increment size have been presented in the literature. ***Bergan et al.*** **[27]**, define a "current stiffness parameter" as a measure of the current degree of non-linearity. ***Crisfield*** **[39]** and ***Ramm*** **[35]**, make use of the following ratio to control the automatic incrementation:

$$\left[\frac{Jd}{J_{i-1}}\right] \quad \text{..... (4.21)}$$

in which **Jd** is the desired number of iterations for convergence, typically 3 to 5. And J_{i-1} is the actual number of iterations required for convergence in the previous load step. This technique which depend on the number of iterations required to achieve convergence in the previous load step, is adopted in this study.

The load incrementation strategies that based on the ratio Jd/J_{i-1} are classified into:

4.5.1.1 Direct Incrementation of the Load Parameter

Crisfield **[39]**, using the modified N-R method, adopted the following procedure to calculate the increment size.

$$\Delta\lambda_i^1 = \Delta\lambda_{i-1}^1\left(\frac{Jd}{J_{i-1}}\right) \quad \text{..... (4.22)}$$

Ramm **[35]**, used the square root of (Jd/J_{i-1}), which results in a smoother response. If an iterative strategy which iterates on the load factor λ_i^j as displacement is adopted, thus allowing load limit points to be passed, then the following expression may be used for the automatic load incrementation.

$$\Delta\lambda_i^1 = \pm\Delta\lambda_{i-1}^1\left(\frac{Jd}{J_{i-1}}\right)^{\gamma} \quad \text{..... (4.23)}$$

in which the exponent γ typically lies in the range (0.5-1.0) and the choice of the correct sign in Equation (4.23) will be discussed later.

4.5.1.2 Incrementation of the Arc-Length

Let the arc-length **li** for load step **i** be defined by **[67]**,

$$\mathbf{l_i^2} = \left(\Delta\lambda_i^1\right)^2 \{vt\}_i^T \{vt\}_i \quad \text{..... (4.24)}$$

The arc-length for use in the current increment can be computed using the arc-length of the previous increment by

$$\mathbf{l_i} = \mathbf{l_{i-1}}\left(\frac{\mathbf{Jd}}{\mathbf{J_{i-1}}}\right)^{\gamma} \quad \text{..... (4.25)}$$

Equation (4.24) can now be solved for the required initial load increment

$$\Delta\lambda_i^1 = \frac{\pm \mathbf{li}}{\sqrt{\{\mathbf{v_t}\}_i^T \{\mathbf{v_t}\}_i}} \quad \text{..... (4.26)}$$

The procedure is commenced with the evaluation of $\mathbf{l_1}$ from the starting load level $\Delta\lambda_1^1$ using equation (4.24).

4.5.1.3 Incrementation of the External Work

The initial load increment is chosen so as to limit the incremental work $\Delta\mathbf{W_i}$ performed by the applied external loads. The incremental work for the ith load step computed by **[67]**,

$$\Delta\mathbf{W_i} = \Delta\mathbf{W_{i-1}}\left(\frac{\mathbf{Jd}}{\mathbf{J_{i-1}}}\right)^{\gamma} \quad \text{..... (4.27)}$$

and $\Delta\lambda_i^1$ is calculated by

$$\Delta\lambda_i^1 = \frac{\pm \Delta\mathbf{W_i}}{\left|\{\mathbf{F_r}\}_i^T \{\mathbf{v_t}\}_i\right|} \quad \text{..... (4.28)}$$

The procedure initiated by computation of $\Delta\mathbf{W_1}$ from Equation (4.28) using specified starting load level $\Delta\lambda^1{}_1$.

4.5.2 Iterative Strategies

Let it be assumed that the jth cycle in the iterative process now takes place, (see Figure (4.16)). In order to minimize the distance between the current internal force state, point **j** in the load space, and the external force state, the load parameter of the external forces should be reduced. Therefore; the change in the load parameter $\Delta\lambda_i^j$ **(j≥2)** is regarded as an additional variable as well as the residual displacements $\{\Delta v_r\}_i^j$. Generally, there are several different constraint equations available for determination of $\Delta\lambda_i^j$. These are summarized below.

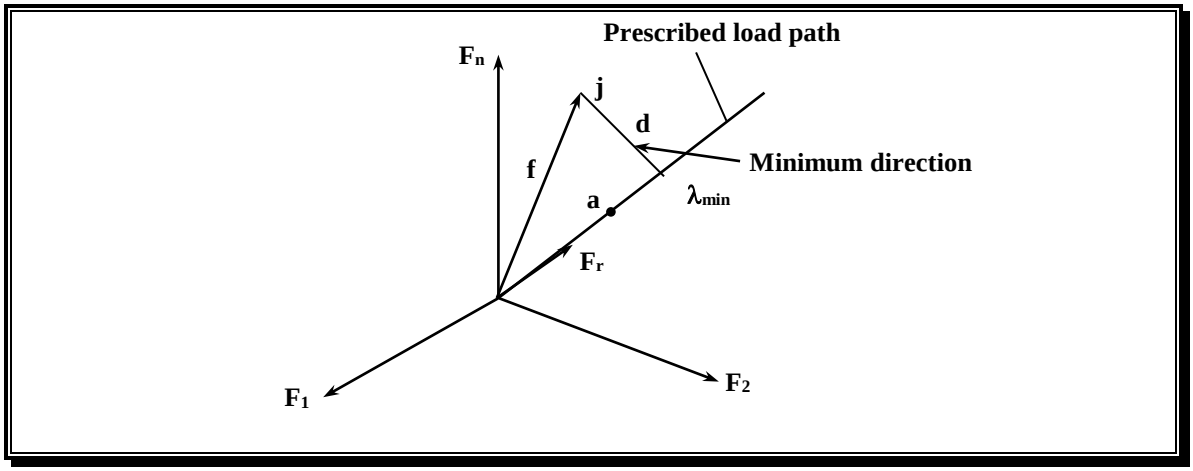

Fig.(4.16): Minimization of Unbalanced Forces .

4.5.2.1 Iteration at Constant Load

Under pure load control, the load parameter is held constant for all iterations **j≥2** and so iteration is performed on the nodal displacements only. In this instance the constraint equation reduces to the expression

$$\Delta\lambda_i^j = 0 \quad \text{..... (4.29)}$$

Iteration at constant load corresponds to the commonly encountered iterations of the modified Newton-Raphson type. Although this iterative strategy does not permit limit points to be passed, it is included here for completeness.

4.5.2.2 Iteration at Constant Arc-Length

The concept of using an arc-length constraint equation to limit the initial load increment $\Delta\lambda_i^1$ was introduced independently by ***Wempner*** **[12]**. The author limit the load step $\Delta\lambda_i^1$ by the constraint equation

$$\{\Delta v1\}_i^{1T}\{\Delta v\}_i^1 + \left(\Delta\lambda_i^1\right)^2\{F_r\}_i^T\{F_r\}_i = I_i^2 \quad \text{..... (4.30)}$$

in which I_i is the generalized arc-length of the tangent at converged state **(i-1)** in load-deformation space. The iterative path adopted by ***Wempner*** then followed a plane normal to the tangent.

The method described above has been modified by ***Crisfield*** **[34]**, in the light of numerical experience and improved suitability for the finite element method. In the modified ***Riks*** method proposed by ***Crisfield***, equation (4.30) is replaced by

$$\{\Delta v_a\}_i^{jT}\{\Delta v_a\}_i^j = l_i^2 \quad \text{..... (4.31)}$$

For all iterations **j**, where $\{\Delta v_a\}_i^j$ are the accumulated displacements within the ith load step:

$$\{\Delta v_a\}_i^j = \{v\}_i^j - \{v\}_{i-1} \quad \text{..... (4.32)}$$

Equation (4.31) corresponds to iterating on a sphere centered at the last converged state (λ_{i-1}, $\{v\}_{i-1}$) and radius 1_i, rather than on a plane as originally proposed by ***Wempner***. The modified ***Riks*** method is slightly less likely to fail **[34]**. From equation (4.32), (4.19) and (4.17), Equation (4.31) can be expanded as

$$\left[\{\Delta v_a\}_i^{j-1} + \Delta\lambda_i^j \{\Delta v_t\}_i + \{\Delta v_r\}_i^j\right]^T \left[\{\Delta v_a\}_i^{j-1} \Delta\lambda_i^j \{\Delta v_t\}_i + \{\Delta v_r\}_i^j\right] - l_i^2 = 0 \text{ ..... (4.33)}$$

which leads to the following quadratic in $\Delta\lambda_i^j$:

$$A(\Delta\lambda_i^j)^2 + B\Delta\lambda_i^j + C = 0 \quad \text{..... (4.34)}$$

where

$$A = \{\Delta v_t\}_i^T \{\Delta v_t\}_i \quad \text{..... (4.35)}$$

$$B = 2\{\{\Delta v_a\}_i^{j-1} + \{\Delta v_r\}_i^j]^T \{\Delta v_t\}_i \quad \text{..... (4.36)}$$

$$C = [\{\Delta v_a\}_i^{j-1} + \{\Delta v_r\}_i^j]^T [\{\Delta v_a\}_i^{j-1} + \{\Delta v_r\}_i^j] - l_i^2 \quad \text{..... (4.37)}$$

Suppose the two roots of Equation (4.34) are denoted $(\Delta\lambda_i^j)$ and $(\Delta\lambda_i^j)_2$. The correct choice of the root is the one that avoids doubling back on the load-deflection response. The angle between the incremental displacement vector before the present iteration and the incremental displacement vector after the current iteration should be positive. For the two possible roots, the corresponding angles are defined by

$$\xi_{1,2} = \left[\{\Delta v_a\}_i^{j-1} + \left(\Delta\lambda_i^j\right)_{1,2} \{\Delta v_t\}_i + \{\Delta v_r\}_i^j\right]^T \{\Delta v_a\}_i^{j-1} \quad \text{..... (4.38)}$$

The correct choice of root $\Delta\lambda_i^j$ is the one which gives a positive angle ξ, unless both angles are positive, in such case the appropriate root is the one which is closest to the linear solution **[34]** to Equation (4.44)

$$\Delta\lambda_i^j = -C / B \quad \text{..... (4.39)}$$

4.5.2.3 Iteration at Constant External Work

Iteration at constant external work is an example of the general method described by ***Powell*** and ***Simons*** **[36]**. For an increment $\Delta\lambda_i^j$ $\{F_r\}$ of external load, the quantity

$$\Delta W_i = \{Fr\}_i^T \{\Delta v\}_i^j \quad \text{..... (4.40)}$$

is an incremental work term. If the external work is to remain unchanged during equilibrium iterations, then $\Delta W_i=0$ the expression for the iterative change in the load parameter $\Delta\lambda_i^j$ is

$$\Delta\lambda_i^j = -\frac{\{F_r\}_i^T \{\Delta v_r\}_i^j}{\{F_r\}_i^T \{v_t\}_i} \quad \text{..... (4.41)}$$

4.5.2.4 Iteration at Minimum Residual Displacement

This iterative strategy has been described by ***Chen*** **[56]**, as the "minimum residual displacement" method and can also be regarded as another special case of the general technique presented by ***Powell*** and ***Simon*** **[36]**.

In this instance, the constraint equation involving $\Delta\lambda_i^j$ is :

$$\frac{\partial}{\partial\Delta\lambda_i^j}\left[\{\Delta v\}_i^{jT} \{\Delta v\}_i^j\right] = 0 \quad \text{..... (4.42)}$$

which guarantees a minimum value for the residual displacement norm in each iteration. Expanding $\{\Delta v\}_i^j$ as defined in Equation (4.17) and evaluating Equation (4.42) furnishes:

$$\Delta\lambda_i^j = -\frac{\{v_t\}_i^T \{\Delta v_r\}_i^j}{\{v_t\}_i^T \{v_t\}_i} \quad \text{..... (4.43)}$$

Because of the different dimensions of transnational and rotational displacement components and to avoid dimensions inconsistency, ***Clarke*** and ***Hancock*** **[67]**, suggested that only the transnational displacement components should be incorporated in the application of equation (4.31). Also, ***Chan*** **[58]**, reported in his paper that such inconsistency in dimensions is actually implied in the arc-length method produced by ***Crisifield*** **[34]**, and ***Ramm*** **[35]**, and he suggested that such inconsistency should be avoided in implementation of Equation (4.43).

Generally, there are many other types of iterative strategies, but the previous iteration strategies are capable to pass the limit points.

However, the four iterative strategies described in this section are used in this study.

4.5.3 The Sign of the Initial Load Increment

In all equations of the initial load incrementation, the sign of the initial load increment can be positive or negative. It is imperative that the correct sign be chosen so that the solution continues to advance the load-deflection response.

Most potential problem in sign determination are encountered at load and displacement limit points.

Crisfield **[34]** and ***Ramm*** **[35]** suggested that the sign of $\Delta\lambda_i^1$ should follow that of the previous increment unless the determinant of the tangent stiffness matrix changes sign. A decreasing determinant gives an indication that a bifurcation or limit point region is being approached.

In the paper of ***Bergan*** **[31]**, it was suggested that the current stiffness parameter could be used for detecting limit points. The reaching of limit point can be detected by checking the sign of the current stiffness parameter. The current stiffness parameter becomes very useful in that it changes sign when passing limit points.

Bergan et al. **[27]**, detect when maxima and minima of the load-deflection curve have been passed by checking the sign of the incremental work.

$$\Delta W_i = \Delta\lambda_i^1 \{v_t\}_i^T \{F_r\}_i \quad \text{..... (4.44)}$$

In the present study, it is found that the determinant technique is efficient for detecting the right sign of initial load increment. Therefore, the sign of $\Delta\lambda_i^1$ should follow that of the previous increment unless the determinant of the tangent stiffness matrix changes it sign which is easily calculated as the product of all the main diagonal terms in the upper-triangular form obtained by using Gaussian elimination.

To demonstrate the basic idea of the determinant technique, consider a typical load-deflection diagram as shown in Figure (4.17). For instance, when taking a trial positive load increment at point **C**, negative displacement is produced giving point $\bar{\mathbf{D}}$ rather than point **D**. negative tangent stiffness matrix gives negative displacement and vice versa. Therefore, the sign reversing must be applied on the initial load increment to advance the load-deflection curve. However, the sign of the tangent stiffness matrix can be determined by checking the sign of determinant of this tangent stiffness matrix which indicates that the sign reversing n the initial load increment must be applied or not.

To avoid the doubling change of the sign of the initial load increment at load limit points when using the load incrementation strategy of external work, the absolute value of $\{F_r\}_i^T\{v_t\}_i$ must be used in Equation (4.28).

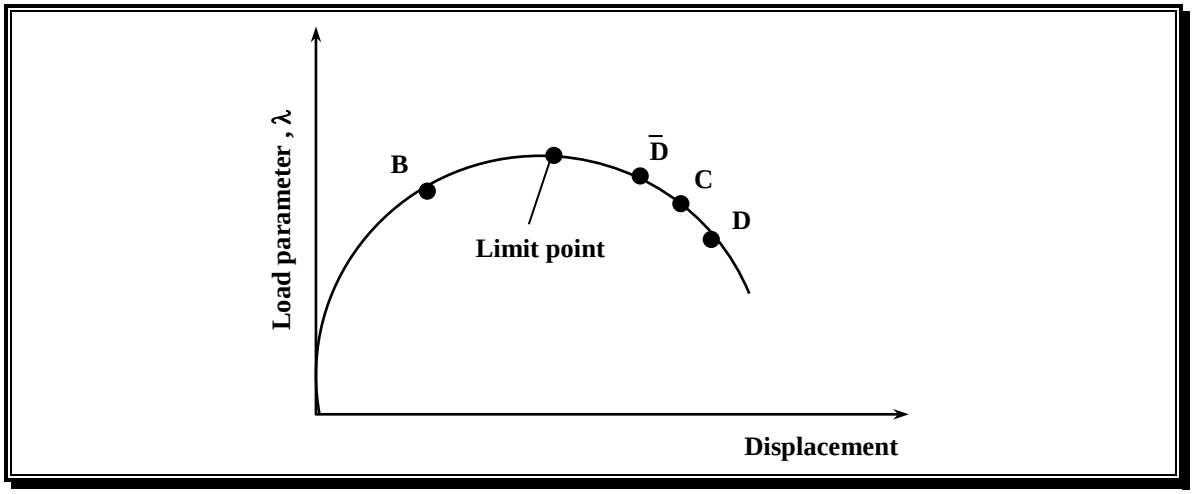

Fig.(4.17): Passing a Limit Point .

4.6 Convergence Criterion

A termination criterion for an iterative process should be used to stop iteration when sufficient accuracy is achieved (i.e. when not further iterations are necessary).

4.6.1 Displacement Criterion

This criterion depends on a comparison between incremental change in the displacement vector **{Δv}** and the cumulative displacement vector **{v}**. In applying this criterion, translations and rotations of the joint should be treated as separate groups, and convergence assumed to occur when the inequality

$$\left[\frac{\sum_{i=1}^{n}(\Delta v)_i^2}{\sum_{i=1}^{n}(v)_i^2}\right]^{(1/2)} \leq \mathbf{tol} \quad \text{..... (4.45)}$$

is satisfied simultaneously and independently for each group. In Equation (4.45) the dimensionless quantity, **tol**, represents a prescribed tolerance.

4.6.2 Force Criteria

This criterion depends on a comparison between the internal force vector {**f**} and the applied load vector {**F**}. In other words, seeking a vector called unbalance force vector to be small within prescribed tolerance. Like the displacement criterion, in applying this criterion the resultant force and moment vector of the joints are treated as separate groups and the convergence is assumed to occur when the inequality

$$\left[\frac{\sum_{i=1}^{n}\left(\{F\}_i-\{f\}_i\right)^2}{\sum_{i=1}^{n}\left(\{F\}_i\right)^2}\right]^{(1/2)} \leq \mathbf{tol} \quad \text{..... (4.46)}$$

is satisfied simultaneously and independently for each group.

4.6.3 Work Done Criteria

This criterion uses a comparison between the work done by the external forces and the work done by the internal forces and convergence occurs when the inequality

$$\left|\frac{W_e - W_i}{W_i}\right| \leq \mathbf{tot} \quad \text{..... (4.47)}$$

is satisfied where

W_e : Is the work done by the external forces,

W_i : Is the work done by the internal forces.

The prescribed tolerance, **tol**, in the inequalities (4.45), (4.46) and (4.47) is chosen to balance accuracy requirements against machine precision.

CHAPTER FIVE

5

COMPUTER PROGRAM, TESTING AND DISCUSSION OF RESULTS

5.1 General

As part of this research, a computer program (NSHEEFF) has been written in Quick Basic 4.5 language to embody the formulation of large displacement and post-buckling analysis of steel frames resting on elastic foundation with non-prismatic members, flexible connections and subjected to static loads including shear effects presented in chapters three and four.

This chapter presents a description of the computer program (NSHEEFF) which is developed in the present study. Furthermore, some examples reported by previous researchers are utilized, in order to verify the reliability and accuracy of the computer program results.

5.2 Properties and Ability of the Program

A computer program (NSHEEFF) is developed in the present study to carry out the large displacement and post-buckling analysis of plane steel frames resting on elastic foundation with flexible connections and non-prismatic members, subjected to static loads including shear effects. The computer program was first introduced by ***Al-Raunduzy*** **[73]**, and it was designed to deal with a large displacement elastic analysis of rigid frames under static and dynamic loads. Such version of the program was designed to treat fixed and free-ended frames only. The post-buckling effects were not considered in that program. Later ***Al-Khafaji H.M.J.*****[85]**, developed ***Al-Raunduyz's*** program to include the post buckling effects and flexible connections.

In the present study, the same static load part of the computer program has been adopted but several developments are inserted to deal with the following: -

1. Non-prismatic frames by **(T.S.M.)** as described in **Chapter Three**.

2. Static load including shear effect by **(T.S.M.)** as described in **Chapter Three**. The **Modified (T.S.M.)** is derived to take into account the effect of the shear.
3. Any type of supports (fixed, free, hinge as well as elastic foundations).

Some of the computer's subroutines are taken from reference **[77]**, and **[85]** after modification. The present computer program has many properties and is designed to deal with many cases. The properties of the program may be summarized as follows:

1. Load Increment.

The computer program (NSFEEFF) is designed to deal with several load incrementation strategies. The basic idea of these strategies is the selection of a suitable external load increment for the first iterative cycle to achieve convergence in the current load increment. The present program is designed to deal with the following load incrementation strategies:

1.Direct incrementation of the load parameter.

2.Incrementation of the arc-length.

3.Incrementation of the external-work..

One can adopt either constant or variable load increments in the static analysis. These strategies achieve the variable load increments. If the constant load increments are required, the load incrementation strategies are not furthering needed and one can applicate the desired proportional equation on the load increment. In the all examples, the variable load increments, using the load incrementation strategies, are adopted because they enable us to trace the entire load-displacement curves by small number of increments. This is achieved due to applying large increments at the beginning and small increments near the limit points.

2. Iterative Process for Equilibrium.

In order to achieved the convergence of iteration process as rapidly as possible, the modified Newton-Raphson method must be used in connection with one of the following iterative strategies:

1.Iteration at constant arc-length.
2.Iteration at constant residual displacement.
3.Iteration at constant external-work.
4.Iteration at constant load.

The selection of an appropriate iterative strategy mainly depends on the structure type and its behavior under subjected loads.

3. Connection Model.

In this program, the connections are considered to have the non-linear moment-rotation characteristics. Such relationships are well known as **Polynomial Model**. A significant difficulty has been encountered in calculating end bending moments and connection rotation due to the presence of a two highly non-linear equations for each beam-column member, this difficulty has been overcome by solving the two non-linear equations by using **Conventional Newton-Raphson Iteration**, or by using the **Approximate Iterative Method**.

4. Detection of Limit Points.

The determinant technique for checking a sign change is used in the present program to enable the program to pass limit point. At the commencement of each load increment, the program monitors the sign of the determinant and when the determinant changes its sign, the sign of the initial load increment will be reversed.

5. Member Coordinate System.

The member tangent stiffness matrix in global coordinates, derived in C**hapter Three**, assumed last configuration of the member so that, the Eulerian coordinate system should be used in which new member coordinates is updated at each iteration.

6. Stability and Bowing Effects.

The present program is designed to deal with all the effects of geometrical non-linearity. However, the analysis that is carried out by this program can be simplified and the necessity of iteration in determining member axial forces can be avoided as follows:

1.Neglected bowing effect, or

2.Neglected stability and bowing effects.

The first approximation can be made by setting $\mathbf{C_b}=0$ in Equation (3-17) and $\mathbf{G_1}=\mathbf{G_2}=0$ and $\mathbf{H}=\pi^2/\lambda^2_o$ in Equation (3-84). The second approximation can be made by setting $\mathbf{C_1}=4$ and $\mathbf{C_2}=2$ without change in addition to the first approximation. The second approximation means that the non-linearity only comes from large displacement effect. For both approximations see Figure (5.1).

7. Linear Analysis.

The program (NSHEEFF) is designed to deal with linear elastic analysis of structures. In such analysis, the deformations are assumed to be small so that the stability effect and bowing effect can be ignored and the

equilibrium equations are formulated on the basis of the undeformed configuration of structures. This analysis can be done as follows:

1.Apply the external loads as one increment.

2.Neglected the stability, bowing and large displacement effects.

3.Neglected any iterative process.

For more details see Figure (5.1).

8. Convergence Criterion.

The displacement criterion presented in chapter four has been used for terminating the iterative process in iterative solution.

5.3 Structure of the Program

The program (NSHEEFF) consists of a main routine and many subroutines. Each one of these subroutines has been designed to deal with a part of the analysis and that part may be repeated more than one time in the main routine. The flow chart of the main routine will be given here only, with a brief description for each subroutine.

The purpose of the main routine is to control and arrange the process in the program. In other words the subroutines will work together under the organization of the main routine. A flow chart that represents the sequence of the operations in this routine is shown in Figure (5.1).

5.4 Applications for Testing the Program

Many examples are taken to verify the reliability of the program (NSHEEFF) and to examine the various solution schemes implemented in the program. Wherever possible, the results are compared with experimental, analytical and/or numerical results obtained by other investigators. These examples are

1. 3-Members extended frame.
2. Portal frame.
3. T-Shaped frame.
4. William's Toggle Frame.
5. Finite Beam on Elastic Foundation.
6. Fixed-Fixed Beam Resting on Elastic Foundation.
7. Fixed-Ended Vierendeel Frame.
8. Fixed-Ended X-Bracing truss Beam.
9. Cantilever Tapered Truss.

Principally, when the structure exhibits stiffening behavior, any of the iterative strategies can be used to get the complete load-displacement

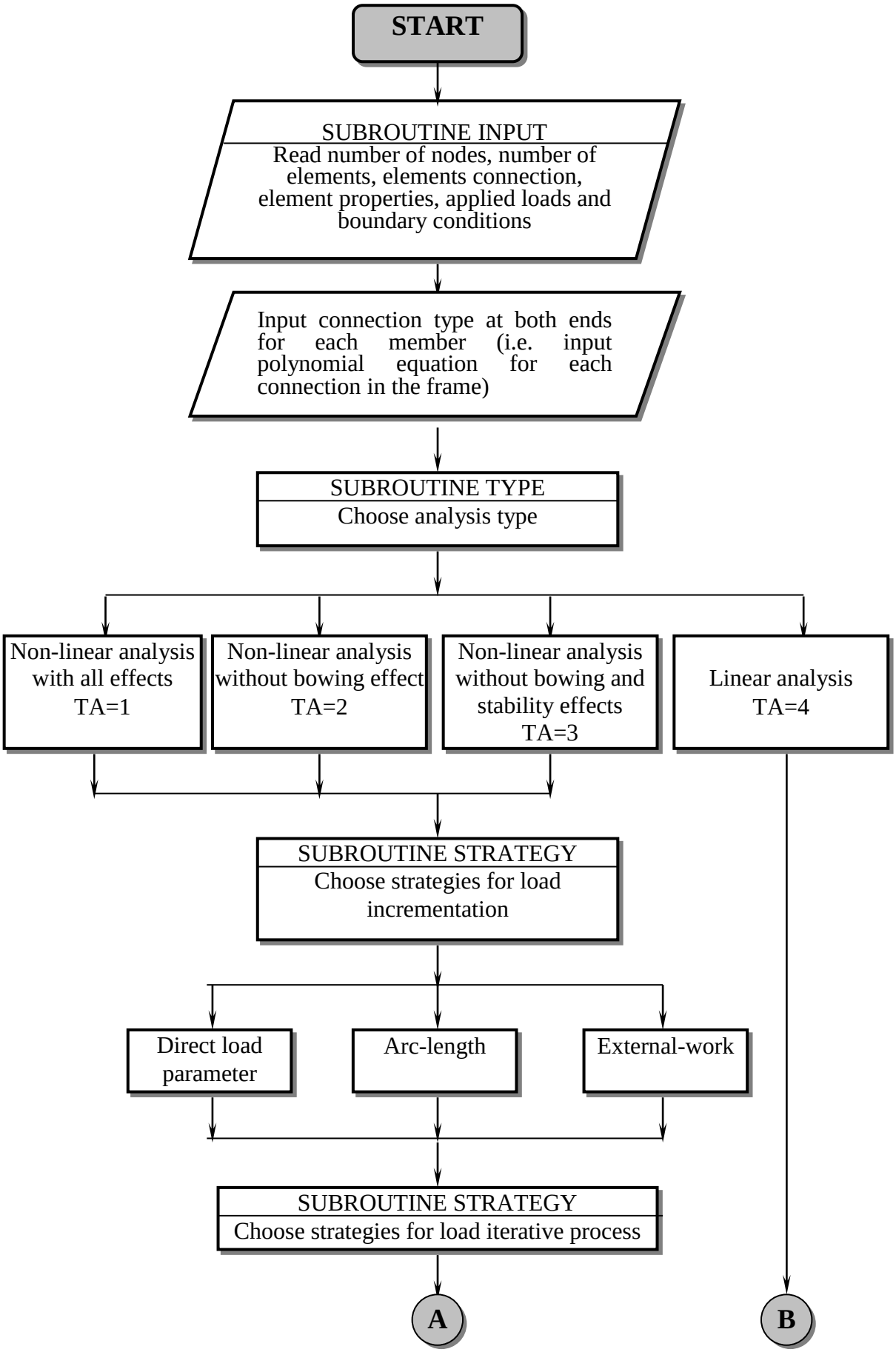

Fig.(5.1) :The Flow Chart of Computer Program (NSHEEFF).

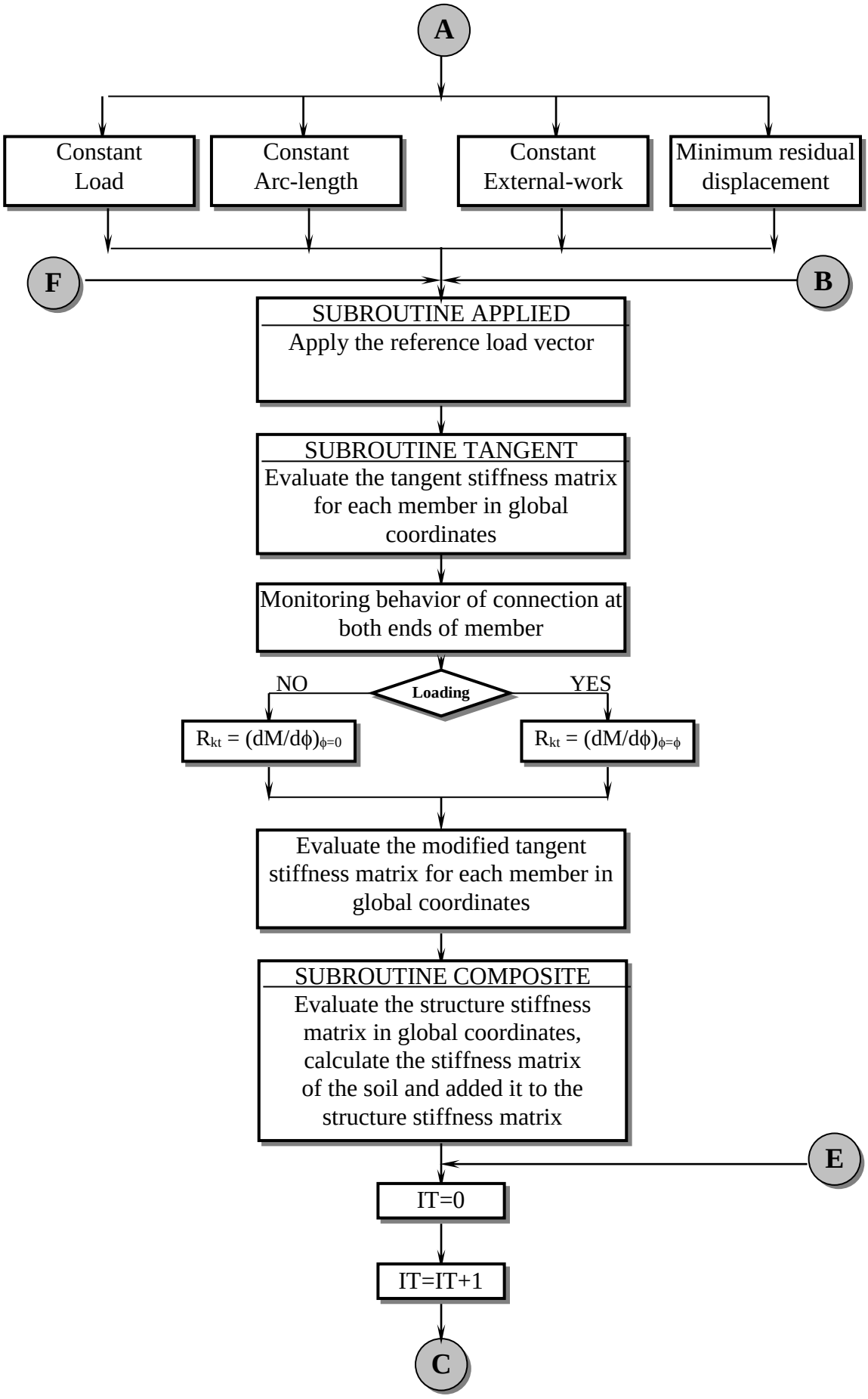

Fig.(5.1) : Continue

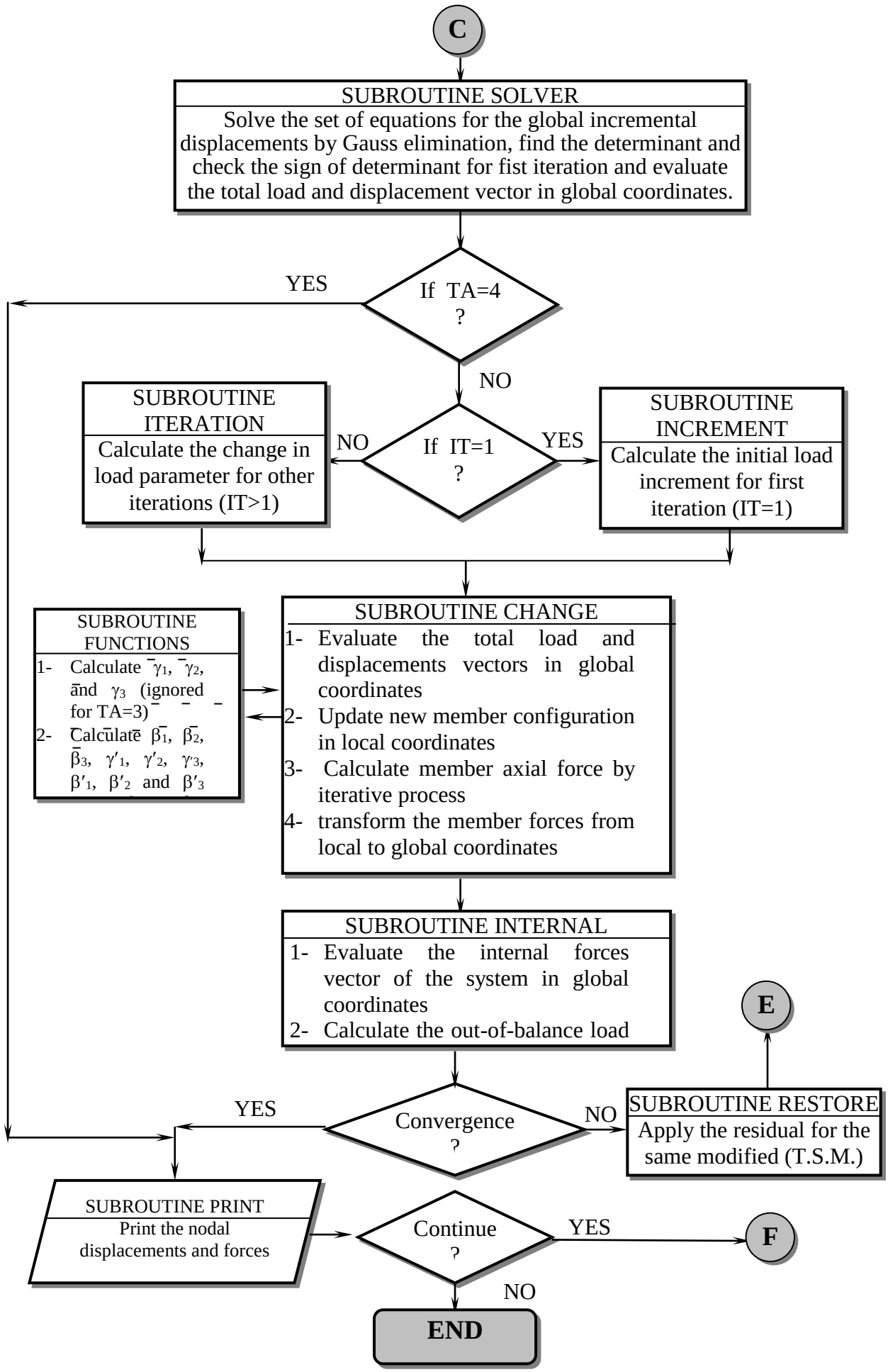

Fig.(5.1) : Continue

Curve, but, when the structure exhibits softening behavior, any of the iterative strategies can be used, except the constant load iterative strategy, to get the complete load-displacement curve. The constant load iterative strategy can be used only when the structure exhibits stiffening behavior.

5.4.1 Example No. 1: (3-Member Extended Frame)

The geometry, properties and load conditions of this example are as shown in Figure (5.2). This example shows very complex behavior for the load-displacement curves include both displacement and load limit points, therefore, it is chosen.

In 1996, ***Al-Raunduzy*** **[73]** solved this case by using the beam-column approach. Also, he used several methods for detecting the instability conditions and the extrapolation method was used to help in detecting such conditions. In his work, he detected a typical limit point at a load stage of 84.55 N. Also, he produced a complete load-displacement curve for vertical displacement of point B (see Figure (5.3)). Because he neglected the post-buckling analysis, the decreasing range in the post-buckling behavior did not appear.

Al-Mutairee in 2000, **[82]** solved this example, by using the constant arc-length incrementation strategy with the arc-length iterative strategy.

AL-Khafaji A.Kh.**[84]** , solved the same example in 2002, but it was resting on elastic foundation with foundation length (**Lf=500 mm**) and soil stiffness (**Kn=50 kN/mm^2**), Figure (5.3) shows this aim .

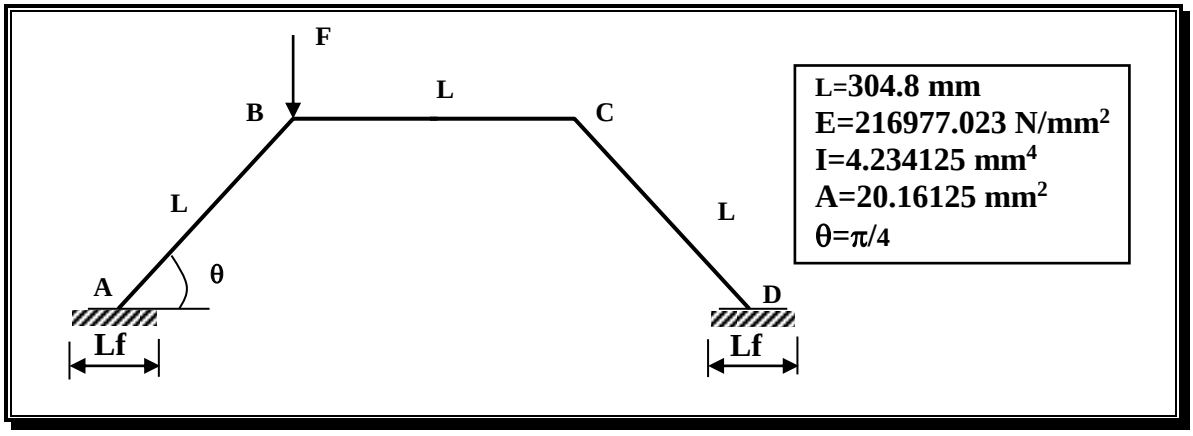

Fig.(5.2) : Geometry and Loading Conditions for Example No.1 .

In the present study, this frame is analyzed by using the arc-length load incrementation strategy and the minimum residual displacement iterative strategy. The reference load is (Fr = 1.5 N) and the desired number of iterations (Jd = 3). The complete load-displacement curve for vertical displacement of point B, horizontal displacement of point B and horizontal displacement of point C are shown in Figure (5.3) and Figure (5.4) respectively. Figure (5.3) shows a typical load-displacement curve including two load extremum points. Also, this Figure shows the load decreasing range in the post-buckling behavior that did not appear in reference **[73].** Finally from this figure it can be noticed that when the frame is resting on elastic foundation, the load resistance is smaller than that obtained when the frame is fixed at joints (A) and (D), by (7.5-20 %) ***AL-Khafaji A.Kh*. [84].**

The load-deflection curves in (**Fig.(5.3)**) show a good agreement with ***Al-Mutairee*** study. Figure (5.4) shows the more complex load-displacement curves for the horizontal displacement at point B&C. these curves show the displacement at a limit point as well as the load limit points.

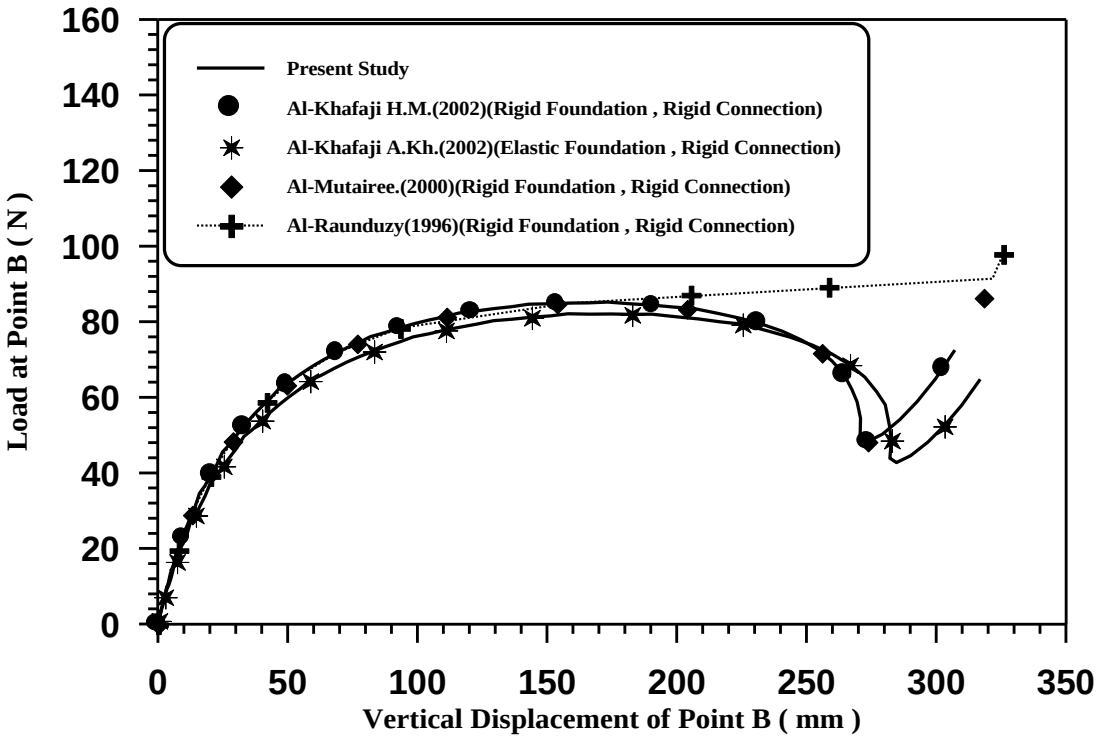

Fig.(5.3): Load-Displacement Curves for Example No.1 .

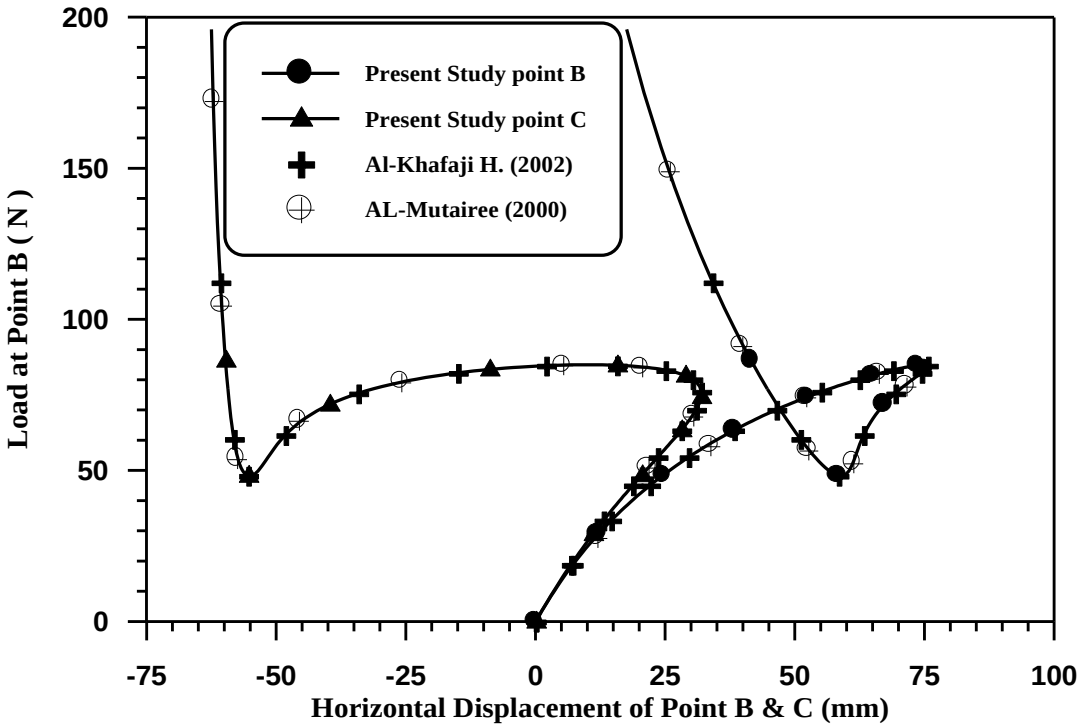

Fig.(5.4) : Load-Displacement Curves for Example No.1 .

5.4.2 Example No. 2: (Portal Frame)

This case aims to check the reliability of the derived modified tangent stiffness matrix in the presence of linear connection and to check the computer program in solving elastic stability problems in the presence of bowing effect as well as the linear connection.

The structure-load system of this example is shown in Figure (5.5). The frame is loaded with two vertical point loads **(F)** at the joints and a small lateral force **(rF)** is applied horizontally to the top of the frame.

Hsiao and ***Hou*** **[55]** produced geometrical non-linear finite element analysis on in-plane frames. They adopted a corotational formulation combined with the small deflection beam theory with the inclusion of the effect of the axial force. Like ***Oran*** and ***Kassimali*** **[21]**, solved this example considering four loading cases for **(r= 0.001, 0.01, 0.1, 0.5)**. Each member of the frame was represented by three equal elements. At each increment, the stiffness matrix updating was only performed at the two iterations of each cycle. The average number of iterations per increment is about nine with tolerance of 10^{-4} .

Wong and ***Tin-Loi*** **[66]** analyzed this example by using the finite element method. They used Newton-Raphson method for the iteration at initial stages with a load step of **(3302 kN)** and translation to the reduced modified arc-length method occurred at a load of **(19816 kN)**. They considered only one loading case of **(r = 0.001).**

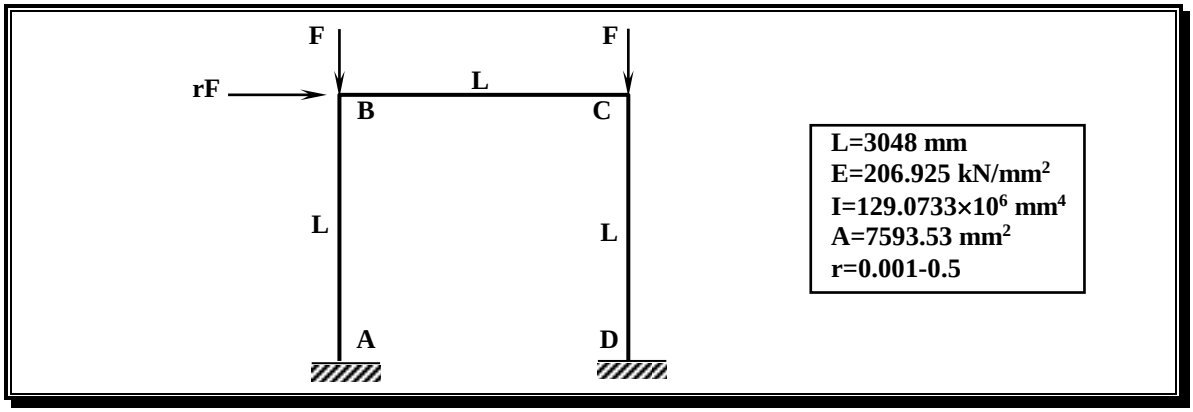

Fig.(5.5): Portal Frame (Geometry and Loading Conditions) .

In the present study, the frame is analyzed by using only three elements (one element for each member). The reference load **(Fr = 15 kN),** the desired number of iterations for convergence **(Jd = 3)**, and the incremental arc-length with iterative minimum residual displacement are used for rigid beam-to-column joint in the frame. And for linear beam-to-column joint with constant stiffness equals to (**10 EI / L**), the desired number of iterations for convergence **(Jd = 2)**, and the incremental arc-length with iterative arc-length are used.

As shown in Figure (5.6) a good agreement is obtained with the references **[21]** and **[66]** and some deviations are detected with the reference **[55]**. Also, the Figures (5.7) and (5.8) indicate that the present study is in a good agreement with respect to the reference **[85].**

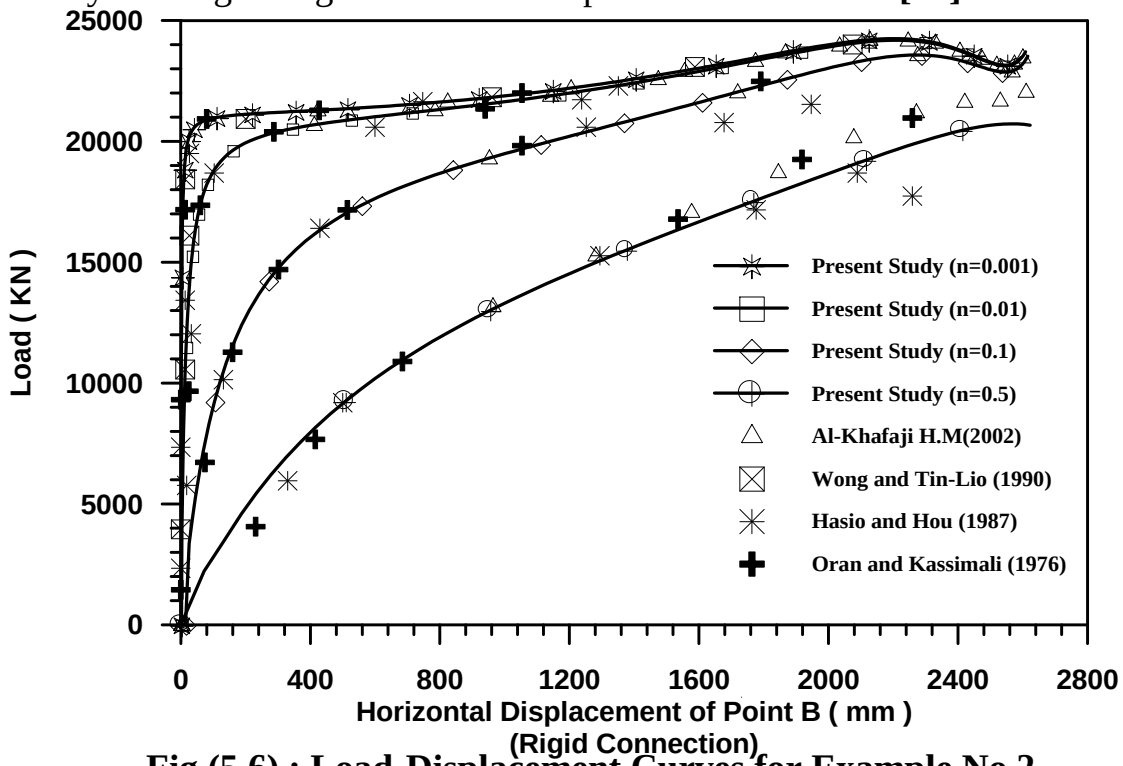

Fig.(5.6) : Load-Displacement Curves for Example No.2 (Rigid Connection) .

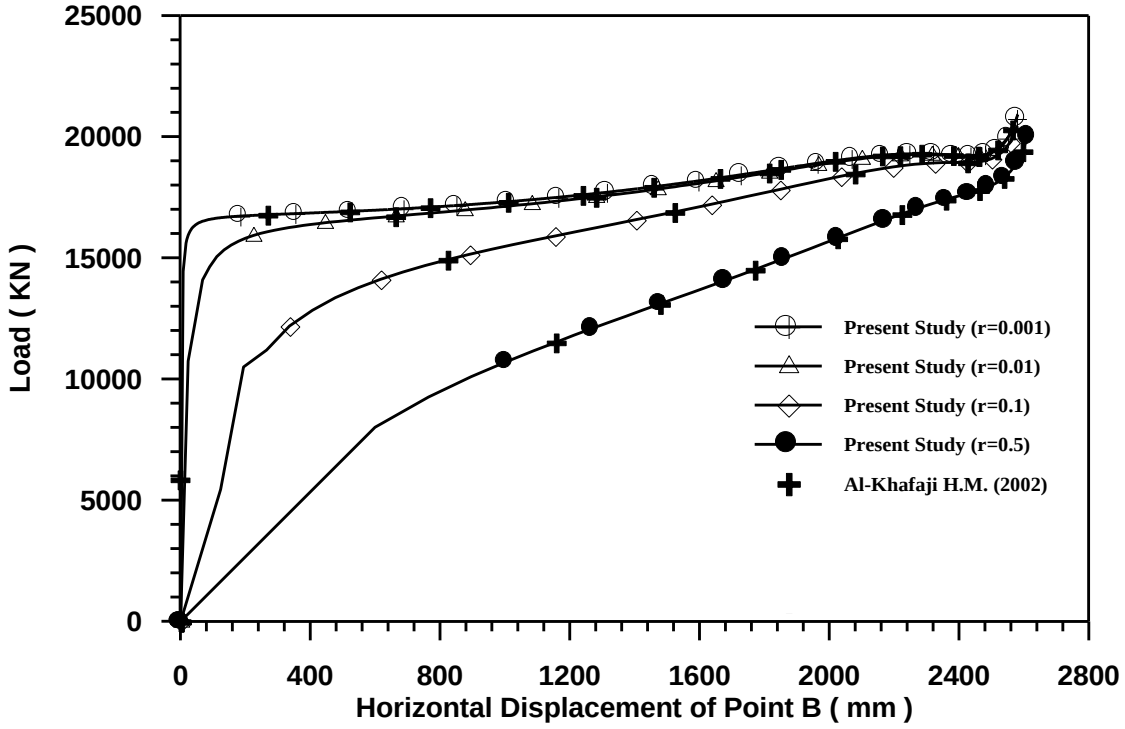

Fig.(5.7): Load-Displacement Curves for Ex. No.2 (Flexible Connection) .

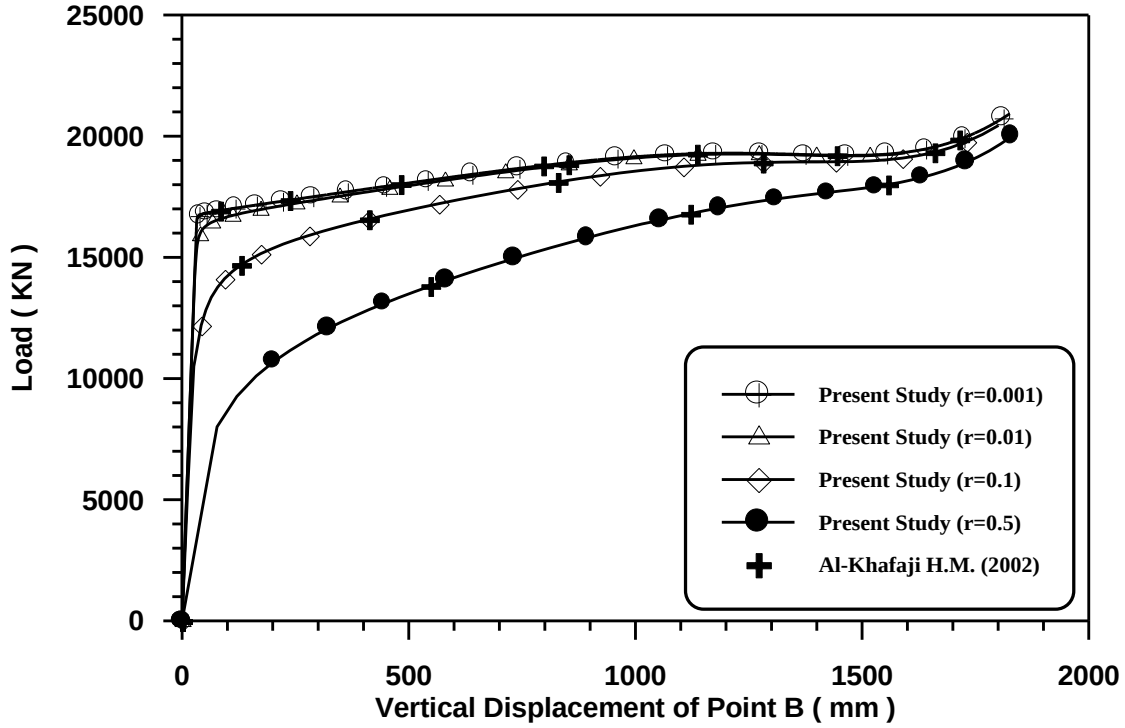

Fig.(5.8) : Load-Displacement Curves for Ex. No.2 (Flexible Connection) .

5.4.3 Example No. 3: (T - Shaped Frame)

In order to investigate the effect of connection flexibility on the behavior of structures, this example is considered here.

The geometry, properties and loading conditions of this example as shown in Figure (5.9). A gain, two cases, i.e. rigid and flexible connection cases, are considered and the behavior of the connection is given by the moment-rotation curve as illustrated in Figure (5.10).

Achintya Haldar and ***Ker-Ming Nee*** in 1988, analyzed this example by using the finite element method. The solution as shown in Figure (5.11) was obtained by using the moment-rotation behavior of the flexible connections as shown in Figure (5.10). In solving the non-linear equations, the Newton-Raphson method with arc-length control is used in tracing the post-buckling behavior. The behavior of flexible connections is represented by an exponential function.

G. Shi and ***S. N. Atluri*** in 1989, **[63]**, analyzed this example by using the complementary energy approach, involving the weak form of the compatibility of the member deformation. The solution as shown in Figure (5.11) was using the same moment-rotation behavior of the flexible connection. In solving the non-linear equations, the Newton-Raphson method with arc-length control is used in tracing the post-buckling behavior. The behavior of flexible connections is represented by the Ramberg-Osgood function.

In the present study, in both cases rigid and flexible the frame is analyzed by using the constant arc-length incrementation strategy with the arc-length iterative strategy. The reference load is **(Fr = 20 Kips)** and the desired number of iterations is **(Jd = 3)**. The load-displacement at point A for both the rigid and flexible connections are plotted in Figure (5.11). The results agree quite well with those given by ***Achintya Haldar*** **and** ***Ker-Ming Nee, G. Shi*** **and** ***S. N. Atluri*** **[63]** and ***AL-Khafaji H.M.*****[85]**, also from this Figure, it can be seen that even under a very small external load **F**, the behavior of the frame with flexible connections is considerably different from that of the rigid connection case. This clearly indicates the importance of consideration of flexible connections in real structures.

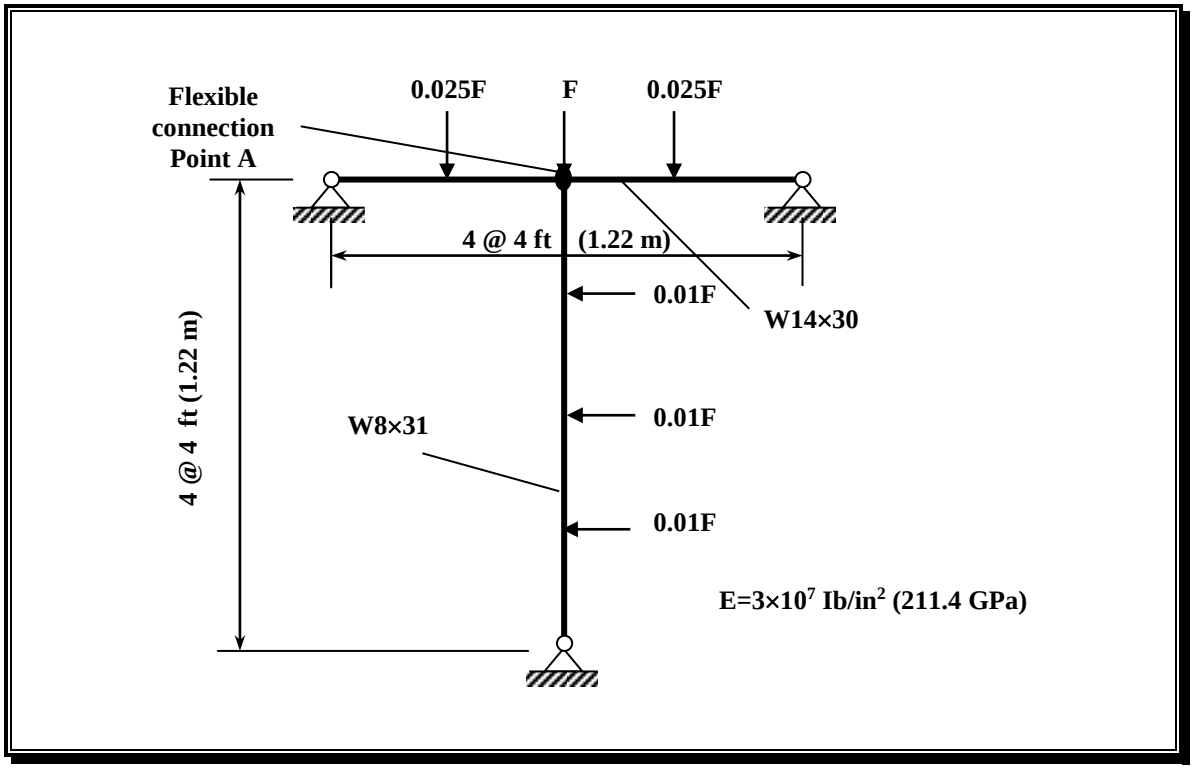

Fig.(5.9): Geometry and Loading Conditions for Example No. 3 .

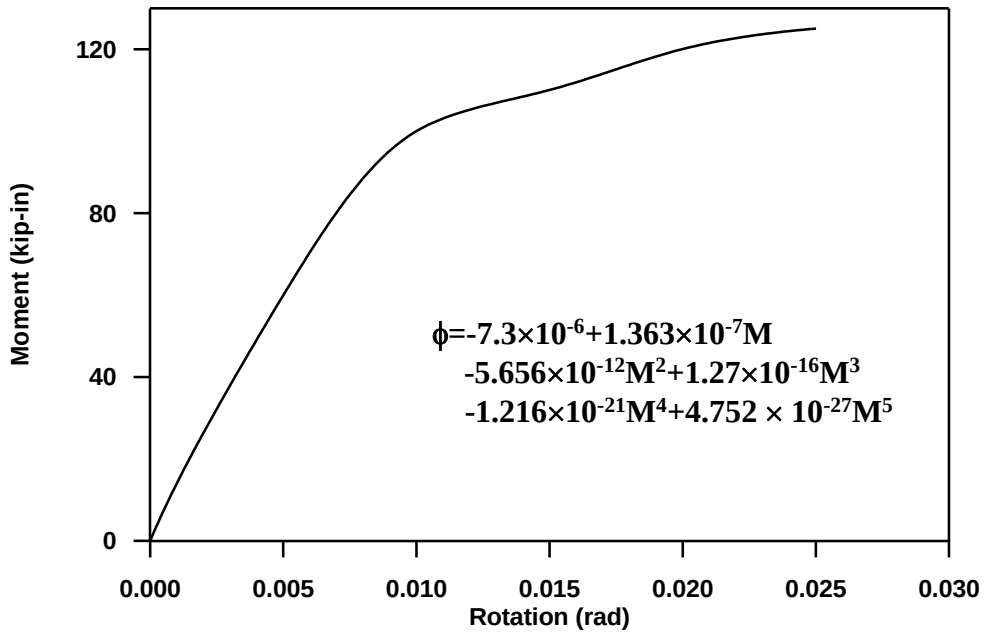

Fig.(5.10): Connection Moment-Rotation Behavior Used for Example No. 3 [63].

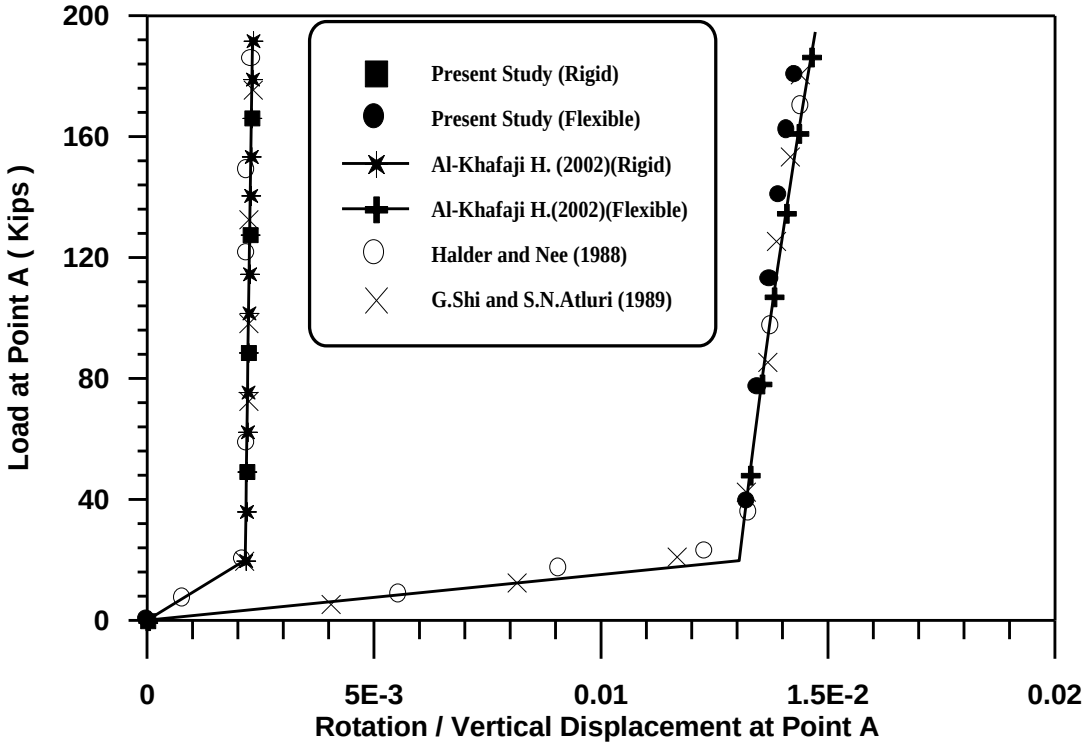

Fig.(5.11): Load-Ratio of Rotation/Translation at Flexible Connection Point A.

5.4.4 Example No. 4: (William's Toggle Frame)

The study of this case aims to checks the accuracy of the proposed method with highly non-linear structure. Figure (5.12) shows the geometry, properties and loading conditions of William's toggle frame to solve non-linear flexible supports, the moment-rotation behavior of which is shown in Figure (5.13).

Many researchers have analyzed this frame by using rigid supports. In 1964, ***William's*** **[8]** presented both experimental and theoretical results for a series of toggle frames. In his theoretical work, he adopted a beam-column model to describe the behavior of individual members of the frames. By solving the differential equations for each member a corrected axial strain expression, including terms up to the second order, was obtained and used for his elastic stability finite deflection and flexural shortening analysis. Results varying from a simple linear to highly complex non-linear analysis, formulated by including more and more terms in the governing equation, were also compared.

Wood and ***Zienkiewicz*** **[25],** employed a total Lagrangian finite element formulation in a continuous approach with paralinear

isoparametric element. They solved this example by using modified Newton-Raphson method with five elements per member.

Hsiao and ***Hou*** **[55]** analyzed this example considering the symmetry of geometry and deformations by taking only half of the frame in the analysis. Five elements were used for discretization and the error tolerance 10^{-4} was used for equilibrium iteration. Also, they used five load increments and the average number of iterations per increment is about seven.

Wong and ***Tin-Loi*** **[66],** discretized the frame into four elements per member and used the incremental-iterative method with load step of 17.8 N (4 Ib). The Newton-Raphson method was used at the initial stages and when the load reached a stage of 142.4 N (32 Ib) a sever deterioration in the stiffness of the structure was detected. The reduced modified arc-length method was automatically activated and the analysis was continued until a critical load of 151.3 N (34 Ib) was reached.

In the present study the toggle frame is analyzed and modeled by two elements only, and also utilizing symmetry. For both rigid and flexible cases the reference load is **(Fr = 1.2 Ib)** and the desired number of iterations for convergence **(Jd = 3)**. The incremental external-work with iterative external-work is used.

The present analysis of the toggle frame is shown in Figures (5.14) and (5.15), compared with results obtained by others. Figures (5.14) and (5.15) shows the load-displacement curves for the vertical displacement of point B. It can be seen that the solution based on the present formulation with all geometrical effects has good agreement with both experimental and theoretical results obtained by others.

For the purpose of comparison, the behavior of this frame with rigid and flexible supports is shown in Figures (5.14) and (5.15), it can be seen that before limit point, the load-deflection behavior of the toggle with rigid supports is quite comparable with that of flexible supports. At or after limit point, however, the toggle with flexible supports deflected more.

This phenomenon can be explained by referring to Figure (5.13). Before limit point, the rotational stiffness of the connection (slope of the moment-rotation curve) is quite considerable. Appreciable more deflection is experienced at or after limit point because of the decreased stiffness as a result of non-linear rotation behavior of the support.

Figure (5.16) shows the present computed relation between the external load and the horizontal reaction at the fixed end. A good agreement is obtained between this study and the other reference.

This example aims to examine the reliability of the interpolation method for calculating the critical loads and critical points. In the present study the first critical load in the rigid analysis is equal to (33.998 lb) and for flexible analysis is equal to (25.974 lb).

It can be seen from the previous figures that the rigidity or stiffness of the support plays a very important role in the post-buckling behavior of the toggle and any other frames.

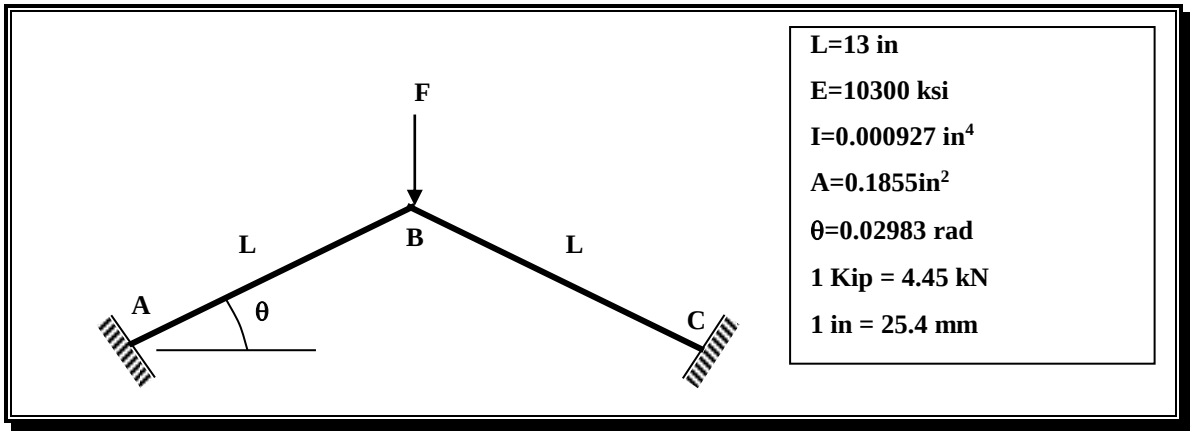

Fig.(5.12) : Toggle Frame (Geometry and Loading Conditions) .

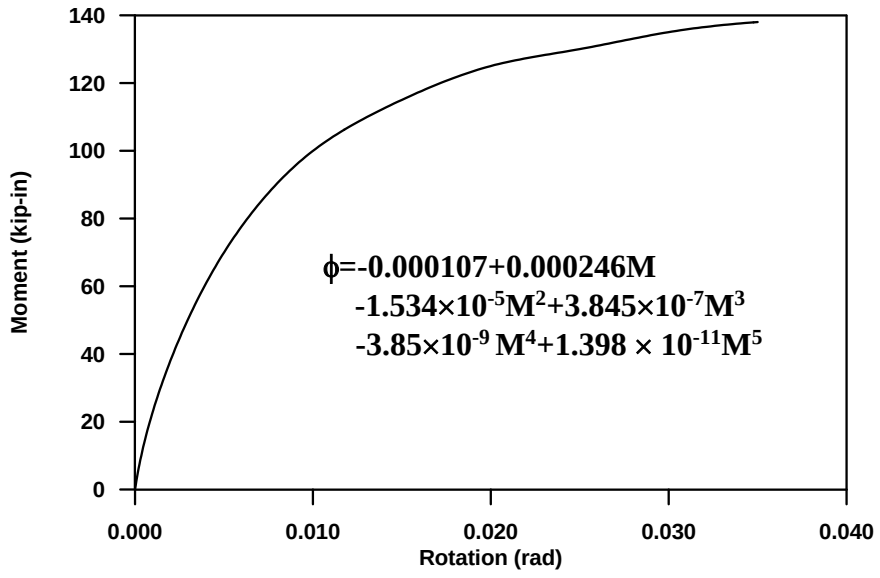

Fig.(5.13): Moment-Rotation Behavior Used for Supports of Toggle Frame [66].

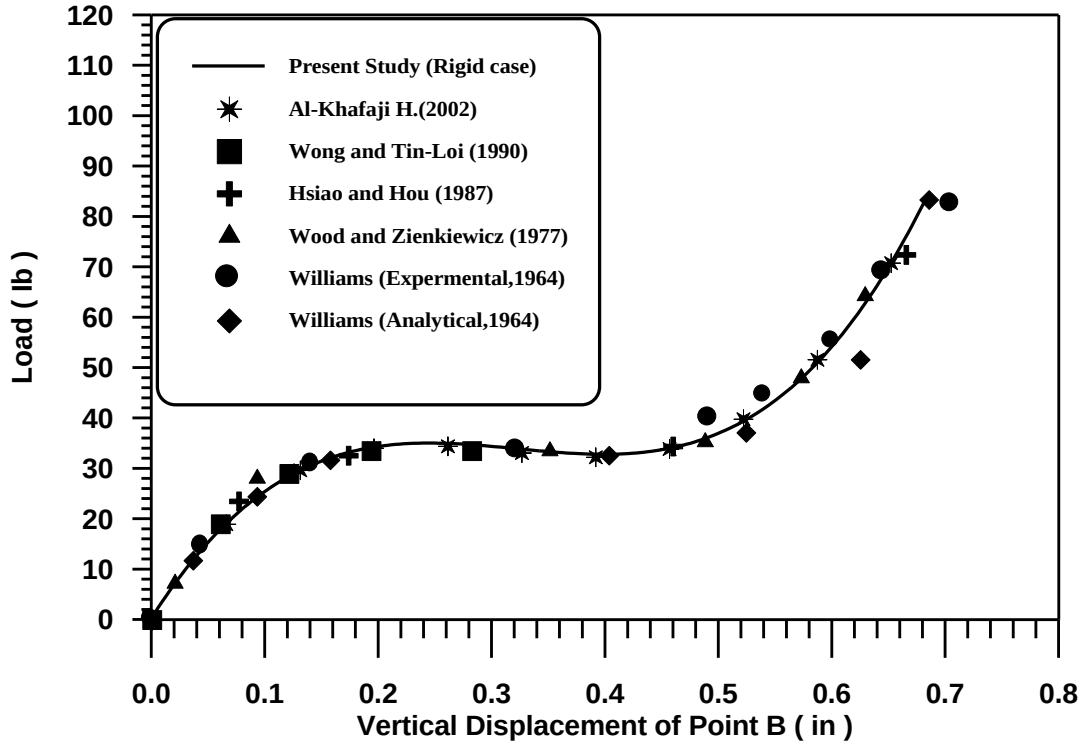

Fig.(5.14): Load-Displacement Curves for Example No.4 .

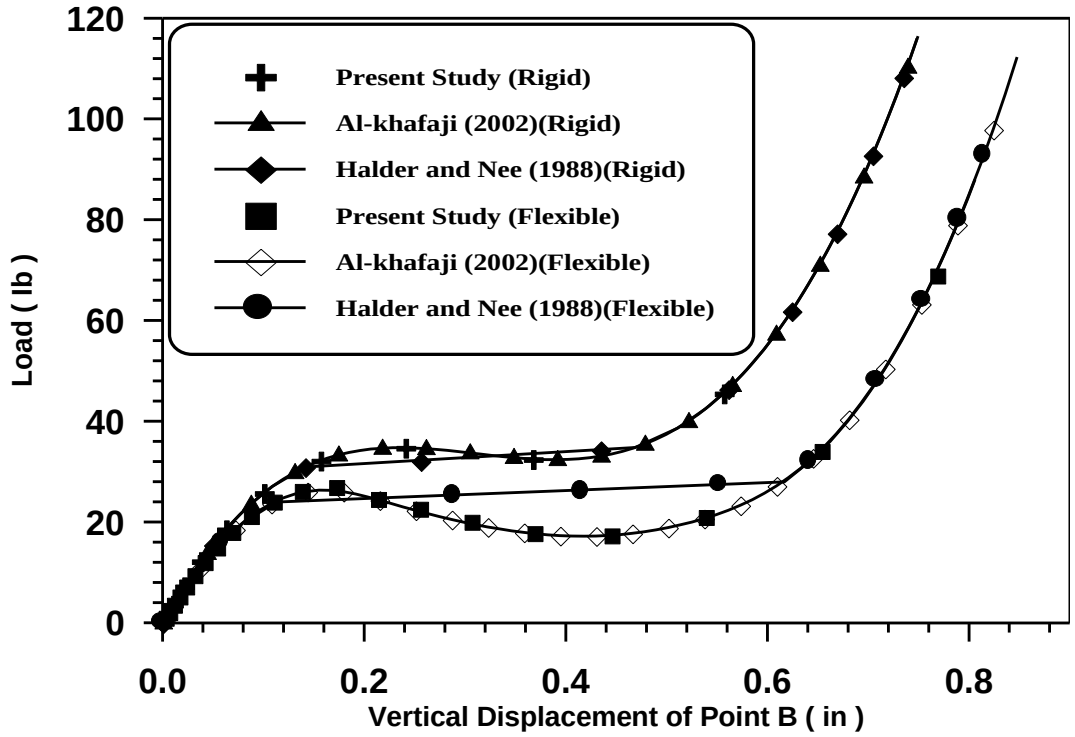

Fig.(5.15): Load-Displacement Curves for Example No.4 .

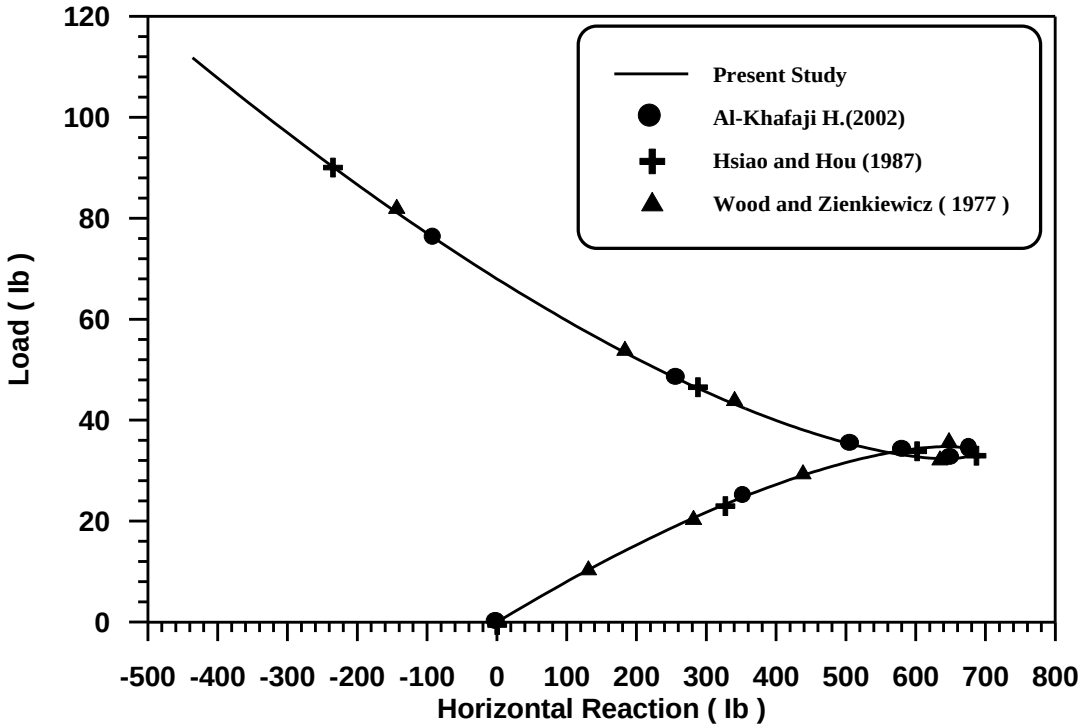

Fig.(5.16) : Load-Horizontal Reaction Curves for Example No. 4 .

5.4.5 Example No. 5: (Finite Beam on Elastic Foundation)

The geometry and loading conditions of finite beam resting on a linear elastic foundation is shown in Fig. (5.17).

M. Hetenyi **[2],** gave the exact solution of this problem in 1946.

Antonio, in 1987, **[59]**, solved the same example by using the finite element method. He needed (13) elements to get the exact value.

AL-Khafaji A.Kh. **[84]**, used the same example and solving it by using A polynomial function in the stiffness of soil in 2002.

In the present study, the approach of lumped spring is used in the analysis of this example. Figure (5.18) shows the load deflection curve for this example. As shown in this figure, there were some differences in the range of **(0-6.66 %)**, between the present study and the results obtained by ***Antonio*** **[59],** and ***AL-Khafaji A.Kh***. **[84],** because the present study used the beam-column element and linear elastic foundation, reference **[59],** used the finite element and non-linear elastic foundation, and reference **[84],** used the beam-column element and non-linear elastic foundation.

Any way a good agreement is achieved between the results obtained in the present study and those obtained by ***Antonio*** **[59],** and ***AL-Khafaji A.Kh***. **[84].**

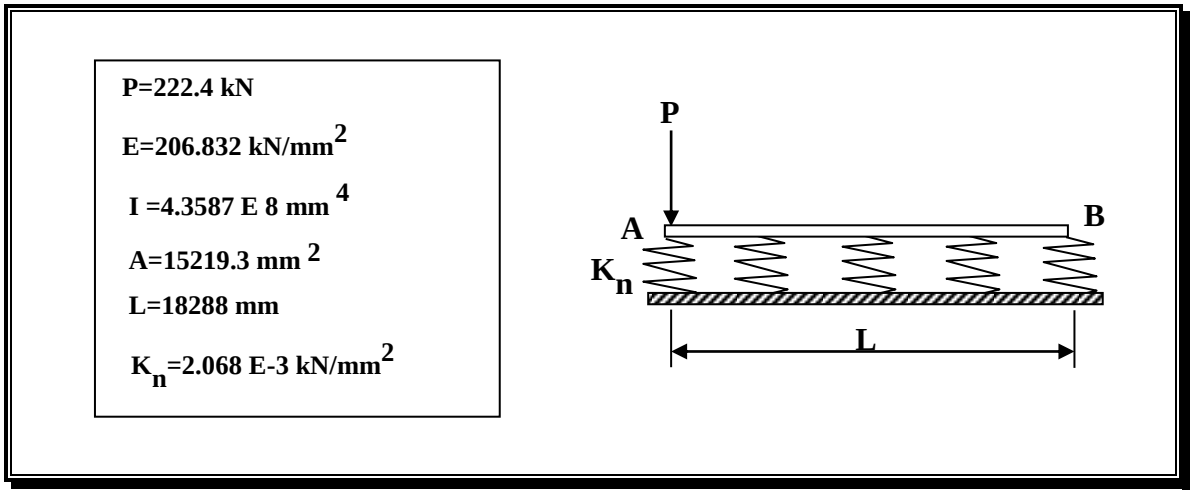

Fig.(5.17) : Geometry and Loading Condition of Example No.5 .

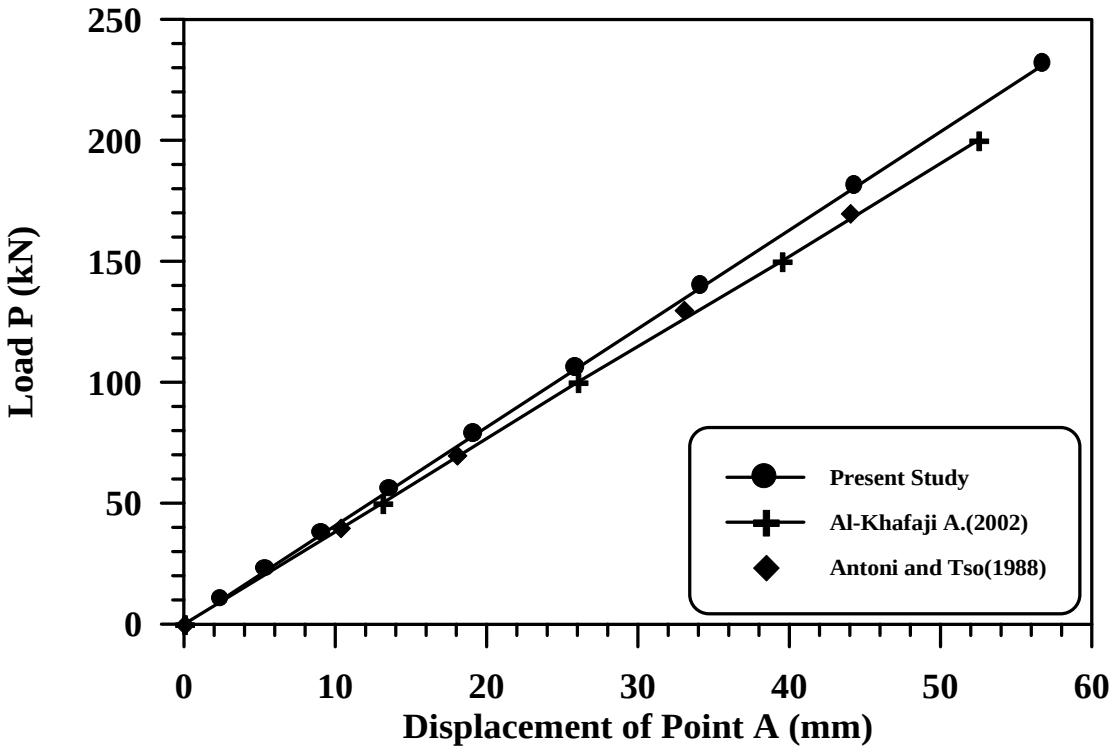

Fig.(5.18) : Load-Displacement Curve of Example No.5 .

5.4.6 Example No. 6: (Fixed-Fixed Beam Resting on Elastic Foundation)

The purpose from choosing this example is to illustrate the effect of the subgrade reaction soil on the behavior of the structure. Fig. (5.19) shows the geometry and loading conditions for this case.

Chen, in 1998, **[78]**, used numerical method for solving this problem. He used the differential quadrature elements method (DQEM),

but he assumed that the modules of subgrade reaction for soil was constant (linear elastic foundation).

During 2002, ***Al-Khafaji A. Kh.*** **[84]**, used the same example and rested it on non-linear elastic foundation, using polynomial function for the soil stiffness.

In the present study, this example is considered to rest on linear elastic foundation.

Fig.(5.20) shows the deflected shapes of this beam .A significant difference is achieved between the results of the linear and non-linear subgrade reaction soil .

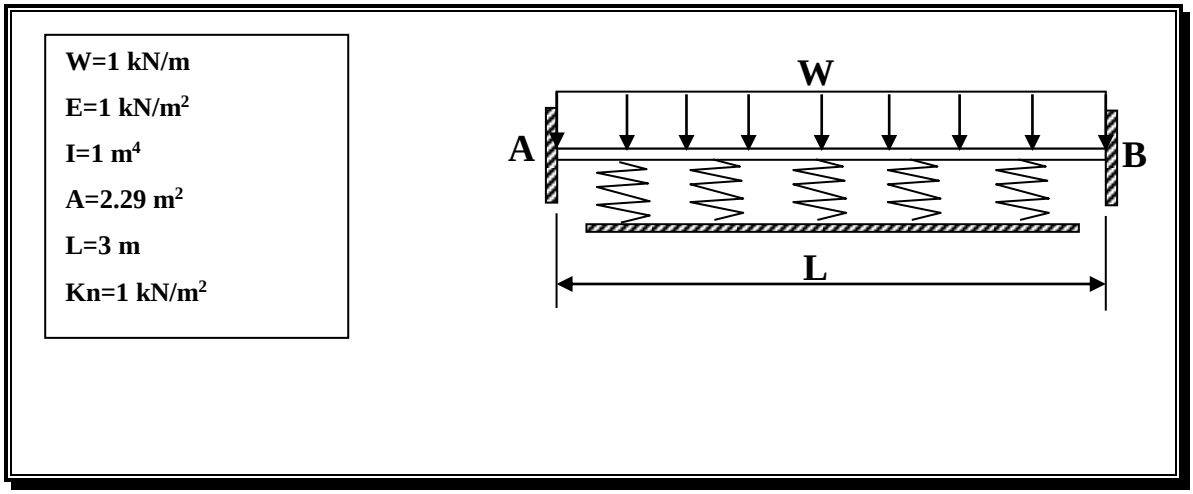

Fig.(5.19) : Geometry and Loading Condition of Example No.6 .

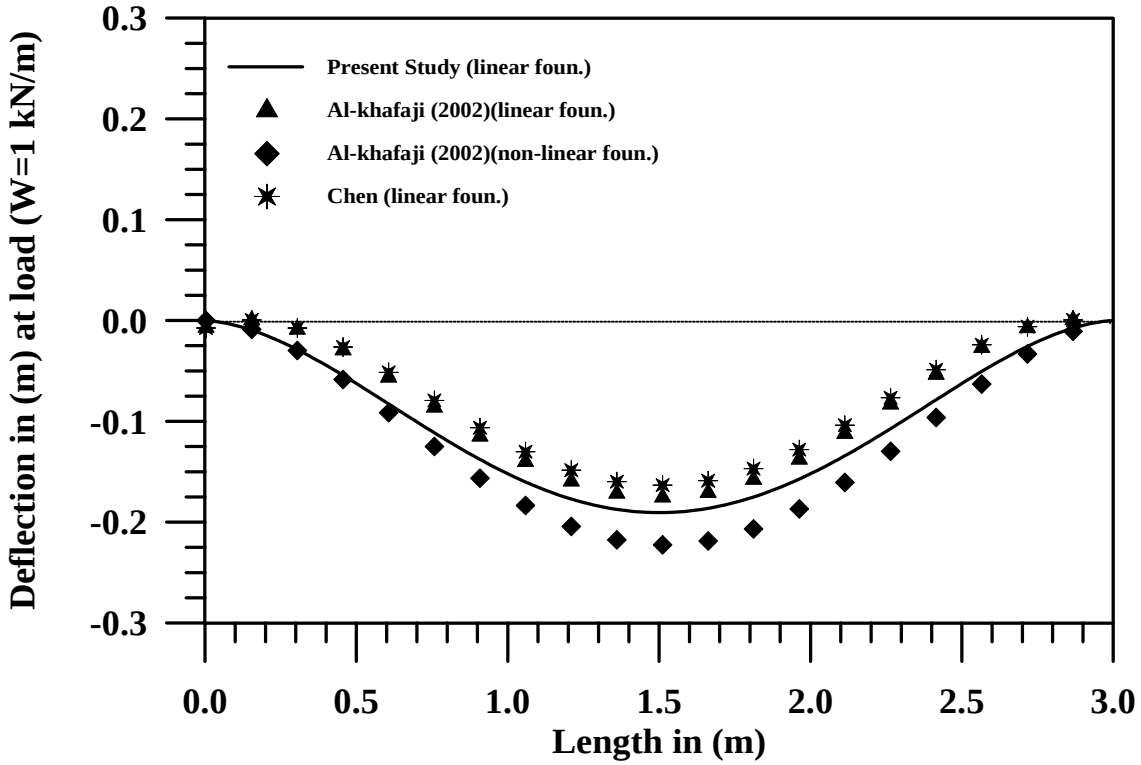

Fig.(5.20) : Load-Displacement Curve of Example No.6 .

5.4.7 Example No. 7: (Fixed-Ended Vierendeel Frame)

To check the reliability of the computer program (NSHEEFF) in solving problems including shear effect, and to verify the effect of shear on the behavior of beam-like lattice structures, the fixed-ended Vierendeel frame has been chosen for this aim.

The geometry, properties and loading condition for this problem are shown in Figure (5.21).

During 1988, ***Mc Callen and Romstad*** **[60]**, was solved this example by using the original geometry of this frame.

Al-Bidairi S.**[76]**, was solved the same frame in 1998, by using the original frame and the equivalent model.

In 1999, ***AL-Quraishi*** **[80]**, solved this example by using the equivalent model.

The structure consists of (**31**) identical members with (**22**) rigid joints. The shear parameter (μ) for each member was calculated and it was found equal to (0.0256), which is too small and can be neglected for this example. Therefore, an equivalent beam, as shown in Figure (5.21b), by using the method presented in chapter three modeled the structure. The model was discreted into four equal elements. The shear parameter for each element is equal to (36.406). The results obtained from the above solutions are shown in Figure (5.22). The results show that the present and the previous solutions for the original structure are very close to each other.

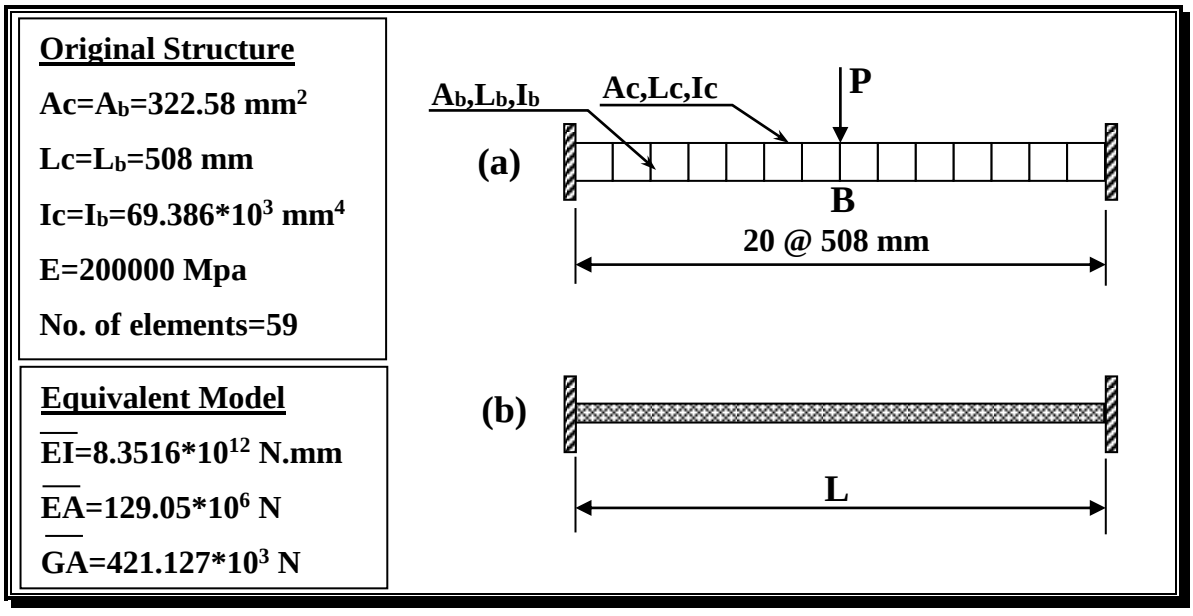

Fig.(5.21) : Geometry and Loading Condition of Example No.7 .

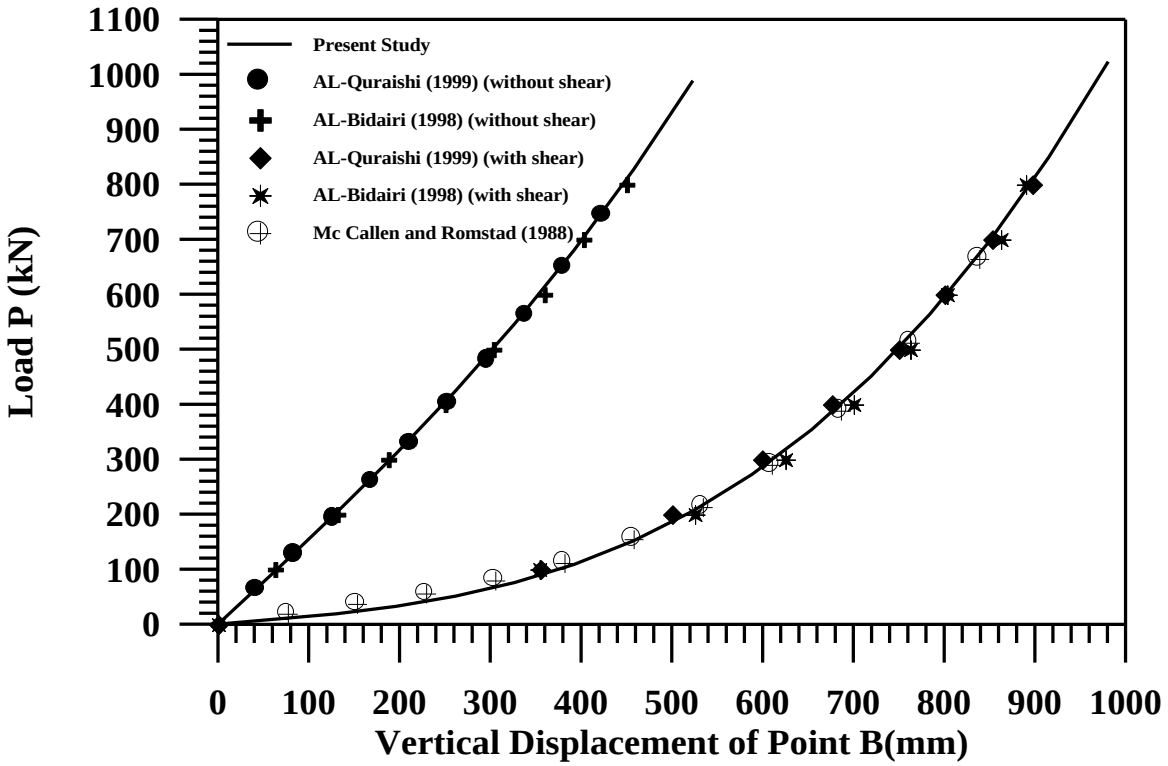

Fig.(5.22) : Load-Displacement Curve of Example No.7 .

5.4.8 Example No. 8: (Fixed-Ended X-Bracing Truss Beam)

To show the effect of the slenderness ratio on the value of the shear parameter (μ) and accordingly on the shear deformations of structures, a fixed-ended X-bracing beam has been chosen for this aim.

The reference of the structure used in this example is an X-bracing cantilever truss beam under static load used by ***Mc Callen*** and ***Romstad*** in 1988 **[60]**. A modification is made for the geometry of the reference structure to get the proposed example as follows: -

1- Fixing the free-end of the cantilever structure.

2- Using the equivalent model for the whole structure.

Other structural properties are kept same as that of the reference structure Figure (5.23) shows the geometry, properties and loading condition for the proposed structure used in this example.

This structure was modeled by an equivalent beam with the properties shown in Figure (5.23b). Then, the equivalent beam-model was analyzed by using different slenderness ratios (**L/d**) and accordingly different values of shear parameter (μ).

In 1998, ***Al-Bidairi*** **[76]**, used the same example and studied the effect of the shear parameter value on the dynamic response of beam –like lattice structures.

Figure (5.24) shows the load-displacement curve of this problem by analyzing it twice, the first one with shear effect and the other without shear effect for three cases of slenderness ratios (**L/d**).

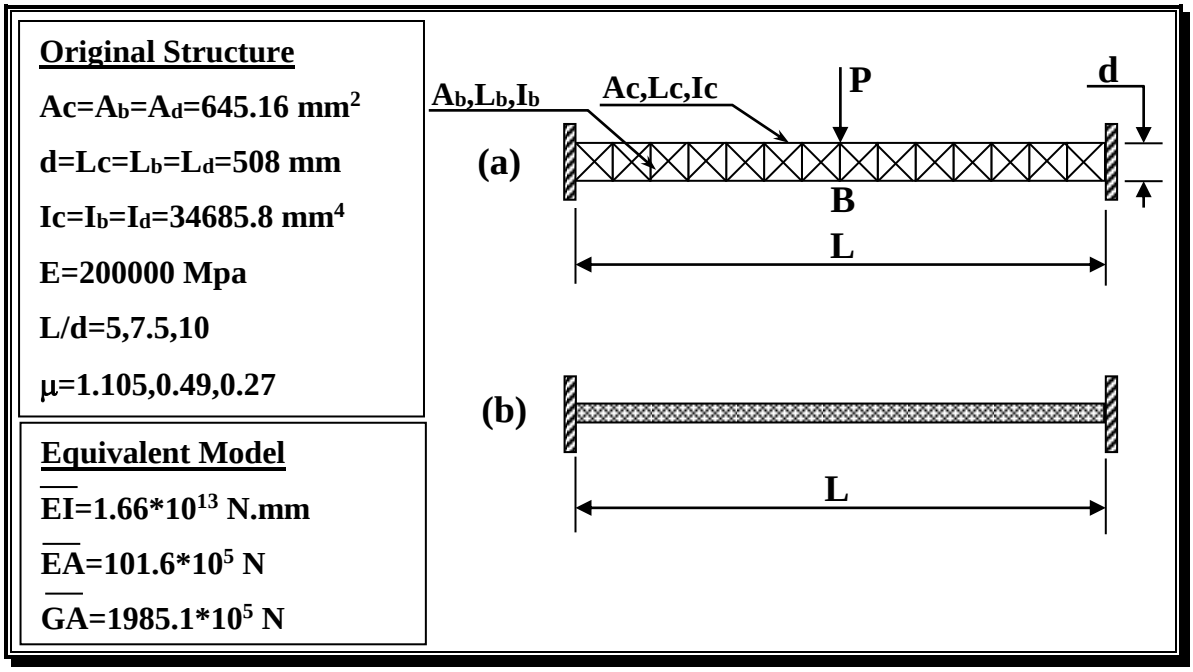

Fig.(5.23) : Geometry and Loading Condition of Example No.8 .

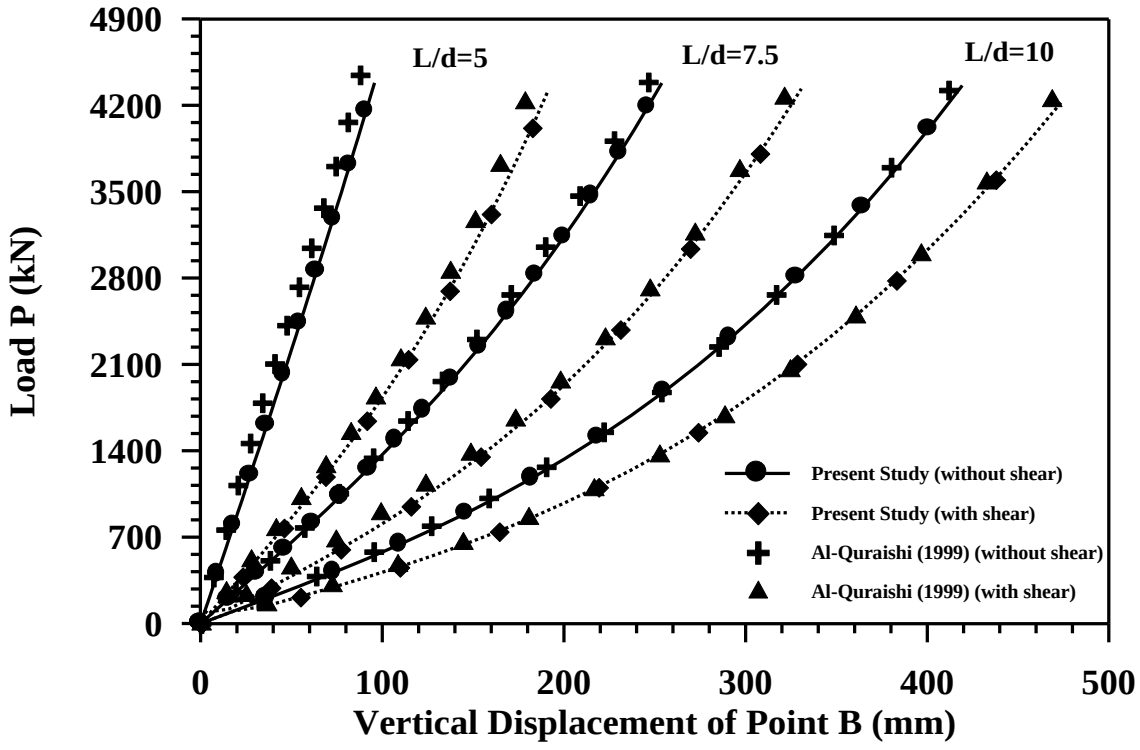

Fig.(5.24) : Load-Displacement Curve of Example No.8 .

5.4.9 Example No. 9: (Cantilever Tapered Truss)

To check the adequacy of the equivalent continuum model of non-prismatic beam-like lattice structure present in this study (see chapter three) and in order to induced the effect of shear on the non-prismatic structure, the analysis of the cantilever tapered truss is considered as an example for study.

Figure (5.25) shows the geometry and loading conditions for the actual and equivalent model of the cantilever tapered truss which is subjected to transverse tip load. Using an equivalent tapered beam-column element as shown in Figure (5.25b) solves the present problem.

Figure (5.26) shows the load-displacement curve of this problem, where a good agreement has been found between the two solutions. This confirms the efficiency of the present method to predict the behavior of non-prismatic beam-like lattice structure. Also the equivalent model was analyzed twice, the first one with shear effect and the other without shear effect, the results are shown in Figure (5.26), where the effect of shear deformation is about 23.33% ***AL-Quraishi*** (1999) **[80]**.

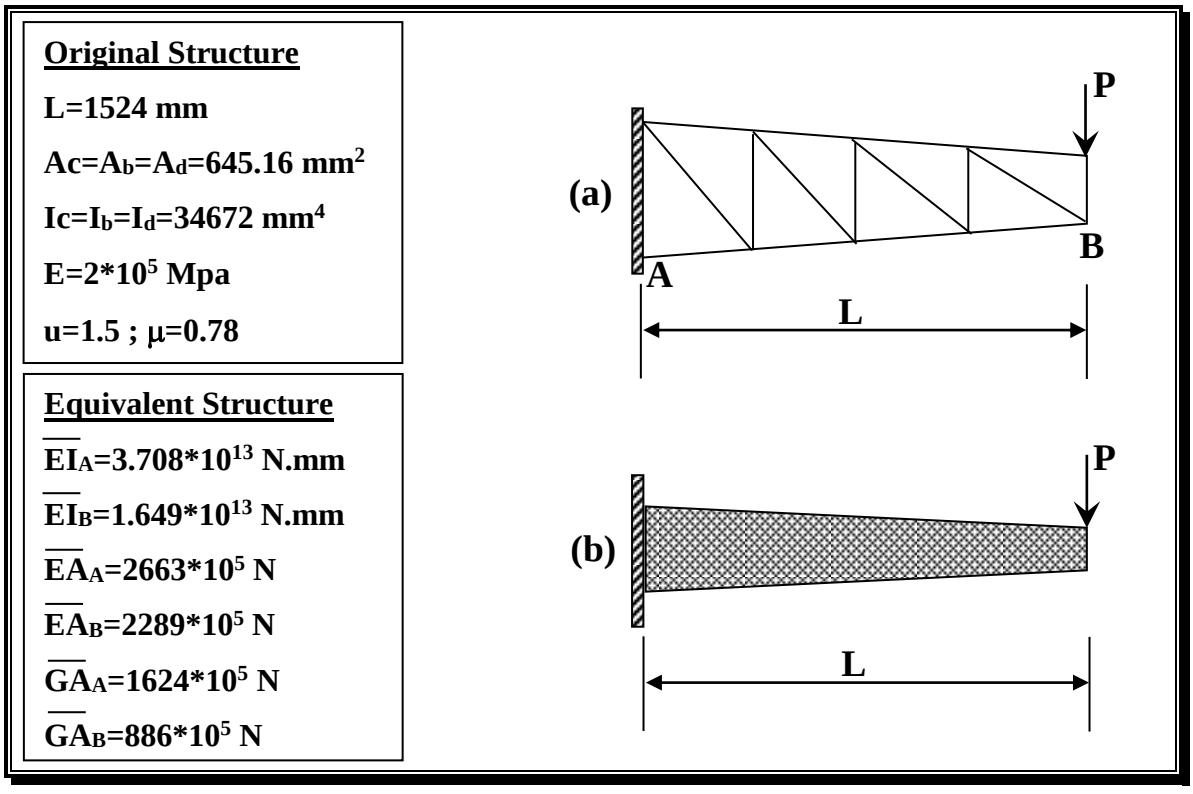

Fig.(5.25) : Geometry and Loading Condition of Example No.9 .

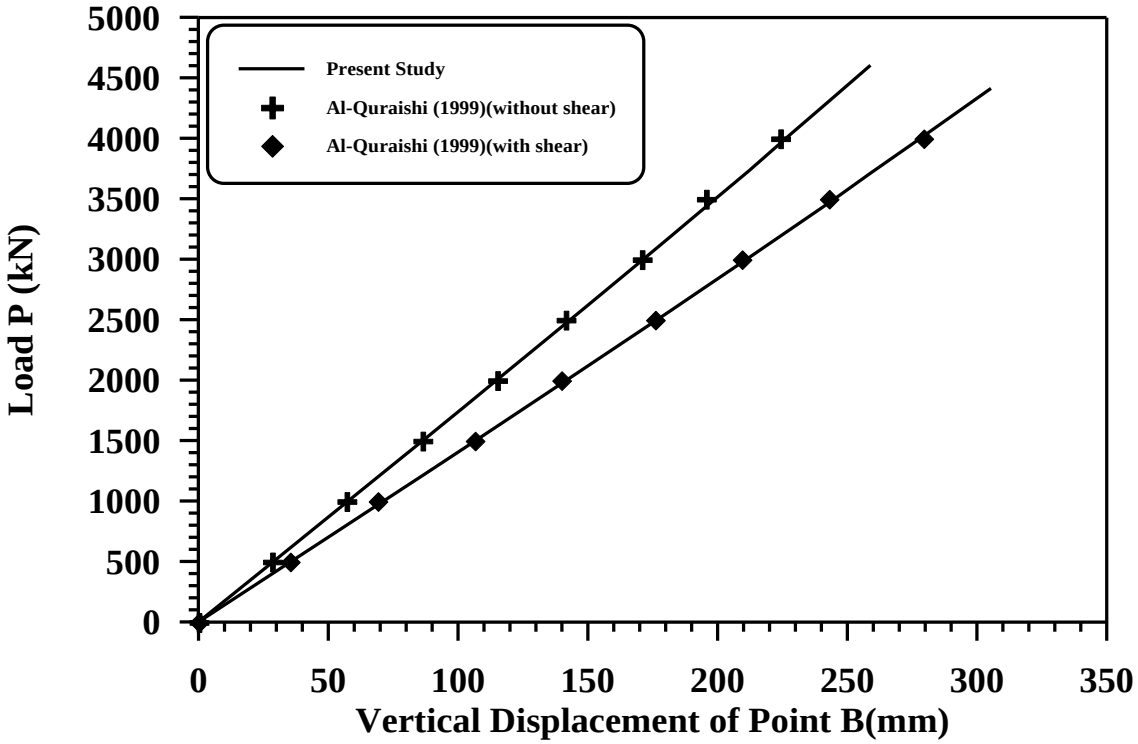

Fig.(5.26) : Load-Displacement Curve of Example No.9 .

REFERENCES

1. Rathbun, J.C., "Elastic Properties of Riveted Connections", Transactions of ASCE, Vol. 107, 1936, pp.(993-1019).
2. Hetenyi , M., " Beams on Elastic Foundation" ,The University of Michigan, USA, 1946.
3. Livesely, R.K. and Chandler, D.B., "Stability Functions For Structural Frameworks", Manchester University Press, Manchester, 1956.
4. Timoshenko, S.P. and Gere, J.M., "Theory of Elastic Stability", Second Edition, MeGraw-Hill Book Co., Inc., New York, 1961.
5. Wang, T.M., Lee, S.L. and Koa, J.S., "Continuous Beam - Column on Elastic Foundation", Journal of Engineering Mechanics, ASCE, Vol.87, No.EM2, April, 1961, pp.55-70.
6. Monforton, G.R. and Wu, T.S., "Matrix Analysis of Semi Rigidly Connected Frames", Journal of Structural Engineering, ASCE, Vol. 89, No.ST6, June, 1963, pp.(13-42).
7. Saffan, S.A., "Nonlinear Behavior of Structural Plane Frames", Journal of the Structural Division, ASCE, Vol. 89, No.ST4, August, 1963, pp.(557-578).
8. Williams, F.W., "An Approach to the Nonlinear Behavior of the Members of a Rigid Jointed Plane Framework with Finite Deflections", The Quarterly Journal of Mechanics and Applied Mathematics, Vol. 17, 1964, pp.(451-469).
9. Somner, W.H., "Behavior of Welded Header Plate Connections", M.Sc. thesis, University of Toronto, Toronto, October 1969.
10. Romstad, K.M. and Subramanian, C.U., "Analysis of Frames with Partial Connection Rigidity", Journal of Structural Division, ASCE, Vol. 96, No.ST11, Nov., 1970, pp.(2283-2300).
11. Lin, F.J., Glauser, E.C. and Jhonston, B.G., " Behavior of Laced and Battened Structural Members " , Journal of Structural Engineering, ASCE, Vol.96,No.ST7,July, 1970,pp. 1377-1401 .
12. Wempner, G.A., "Discrete Approximations Related to Nonlinear Theories of Solids", International Journal of Solids Structures, Vol. 7, 1971, pp.(1581-1599).
13. Oran, C., "Tangent Stiffness in Plane Frames", Journal of the Structural Division, ASCE, Vol. 99,No.ST6, June, 1973, pp.(973-985).
14. Renton, J.D. , " Buckling of Long, Regular Trusses " , Journal of Solids Structures, Vol.9, 1973, pp. 1489-1500.
15. Oran, C., "Geometric Nonlinearity in Nonprismatic Members", Journal of the Structural Division, ASCE, Vol. 100,No.ST7, July, 1974, pp.(1473-1487).

16. James, M.E., Kozik, T.J. and Martinez, J.E., "Effect of Curvature on Nonlinear Frame Analysis", Journal of the Structural Division, ASCE, Vol. 100, No.ST7, July, 1974, pp.(1451-1458).

17. Lightfoot, E. and Le Messurier, A.P., "Elastic Analysis of Frameworks with Elastic Connections", Journal of Structural Division, ASCE, Vol. 100, No.ST6, June, 1974, pp.(1297-1309).

18. Noor, A.K., " Non-Linear Analysis of Space Trusses " , Journal of Structural Division , ASCE, Vol.100, No.ST3, March, 1974, pp.533-548.

19. Gupta,S.D.,"Axially Constrained Beam on Elastic Foundation",International Journal of Mechanical Science ,Vol.16 , 1974 ,pp. 305-310.

20. Frye, M.J. and Morris, G.A., "Analysis of Flexibily Connected Steel Frames", Canadian Journal of Civil Engineering, Vol. 2, No. 3, Sept., 1975, pp.(280-291).

21. Oran, C. and Kassimali, A., "Large Deformations of Framed Structures Under Static and Dynamic Loads", International Journal of Computers and Structures, Vol. 6, No. 6, December 1976, pp. (539-547).

22. Chen, W.F. and Atusta, T., "Theory of Beam-Column", Vol. 1, Inplane Behavior and Design, McGraw-Hill Inc., New York, 1976.

23. Avent ,R.R. ,Bounin ,D., and Rhee , H.C. , " Analysis of Beam - Column on Elastic Supports " , Journal of The Structural Division,ASCE,Vol.102 , No.St3, March, 1976 , pp.691-699.

24. Wang, J.T. , " Buckling of Cantilever Bars on Elastic Foundation " , Journal of Engineering Mechanics , ASCE , Vol.102 ,No.EM4,Aug., 1976,pp.731-735.

25. Wood, R.D. and ZienKiewicz, O.C., "Geometrically Nonlinear Finite Element Analysis of Beams, Frames, Arches and Axisymmetric Shells", International Journal of Computers and Structures, Vol. 7, No. 5, 1977, pp.(725-735).

26. Mondkar, D.P. and Powell, G.H., "Finite Element Analysis of Nonlinear Static and Dynamic Response", International Journal for Numerical Methods in Engineering, Vol. 11, 1977, pp.(499-520).

27. Bergan, P.G., Horrigmoe, G., Krakeland, B. and Soreide, T.H., "Solution Techniques for Nonlinear Finite Element Problems", International Journal for Numerical Methods in Engineering, Vol. 12, 1978, pp.(1677-1696).

28. Bergan, P.G. and Soreide, T.H., "Solution of Large Displacement and Instability Problems Using the Current Stiffness Parameter", in Finite Elements in Nonlinear Mechanics (Edited by Bergan, P.G. et al.), Tapir, Trondheim, 1978, pp.(647-669).

29. AL-Sarraf, S.Z., " Elastic Instability of Structures on or Driven into Elastic Foundations " ,The Structural Engineering ,Vol.56 B, No.1,1978 ,pp.13-19.

30. Al-Sarraf, S.z., "Elastic Instability of Frames with Uniformly Tapered Members", The Structural Engineer, Vol. 57B, No. 1, March, 1979, pp.(18-24).

31. Bergan, P.G., "Solution Algorithms for Nonlinear Structural Problems", International Journal of Computers and Structures, Vol. 12, 1980, pp.(497-509).

32. Beaufait, F.W.,and Hoadley ,P.W. " Analysis of Elastic Beams on Nonlinear Foundations", International Journal of Computers and Structures,Vol.12, No.5 , Nov.1980, pp.669-676.

33. Moncarz, P.D. and Gerstle, K.H., "Steel Frames with Nonlinear Connections", Journal of Structural Division, ASCE, Vol. 107, No.ST8, Aug., 1981, pp.(1427-1441).

34. Crisfield, M.A., "A Fast Incremental/Iterative Solution Procedure that Handles Snap-Through", International Journal of Computers anf Structures, Vol. 13, No. 1, 1981, pp.(55-62).

35. Ramm, E., "Strategies for Tracing the Nonlinear Response Near Limit Points", in W. Wunderlich et al. (eds.), Nonlinear Finite Element Analysis in Structural Mechanics, Springer-Verlag, Berlin, 1981, pp.(63-89).

36. Powell, G. and Simons, J., "Improved Iteration Strategy for Nonlinear Structures", International Journal For Numerical Methods in Engineering, Vol. 17, 1981, pp.(1455-1467).

37. Jones, S.W., Kirby, P.A. and Nethercot, D.A., "Columns with Semi Rigid Joints", Journal of Structural Division, Vol. 108, No.ST2, Feb., 1982, pp.(361-372).

38. Freydoon, A., "Drift of Flexibly Connection Frames", Journal of Computers and Structures, Vol. 15, No. 2, December, 1982, pp.(103-108).

39. Crisfield, M.A., "Numerical Analysis of Structures", in J. Rhodes and A.C. Walker (eds.), Developments in Thin-Walled Structures-I, Applies Science, London, 1982, pp.(235-284).

40. Svensson S.E., and Kragerup J., " Collapse Loads of Laced Columns " , Journal of Division ,ASCE, Vol.108, No.ST6, June, 1982, pp.1367-1386.

41. Wen, R.K. and Rahimzadah, J., "Nonlinear Elastic Frame Analysis by Finite Element", Journal of Structural Engineering, ASCE, Vol. 109, No. 8, August, 1983, pp.(1952-1971).

42. Kassimali, A., "Large Deformation Analysis of Elastic-Plastic Frames", Journal of Structural Engineering, ASCE, Vol. 109, No.ST8, August, 1983, pp.(1869-1886).

43. Gelu Onu, " Shear Effect in Beam Stiffness Matrix " , Journal of Structural Engineering , ASCE, Vol.109, No.9, September, 1983, pp.2216-2221.

44. Ang, K.M. and Morris, G.A., "Analysis of Three-Dimentional Frames with Flexible Beam-Column Connections", Canadian Journal of Civil Engineering, Vol. 11, No. 2, June, 1984, pp.(245-254).

45. Kani, I.M., McConnel, R.E. and See, T., "The Analysis and Testing of a Single Layer Shallow Braced Dome", in Proceeding of 3rd International Conference on Space Structures, University of Surrey, 1984, pp.(613-618).

46. Banerjee, J.R. and Williams, F.W., "Exact Bernoulli-Euler Dynamic Stiffness Matrix for a Range of Tapered Beams", International Journal for Numerical Methods in Engineering, Vol. 21, 1985, pp.(2289-2302).

47. Yu, C.H. and Shanmugam, N.E., "Stability of Frames with Semi Rigid Joints", International Journal of Computers and Structures, Vol.23, No.5, 1986, pp.(634-648).

48. Yankelevsky, D.Z., and Eisenberger,M., " Analysis of a Beam - Column on Elastic Foundation" , International Journal of Computers and Structures, Vol.23 , No.3 , 1986, pp.351-356.

49. Yee, Y.L. and Melchers, R.E., "Moment-Rotation Curves for Bolted Connections", Journal of Structural Engineering, ASCE, Vol. 112, No.3, March, 1986, pp.(615-634).

50. Razaqpur ,A.G. , " Stiffness of Beam - Columns on Elastic Foundation with Exact Shape Functions" ,International Journal of Computers and Structures, Vol.24, No.5 ,1986 , pp.813-819.

51. Al-Sarraf, S.Z., "Shear Effect on The Elastic Stability of Frames", The Structural Engineer, Vol. 64B, No. 2, June, 1986, pp.43-47.

52. American Institute of Steel Construction, Inc., "Load and Resistance Factor Design Specification for Structural Steel Building", First Edition, Chicago, USA, 1986.

53. Chajes, A. and Churchill, J.E., "Nonlinear Frame Analysis by Finite Element Methods", Journal of Structural Engineering, ASCE, Vol. 113, No. 6, June, 1987, pp.(1221-1235).

54. Morris, G.A. and Packer, J.A., "Beam-to-Column Connections in Steel Frames", Canadian Journal of Civil Engineering, Vol. 14, No. 1, Feb., 1987, pp.(68-76).

55. Hsiao, K.M. and Hou, F.Y., "Nonlinear Finite Element Analysis of Elastic Frames", International Journal of Computers and Structures, Vol. 26, No. 5, 1987, pp.(693-701).

56. Chen, W.F. and Lui, E.M., "Effects of Joint Flexibility on the Behavior of Steel Frames", Journal of Computers and Structures, Vol. 26, No. 5, September, 1987, pp.(719-732).

57. G.E. Blandford, "Static Analysis of Flexibly Connected Thin-Walled Plane Frames", International Journal of Computers and Structures, Vol. 28, No. 1, February, 1988, pp.(105-113).

58. Chan, S.L., "Geometric and Material Nonlinear Analysis of Beam-Columns and Frames Using the Minimum Residual Displacement Method", International Journal for Numerical Methods in Engineering, Vol. 26, 1988, pp.(2657-2669).

59. Antoni,S.F.,and Tso,F.K.,"Finite Element Analysis of 3-D Beam – Columns on a Nonlinear Foundation " , International Journal of Computers and Structures , Vol.28, No.6 ,1988, pp.699-715.

60. Mc Callen, D.B., and Romstad, K.M., "A Continuum Model For The Non-Linear Analysis of Beam-Like Lattice Structures " , International Journal of Computers and Structures, Vol.29, No.2, 1988, pp.177-197.

61. Yankelevsky,D.Z., and Eisenberger,M.,and Adin ,M.A., "Analysis of Beams on Nonlinear Winkler Foundation", International Journal of Computers and Structures,Vol.31,No.2 ,Dec.1989,pp.287-292.

62. American Institute of Steel Construction, Inc., "Manual of Steel Construction-Allowable Stress Design", Ninth Edition, Chicago, USA, 1989.

63. Shi, G. and Atluri, S.N. "Static and Dynamic Analysis of Space Frames with Nonlinear Flexible Connections", International Journal for Numerical Methods in Engineering, Vol. 28, No. 28, April, 1989, pp.(2635-2650).

64. Meek, J.L. and Loganathan, S., "Large Displacement Analysis of Space-Frame Structures", Computer Methods in Applied Mechanics and Engineering, Vol. 72, 1989, pp.(57-75).

65. Haldar, A. and Nee, K.M., "Elasto-Plastic Large Deformation Analysis of PR Steel Frames for LRFD", Journal of Computers and Structures, Vol. 31, No. 5, February, 1989, pp.(811-823).

66. Wong, M.B. and Tin-Loi, F., "Geometrically Nonlinear Analysis of Elastic Framed Structures", International Journal of Computers and Structures, Vol. 34, No. 4, 1990, pp.(633-640).

67. Clarke, M.j. and Hancock, G.J., "Study of Incremental-Iterative Strategies for Nonlinear Analysis", International Journal for Numerical Methods in Structures, Vol. 29, 1990, pp.(1365-1391).

68. Avent, R.R., R.R.A. Issa, and M.L.Chaw, " Discrete Field Stability Analysis of Planar Trusses ", Journal of Structural Engineering, ASCE, Vol.117, No.2, February, 1991, pp.423-439.

69. Fuji, F., Choong, K.K. and Gong, S.X., "Variable Displacement Control to Overcome Turning Points of Nonlinear Elastic Frames", International Journal of Computers and Structures, Vol. 44, No. 12, 1992, pp.(133-136).

70. Paramaisvam, V. , S.P.T.R.Gowda, and D.M.Raj, "Timoshenko Beam Finite Element with Four DOF and Convergence of $O(h^4)$ " , International Journal of Computers and Structures, Vol.43, 1992, pp.1187-1189.

71. Al-Sadder, S.Z.R., "Large Displacement Elastic-Plastic Stability Analysis of Plane Steel Frames with Nonlinear Connections", M.Sc. thesis, University of Baghdad, December 1994.

72. Alwash, N.A., " Non-Linear Behavior and Optimal Design of Reinforced Concrete Vierndeel Truss ", Ph.D. Thesis presented to the University of Technology, Building and Construction Department, December 1995.

73. Al-Raunduzy, A., "Large Displacement Elastic Stability Analysis of Plane Steel Frames Under Static and Dynamic Loads", M.Sc. thesis, University of Technology, January 1996.

74. Sideek, KH.F., "Shear And Three-Dimensional Large Deformation Effects on Stability of Cables " , M.Sc. thesis, University of Technology, 1997.

75. Al-Hachami, E.K.,"Large Displacement Analysis of Structures with Applications to Piles and Submarine Pipelines ", Ph.D. Thesis, University of Technology, Baghdad, 1997.

76. Al-Bidairi, S., "Large Displacement Elastic Stability Analysis of Plane Steel Frames Including Shear and Damping Effects", M.Sc. thesis, University of Babylon, December 1998.

77. Al-Uraiby, B., "Large Displacement and Post-Buckling Analysis of Frames with Non-prismatic Members", M.Sc. thesis, University of Babylon, November 1998.

78. Chen, C.N., "Solution of Beam on Elastic Foundation by DQEM", Journal of Engineering Mechanics ,Vol.124,No.12,Dec.1998,pp.1381-1384.

79. Al-Damerchi, H., "Large Displacement Elastic-Plastic Nonlinear Behavior With Non-prismatic Members", M.Sc. thesis, University of Technology, 1998.

80. Al-Quraishi H.A.A., " Large Displacement Elastic Stability Analysis of Plane Frame Including Shear Effect ", M.Sc. thesis, University of Technology, 1999.

81. T. Hong, J.G. Teng and Y.F. Luo, " Axisymmetric shell and plates on tensionless elastic foundations", International Journal of Solids and Structures, 1999, pp. 5277-5300.

82. Al-Mutariee, H., "Large Displacement and Post-Buckling Analysis of Non-prismatic Frames Under Static and Dynamic Loads", M.Sc. thesis, University of Babylon, December 2000.

83. AL-Rubai, Q.K., " Large Displacement Elastic Stability Analysis of Plane Structure Under Static Loads and Resting on Nonlinear Winkler Foundation" M.Sc. Thesis, University of Technology, Baghdad, 2001.

84. Al-Khafaji A.Kh. , " Large Displacement & Post-buckling Analysis of Plane Steel Structures With Non-Prismatic Members Resting on Elastic Foundation ", M.Sc., thesis, University of Babylon, January 2002.

85. AL-Khafaji H.M.J., " Large Displacement & Post-buckling Analysis of Plane Steel Frames With Non-Prismatic Members & Non-Linear Flexible Connections Under Static Loads ", M.Sc., thesis, University of Babylon, January 2002.

Table (2.1): Mathematical modeling of connection M-ϕ behavior [54]

Connection	Reference	Description of model	M-ϕ curve
Single web angle	____	____	____
Web side plate	Richard *et al*. (1980)	Dimensionless equation based upon non-linear finite element analysis of several connections	
Double web angle	Lothers (1951)	Linear equations for initial stiffness and connection moment capacity, based upon elastic analysis of web angles	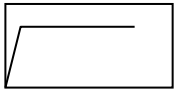
	Lewitt *et al.*(1969)	Two equations based upon elastic and plastic analyses, with intermediate transition. Equaion contain factor evaluated	
End plate	Tary and Cardinal (1981)	Equations for initial M-ϕ curve (almost linear) and ultimate moment capacity, based on parametric study using parametric study using finite-element program	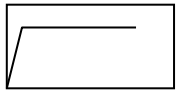

Connection	Reference	Description of model	M-ϕ curve
Header plate	____	____	____
End plate	Krishnamrthy *et al.* (1979)	Equation for initial M-ϕ curve (almost linear), based on parametric study using two dimensional elastic-plastic finite-element program	
	Johnson and Law (1981)	Linear equations for intial stiffness and plastic moment capacity, based upon elastic and yield line analysis, respectively	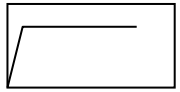
Top and Seat angle	Lothers (1951)	Linear equations for initial stiffness and connection moment capacity, based on elastic analysis	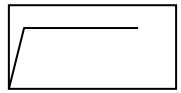
	Maxwell *et al.*, (1981)	Linear equations for initial stiffness and ultimate moment, based on finite – element analysis of several connections	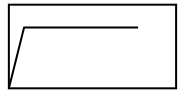

APPENDIX A

STABILITY AND BOWING FUNCTIONS WITH THEIR DERIVATIVES FOR PRISMATIC MEMBERS

A.1 Stability functions [13]

1. Compressive axial force, (q>0):-

$$C_1 = \frac{\phi(\sin\phi - \phi\cos\phi)}{2(1-\cos\phi) - \phi\sin\phi} \quad \text{.....(A.1)}$$

$$C_2 = \frac{\phi(\phi - \sin\phi)}{2(1-\cos\phi) - \phi\sin\phi} \quad \text{.....(A.2)}$$

where

$$\phi^2 = \frac{QL^2}{EI} = \pi^2 q \quad \text{.....(A.3)}$$

2. Zero axial force, (q=0): -

$$C_1 = 4 \quad \text{.....(A.4)}$$

$$C_2 = 2 \quad \text{.....(A.5)}$$

3. Tensile axial force, (q<0): -

$$C_1 = \frac{\psi(\psi\cosh\psi - \sinh\psi)}{2(1-\cosh\psi) + \psi\sinh\psi} \quad \text{.....(A.6)}$$

$$C_2 = \frac{\psi(\sinh\psi - \psi)}{2(1-\cosh\psi) + \psi\sinh\psi} \quad \text{.....(A.7)}$$

where

$$\psi^2 = -\frac{QL^2}{EI} = -\pi^2 q \quad \text{.....(A.8)}$$

A.2 Bowing functions [7]: -

$$b_1 = \frac{(C_1 + C_2)(C_2 - 2)}{8\pi^2 q} \quad \text{.....(A.9)}$$

$$b_2 = \frac{C_2}{8(C_1 + C_2)} \quad \text{.....(A.10)}$$

A.3 Derivatives with respect to q [42]: -

$$C_1' = -2\pi^2 (b_1 + b_2) \quad \text{.....(A.11)}$$

$$C_2' = -2\pi^2 (b_1 - b_2) \quad \text{.....(A.12)}$$

$$b_1' = -\frac{(b_1 - b_2)(C_1 + C_2) + 2C_2 b_1}{4q} \quad \text{.....(A.13)}$$

$$b_2' = \frac{\pi^2 (16 b_1 b_2 - b_1 + b_2)}{4(C_1 + C_2)} \quad \text{.....(A.14)}$$

A.4 Series Expressions [42]

The closed form expressions of stability and bowing functions and their derivatives become singular at q=0. As a result, computational difficulties are encountered in the evaluation of functions for small values of q. these difficulties can be avoided by using the series expansion of these functions as given by **Kassimali**. The series expressions which are valid for the small values of compressive and tensile axial force, were used within the range of (-0.1≤q≤0.1) in the numerical solution presented in this study. The series expressions are:

$$C_1 \approx 4 - \frac{2}{15}\pi^2 q - \frac{11}{6300}\pi^4 q^2 - \frac{1}{27000}\pi^6 q^3 \quad \text{.....(A.15)}$$

$$C_2 \approx 2 + \frac{1}{30}\pi^2 q + \frac{13}{12600}\pi^4 q^2 + \frac{11}{378000}\pi^6 q^3 \quad \text{.....(A.16)}$$

$$b_1 \approx \frac{1}{40} + \frac{1}{2800}\pi^2 q + \frac{1}{168000}\pi^4 q^2 + \frac{37}{388080000}\pi^6 q^3 \quad \text{.....(A.17)}$$

$$b_2 \approx \frac{1}{24} + \frac{1}{720}\pi^2 q + \frac{1}{20160}\pi^4 q^2 + \frac{37}{604800}\pi^6 q^3 \quad \text{.....(A.18)}$$

$$C_1' \approx -\frac{2}{15}\pi^2 - \frac{11}{3150}\pi^4 q - \frac{1}{9000}\pi^6 q^2 \quad \text{.....(A.19)}$$

$$C_2' \approx \frac{1}{30}\pi^2 + \frac{13}{6300}\pi^4 q + \frac{11}{126000}\pi^6 q^2 \quad \text{.....(A.20)}$$

$$b_1' \approx \frac{1}{2800}\pi^2 + \frac{1}{84000}\pi^4 q + \frac{27}{129360000}\pi^6 q^2 \quad \text{.....(A.21)}$$

$$b_2' \approx \frac{1}{720}\pi^2 + \frac{1}{10080}\pi^4 q + \frac{1}{201600}\pi^6 q^2 \quad \text{.....(A.22)}$$

Finally, the stability and bowing functions are shown graphically in Figures (A.1) and (A.2).

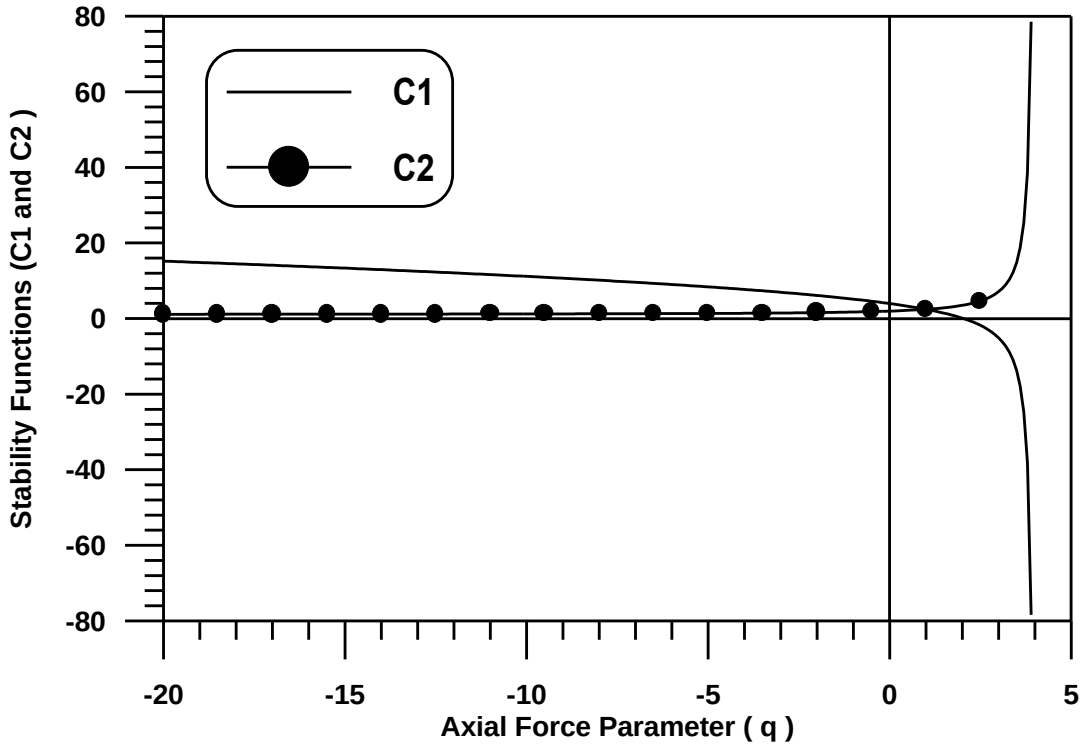

Fig.(A-1): Stability Functions-Axial Force Parameter Curves .

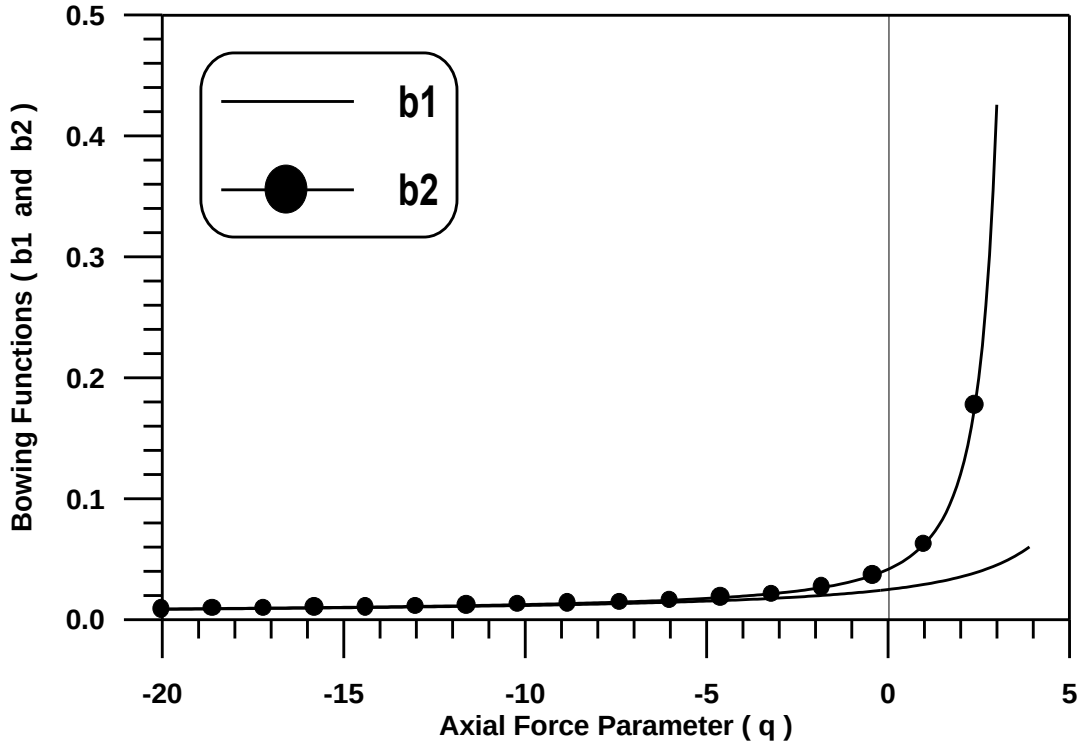

Fig.(A-2): Bowing Functions-Axial Force Parameter Curves .

APPENDIX (B)

EVALUATION OF THE DERIVATIVES OF THE STABILITY AND BOWING FUNCTIONS OF NON-PRISMATIC MEMBER BY FINITE DIFFERENCE METHOD

The first and second derivatives of C_i (i=1, 2), with respect to $\mathbf{q_o}$ can be obtained directly by using the finite difference method as follows:

$$\mathbf{C_1'} = \frac{\mathbf{C_1(q+\Delta q) - C_1(q-\Delta q)}}{\mathbf{2\Delta q}} \quad \text{.....(B.1)}$$

$$\mathbf{C_2'} = \frac{\mathbf{C_2(q+\Delta q) - C_2(q-\Delta q)}}{\mathbf{2\Delta q}} \quad \text{.....(B.2)}$$

$$\mathbf{C_1''} = \frac{\mathbf{C_1(q+\Delta q) - 2\ C_1(q) + C_1(q-\Delta q)}}{\mathbf{(\Delta q)^2}} \quad \text{.....(B.3)}$$

$$\mathbf{C_2''} = \frac{\mathbf{C_2(q+\Delta q) - 2\ C_2(q) + C_2(q-\Delta q)}}{\mathbf{(\Delta q)^2}} \quad \text{.....(B.4)}$$

where the values of C_i at (q, q±Δq) can be obtained by using the equations of appendix A. also, the value of q can be obtained by using equation (3.60). However, the equations of γ_i', β_i and β_i' (i=1, 2, 3), become,

$$\boldsymbol{\gamma_1'} = \mathbf{D^{\varphi m/4}\, C_1'(q)} \quad \text{.....(B.5)}$$

$$\boldsymbol{\gamma_2'} = \mathbf{D^{(1+\varphi)m/4}\, C_2'(q)} \quad \text{.....(B.6)}$$

$$\boldsymbol{\gamma_3'} = \mathbf{u^{(1+\phi/2)m/4}\, C_1'(q)} \quad \text{.....(B.7)}$$

$$\boldsymbol{\gamma_1'} = \mathbf{D^{\varphi m/4}\, C_1'(q)} \quad \text{.....(B.8)}$$

$$\boldsymbol{\beta_2} = -\frac{\mathbf{D^{(1+\varphi)m/4}\, C_2'(q)}}{\mathbf{2\pi^2}} \quad \text{.....(B.9)}$$

$$\boldsymbol{\beta_3} = -\frac{\mathbf{D^{(1+\varphi/2)m/4}\, C_1'(q)}}{\mathbf{2\pi^2}} \quad \text{.....(B.10)}$$

$$B_2 = -\frac{D^{(1+\varphi)m/4}\, C_2'(q)}{2\pi^2} \quad \text{.....(B.11)}$$

$$\beta_2' = -\frac{D^{(1+\varphi)m/4}\, C_2''(q)}{2\pi^2} \quad \text{.....(B.12)}$$

$$\beta_3' = -\frac{D^{(1+\varphi/2)m/4}\, C_1''(q)}{2\pi^2} \quad \text{.....(B.13)}$$

The value of Δq depends on the required accuracy. When the value is too large or too small, the program will fail to coverage, therefore it is usually in the range (10^{-2}-10^{-4}).

Certificate

We certify that the preparation of this thesis was under our supervision at the University of Babylon in partial fulfillment of the requirements for the degree of Master of Science in Civil Engineering.

Signature :
Name : *Dr. Nameer A. Alwash*
Date: / / 2002

Signature :
Name : *Prof. Dr. Sabeeh Z. Al-Sarraf*
Date: / / 2002

Certificate

We certify as an examining committee that we have read this thesis entitled "**Post-Buckling Analysis of Plane Steel Frames on Elastic Foundation with Flexible Connection**", and examined the student (**Jawad Talib Aboudi**) in it's content and what related to it, and found it meets the standard of a thesis for the Degree of Master of Science in Structural Engineering.

Signature :

Name : *Prof. Dr. Sabeeh Z. Al-Sarraf*
(Supervisor**)**

Date: / / 2002

Signature :

Name:*Assis. Prof. Dr. Nameer A.Alwash*
(Supervisor**)**

Date: / / 2002

Signature :

Name:*Assis. Prof. Dr.Bayan S. Al-Nu'man*
(Member**)**

Date: / / 2002

Signature :

Name:*Assis. Prof. Dr. Ammar Y. Ali*
(Member**)**

Date: / / 2002

Signature :
Name:*Assis. Prof. Dr. Ing Ali AL-Athary*
(Chairman**)**

Date: / / 2002

Approval of the Civil Engineering Department
Head of the Civil Engineering Department

Signature:

Name: *Assis. Prof. Dr. Nameer A. Alwash*

Date: / / 2002

Approval of the Deanery of the College of Engineering
Dean of the College of Engineering

Signature:

Name: *Prof. Dr. Abdul Amir S. Resen*
Dean of the College of Engineering

Date: / / 2002